



**UNIVERSITY OF IOANNINA**

**SCHOOL OF SCIENCES**

**DEPARTMENT OF CHEMISTRY**

**DEVELOPMENT OF ANALYTICAL METHODS FOR THE HPLC-BASED  
DETERMINATION OF SULFONAMIDES AFTER MICROEXTRACTION WITH  
NOVEL (NANO)MATERIALS**

**CHATZIMITAKOS THEODOROS**  
CHEMIST

**DOCTORAL THESIS**

**IOANNINA 2020**

This thesis was funded by General Secretariat for Research and Technology (GSRT)  
and Hellenic Foundation for Research and Innovation (HFRI)





**ΠΑΝΕΠΙΣΤΗΜΙΟ ΙΩΑΝΝΙΝΩΝ**

**ΣΧΟΛΗ ΘΕΤΙΚΩΝ ΕΠΙΣΤΗΜΩΝ**

**ΤΜΗΜΑ ΧΗΜΕΙΑΣ**

**ΑΝΑΠΤΥΞΗ ΑΝΑΛΥΤΙΚΩΝ ΜΕΘΟΔΩΝ ΓΙΑ ΤΟΝ ΥΓΡΟΧΡΩΜΑΤΟΓΡΑΦΙΚΟ  
ΠΡΟΣΔΙΟΡΙΣΜΟ ΣΟΥΛΦΟΝΑΜΙΔΙΩΝ ΜΕΤΑ ΑΠΟ ΜΙΚΡΟΕΚΧΥΛΙΣΗ ΜΕ  
ΚΑΙΝΟΤΟΜΑ (ΝΑΝΟ)ΎΛΙΚΑ**

**ΧΑΤΖΗΜΗΤΑΚΟΣ ΘΕΟΔΩΡΟΣ**  
**ΧΗΜΙΚΟΣ**

**ΔΙΔΑΚΤΟΡΙΚΗ ΔΙΑΤΡΙΒΗ**

**ΙΩΑΝΝΙΝΑ 2020**

Η παρούσα διδακτορική διατριβή υλοποιήθηκε με υποτροφία της Γενικής  
Γραμματείας Έρευνας και Τεχνολογίας και του Ελληνικού Ιδρύματος Έρευνας και  
Καινοτομίας



«Η έγκριση της διδακτορικής διατριβής από το Τμήμα Χημείας της Σχολής Θετικών Επιστημών,  
του Πανεπιστημίου Ιωαννίνων δεν υποδηλώνει αποδοχή των γνώμων του συγγραφέα Ν.

5343/32, άρθρο 202, παράγραφος 2»



Ορισμός Τριμελούς Συμβουλευτικής Επιτροπής από τη Συνέλευση: 923<sup>A</sup>/29-1-2016

Μέλη Τριμελούς Συμβουλευτικής Επιτροπής:

Επιβλέπων: Κωνσταντίνος Σταλίκας, Καθηγητής Τμ. Χημείας, Παν/μιο Ιωαννίνων

Μέλη: Τριαντάφυλλος Αλμπάνης, Καθηγητής Τμ. Χημείας, Παν/μιο Ιωαννίνων

Βικτωρία Σαμανίδου, Καθηγήτρια Τμ. Χημείας, ΑΠΘ

Ημερομηνία ορισμού θέματος από τη Συνέλευση: 924<sup>A</sup>/26-2-2016, όπως τροποποιήθηκε από τη Συνέλευση: 1001<sup>A</sup> /21-6-2019

Θέμα: <<Ανάπτυξη αναλυτικών μεθόδων για τον υγροχρωματογραφικό προσδιορισμό σουλφοναμιδίων μετά από μικροεκχύλιση με καινοτόμα (νάνο)υλικά>>

<<Development of analytical methods for the HPLC-based determination of sulfonamides after microextraction with novel (nano)materials>>

**ΟΡΙΣΜΟΣ ΕΠΤΑΜΕΛΟΥΣ ΕΞΕΤΑΣΤΙΚΗΣ ΕΠΙΤΡΟΠΗΣ ΑΠΟ ΤΗ ΣΥΝΕΛΕΥΣΗ:** 1016<sup>A</sup>/14-5-2020

1. Κωνσταντίνος Σταλίκας, Καθηγητής Τμ. Χημείας, Παν/μιο Ιωαννίνων
2. Τριαντάφυλλος Αλμπάνης, Καθηγητής Τμ. Χημείας, Παν/μιο Ιωαννίνων
3. Βικτωρία Σαμανίδου, Καθηγήτρια Τμ. Χημείας, ΑΠΘ
4. Ιωάννης Ρούσσης, Καθηγητής Τμ. Χημείας, Παν/μιο Ιωαννίνων
5. Αθανάσιος Βλεσσίδης, Καθηγητής Τμ. Χημείας, Παν/μιο Ιωαννίνων
6. Βασίλειος Σακκάς, Αναπλ. Καθηγητής Τμ. Χημείας, Παν/μιο Ιωαννίνων
7. Δημοσθένης Γκιώκας, Αναπλ. Καθηγητής Τμ. Χημείας, Παν/μιο Ιωαννίνων

Έγκριση Διδακτορικής Διατριβής με βαθμό <<Άριστα (δέκα-10)>> στις 29-6-2020

Η Πρόεδρος του Τμήματος Χημείας  
Λουλούδη Μαρία, Καθηγήτρια

Η Γραμματέας του Τμήματος  
Ξανθή Τουτουτζόγλου





**ΠΑΝΕΠΙΣΤΗΜΙΟ ΙΩΑΝΝΙΝΩΝ**  
**ΣΧΟΛΗ ΘΕΤΙΚΩΝ ΕΠΙΣΤΗΜΩΝ**  
**ΤΜΗΜΑ ΧΗΜΕΙΑΣ**  
**ΤΟΜΕΑΣ ΑΝΟΡΓΑΝΗΣ ΚΑΙ ΑΝΑΛΥΤΙΚΗΣ ΧΗΜΕΙΑΣ**

Προς την Γραμματεία του Τμήματος Χημείας  
του Πανεπιστημίου Ιωαννίνων

Ιωάννινα 29 Ιουνίου 2020

**ΠΡΑΚΤΙΚΟ ΕΠΤΑΜΕΛΟΥΣ ΕΞΕΤΑΣΤΙΚΗΣ ΕΠΙΤΡΟΠΗΣ ΤΟΥ ΥΠΟΨΗΦΙΟΥ**  
**ΔΙΔΑΚΤΟΡΑ κ. ΘΕΟΔΩΡΟΥ ΧΑΤΖΗΜΗΤΑΚΟΥ**

Σήμερα στις 29 Ιουνίου 2020 και ώρα 14:30 μμ, η επταμελής εξεταστική επιτροπή αποτελούμενη από τους:

1. Κωνσταντίνο Σταλικά, Καθηγητή Τμ. Χημείας, Παν/μίου Ιωαννίνων (επιβλέποντα)
2. Τριαντάφυλλο Αλμπάνη, Καθηγητή Τμ. Χημείας, Παν/μίου Ιωαννίνων
3. Βικτωρία Σαμανίδου, Καθηγήτρια Τμ. Χημείας, ΑΠΘ
4. Ιωάννη Ρούσση, Καθηγητή Τμ. Χημείας, Παν/μίου Ιωαννίνων
5. Αθανάσιο Βλεσσίδη, Καθηγητή Τμ. Χημείας, Παν/μίου Ιωαννίνων
6. Βασίλειο Σακκά, Αναπλ. Καθηγητή Τμ. Χημείας, Παν/μίου Ιωαννίνων
7. Δημοσθένη Γκιώκα, Αναπλ. Καθηγητή Τμ. Χημείας, Παν/μίου Ιωαννίνων

που ορίστηκε με την απόφαση του Τμήματος Χημείας (Συνεδρίαση 1016/14-5-2020), συνήλθε με τηλεδιάσκεψη μέσω της διαδικτυακής πλατφόρμας MS TEAMS και παρακολούθησε τη δημόσια παρουσίαση της διατριβής του υποψήφιου διδάκτορα κ. Θεόδωρου Χατζημητάκου με θέμα: "**Ανάπτυξη αναλυτικών μεθόδων για τον υδροχρωματογραφικό προσδιορισμό σουλφοναμιδίων μετά από μικροεκχύλιση με καινοτόμα (νανο)υλικά. Αγγλικός τίτλος: Development of analytical methods for the HPLC-based determination of sulfonamides after microextraction with novel (nano)materials**".

Ο κ. Χατζημητάκος ανέπτυξε επί σαράντα λεπτά τα κυριότερα αποτελέσματα της διατριβής του, απάντησε σε ερωτήσεις του ακροατηρίου και ακολούθως σε ερωτήματα της εξεταστικής επιτροπής. Στη συνέχεια, ο κ. Χατζημητάκος και το ακροατήριο αποχώρησαν από την τηλεδιάσκεψη και η επταμελής εξεταστική επιτροπή μετά από σύσκεψη και λεπτομερή συζήτηση έκρινε ότι η διατριβή είναι πρωτότυπη και συμβάλλει στην εξέλιξη της επιστήμης κι έτσι αποφάσισε ομόφωνα να προτείνει στη Γενική Συνέλευση Ε.Σ. την απονομή στον κ. Θεόδωρο Χατζημητάκο του τίτλου του διδάκτορα του Τμήματος Χημείας του Πανεπιστημίου Ιωαννίνων, με βαθμό "Άριστα" (δέκα-10).

**Η Εξεταστική Επιτροπή**

Κωνσταντίνος Σταλικάς, Καθηγητής

Τριαντάφυλλος Αλμπάνης, Καθηγητής

Βικτωρία Σαμανίδου, Καθηγήτρια

Ιωάννης Ρούσσης, Καθηγητής

Αθανάσιος Βλεσσίδης, Καθηγητής

Βασίλειος Σακκάς, Αναπλ. Καθηγητής

Δημοσθένης Γκιώκας, Αναπλ. Καθηγητής





## ΠΡΟΛΟΓΟΣ

Η παρούσα διδακτορική διατριβή με τίτλο: *“Development of analytical methods for the hplc-based determination of sulfonamides after microextraction with novel (nano)materials”* εκπονήθηκε στο Εργαστήριο Αναλυτικής Χημείας του Τμήματος Χημείας του Πανεπιστημίου Ιωαννίνων, υπό την επίβλεψη του Καθηγητή Κωνσταντίνου Σταλίκας. Για την υλοποίηση της παρούσας διδακτορικής διατριβής χορηγήθηκε υποτροφία από το Ελληνικό Ίδρυμα Έρευνας και Τεχνολογίας (ΕΛΙΔΕΚ) και από τη Γενική Γραμματεία Έρευνας και Τεχνολογίας (ΓΓΕΤ).

Δοθείσης της ευκαιρίας, θα ήθελα να εκφράσω τις ευχαριστίες μου σε ανθρώπους οι οποίοι με βοήθησαν, ο καθένας με τον δικό του ξεχωριστό τρόπο, όχι μόνο να ολοκληρώσω τη παρούσα έρευνα αλλά να είναι και ιδιαίτερα εποικοδομητική.

Δικαιωματικά, ο πρώτος άνθρωπος στον οποίο οφείλω ολόψυχες ευχαριστίες είναι ο Καθηγητής του Τμήματος Χημείας του Πανεπιστημίου Ιωαννίνων, Κωνσταντίνος Σταλίκας, κοντά στον οποίον είχα τη χαρά και την τιμή να εκπονήσω τη διδακτορική διατριβή. Η αδιάκοπη επιστημονική του καθοδήγηση, οι υψηλές απαιτήσεις του και οι συνεχείς προτροπές για την όσο το δυνατόν αρτιότερη διεξαγωγή όλων των σταδίων της μελέτης αυτής, λειτούργησαν ως φάρος για την ορθή αποπεράτωση της διατριβής αυτής. Τον ευχαριστώ που μου μεταλαμπάδευσε τα φώτα της επιστήμης του, τις εμπειρίες και τον επιστημονικό τρόπο σκέψης, τα οποία σμίλευσαν την έως τώρα επιστημονική μου κατάρτιση και πορεία. Τον ευχαριστώ για όλον τον προσωπικό χρόνο και κόπο που αφιέρωσε πέραν των υποχρεώσεων του και για την αδιάκοπη αρωγή και υποστήριξή του σε επιστημονικά θέματα πέραν της παρούσας διατριβής. Κυρίως όμως θα ήθελα να τον ευχαριστήσω γιατί αποτελεί πρότυπο, όχι μόνο ως επιστήμονας και εκπαιδευτικός αλλά και ως άνθρωπος.

Συνεχίζοντας, θέλω να ευχαριστήσω θερμά τον κ. Τριαντάφυλλο Αλμπάνη, Πρύτανη και Καθηγητή του Τμήματος Χημείας του Πανεπιστημίου Ιωαννίνων, για την πολύτιμη βοήθεια που μου προσέφερε, όταν τη χρειάστηκα καθώς και την κ. Βικτωρία Σαμανίδου, Καθηγήτρια του Τμήματος Χημείας του Αριστοτελείου Πανεπιστημίου Θεσσαλονίκης για τα σχόλια και τις παρατηρήσεις της σε επιστημονικά θέματα. Επιπλέον, τους ευχαριστώ

και τους δυο τόσο για την προθυμία τους να είναι μέλη της τριμελούς συμβουλευτικής μου επιτροπής, καθώς και για τον χρόνο που διέθεσαν για να μελετήσουν την παρούσα εργασία.

Ένα τεράστιο ευχαριστώ οφείλω στην κ. Κασούνη Αθανασία, μεταδιδακτορική ερευνήτρια στο Εργαστήριο Φυσικοχημείας Βιολογικών Συστημάτων του Τμήματος Βιολογικών Εφαρμογών και Τεχνολογιών του Πανεπιστημίου Ιωαννίνων για τις πολυάριθμες ώρες που περάσαμε μαζί στο εργαστήριο και μοιραζόμασταν τις ανησυχίες, το άγχος, τα όνειρα και τις ελπίδες μας, κάνοντας τις πολύωρες αναμονές ευχάριστες. Επιπλέον την ευχαριστώ για όλη τη βοήθεια που μου προσέφερε (πρακτική και ψυχολογική) και για την άψογη συνεργασία που διατηρούμε έως και σήμερα.

Ένα μεγάλο ευχαριστώ οφείλω και στον Καθηγητή του Τμήματος Χημείας Jared Anderson του Iowa State University για την άψογη συνεργασία και την παροχή των μαγνητικών ιοντικών υγρών στα οποία στηρίχτηκε η ανάπτυξη μιας εκ των τεσσάρων αναλυτικών μεθόδων. Επίσης, θα ήθελα να ευχαριστήσω τον Καθηγητή του τμήματος Χημείας κ. Δημήτριο Πετράκη για τις μετρήσεις ποροσιμετρίας αζώτου με την μέθοδο BET, καθώς και για τη λήψη των εικόνων SEM, καθώς και την κ. Παπαχριστοδούλου Χριστίνα για την μελέτη των δειγμάτων με Περίθλαση Ακτίνων Χ.

Επιπλέον, θα ήθελα να ευχαριστήσω ιδιαίτερα την κ. Βασιλική Εξάρχου, Επιστημονική/Τεχνική υπεύθυνη Έργων στην Ευρωπαϊκή Επιτροπή, παρότι πέρασαν χρόνια από την συνεργασία μας, για την όρεξη και την αγάπη για την έρευνα που μου μετέδωσε και για την εμπιστοσύνη της στο πρόσωπο μου, η οποία αποτέλεσε κύριο βήμα για την έναρξη της σταδιοδρομίας μου. Τέλος την ευχαριστώ για τη βοήθεια που μου προσφέρει έως και σήμερα.

Επιπλέον, θα ήθελα να ευχαριστήσω τον καθηγητή κ. Βλεσσίδα Αθανάσιο, τον επίκουρο καθηγητή κ. Γκιώκα Δημοσθένη, τον αναπληρωτή καθηγητή κ. Σακκά Βασίλειο και την κ. Αγγελική Φλώρου για τη βοήθεια τους όλα αυτά τα χρόνια σε ό,τι χρειάστηκα αλλά κυρίως για το ευχάριστο κλίμα και τη φιλική και πρόσχαρη συμπεριφορά τους.

Έπειτα, θα ήθελα να ευχαριστήσω το Ελληνικό Ίδρυμα Έρευνας και Τεχνολογίας (ΕΛΙΔΕΚ) και τη Γενική Γραμματεία Έρευνας και Τεχνολογίας (ΓΓΕΤ) για την υποτροφία που μου χορήγησαν.

Τέλος, θα ήθελα να εκφράσω το μεγαλύτερο ευχαριστώ στην οικογένεια μου και ιδίως στη μητέρα μου Γαϊτανίδου Σωτηρία, η οποία μέσα από τον καθημερινό της αγώνα και τις θυσίες, μου παρείχε όσα χρειαζόμουν για να ασχολούμαι απρόσκοπτα με τις σπουδές μου. Η ηθική συμπαράσταση που μου προσέφεραν όλα αυτά τα χρόνια και η υποστήριξή τους είναι ανεκτίμητη.



**αἰὲν ἀριστεύειν καὶ ὑπεῖροχον ἔμμεναι ἄλλων**

**«Πάντα να είσαι πρώτος και ανώτερος από τους άλλους »**

***Ομήρου Ιλιάδα, ραψωδία Ζ, στ. 208***





## Περιεχόμενα

ΠΡΟΛΟΓΟΣ.....	1
Περιεχόμενα.....	7
SUMMARY .....	11
ΠΕΡΙΛΗΨΗ .....	15
ABBREVIATIONS.....	19
LIST OF FIGURES .....	21
LIST OF TABLES .....	25
CHAPTER 1: Introduction.....	27
1.1 Sulfonamides .....	27
1.1.1 Historical background.....	27
1.1.2 Mechanism of action.....	32
1.1.2.1 Sulfacetamide (SA) .....	33
1.1.2.2 Sulfadiazine (SD).....	33
1.1.2.3 Sulfapyridine (SP) .....	34
1.1.2.4 Sulfathiazole (STZ) .....	34
1.1.2.5 Sulfamerazine (SM) .....	35
1.1.2.6 Sulfamethazine (SMZ) .....	35
1.1.2.7 Sulfamethoxyipyridazine (SMP) .....	37
1.1.2.8 Sulfachloropyridazine (SCP).....	37
1.1.2.9 Sulfamethoxazole (SMX) .....	37
1.1.2.10 Sulfadimethoxine (SDM) .....	38
1.1.2.11 Sulfisoxazole (SIX).....	38
1.1.2.12 Sulfaquinoxaline (SQX) .....	39
1.1.3 Usage of SAs and associated risks .....	39
1.1.4 Overview of sample preparation procedures for sulfonamides detection.....	40
1.1.4.1 Sample preparation procedures for milk samples .....	42
1.1.4.2 Sample preparation procedures for egg samples .....	48
1.1.4.3 Sample preparation procedures for water samples .....	48
1.1.4.4 Sample preparation procedures for pork and chicken samples .....	54
1.1.4.5 Sample preparation procedures for honey samples .....	57
1.1.4.6 Sample preparation procedures for fish samples .....	57
1.1.4.7 Sample preparation procedures for animal feeds samples .....	58

1.1.5 Objectives and Scope .....	63
1.2 References.....	64
Chapter 2: Graphene-functionalized melamine sponges for microextraction of sulfonamides from food and environmental samples .....	77
2.1 Introduction.....	77
2.2 Material and methods.....	80
2.2.1 Chemicals and reagents .....	80
2.2.2 Instrumentation .....	80
2.2.3 Graphene oxide (GO) synthesis.....	81
2.2.4 Functionalization of melamine sponges .....	81
2.2.5 Extraction procedure.....	82
2.2.6 Sample preparation.....	82
2.3 Results and discussion.....	83
2.3.1 Characterization of the GMeS .....	83
2.3.2 Synthesis optimization .....	87
2.3.2.1 GO concentration and hydrazine quantity.....	89
2.3.2.2 Microwave intensity and time .....	91
2.3.2.3 Times of functionalization.....	92
2.3.3 Optimization of the proposed procedure .....	93
2.3.3.1 Effect of the pH-mechanism of interaction.....	93
2.3.3.2 Effect of the ionic strength.....	95
2.3.3.3 Other extraction parameters .....	97
2.3.3.4 Elution conditions.....	98
2.3.4 Method validation .....	99
2.3.5 Comparison with other analytical methods.....	106
2.4 Conclusions.....	107
2.5 References.....	111
Chapter 3: Melamine sponge decorated with copper sheets as a material with outstanding properties for microextraction of sulfonamides prior to their determination by high-performance liquid chromatography.....	115
3.1 Introduction.....	115
3.2 Material and methods.....	117
3.2.1 Chemicals and reagents .....	117
3.2.2 Instrumentation .....	117

3.2.3	Decoration of melamine sponge with copper sheet .....	118
3.2.4	Extraction procedure .....	118
3.2.5	Sample preparation .....	119
3.3	Results and discussion .....	120
3.3.1	Characterization .....	120
3.3.2	Synthesis optimization .....	122
3.3.2.1	Copper salt .....	122
3.3.2.2	Copper acetate concentrations and reduction conditions .....	123
3.3.2.3	Synthesis pH, time and temperature .....	126
3.3.2.4	Times of modification and synthesis scale-up .....	127
3.3.3	Optimization of the proposed procedure .....	128
3.3.3.1	Effect of pH-mechanism of interaction .....	128
3.3.3.2	Effect of the ionic strength .....	131
3.3.3.3	Other extraction parameters .....	132
3.3.3.4	Elution conditions .....	134
3.3.4	Method validation according to the commission decision 657/2002/EC .....	135
3.3.4.1	Linearity and sensitivity .....	135
3.3.4.2	Selectivity .....	135
3.3.4.3	Accuracy and precision .....	136
3.3.4.4	Decision limit and detection capability .....	139
3.4	Conclusions .....	142
3.5	References .....	146
Chapter 4: Enhanced magnetic ionic liquid-based dispersive liquid-liquid microextraction of triazines and sulfonamides through a one-pot, pH-modulated approach .....		151
4.1	Introduction .....	151
4.2	Material and methods .....	154
4.2.1	Chemicals and reagents .....	154
4.2.2	Instrumentation .....	155
4.2.3	MIL synthesis .....	155
4.2.4	Sample preparation .....	156
4.2.5	Extraction procedure .....	156
4.3	Results and discussion .....	157
4.3.1	Selection of the solid supporting material .....	157

4.3.2 Optimization of extraction .....	159
4.3.2.1 pH-modulation for extraction .....	160
4.3.2.2 Ionic strength .....	161
4.3.2.3 Other extraction parameters .....	163
4.3.3. Analytical figures of merit .....	164
4.4 Conclusions.....	171
4.5 References.....	173
Chapter 5: Zinc ferrite as a magnetic sorbent for the dispersive micro solid-phase extraction of sulfonamides and their determination by HPLC .....	177
5.1 Introduction.....	177
5.2 Materials and methods .....	178
5.2.1 Chemicals and reagents .....	178
5.2.2 Instrumentation .....	178
5.2.3 Zinc ferrites synthesis.....	179
5.2.4 Ultrasound-assisted dispersive micro solid-phase procedure .....	179
5.2.5 Sample preparation.....	180
5.3 Results and discussion.....	181
5.3.1 Synthesis optimization .....	181
5.3.1.1 Effect of zinc salt .....	181
5.3.1.2 Zinc-to-iron molar ratio in the co-precipitation process.....	182
5.3.1.3 Reaction temperature, time and calcination .....	183
5.3.2 Characterization .....	184
5.3.3 Optimization of the extraction procedure .....	186
5.3.3.1 Effect of the pH – Mechanism of interaction.....	186
5.3.3.2 Ionic strength .....	187
5.3.3.3 Other extraction parameters .....	188
5.3.4 Optimization of the elution conditions .....	190
5.3.5 Method validation.....	190
5.4 Conclusions.....	195
5.5 References.....	197
Appendix: Commission Decision 657/2002/EC.....	199
Conclusions .....	203
List of Book Chapters, Journal Papers and Conference Presentations .....	205

## SUMMARY

Antibiotics are well-known for their theraceutical applications. However, in the last years, their presence in the environment and food products has raised concerns. To address the issue, regulatory agencies have set maximum residue limits for most of them. Sulfonamides (SAs) are the first class of commercially available antibiotics and among the most commonly used ones. This is the reason why many analytical methods are being developed for SAs detection. In this Ph.D. thesis, four new sorbents ((nano)materials) are developed and utilized in sample preparation procedures, to extract SAs from food and environmental matrices and as a consequence, four analytical methods are developed. SAs were separated using an HPLC system and detected/quantified using a diode array detector. The sulfonamides employed are: sulfacetamide, sulfathiazole, sulfadiazine, sulfapyridine, sulfamerazine, sulfamethazine, sulfamethoxypyridazine, sulfachloropyridazine, sulfamethoxazole, sulfadimethoxine, sulfisoxazole and sulfaquinoxaline.

In the first method, melamine sponges are functionalized with graphene (GMeS) and used as an adsorbent. The sponges are prepared by an easy, one-step procedure, which complies with the principles of green chemistry and is proved advantageous over previously described synthesis methods. The applicability of the GMeS in extraction procedures is studied and an analytical method for the determination of sulfonamides in milk, eggs and lake water is developed and validated according to SANCO/12571/2013 guideline. The method is highly accurate and reproducible, while the limits of quantification are found to be fairly low ( $0.31\text{-}0.91\ \mu\text{g kg}^{-1}$ ,  $0.96\text{-}1.32\ \mu\text{g kg}^{-1}$  and  $0.10\text{-}0.29\ \mu\text{g L}^{-1}$  in the case of milk, eggs and lake water, respectively). Furthermore, the method is exempt from matrix effects, since the microextraction procedure serves not only as such but also as a clean-up step. Some additional advantages of the proposed procedure are the low cost and environmentally friendly synthesis, efficiency and the high extraction recoveries.

In the second study, the modification/loading of melamine sponge with metallic copper sheets (CuMeS) is discussed. The CuMeS is prepared in a fast, single-step procedure, where the concurrent production of copper oxides is avoided. The as-prepared CuMeS is utilized to develop a sensitive and selective sample preparation procedure to extract SAs from milk and water samples. The surface of the resulting CuMeS, after drying is rendered hydrophobic enabling hydrophobic interactions with analytes. This is the first time that the benefits of the high affinity of copper for SAs are reaped for analytical purposes. Due to the high selectivity for SAs, the proposed CuMeS-based procedure acts both as an extraction and a clean-up step for their quantitative determination. The analytical method developed, which is based on the extractive potential of CuMeS, has the merits of wide linearity (including concentrations above and below the maximum residue limit of SAs), low limits of quantification ( $0.025\text{--}0.057\ \mu\text{g L}^{-1}$  for lake water and  $0.23\text{--}1.05\ \mu\text{g L}^{-1}$  for milk samples), high enrichment factors and highly satisfactory recoveries and repeatability. The analytical method is validated according to the Commission Decision 657/2002/EC.

With respect to the third method, an enhanced variant of magnetic ionic liquid (MIL)-based dispersive liquid-liquid microextraction is put forward. The procedure combines a water-insoluble solid support and the  $[\text{P}_{66614}^+][\text{Dy(III)}(\text{hfacac})_4^-]$  MIL, in a one-pot, pH-modulated procedure for the microextraction of triazines (TZs) and SAs. The solid supporting material is mixed with the MIL to overcome difficulties concerning the weighing of MIL and to control the uniform dispersion of the MIL, rendering the whole extraction procedure more reproducible. The pH-modulation during the extraction step enables the one-pot extraction of SAs and TZs, from a single sample, in 15 min. Overall, the new analytical method developed enjoys the benefits of sensitivity (limits of quantification:  $0.034\text{--}0.091\ \mu\text{g L}^{-1}$ ) and precision (relative standard deviation: 5.2-8.1%), while good recoveries (i.e., 89-101%) are achieved from lake water and effluent from a municipal wastewater treatment plant. Owing to all of the above, the new procedure can be used to determine the concentrations of SAs and TZs at levels below the maximum residue limits.

Finally, for the development of the last method, zinc ferrites were used in a magnetic, ultrasound-assisted dispersive micro solid-phase procedure. Although zinc is known to have a high affinity for sulfonamides, there are no sample preparation procedures based on this property. The synthesis of zinc ferrites is straightforward, and the resulting materials exhibit favorable magnetic properties for their harvesting after extraction. Zinc ferrites can efficiently and selectively extract SAs from lake water and egg samples. The new procedure exhibits low limits of quantification (0.06 up to 0.11  $\mu\text{g L}^{-1}$ ), low matrix effect (from -8% to 8%), acceptable recoveries (88-101%) and satisfactory enrichment factors (111-141). Moreover, the method has a wide linear range (up to 250  $\mu\text{g L}^{-1}$ ) making it possible the determination of sulfonamides at concentrations above or below the maximum residue limit. Due to the aforementioned merits as well as the simplicity, the few synthetic steps required and the efficiency of sample preparation, the developed method can be used for routine analysis of sulfonamides.





## ΠΕΡΙΛΗΨΗ

Τα αντιβιοτικά είναι ευρέως διαδεδομένα για τις θεραπευτικές τους ιδιότητες. Ωστόσο, τα τελευταία χρόνια εκφράζονται ανησυχίες σχετικά με την ύπαρξή τους στο περιβάλλον και στα τρόφιμα. Για να περιοριστεί το πρόβλημα, οι νομοθετικές αρχές έχουν θεσπίσει ανώτατα επιτρεπτά όρια για τα περισσότερα αντιβιοτικά. Τα σουλφοναμίδια (sulfonamides, SAs) είναι η πρώτη κατηγορία εμπορικά διαθέσιμων αντιβιοτικών και παραμένουν από τις πιο δημοφιλείς. Αυτός είναι και ο λόγος για τον οποίο αναπτύσσονται πολλές αναλυτικές μέθοδοι για τον προσδιορισμό τους. Στο πλαίσιο της παρούσας διδακτορικής διατριβής, αναπτύχθηκαν τέσσερα (νανο)υλικά και χρησιμοποιήθηκαν σε τεχνικές προκατεργασίας δείγματος, προκειμένου να γίνει εκχύλιση των SAs από περιβαλλοντικά δείγματα και δείγματα τροφίμων και κατά συνέπεια, προέκυψαν τέσσερις νέες αναλυτικές μέθοδοι. Πραγματοποιήθηκε διαχωρισμός των SAs χρησιμοποιώντας υγρή χρωματογραφία (HPLC) και η ταυτοποίηση/ποσοτικοποίηση των ενώσεων επετεύχθη με έναν ανιχνευτή συστοιχίας διόδων (diode array detector). Τα σουλφοναμίδια τα οποία εξετάστηκαν είναι τα εξής: σουλφακεταμίδιο, σουλφαθειαζόλη, σουλφαδιαζίνη, σουλφαπυριδίνη, σουλφαμεραζίνη, σουλφαμεθαζίνη, σουλφαμεθοξυπυριδαζίνη, σουλφαχλωροπυριδαζίνη, σουλφαμεθοξαζολη, σουλφαδιμεθοξίνη, σουλφισοξαζολη, και σουλφακιννοξαλίνη.

Για την ανάπτυξη της πρώτης μεθόδου, σπόγγοι μελαμίνης τροποποιήθηκαν με γραφένιο (graphene-modified melamine sponges, GMeS) και χρησιμοποιήθηκαν ως προσροφητικό υλικό. Οι τροποποιημένοι σπόγγοι μελαμίνης παρασκευάστηκαν με μια απλή διαδικασία που ολοκληρώθηκε σε ένα στάδιο και η οποία όχι μόνο είναι σύμφωνη με τις αρχές της πράσινης Χημείας, αλλά πλεονεκτεί σε σχέση με προηγούμενες μεθόδους που αναφέρονται στη βιβλιογραφία σε σχέση με τη σύνθεση τροποποιημένων σπόγγων μελαμίνης με γραφένιο. Μελετήθηκε η καταλληλότητα των GMeS για την εκχύλιση των SAs και αναπτύχθηκε μια αναλυτική μέθοδος για τον προσδιορισμό τους σε δείγματα γάλακτος, αυγών και νερού λίμνης. Η μέθοδος που αναπτύχθηκε επικυρώθηκε σύμφωνα με την οδηγία SANCO/12571/2013 και αποδείχθηκε ότι είναι ακριβής και επαναλήψιμη, ενώ τα όρια ποσοτικοποίησης είναι χαμηλά ( $0,31-0,91 \mu\text{g kg}^{-1}$ ,

0,96-1,32  $\mu\text{g kg}^{-1}$  και 0,10-0,29  $\mu\text{g L}^{-1}$  για τα δείγματα γάλακτος, αυγών και νερού λίμνης, αντίστοιχα). Επιπλέον, δεν παρατηρήθηκε σημαντική επίδραση από τα μελετούμενα υποστρώματα, καθώς η τεχνική μικροεκχύλισης που αναπτύχθηκε λειτουργεί και ως στάδιο καθαρισμού. Το χαμηλό κόστος, η φιλική προς το περιβάλλον σύνθεση και οι υψηλές ανακτήσεις είναι μερικά ακόμα από τα πλεονεκτήματα της μεθόδου που αναπτύχθηκε.

Για την ανάπτυξη της δεύτερης μεθόδου τροποποιήθηκαν σπόγγοι μελαμίνης με μεταλλικά φύλλα χαλκού (CuMeS). Οι CuMeS παρασκευάστηκαν με μια γρήγορη διαδικασία που ολοκληρώθηκε σε ένα στάδιο (χωρίς τη δημιουργία οξειδίων του χαλκού) και χρησιμοποιήθηκαν για την ανάπτυξη μιας ευαίσθητης και εκλεκτικής μεθόδου προκατεργασίας για την εκχύλιση SAs από δείγματα γάλακτος και νερού λίμνης. Η επιφάνεια των παρασκευασμένων CuMeS, μετά τη ξήρασή τους καθίσταται υδρόφοβη, γεγονός που επιτρέπει την ανάπτυξη υδρόφοβων αλληλεπιδράσεων. Επιπλέον, είναι η πρώτη φορά που αξιοποιείται η μεγάλη συγγένεια του χαλκού για τα SAs στην αναλυτική χημεία. Λόγω της μεγάλης εκλεκτικότητας, η μέθοδος που αναπτύχθηκε αποτελεί τόσο ένα βήμα εκχύλισης, όσο και ένα βήμα καθαρισμού για τον ποσοτικό προσδιορισμό των SAs. Η αναλυτική μέθοδος έχει ευρεία γραμμική περιοχή (η οποία περιλαμβάνει συγκεντρώσεις μεγαλύτερες και μικρότερες από το ανώτατο επιτρεπτό όριο που έχει θεσπιστεί για τα SAs), χαμηλά όρια ποσοτικοποίησης (0,025–0,057  $\mu\text{g L}^{-1}$  για δείγματα νερού λίμνης και 0,23–1,05  $\mu\text{g L}^{-1}$  για δείγματα γάλακτος), ιδιαίτερα ικανοποιητικές ανακτήσεις και καλή αναπαραγωγιμότητα. Η μέθοδος επικυρώθηκε σύμφωνα με την απόφαση Commission Decision 657/2002/EC.

Η τρίτη μέθοδος αποτελεί μια βελτιωμένη παραλλαγή της μικροεκχύλισης διασποράς υγρού-υγρού με χρήση μαγνητικών ιοντικών υγρών. Η διαδικασία συνδυάζει ένα αδιάλυτο στο νερό υποστηρικτικό υλικό και το ιοντικό υγρό  $[\text{P}_{66614}^+][\text{Dy(III)}(\text{hfacac})_4^-]$  και μέσω της μεταβολής pH στο ίδιο δείγμα επιτρέπει την ταυτόχρονη μικροεκχύλιση των SAs και των τριαζινών. Το στερεό υπόστρωμα αναμιγνύεται με το μαγνητικό ιοντικό υγρό προκειμένου να ξεπεραστούν οι δυσκολίες που αντιμετωπίζονται κατά τη ζύγιση

του μαγνητικού ιοντικού υγρού και για να καταστεί πιο ομοιόμορφη η διασπορά του, καθιστώντας την προτεινόμενη μέθοδο πιο επαναλήψιμη. Η μεταβολή του pH του δείγματος κατά το στάδιο της εκχύλισης επιτρέπει την εκχύλιση των SAs και των τριαζινών από το ίδιο δείγμα μέσα σε 15 λεπτά. Η νέα αυτή αναλυτική μέθοδος είναι ευαίσθητη (όρια ποσοτικοποίησης: 0,034-0,091  $\mu\text{g L}^{-1}$ ) και επαναλήψιμη (σχετική τυπική απόκλιση: 5,2-8,1%), ενώ επιτυγχάνει καλές ανακτήσεις (89-101%) για δείγματα νερού λίμνης και βιολογικού καθαρισμού.

Τέλος, αναπτύχθηκε μια αναλυτική μέθοδος βασισμένη σε φερρίτες ψευδαργύρου σε μια διαδικασία μικροεκχύλισης διασποράς μαγνητικής στερεάς φάσης, υποβοηθούμενη από υπερήχους. Παρόλο που είναι γνωστό ότι ο ψευδάργυρος εμφανίζει μεγάλη συγγένεια για τα SAs, δεν υπάρχουν μέθοδοι προκατεργασίας δείγματος που να βασίζονται σε αυτήν την ιδιότητα. Η σύνθεση των φερριτών του ψευδαργύρου γίνεται απευθείας και το προκύπτον υλικό εμφανίζει αξιόλογες μαγνητικές ιδιότητες, οι οποίες επιτρέπουν τη συλλογή τους μετά την εκχύλιση. Οι φερρίτες ψευδαργύρου μπορούν να εκχυλίσουν αποδοτικά και εκλεκτικά τα SAs από δείγματα νερού λίμνης και αυγών. Η νέα διαδικασία επιτυγχάνει χαμηλά όρια ποσοτικοποίησης (0,06 μέχρι 0,11  $\mu\text{g L}^{-1}$ ), αποδεκτές ανακτήσεις (88-101%), ικανοποιητικούς συντελεστές προσυγκέντρωσης (111-141), ενώ επηρεάζεται ελάχιστα από το υπόστρωμα (από -8% έως 8%). Επιπλέον, η μέθοδος έχει μεγάλη γραμμική περιοχή (μέχρι τα 250  $\mu\text{g L}^{-1}$ ) γεγονός που επιτρέπει τον προσδιορισμό των SAs σε μεγαλύτερες και μικρότερες συγκεντρώσεις από το ανώτατο επιτρεπτό όριο. Λόγω των προαναφερθέντων πλεονεκτημάτων, της απλότητας, ευκολίας σύνθεσης του προσροφητικού και την αποδοτικότητα της όλης διαδικασίας, η μέθοδος που αναπτύχθηκε μπορεί να χρησιμοποιηθεί σε αναλύσεις ρουτίνας για τα σουλφοναμίδια.



## ABBREVIATIONS

SAs: Sulfonamides

SA: Sulfacetamide

STZ: Sulfathiazole

SD: Sulfadiazine

SP: Sulfapyridine

SM: Sulfamerazine

SMZ: Sulfamethazine

SMP: Sulfamethoxypyridazine

SCP: Sulfachloropyridazine

SMX: Sulfamethoxazole

SDM: Sulfadimethoxine

SIX: Sulfisoxazole

SQX: Sulfaquinoxaline

SAA: Sulfanilamide

SCIZ: Sulfaclozine

SCR: Sulfachloro-pyrazine

SDO: Sulfadoxine

SDMD: Sulfadimidine

SFM: Sulfameter

SIA: Sulfisoxazole

SMD: Sulfamethoxydiazine

SML: Sulfamethizole

SMD: Sulfamethoxydiazine

SMM: Sulfamonomethoxine

ACN: Acetonitrile

DDW: Double distilled water

GO: Graphene oxide

G: Graphene

GMeS: Graphene functionalized melamine sponges

MeS: Melamine sponges

SPE: Solid phase extraction

LC-ESI-MS/MS: Liquid Chromatography-Electrospray Ionization-Tandem Mass Spectrometric

HPLC: High-performance liquid chromatography

QuEChERS: Quick Easy Cheap Effective Rugged Safe

PSA: Primary secondary amine

DAD: Diode array detector

RSD: Relative standard deviation

EF: Enrichment Factor

## LIST OF FIGURES

Figure 1: General structure of sulfonamides.....	28
Figure 2: Mechanism of action of sulfonamide antibiotics.....	36
Figure 3: SEM images of MeS before (A) and after (B) functionalization with graphene (GMeS)...	83
Figure 4: SEM images of MeS in various magnifications (scale bars: 100 $\mu\text{m}$ (A), 50 $\mu\text{m}$ (B), 20 $\mu\text{m}$ (C), 20 $\mu\text{m}$ (D) and 10 $\mu\text{m}$ (E)).....	84
Figure 5: SEM images of GMeS in various magnifications (scale bars: 100 $\mu\text{m}$ (A), 100 $\mu\text{m}$ (B), 50 $\mu\text{m}$ (C), 20 $\mu\text{m}$ (D), 20 $\mu\text{m}$ (E) 10 $\mu\text{m}$ (F) 5 $\mu\text{m}$ (G) and 5 $\mu\text{m}$ (H)).....	85
Figure 6: XRD spectrum of graphite. ....	86
Figure 7: XRD spectrum of graphene oxide.....	86
Figure 8: XRD spectrum of GMeS.....	87
Figure 9: Images of (A) water droplet on the surface of a GMeS, (B) contact angle of a water droplet, (C) MeS and GMeS in a glass beaker with water, (D) GMeS immersed in water and (E) GMeS on top of a dandelion flower. ....	88
Figure 10: % Extraction yield of GMeS cubes, prepared using various concentrations of GO. ....	89
Figure 11: % Extraction yield of GMeS cubes, prepared using various amounts of hydrazine.....	90
Figure 12: % Extraction yield of GMeS cubes, prepared using various intensities of microwave. ..	91
Figure 13: % Extraction yield of GMeS cubes, prepared by microwaving for various times. ....	92
Figure 14: Effect of the pH on the adsorption efficiency of the SAs on GMeS. ....	94
Figure 15: Adsorption efficiency of the proposed method in solutions containing different concentrations of NaCl.....	96
Figure 16: Adsorption efficiency of the proposed method in solutions containing different concentrations of $\text{Na}_2\text{SO}_4$ . ....	96
Figure 17: Effect of sample volume, amount of adsorbent and extraction time on the efficiency of the method.....	98
Figure 18: Chromatograms of a blank milk sample (lower purple line) and a spiked milk sample, at 270 nm. Peak assignment: sulfacetamide (SA), sulfadiazine (SD), sulfapyridine (SP), sulfamerazine (SM), sulfamethazine (SMZ), sulfamethoxypyridazine (SMP), sulfachloropyridazine (SCP), sulfamethoxazole (SMX), sulfadimethoxine (SDM).....	100
Figure 19: Chromatograms (270 nm) of a blank egg sample (lower purple line) and an egg sample spiked with 50 $\mu\text{g kg}^{-1}$ of SAs (upper black line). ....	100
Figure 20: Chromatograms (270 nm) of a blank lake water sample (lower purple line) and a lake water sample spiked with 50 $\mu\text{g L}^{-1}$ of SAs (upper black line). ....	101

Figure 21: XRD pattern of CuMeS. ....	120
Figure 22: SEM images of MeS (A–D) and CuMeS (E–H) in various magnifications (scale bars: 500 $\mu\text{m}$ (A, E), 100 $\mu\text{m}$ (B, F), 50 $\mu\text{m}$ (C, G) and 20 $\mu\text{m}$ (D, H)).....	121
Figure 23: Copper mirror formed on the surface of the reaction glass beaker during decoration of MeS (A). The produced CuMeS (B) and its behavior in water (C, D).....	121
Figure 24: Effect of copper acetate concentration on the adsorption efficiency of the resulting CuMeS for a mixture of 10 SAs ( $150 \mu\text{g mL}^{-1}$ each) (number of replicate analysis=3).....	124
Figure 25: Effect of hydrazine concentration on the adsorption efficiency of the resulting CuMeS for a mixture of 10 SAs ( $150 \mu\text{g mL}^{-1}$ each) (number of replicate analysis=3).....	126
Figure 26: Effect of the pH on the adsorption efficiency of CuMeS for a mixture of 10 SAs ( $150 \mu\text{g mL}^{-1}$ each) (number of replicate analysis=3).....	129
Figure 27: Effect of the ionic strength of the sample on the adsorption efficiency of the method for a mixture of 10 SAs ( $150 \mu\text{g mL}^{-1}$ each) (number of replicate analysis=3).....	132
Figure 28: Effect of sample volume, amount of adsorbent and extraction time on the efficiency of the method (number of replicate analysis = 3).....	133
Figure 29: Chromatograms (at 270 nm) of a blank lake water sample (lower purple line) and a lake water sample spiked with $50 \mu\text{g L}^{-1}$ of SAs (upper black line). ....	136
Figure 30: Chromatograms (at 270 nm) of a blank milk sample (lower purple line) and a milk sample spiked with $50 \mu\text{g L}^{-1}$ of SAs (upper black line).....	139
Figure 31: Effect of sample pH on the extraction of a mixture of SAs and TZs, containing $100 \mu\text{g L}^{-1}$ of each (number of replicate analysis = 3). ....	160
Figure 32: Addition of different salts to increase the ionic strength of the solution and the respective extraction efficiency for a mixture of SAs and TZs, containing $100 \mu\text{g L}^{-1}$ of each (number of replicate analysis = 3). ....	162
Figure 33: Effect of sample volume and amount of extracting phase on the efficiency of the method (number of replicate analysis = 3). ....	164
Figure 34: Chromatograms of the extract (obtained with the proposed procedure) of an effluent from municipal treatment plant, spiked with $50 \mu\text{g L}^{-1}$ SAs and TZs (two upper) and non-spiked (two lower), at two different wavelengths. Peak assignment: 1. sulfadiazine, 2. sulfapyridine, 3. sulfamerazine, 4. sulfamethazine, 5. sulfamethoxypridazine, 6. sulfachloropyridazine, 7. sulfamethoxazole, 8. sulfisoxazole, 9. sulfadimethoxine, 10. terbuthryn, 11. atrazine, 12. propazine, 13. Terbuthylazine.....	166
Figure 35: Effect of using different zinc salts during the synthesis of zinc ferrites on their adsorption efficiency for SAs (number of replicate analysis = 3).....	182



Figure 36: Effect of different zinc: iron molar ratios during the synthesis of zinc ferrites on their adsorption efficiency for SAs (number of replicate analysis = 3).....	183
Figure 37: XRD pattern of the synthesized zinc ferrites.....	184
Figure 38: Magnetization curves of the synthesized zinc ferrite. ....	185
Figure 39: Nitrogen adsorption-desorption isotherms for the synthesized zinc ferrite. ....	185
Figure 40: Effect of the pH on the adsorption efficiency of SAs on zinc ferrites (number of replicate analysis = 3). ....	187
Figure 41: Effect of increasing ionic strength on the adsorption efficiency of SAs from zinc ferrites (number of replicate analysis = 3). ....	188
Figure 42: Effect of different sample volume, sorbent mass and extraction time on the adsorption efficiency of SAs from zinc ferrites (number of replicate analysis = 3). ....	189
Figure 43: Chromatogram of the extract obtained with the developed procedure from egg sample spiked with 3.75 $\mu\text{g mL}^{-1}$ of each sulfonamide; 1: sulfacetamide; 2: sulfadiazine; 3: sulfapyridine; 4: sulfamerazine; 5: sulfathiazole; 6: sulfamethazine; 7: sulfamethoxypyridazine; 8: sulfachlorpyridazine; 9: sulfamethoxazole; 10: sulfisoxazole; 11: sulfadimethoxine; 12: sulfaquinoxaline .....	194



## LIST OF TABLES

Table 1: Chemical structures and physicochemical characteristics of SAs .....	29
Table 2: Analytical methods developed for the determination of SAs in milk .....	45
Table 3: Analytical methods developed for the determination of SAs in eggs .....	50
Table 4: Analytical methods developed for the determination of SAs in water .....	52
Table 5: Analytical methods developed for the determination of SAs in pork and chicken meat ..	55
Table 6: Analytical methods developed for the determination of SAs in honey .....	59
Table 7: Analytical methods developed for the determination of SAs in fish.....	61
Table 8: Analytical methods developed for the determination of SAs in animal feeds.....	62
Table 9: Analytical characteristics of the proposed method for SAs determination in milk; LOQ: limit of quantification, RSD: relative standard deviation, enrichment factor (ratio of the peak area after the extraction and a standard), matrix effect (calculated by the areas of spiked extraction solution and spiked matrix samples).....	102
Table 10: Analytical characteristics of the proposed method for SAs determination in eggs; LOQ: limit of quantification, RSD: relative standard deviation, enrichment factor (ratio of the peak area after the extraction and a standard), matrix effect (calculated by the areas of spiked extraction solution and spiked matrix samples).....	103
Table 11: Analytical characteristics of the proposed method for SAs determination in lake water; LOQ: limit of quantification, RSD: relative standard deviation, enrichment factor (ratio of the peak area after the extraction and a standard), matrix effect (calculated by the areas of spiked extraction solution and spiked matrix samples) .....	104
Table 12: Summary of the analytical characteristics of the developed method for each matrix; LOQ: limit of quantification, RSD: relative standard deviation, enrichment factor (ratio of the peak area after the extraction and a standard), matrix effect (calculated by the areas of spiked extraction solution and spiked matrix samples) .....	105
Table 13: Comparison of the developed procedure with other analytical methods.....	108
Table 14: Analytical characteristics of the proposed method for SAs determination in lake water .....	137
Table 15: Analytical characteristics of the proposed method for SAs determination in milk samples .....	138
Table 16: Relative standard deviations of lake water samples spiked with three different concentrations of SAs.....	140

Table 17: Relative standard deviations of milk samples spiked with three different concentrations of SAs.....	141
Table 18: Comparison with other analytical methods .....	143
Table 19: Analytical figures of merit of the developed MIL-based microextraction procedure....	167
Table 20: Enrichment factors (EF), Extraction percentages (E%), Relative standard deviations (RSD) and Relative recoveries of the developed MIL-based microextraction procedure .....	168
Table 21: Comparison of the developed procedure with other analytical methods.....	169
Table 22: Analytical figures of merit of the developed ultrasound-assisted dispersive micro solid-phase procedure for SAs detection in egg and lake water samples .....	192
Table 23: Relative standard deviations and relative recoveries of SAs from egg and lake water samples with the developed ultrasound-assisted dispersive micro solid-phase procedure .....	193

# CHAPTER 1: Introduction

## 1.1 Sulfonamides

### 1.1.1 Historical background

Human beings have always been concerned about the well-being since the beginning of recorded history. However, human is faced with numerous abnormal conditions that negatively affect health and cause diseases. Among various diseases, infectious diseases had always been, and still remain the leading cause of deaths, worldwide [1,2]. From the various microorganisms that cause infectious diseases, bacteria have caused tremendous havoc in human history. Representative examples are the Plague of Athens (429-426 BC), the Plague of Justinian (541-542) and Black Death (1331-1352) [1–3]. To treat bacterial diseases, various remedies has been used, until the late 19th century, when scientists began to study various chemical compounds for their antibacterial properties and antibiotics were discovered. Although the first antibiotic (penicillin) was discovered by Alexander Fleming in 1928, it was not until 1932 that the first antibiotic became commercially available under the brand-name Prontosil [4,5]. The generic name of Prontosil is p-sulfamidocrisoidine and was discovered by the German pathologist Gerhardt Domagk. He found that mice suffering from streptococcal septicemia were cured, upon treatment with Prontosil. Later on, it was found that the antibacterial activity was not achieved by prontosil itself, but by sulfanilamide which is produced by the *in vivo* degradation of prontosil. Following his publication “*A Contribution to Chemotherapy of Bacterial Infections*”, Domagk paved the way for the development of various sulfa drugs, which revolutionized medicine [5,6].

Sulfa drugs or sulfonamides (SAs) are a broad-spectrum class of antibacterial compounds that are active against both gram-negative and gram-positive bacteria, as well as against some protozoa [7,8]. Sulfonamides contain a sulfonamide group ( $R-S(=O)_2-NR_2$ ) connected to a benzene ring that contains an amino group in the para position (Figure 1).

Numerous SAs have been synthesized by using various substitution groups at N<sub>1</sub> and a few more by substituting a hydrogen atom from N<sub>4</sub> for another group [9]. Owing to their big success as antibiotics, in a very short time, a lot of SAs have been synthesized. Sulfonamides are synthesized by many approaches, with the most common being the reaction of sulfonyl chlorides with amines, as depicted in the chemical equation (1).

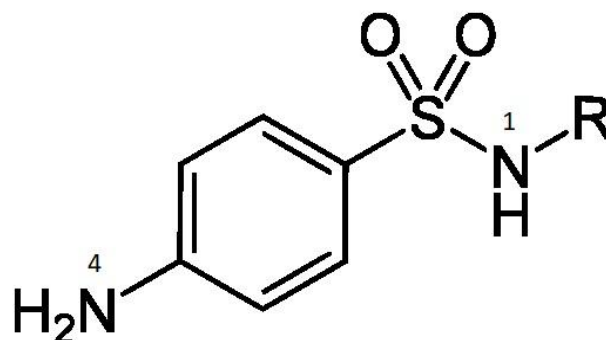


Figure 1: General structure of sulfonamides.

Today, the number of existing SAs is estimated to be greater than 5000, although only 33 are used for medicinal purposes [5,10]. The presence of different substitution groups results in SAs with different pharmacokinetic and physicochemical properties. Although SAs are hardly soluble in water, their amphoteric properties can help tune their solubility [11]. At pH between 2 and 3, the basic aromatic amino group (N<sub>4</sub>) is protonated and at pH between 5-8, the amide nitrogen (N<sub>1</sub>) is deprotonated. Thus, at acidic environment (pH<2) SAs are positively charged and negatively charged at less acidic one (pH>5). The above are the reasons that SAs are classified into: (I) absorbable oral SAs, (II) non-absorbable SAs and (III) topical SAs [9]. The structures of SAs used in this thesis, along with some physicochemical characteristics are presented in Table 1.

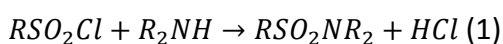
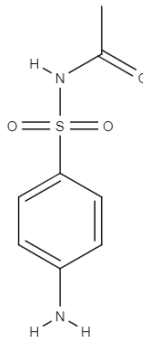
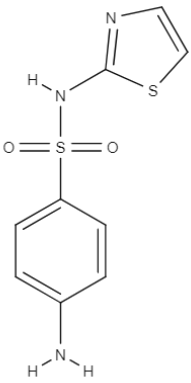
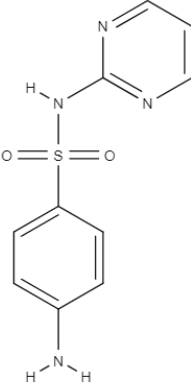
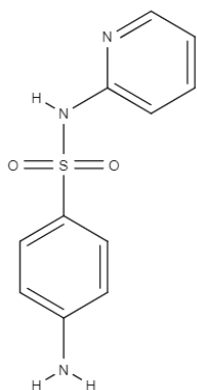


Table 1: Chemical structures and physicochemical characteristics of SAs

Sulfonamide	Chemical structure	$pK_a$	$\log K_{ow}$
Sulfacetamide (SA)		2.14 4.3	-0.96
Sulfathiazole (STZ)		2.14 7.2	0.05
Sulfadiazine (SD)		2.01 6.36	-0.12

---

Sulfapyridine  
(SP)



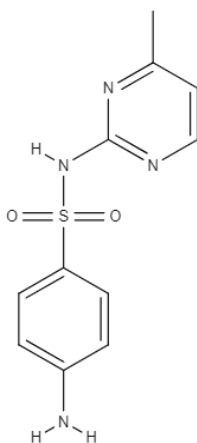
2.63

6.24

0.35

---

Sulfamerazine  
(SM)



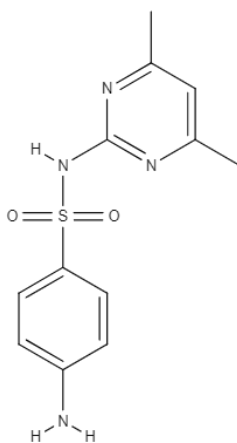
2.01

6.99

0.14

---

Sulfamethazine  
(SMZ)

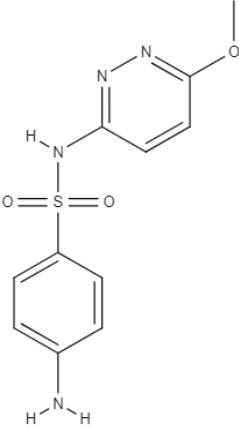
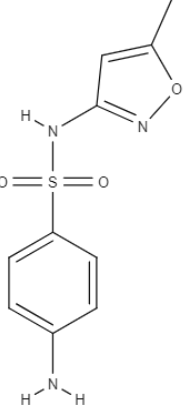
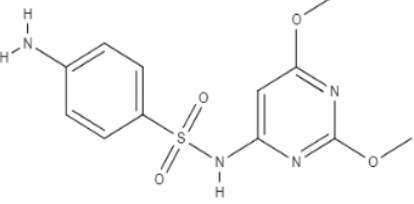


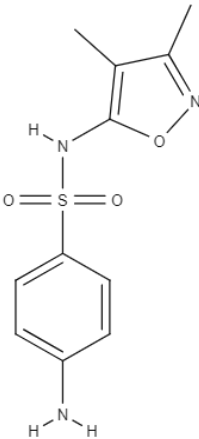
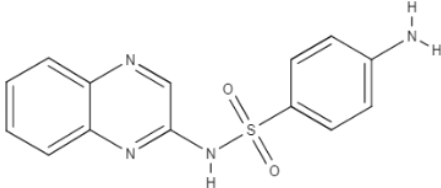
2.65

7.6

0.14



Sulfamethoxypyridazine (SMP)		2.02 6.84	0.32
Sulfachloropyridazine (SCP)		1.8 5.9	1.02
Sulfamethoxazole (SMX)		1.6 5.7	0.89
Sulfadimethoxine (SDM)		1.95 6.21	1.56

Sulfisoxazole (SIX)		1.5 5.0	1.01
Sulfaquinoxaline (SQX)		2.13 6.79	1.68

### 1.1.2 Mechanism of action

In order for bacteria to replicate, DNA replication must be carried out. To do so, purine and pyrimidine bases are needed. Bacteria synthesize these bases using tetrahydrofolic acid, which is produced by dihydrofolic acid in the presence of dihydrofolate reductase. Dihydrofolic acid is produced by the reaction of dihydropteroic acid with glutamic acid. Dihydropteroic acid is produced by the reaction of *p*-aminobenzoic acid and pteridine in the presence of dihydropteroate synthase. The antibacterial activity of SAs is owing to their competitive inhibitory properties for the dihydropteroate synthase and thus, inhibiting the aforementioned synthetic pathways, depriving bacteria of tetrahydrofolic acid, which is essential for cellular replication (Figure 2) [11]. Due to this mechanism of action, SAs can be effectively used as bactericidal agents against a broad spectrum of bacteria, including both Gram-positive and Gram-negative species, such as *Streptococcus*, *Salmonella*, *Staphylococcus*, *Escherichia*, etc. while no activity is presented in humans, since dihydrofolic acid can be obtained directly from food, resulting in the undisrupted

synthesis of tetrahydrofolic acid [12]. According to their duration of activity, SAs are classified into: (I) short-acting (3-8 h), (II) intermediate-acting (8-18 h) and long-acting (>35 h) [9]. SAs have been used, so far, to treat numerous diseases, such as urinary tract infections, conjunctivitis, toxoplasmosis, meningitis, rheumatic fever, etc. In addition, each SA exhibits also a unique activity that potentiates its use for other diseases [13]. As a result of more than 50 years of therapeutic use, bacterial resistance to SAs is widespread, with approximately 40% of *Escherichia coli* species, to be nowadays, resistant. Although this has limited their effectiveness, the combination of SAs with other medications has extended their application range and further increased their use.

#### **1.1.2.1 Sulfacetamide (SA)**

Sulfacetamide is used for the treatment of bacterial vaginitis, keratitis, acute conjunctivitis, and blepharitis. As cream is used to treat skin infections and as eye drops to treat eye infections. On the skin, it is used to treat acne and seborrheic dermatitis. Its sodium salt has been used for many years to treat erythema and inflammatory lesions of rosacea. Also, it is combined with sulfur in lotions, creams, foams, etc. for the treatment of acne rosacea (rosacea with papules, pustules, or both). The side effects of its usage include transient ophthalmic burning, drug-induced lupus erythematosus, superinfections, severe allergic reactions (tightness in the chest, swelling in the face, mouth, lips, and tongue). More importantly, life-threatening conditions may appear, such as Stevens-Johnson syndrome, erythema multiforme, toxic epidermal necrolysis and can also cause nephrotoxicity [14].

#### **1.1.2.2 Sulfadiazine (SD)**

Sulfadiazine is a short-acting SA, rapidly absorbed from the gastrointestinal tract. It exhibits the strongest antimicrobial activity, among all SAs. It is used as a first-line antibiotic for *Mycobacterium smegmatis*, *Nocardia asteroides* & *brasiliensis* (causing nocardiosis) and as a second-line treatment for bacterial otitis media caused by *Haemophilus influenzae*, recurrent rheumatic fever and wound sepsis. Sulfadiazine is

commonly administered along with pyrimethamine and folinic acid to treat toxoplasmosis. Although it belongs to the SAs groups that are commonly used to treat urinary tract infections, the use of sulfadiazine is avoided owing to its low solubility and nephrotoxicity [15]. Also, its use is avoided by people who have liver and/or kidney problems or porphyria. Its use exhibits some side effects including diarrhea, headache, reversible oligospermia, nausea, allergic reactions, rash, hypersensitivity, thrombocytopenia, thyroid function disturbance and crystalluria [16].

#### ***1.1.2.3 Sulfapyridine (SP)***

Sulfapyridine is one of the first discovered SAs. However, sulfapyridine does not work for any kind of infection as other SAs do. Sulfapyridine may cause some serious side effects, which prevented its prescription for treat human infections, except for the treatment of linear IgA disease (a rare immune-mediated skin blistering disease) and dermatitis herpetiformis (Duhring's disease). Its use is avoided since it can cause blood problems, leading to certain infections, slow healing, bleeding of the gums and hematuria. Other side effects include aching of joints and muscles, redness, blistering, peeling, or loosening of the skin, lower back pain, pain or burning while urinating, swelling of the front part of neck and sensitivity to sunlight [14,16].

#### ***1.1.2.4 Sulfathiazole (STZ)***

Sulfathiazole is commonly used in aquaculture and is typically found in aquatic ecosystems. It exists in various forms, out of which the imine tautomer is dominant. In this tautomer, the proton resides on the ring nitrogen. Sulfathiazole is extensively used in aquaculture, livestock production and human medicine to treat bacterial, protozoal and fungal infections. It is used either alone or in combination with other SAs for the disinfection of aquariums. Sulfathiazole is commonly used in cattle to treat bovine respiratory disease complex (shipping fever complex), calf diphtheria, necrotic pododermatitis (foot rot) and acute metritis. It is administered to pigs for the treatment of bacterial pneumonia and porcine colibacillosis (bacterial scours). It is commonly

combined with chlortetracycline and penicillin to improve feed efficiency and promote weight gain, as well as reduce the incidence of cervical abscesses and treat bacterial swine enteritis (salmonellosis or necrotic enteritis and vibronic dysentery [14,17].

#### ***1.1.2.5 Sulfamerazine (SM)***

Sulfamerazine is one of the four approved antibiotics in the USA and one of the 30 approved ones in Japan, for use in aquaculture. It has been used in aquaculture since 1948 and contributed significantly to the commercial success of many aquaculture hatcheries [18]. It is administered to humans to treat bronchitis, prostatitis and urinary tract infections. However, it can cause nausea, vomiting, diarrhea, hypersensitivity reactions and displace bilirubin from albumin binding sites causing jaundice or kernicterus in newborns. Hematologic effects such as anemia, agranulocytosis, thrombocytopenia and hemolytic anemia may also occur [19].

#### ***1.1.2.6 Sulfamethazine (SMZ)***

Sulfamethazine is used to treat or prevent infections, such as pneumonia, intestinal infections (especially coccidia), soft tissue infections and urinary tract infections. Also, it is widely used in veterinary medicine in combination with chlortetracycline and penicillin in pigs for maintenance of weight gain in the presence of atrophic rhinitis, growth promotion and increased feed efficiency. Sulfamethazine is also effective against a wide variety of diseases in food-producing animals. Common therapeutic uses in other animals include treatment of bovine respiratory disease complex, control of coccidiosis, treatment of necrotic pododermatitis, calf diphtheria, colibacillosis, bacterial pneumonia, bacterial swine enteritis, acute fowl cholera, pullorum disease, and acute mastitis. Sulfamethazine may cause nausea, vomiting, diarrhea and hypersensitivity reactions. Hematologic effects such as anemia, agranulocytosis, thrombocytopenia and hemolytic anemia in patients with glucose-6-phosphate dehydrogenase deficiency may also occur. Sulfamethoxazole may displace bilirubin from albumin binding sites causing jaundice or kernicterus in newborns [20].

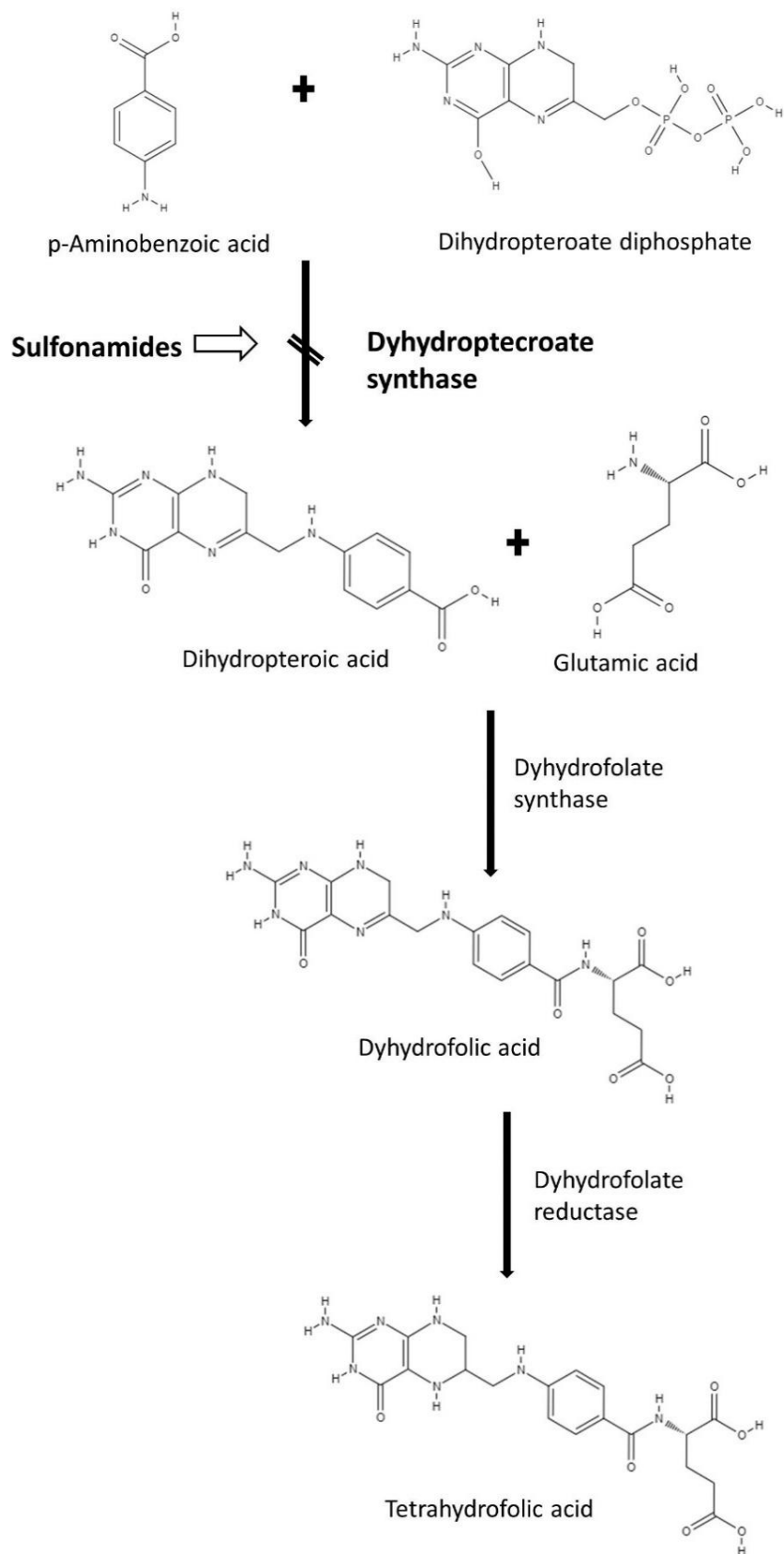


Figure 2: Mechanism of action of sulfonamide antibiotics.

#### ***1.1.2.7 Sulfamethoxyipyridazine (SMP)***

Sulfamethoxyipyridazine is used in the treatment of Dermatitis herpetiformis while it serves as an alternative therapy to Dapsone for ulcerative colitis. Its activity is exhibited in the bower area, where it reduces the inflammation and other symptoms of the disease. In addition, sulfamethoxyipyridazine enteric-coated tablets are used to treat adults and children with rheumatoid arthritis, in patients who have not been helped by or who cannot tolerate other medicines for rheumatoid arthritis. Its use may cause many side effects such as sudden weakness or ill feeling, fever, chills, cold or flu symptoms, sore throat, cough, trouble breathing, painful mouth sores, red or swollen gums, rapid heart rate, rapid and shallow breathing, cough with yellow or green mucus, wheezing, pain when swallowing, fainting, skin sores, pale skin, easy bruising, stabbing chest pain, unusual bleeding or jaundice [14,16].

#### ***1.1.2.8 Sulfachloropyridazine (SCP)***

Sulfachloropyridazine has been used to treat acute urinary tract infections in pediatric patients and for the treatment, control, prevention, and improvement of conditions and symptoms of microbial infections in animals, urinary tract bacterial infections and respiratory tract bacterial infections. It is widely used in poultry farming and less often in cattle and swine. Possible side-effects that may occur are hypersensitivity, anemia, nausea, skin rashes, sore throats or mouth ulcers, headache thrush, diarrhea, vomiting and high levels of potassium in the blood [21].

#### ***1.1.2.9 Sulfamethoxazole (SMX)***

Sulfamethoxazole is used for bacterial infections, such as urinary tract infections, bronchitis, and prostatitis. Also, it is commonly used in combination with trimethoprim to treat ear infections, urinary tract infections, bronchitis, traveler's diarrhea, shigellosis, and *Pneumocystis jiroveci* pneumonia. Its use may cause severe stomach pain, skin rash, bloody diarrhea (even months later than the last dose), yellowing of skin or eyes, seizure, new or unusual joint pain, bruising, swelling, increased thirst, dry mouth, fruity breath odor, an electrolyte imbalance, and low blood cell counts [14].

#### 1.1.2.10 Sulfadimethoxine (SDM)

Sulfadimethoxine is a long-lasting sulfonamide antimicrobial medication used in veterinary medicine. It is used to treat many infections, including respiratory, urinary tract, enteric, and soft tissue infection and can be given as a standalone or combined with ormetoprim to broaden the target range. Its use treats skin and soft-tissue infections in dogs caused by *Staphylococcus aureus* or *E. coli* and bovine respiratory disease complex, necrotic pododermatitis (foot rot), pneumonia when caused by *Pasteurella*, and calf diphtheria caused by *Fusobacterium necrophorum*. It protects poultry from fowl cholera and coccidiosis by *Eimeria* and treat salmon and trout for furunculosis. Common side effects in dogs include vomiting, fever, keratoconjunctivitis sicca, decreased appetite, acute liver inflammation characterized by yellowing of the skin, crystal or stone formation in the urinary tract, urticaria (hives), polyarthritis, facial swelling and eyes, and diarrhea. Less common side effects include allergic reactions including anaphylaxis and immune reactions, anemia (low red blood cells) and low white blood cells [14,16].

#### 1.1.2.11 Sulfisoxazole (SIX)

Sulfisoxazole is sometimes administered in combination with erythromycin or phenazopyridine. It is used for the treatment of acute, recurrent or chronic urinary tract infections, meningococcal meningitis, acute otitis media, nocardiosis, chancroid, toxoplasmosis, trachoma, inclusion conjunctivitis, malaria and other bacterial infections caused by *Escherichia coli*, *Klebsiella-Enterobacter*, and staphylococcus. Its use may cause hypersensitivity, anaphylaxis, erythema multiforme, toxic epidermal necrolysis, angioedema, arteritis and vasculitis, serum sickness, conjunctival and scleral injection, generalized allergic reactions, and allergic myocarditis, dermatologic (exfoliative dermatitis, rash, pruritus, photosensitivity, periarteritis nodosa, systemic lupus erythematosus, and generalized skin eruptions), hematologic (agranulocytosis, leukopenia, thrombocytopenia, aplastic anemia, purpura, hemolytic anemia, eosinophilia, clotting disorders including hypoprothrombinemia, hypofibrinogenemia, sulfhemoglobinemia, and methemoglobinemia), cardiovascular (tachycardia, palpitations, syncope, cyanosis, angioedema, arteritis, and vasculitis, gastrointestinal (pseudomembranous colitis, nausea,



emesis, anorexia, abdominal pain, diarrhea, gastrointestinal hemorrhage, melena, flatulence, glossitis, stomatitis, enlarged salivary gland, and pancreatitis), hepatic (hepatitis, hepatocellular necrosis, and jaundice), renal (acute renal failure, nephritis, and nephrosis with oliguria and anuria), genitourinary (crystalluria, hematuria, and urinary retention) and nervous system side effects (headache, dizziness, peripheral neuritis, paresthesia, convulsions, drowsiness, hearing loss, insomnia, tinnitus, vertigo, ataxia, and intracranial hypertension). Due to its many side effects, its use is significantly limited [14].

#### **1.1.2.12 Sulfaquinoxaline (SQX)**

Sulfaquinoxaline is a veterinary medicine that can be given to cattle and sheep to treat coccidiosis. Although its antibacterial potential is low, it has high anticoccidial potential and is known to have anti-leucocytozoon potential. It is used for the treatment, control and/or prevention of fowl typhoid, fowl cholera, infectious enteritis, malaria infections, and parasitic disease. Prolonged administration of sulfaquinoxaline may result in the deposition of crystals in the kidney or interference with normal blood clotting. Also, its use may cause some side effects such as anorexia, nausea, urge to vomit, diarrhea, tiredness, abnormal, skin pigmentation and abnormal bruising [14].

#### **1.1.3 Usage of SAs and associated risks**

The wide applicability of SAs along with their low cost and high efficiency skyrocketed their use in veterinary medicine to such a degree that even today, almost 100 years after their discovery, they are the second most employed class of antibiotics, after tetracyclines, in Europe [22][7,23]. Moreover, it is noteworthy that SAs are used aside from their antibacterial activity, as feed additives for livestock animals in order to promote their growth and productivity, although it is forbidden in many countries and in Europe (since 2006) [7]. Every year in Europe, around 900 tons of SAs are sold to be consumed by food-producing animals. In Denmark, in 2009, for every kg of meat produced the consumption of SAs was 4.82 mg for pork, 17.2 mg for cattle, 0.033 mg for poultry and 58.5 mg for fish [24]. The extensive use of SAs inevitably results in two major

problems. The first one is the introduction of SAs into the biosphere. It is estimated that each year, more than 20,000 tons of SAs are introduced into the biosphere [11]. Discharges from pharmaceutical companies and farms, burden surface and ground waters with SAs. Another major source of SAs for the environment is human and animal food-chain waste. The concentration of SAs in environmental samples increases in the following order: seawater < groundwater < surface water < treated wastewater < untreated municipal wastewater < hospital wastewater < activated sludge < soil < agricultural runoff < landfill leakage < manure.

The discharge of SAs in the environment has a great impact on the ecosystems, since bacteria, that develop resistance to antibiotics prevail, posing a future threat to animals and humans [22][11][25]. The second major problem arises from the uncontrolled use of SAs in veterinary practices, which combined with misconduct of animal prophylaxis and treatment or non-compliance with regulation regarding the time before slaughter results in the presence of SAs residues in animal-derived food products, such as milk and dairy products, eggs, meat, etc. [26–29]. One way or another, humans are systematically exposed to SAs which raises numerous health-related issues. Allergic reactions, leukocyte production inhibition alteration of the intestinal microflora and promotion of sustainable forms of pathogens classify SAs as harmful for human health, while based on different risk assessment criteria, the SAs are classified as highly toxic and carcinogenic [11,30] [22,25].

#### **1.1.4 Overview of sample preparation procedures for sulfonamides detection**

The hazardous nature of SAs has led regulatory agencies to establish maximum residue limits to strictly regulate SAs residues in food products, in order to safeguard human health [7,26]. For instance, the maximum residue limit of SAs in the European Union is  $100 \mu\text{g L}^{-1}$  for milk (for each sulfonamide individually and for all SAs in the sample), while this is also the limit set in many other countries [7,31]. More information about Commission Decision 657/2002/EC are given in Appendix. Although many years have passed since concerns have arisen about antibiotic residues in the environment and

foodstuffs, monitoring their levels according to local and international environmental regulations still remains as important as ever [32,33]. It is noteworthy that cases of detected sulfonamides in food samples are more frequent (20%) than other classes of antibiotics (e.g. tetracyclines: 8%, oxazolidinones: 8%), as evidenced in an earlier report [7]. In order to ensure safety, reliable analytical methods are needed to detect SAs residues. As the complexity of food products and environmental samples is high and SAs are found in trace amounts, their detection poses a challenge [34]. The selection and optimization of the appropriate sample preparation procedure qualify as essential for the development of a successful method. Considering the drawbacks of existing methods and the importance of sample preparation, the development of new or alternative sample preparation procedures not only is more than welcome but may be a necessity.

Up to now, many analytical methods have been developed for SAs determination, employing different sample preparation procedures, such as solid-phase extraction, salting-out liquid-liquid extraction, fabric-phase sorptive extraction, etc. [7,32,35–38]. Each of them has its pros and cons as they are suitable for certain applications. The modern trend for 'greener' chemical analyses has led to the development of microscale extraction approaches towards minimizing the organic solvent consumption, while maximizing sample throughput and extraction efficiency of the analytes. Microextraction is an extraction technique where the volume of the extracting phase is very small in relation to the volume of the sample [39]. It is not necessarily an exhaustive extraction procedure, in contrast to the classical liquid-liquid extraction and solid-phase extraction, signifying that possibly only a fraction of the analyte may finally be subjected to analysis. Hence, it is not surprising that microextraction, in the modes of solid-phase microextraction, dispersive solid-phase microextraction, magnetic solid-phase extraction, pipette-tip solid-phase extraction, etc., has come to the forefront of analytical chemistry in the past few years. An overview of existing sample preparation methods for SAs determination in each food matrix is presented in the following sub-sections so that the recent trends can be seen.

#### *1.1.4.1 Sample preparation procedures for milk samples*

Milk is a nutritious wholesome food that is widely being consumed worldwide. Since it is a good source of protein and calcium it is commonly added in children's diet. Moreover, it is a necessary ingredient for many other foodstuffs commonly produced, such as sweets or other dairy products. In recent years, many sample preparation procedures have been developed for the detection of SAs in milk samples. Despite the sample preparation procedure, proteins of milk are discarded and usually fat is removed following a defatting process. One of the most common sample preparation procedures is liquid-liquid extraction. She et al. added acetonitrile to milk samples and after homogenization added anhydrous sodium sulfate [40]. After centrifugation, the upper phase was collected and after evaporation to dryness and reconstitution with a water and acetonitrile mixture, they defatted the new solution with acetonitrile saturated hexane. Then, they injected the lower phase into a UPLC-MS/MS system. Using this procedure, they could detect 24 SAs in milk samples with recoveries ranging between 60.5% and 116.6%, while the relative standard deviation was between 2.9% and 18.6%. In another study, the authors added a small quantity of acetic acid in milk and then added ethyl acetate to extract SAs [41]. After transferring the organic layer in another tube and evaporating to dryness, the residue was cleaned by using successively 6 mol L<sup>-1</sup> hydrochloric acid solution and petroleum ether. Then, 3.5 mol L<sup>-1</sup> sodium acetate solution was added along with ethyl acetate and after thorough mixing, the supernatant was transferred to another vial, dried and reconstituted with methanol and sodium acetate solution. This way, a method validated according to Brazilian Regulation 24/2009 for three sulfonamides resulted and recoveries were close to 100%. Similar procedures were followed by Tolika et al. and Unsal et al., who achieved recoveries in the range of 93.9-111.3% and 91%-114%, for 10 and 14 SAs respectively [42,43].

Dai et al. precipitated milk proteins by adding perchloric acid solution and then used an Oasis hydrophilic-lipophilic-balanced solid-phase extraction column to purify the upper layer before capillary zone electrophoresis [44]. The recoveries with this procedure (79.5-

112.4%) were less satisfactory, compared to previous methods, while the relative standard deviation was low (2.1-2.8%). Similar procedures were followed by Hou et al. [45] and Dmitrienko et al. [26]. In the first case, authors used OASIS MCX SPE cartridge to purify the deproteinated sample, while in the second study, authors used hypercrosslinked polystyrene as a sorbent in an SPE cartridge to purify the deproteinated and defatted milk sample. Following the two abovementioned methods, good recoveries are achieved while their reproducibility is relatively low.

Under the principle of dispersive solid-phase extraction, quite a few sample preparation procedures have been developed. An et al. synthesized a polyethylene glycol-molybdenum disulfide composite material which was used for the extraction of eight SAs [46]. The recoveries achieved were between 60.5% and 110.9% and the precision of the method was between 0.32% and 9.83%. Similarly, Jia et al. developed a metal-organic framework/graphite oxide material as a sorbent [47]. They selected MIL-101(Cr) owing to its large surface area, numerous unsaturated metal sites, high porosity, excellent chemical stability, and inexpensiveness and functionalized it with graphite oxide due to its plenty epoxy, carboxyl, and hydroxyl functional groups. This composite was used to develop a dispersive solid-phase extraction procedure for 12 SAs from milk samples and authors achieved recoveries in the range of 79.83-103.8% and relative standard deviation <10%.

Sorbents with magnetic properties have also been synthesized and used in magnetic solid-phase extraction procedures. Magnetic carbon nanotubes have been functionalized with thiol groups and a method was developed for the extraction of four SAs that has a wide linear range (0.1-500  $\mu\text{g L}^{-1}$ ) [48]. Fu et al. functionalized amino-terminated magnetic carbon nanotubes using isocyanates and found that among p-tolyl isocyanate and octadecyl isocyanate the first yielded a sorbent with better extractive properties for SAs [49]. Using the developed procedure, they extracted 13 SAs from milk samples and using HPLC-HRMS they achieved very low limits of detection (2-10  $\text{ng L}^{-1}$ ) and relative recoveries

between 0.9% and 6.9%. Other composites that have been developed include  $\text{CoFe}_2\text{O}_4$ -graphene [50], magnetite/silica/poly (methacrylic acid-co-ethyleneglycoldimethacrylate) composite microspheres [51] and magnetic hypercrosslinked polystyrene [52].

Finally, a few other sample preparation procedures have been developed, under various principles. For instance, Huang et al. coated polydimethylsiloxane magnetic stir bars with a monolithic material (vinyl imidazole-divinylbenzene) [53]. Using a UV detector, the authors achieved low limits of detection ( $1.3\text{-}7.90 \mu\text{g L}^{-1}$ ) and a wide linear range ( $10\text{-}1000 \mu\text{g L}^{-1}$ ). Yu et al. coated stir bars with C18-silica particles [54]. The new stirring bars were used in a stir bar sorptive extraction procedure with low limits of detection ( $0.04\text{-}0.97 \mu\text{g L}^{-1}$ ) and satisfactory recoveries (87-120%). Two pipette tip solid-phase extraction procedures have been developed using nanostructured polyaniline [55] and graphene [56]. These methods have the benefit of using small amounts of sorbent (7.4 mg nanostructured polyaniline and 3 mg graphene). In a similar study, Gao et al. developed a water-compatible poly (hydroxyethyl methacrylate) polymer and used it in a miniaturized syringe assisted extraction, instead of using a pipette tip [57]. Karageorgou et al. functionalized cellulose fabric with four sol-gel coatings (sol-gel poly(ethylene glycol), sol-gel poly(tetrahydrofuran), sol-gel C18 and sol-gel poly(ethylene glycol)-block-poly(propylene glycol)-block-poly(ethylene glycol) (sol-gel PEG-PPG-PEG)) [58]. Out of them all, cotton coated with poly (ethylene glycol) sol-gel yielded the optimum results, since it is suitable for polar analytes. Two other procedures have been developed using ionic liquids. The first one is an ionic liquid-based aqueous two-phase system extraction [59] and the second one is an ionic liquid-based microwave-assisted dispersive liquid-liquid microextraction [60]. These methods consume less organic solvent compared to liquid-liquid extraction and have fewer interferences from the sample matrix. A summary of analytical methods developed for SAs determination in milk is given in Table 2.

Table 2: Analytical methods developed for the determination of SAs in milk

Analytes	Method	Sorbent	Extraction time (min)	Linear range ( $\mu\text{g L}^{-1}$ )	LOD ( $\mu\text{g L}^{-1}$ )	RSD (%)	Recovery (%)	Reference
SMX, SD, SMZ, SDM, SM	Dispersive solid phase extraction and HPLC-UV	SMX imprinted acrylamide functionalized silica nanoparticles	45 (+ 10 min centrifugation)	50-20000	2.81-14.6	3.5-7.5	69.8-87.4	[61]
SD, STZ, SMZ, SMP, SCP, SMX, SIX, SDM, SQX	Magnetic dispersive solid phase extraction and HPLC-DAD	Magnetite-embedded with silica functionalized with phenyl chains	~20	30-800	7-14	<10	81.8-114.9	[62]
SM, SML, SDX, SMX, SIX	Dispersive solid phase extraction and HPLC-UV	CoFe <sub>2</sub> O <sub>4</sub> -graphene	22 (+ 5 min precondition)	20-50000	1.16-1.59	2.4-4.3	62.0-104.3	[50]
SD, SM, SMZ, SML, SMX, SDM	Stir bar sorptive extraction and HPLC-MS/MS	C <sub>18</sub> coated stir bar	10 (+10 min elution)	0.1-2000	0.9-10.5	7.3-16.7	87-120	[63]
SCP, STZ, SP, SMD, SM, SMZ, SMP, SDM, SML, SA SMM	Dispersive solid phase extraction and HPLC-MS	magnetite/silica/poly (methacrylic acid-co-ethylene glycol dimethacrylate)	15	0.05-20	0.0005-0.0495	<13	87.6-115.6	[51]
SP, SMZ, SMZ, SCP, SMP, SIX, SDM, SD, STZ, SM, SMD, SMX	Magnetic solid phase extraction	Functionalization of amino terminated carbon nanotubes with isocyanates	5	0.5-100	0.002-0.01	0.9-6.9	81.5-108.9	[49]

SD, SP, SMX	Pipette tip solid phase extraction coupled with HPLC	Nanostructured polyaniline	15	50-50000	9.5-16.5	2.5-11.1	92.4-104.9	[55]
SD, SMM, SMZ	Magnetic micro-solid phase extraction and HPLC-DAD	Thiol-functionalized magnetic carbon nanotubes	2	0.1-500	0.02-1.5	0.3-7.7	80.7-116.2	[48]
SD, SM, SMZ	Tube Solid-Phase Microextraction Coupled with Capillary Electrophoresis-Laser Induced Fluorescence	Graphene-embedded porous polymer monolithic column prepared	25	2.0-500	0.25-0.47	1.8-6.8	91.1-94.6	[32]
SMP, SMZ, SMX, SCP	Magnetic solid-phase extraction and HPLC	Magnetic hypercrosslinked polystyrene	40	10-400	2.0-2.5	3-10	84-105	[64]
SD, SP, SM, SMZ, SMZ, SMP, SMM, SCP, SDX, SMX, SQX, SDM	Micro-solid phase extraction coupling with UHPLC-MS/MS	MIL-101(Cr)@GO	20	100-50000	0.012-0.145	<10	79.8-103.8	[47]
SD, SM, SMZ, SMZ, SMX, SDM	Stir bar sorptive extraction and HPLC	C18-coated stir bar	10	0.1-2000	0.04-0.97	7.3-16.7	87-120	[54]



SM, SMZ, SDX, SMZ, SIZ	Magnetic solid phase extraction	CoFe <sub>2</sub> O <sub>4</sub> -graphene nanocomposite	22	20—50000	<1.59	4.3 -6.5	62-104	[65]
SD, SMM	Self-assembly miniaturized syringe assisted extraction (mini- SAE) and HPLC	Water-compatible poly (hydroxyethyl methacrylate) polymer	30	7.0-700	0.19- 0.87	≤6.5	85.6 -100.3	[57]
SA, SP, SD, STZ, SM, SMZ, SMX, SIX, SMZ, SMP, SMM, SM, SCP, SDX, SQX, SDM,	SPE and HPLC	Oasis® MCX cartridges	5	0-100	-	11-15	87-119	[45]
ST, SMD, SMZ, SDM, SPP, SNT	Ionic liquid-based aqueous two- phase system extraction	1-butyl-3- methylimidazolium tetrafluoroborate ([C4MIM]BF <sub>4</sub> )	15	8.55—1036.36	2.04—2.84	0.56- 12.20	72.32—108.96	[59]
SD, SMZ, SMM, SMX, SQX	Stir bar sorptive extraction and HPLC	Poly (VI-DB) monolithic	180	10—1000	1.30—7.90	8.3-10.9	57.7-113	[53]

#### *1.1.4.2 Sample preparation procedures for egg samples*

Most of the published sample preparation procedures for SAs determination in egg samples are related to solid-phase extraction. Cruz et al. added acetonitrile to homogenized egg samples and centrifuged the mixture so that proteins could precipitate [66]. After collecting the supernatant, an SPE C18 cartridge was used to clean-up the sample. Similarly, Li et al. precipitated egg proteins using acetonitrile and then used 4.0 mg of graphene oxide/chitosan composite (as sorbent) in an SPE cartridge to clean the sample [33]. Both procedures are simple, have low organic solvent consumption and are relatively fast. Premarathne et al. used ethyl acetate to extract SAs from egg samples, followed by a defatting procedure using n-heptane [28]. Such an extraction step was also employed by Tolika et al., without the defatting step [67]. However, the obtained extract was cleaned up using an OASIS HLB SPE cartridge before injecting the sample in an HPLC system. Xu et al. synthesized magnetic multiwalled carbon nanotubes and utilized it as a sorbent in a magnetic solid-phase extraction procedure for the isolation of SAs from egg samples [68]. This sorbent could easily be reused without a significant reduction of the extraction recoveries serving as an alternative to previous methods. A summary of analytical methods developed for SAs determination in eggs is given in Table 3.

#### *1.1.4.3 Sample preparation procedures for water samples*

Although it would be expected that water would be the main target of most studies, this is not the case. This is because the indigenous concentration of SAs in water bodies is lower, compared to animal-derived food products. However, it is not less important than other food products, because it is consumed daily in higher quantities. Yuan et al. proposed the use of Oasis HLB cartridges for SAs extraction [69]. They also proposed the addition of disodium ethylenediaminetetraacetic acid to complex metal ions and multivalent cations. With this procedure, four SAs and their acetylated metabolites can be extracted. A more sophisticated sorbent (hybrid monolith of polypyrrole-coated graphene oxide incorporated into a polyvinyl alcohol cryogel) has been developed by Chullasat et al. [70]. The large surface areas with many adsorption sites of polypyrrole

and graphene oxide facilitate the high adsorption of sulfonamides while the high porosity of the polyvinyl alcohol cryogel helps reduce the backpressure that occurs in a conventional packed solid-phase extraction cartridge. Peixoto et al. developed a micro solid-phase extraction procedure by placing Empore mixed-mode ion exchange polystyrene divinylbenzene sulfonated (SDB-RPS) disks into disk holders, connected to a peristaltic pump [71]. This way, many samples can be analyzed at the same time while its simplicity potentiates it for use in laboratories. To further automatize the extraction procedure an on-line solid-phase extraction-liquid chromatography-tandem mass spectrometry system was developed [72]. Minimum sample manipulation, sample volume, time and solvents savings, and improved throughput are among the main advantages provided by this technique.

Magnetic sorbents have also been developed and utilized in magnetic solid-phase extraction procedures. Zhao et al. synthesized core-shell magnetite and molybdenum disulfide nanocomposite by growing two-dimension ultrathin molybdenum disulfide sheets with a thickness of approximately 20 nm on the surface of magnetite [73]. The synthesized material was used in a dispersive solid-phase extraction procedure, with which a wide linear range ( $1.0\text{-}1000\text{ ng L}^{-1}$ ), low limits of detection ( $0.20\text{-}1.15\text{ ng L}^{-1}$ ), satisfactory repeatability and reproducibility (relative standard deviation  $< 10\%$ ) and excellent recoveries (between  $80.20\%$  and  $108.6\%$ ) can be achieved. Similarly, Tolmacheva et al. synthesized magnetic hypercrosslinked polystyrene particles, that were used in a similar procedure and the analytical figures of merit of the developed procedure were similar to the previous study (recoveries:  $84\text{-}105\%$ , relative standard deviation:  $3\text{-}10\%$ , limit of detection:  $0.21\text{-}0.33\text{ }\mu\text{g L}^{-1}$ ) [64]. Finally, Sun et al. adsorbed the cation surfactant octadecyl trimethyl ammonium bromide onto magnetite nanoparticles to form mixed hemimicelles which were used in a magnetic mixed hemimicelles solid-phase extraction procedure for the extraction of SAs from environmental water samples [74]. A big sample volume could be analyzed with this method ( $500\text{ mL}$ ) giving a high preconcentration factor ( $\sim 1000$ ) and the relative standard deviations were low ( $1\text{-}6\%$ ). A summary of analytical methods developed for SAs determination in water is given in Table 4.

Table 3: Analytical methods developed for the determination of SAs in eggs

Analytes	Method	Sorbent	Extraction time (min)	Linear range ( $\mu\text{g/L}$ )	LOD ( $\mu\text{g L}^{-1}$ )	RSD (%)	Recovery (%)	Reference
SMX, SD, SMZ, SDM, SM	Dispersive solid-phase extraction and HPLC-UV	SMX imprinted acrylamide functionalized silica nanoparticles	45	50-20000	2.81-14.6	2.3-6.3	73.2-89.1	[61]
SM, SML, SDX, SMX, SIX	Solid phase extraction and HPLC-UV	Graphene oxide/chitosan	~10	10-10000	0.71-0.98	5.2-13.5	75.3-105.2	[33]
SD, STZ, SP, SM, SMZ, SMP, SCP, SMX, SMM, SDM, SIA	Polymer monolith microextraction and HPLC-MS	Porous nanofibers	20	5-2000	0.4-9.8	< 11.8	80.4-119.8	[75]
SD, SMD, SMM, SQX, SM, SDM	Magnetic solid phase extraction and HPLC-MS	Magnetic multiwalled carbon nanotubes	15	10-1000	1.4-2.8	2.9-8.3	73.8-96.2	[76]
SD, STZ, SP, SM, SMZ, SMP	Liquid-liquid extraction and HPLC- DAD	-	30	50-150	108-116	<12	80.7-103.7	[77]
SD, SP, SM, SMZ, SCP, SMX, SDX, SDM	QuEChERS	Primary, secondary amine	5	13.6-1000	4.1- 26.6	<10	65.9 -88.1	[78]

SDM, SMZ, SQXNa, SAM, SCP, SD, SM, SMXZ, STZ, SMP	Solid phase extraction and LC- ESI-MS/MS	-	15	0-200	-	8.5-27.2	87 -116	[66]
SD, SM, SDMD, STZ, SMX, SMP, SCP, SDX SIA	SPE with HPLC analysis	Multiwalled carbon nanotubes	24	0.2-100	0.0041–0.01	2.5–7.8	66–86%	[79]
SD, SP, SM, SMZ, SMM, SCP, SD	Micro-solid phase extraction with HILIC-HPLC/MS	Poly-MAA-EDMA monolith	-	10-100	0.9–9.8	0.8–12.5	80–120	[80]

Table 4: Analytical methods developed for the determination of SAs in water

Analytes	Method	Sorbent	Extraction time (min)	Linear range (µg/L)	LOD (µg/L)	RSD (%)	Recovery (%)	Reference
SD, SDMD, STZ	Magnetic dispersive solid phase extraction and HPLC-DAD	Fe <sub>3</sub> O <sub>4</sub> -graphene oxide	20	200-20000	50-100	5.38-9.03	67.4-119.9	[81]
SMP, SMZ, SMX, SCP	Magnetic solid-phase extraction with HPLC	Magnetic hypercrosslinked polystyrene	40	2-200	0.21–0.33	3-9	84–95	[52]
SP, SD, SMZ,	SPE-LC-MS/MS	Oasis HLB	5	0.5 -50	0.01-0.06	< 9.6	77.7%–148.1%	[69]
SMX, SMD, SDM, SQX	Magnetic mixed hemimicelles solid-phase extraction coupled with HPLC–UV detection	OTMABr-coated magnetite nanoparticles	15	0.10–10	0.024-0.030	1-6	70–102	[74]
sulfathiazole, sulfamethoxazole sulfadimethoxine	Bar Adsorptive Microextraction and HPLC-DAD	Polystyrene-divinylbenzene polymer	90	0.16 to 8.00	0.08 -0.16	< 15.2	63.8- 84.2	[82]
SMX, SMM, SD	Mixed matrix membrane microextraction	Molecularly imprinted silica gel incorporated with agarose polymer matrix	30	1–500	0.06–0.17	<10	80–96%	[83]

Perfluoroalkane sulfonamides	Solid-phase microextraction and HPLC-MS	Poly (1H,1H,2H,2H-nonafluorohexyl acrylate/vinyboronic anhydride pyridine complex-co-ethylenedimethacrylate)	60	0.0025–30.0	0.13–1.45	0.9–11	80.3% to 119%	[84]
SD, STZ, SM, SMM, SDM	Solid phase extraction	Polypyrrole-coated graphene oxide incorporated into a polyvinyl alcohol cryogel	-	200- 100000	0.1 -0.2	<5	85.5- 99	[70]
STZ, SMD, SMZ, SDM, SPP, SNT	Ionic liquid-based aqueous two-phase system extraction	1-butyl-3-methylimidazolium tetrafluoroborate	15	0.05-5	0.011-0.018	3.1-6.5	98-105	[59]

#### *1.1.4.4 Sample preparation procedures for pork and chicken samples*

As mentioned above, SAs are also present in the animal meat. Therefore, sample preparation procedures for solid samples have also been developed. In the majority of the published studies, a liquid extraction step is carried out to the homogenized tissue sample, prior to the main extraction step, so that SAs are transferred from the solid sample to a liquid phase. For instance, Cheong et al. used hexane saturated acetonitrile to blend chicken breast or liver samples and then transferred the organic phase to another tube, where it was evaporated to dryness [85]. The residue was extracted with methylene chloride and then injected into an HPLC system. A similar procedure was followed by Premarathne et al. who used ethyl acetate instead of methylene chloride [77]. In some other studies, the extract was purified using Bond-Elute C18 SPE cartridges [86], Oasis HLB SPE cartridges [87], SPE cartridges packed with multi-walled carbon nanotubes [88] or dual-dummy-template molecularly imprinted polymer [89]. Alternatively, instead of purifying the obtained extract with an SPE procedure, dispersive solid-phase extraction procedures have also been developed that use multi-walled carbon nanotubes [90],  $\text{Fe}_3\text{O}_4@JUC-48$  (a hybrid cadmium carboxylate based metal-organic framework with 1,4-biphenyl dicarboxylic acid as the O-donor ligand) [91], thiol-functionalized magnetic carbon nanotubes [48] or yolk-shell  $\text{Fe}_3\text{O}_4@$ graphitic carbon submicroboxes [92], as sorbents. Finally, owing to the solid nature of the samples, matrix solid-phase dispersion procedures are applicable. To this end, Yu et al. developed such a procedure where the sample is blended in a mortar along with C18 and disodium ethylenediaminetetraacetic acid and oxalic acid [93]. After adding anhydrous sodium sulfate the mixture is placed in a pre-plugged syringe barrel and hexane is used to wash the blend and elute lipids, whereas SAs are eluted with acetonitrile and dichloromethane. In another study, Wang et al. used mixed-template molecularly imprinted polymer in a matrix solid-phase dispersion procedure to extract simultaneously fluoroquinolones, tetracyclines and SAs from meat samples [94]. A summary of analytical methods developed for SAs determination in pork and chicken meat, is given in Table 5.



Table 5: Analytical methods developed for the determination of SAs in pork and chicken meat

Analytes	Method	sorbent	Extraction time (min)	Linear range ( $\mu\text{g}/\text{Kg}$ )	LOD ( $\mu\text{g}/\text{Kg}$ )	RSD (%)	Recovery (%)	Reference
SD, SM, SMZ, SMM, SDX, SMZ, SQX, SDM, SA, ST, SP	Solid-Phase Extraction and HPLC-MS	Multiwalled Carbon Nanotubes	20	0.0015–10	0.3-1.5	<10	70–90	[88]
SMZ, SD, SMX, SM	Dispersive magnetic solid-phase extraction and HPLC-UV	Fe <sub>3</sub> O <sub>4</sub> @graphitic carbon submicroboxes	15	5-6250	0.46–2.24	2.5-9.2	77.2–118.0	[92]
SD, STZ, SMR, SMZ, SMP	Magnetic solid phase extraction and HPLC-UV	Core/shell structured Fe <sub>3</sub> O <sub>4</sub> @JUC-48 magnetic nanocomposite	35	3.97–1000	1.73-5.23	<4.5	76.1- 102.6	[91]
SMM, SMZ, SP, SDM, SIA, SD, SM, SPA, SQX	QuEChERS and HPLC-MS	Primary secondary amine (PSA)	30	0.125-12.5	0.01-0.03	1-6.3	74.0-100.3	[95]
SD, SMZ, SMP, SDM, SMM, SMZ,	Solid phase dispersion	MMIP polymer	15	5-1000	0.5–3.0	1.7-3.1	74.5–102.7	[94]

SD, SM, SMZ, SMM, SMX	Pipette tip solid phase extraction and HPLC	SNW-1@PAN nanofiber	-	5-125	1.7-2.7	5.4-9.2	86-111	[96]
SD, SMZ, SMP, SDM, SMM, SMZ, SQ, SCP	Solid phase extraction and HPLC	Dual-dummy- template molecularly imprinted polymer	-	-	1.0-3.4	1.2-3.4	86.1-109.4	[89]

#### *1.1.4.5 Sample preparation procedures for honey samples*

As happens with previous samples, most of the sample preparation techniques are based on solid-phase extraction. In many cases, before the extraction, a hydrolysis step is carried out, so that sugar-bound SAs are released. For instance, Dluhosova et al. added trichloroacetic acid in honey samples and then used a liquid-liquid extraction procedure (using acetonitrile and ethyl acetate) to isolate SAs [97]. Tolgyesi et al. hydrolyzed honey samples by adding acetic acid and then, they cleaned the samples with Oasis HLB SPE cartridges [98]. Li et al. developed a similar procedure where no hydrolysis takes place but use a self-assembled SPE cartridge packed with graphene oxide and chitosan extracts directly the SAs. The relative standard deviation of the developed method was between 3.5 and 7.1 % [33]. In another study, the authors presented a novel extraction method using acid hydrolysis and salting-out liquid-liquid extraction using tetrahydrofuran [37]. According to authors, similar methods that use acetonitrile as a solvent instead of tetrahydrofuran usually present a wider linear dynamic range but have much lower recoveries. Furthermore, with this method, no SPE clean-up steps or filtering with syringe filters are needed, thus, lowering the overall cost. A summary of analytical methods developed for SAs determination in honey is given in Table 6.

#### *1.1.4.6 Sample preparation procedures for fish samples*

Similarly, to the other meat tissue samples, fish samples are usually homogenized prior to the extraction step. Storey et al. developed a method for the analysis of 13 SAs in fish tissues (catfish, eel, pangasius, sablefish, tilapia, swai, salmon, and trout) [99]. The tissue is mixed with ethylenediaminetetraacetic acid-McIlvaine buffer, double-extracted with acetonitrile, p-toluenesulfonic acid and N, N, N', N'-tetramethyl-p-phenylenediamine dihydrochloride and then analyzed. Dasenaki et al. used a liquid extraction step to isolate SAs from fish tissue and then used a Zorbax Eclipse Plus C18 column to clean up the extract [100]. Nunes et al. employed a QuEChERS approach for the analysis of SAs in tilapia fillet [101]. Shen et al. published a study describing a micro-scale matrix solid-phase dispersion technique, using hydrophilic-lipophilic balanced material as sorbent and

a pipette tip as the cartridge [102]. The whole procedure is completed in 13 min (5 min for extraction and 8 min for separation and detection) and consumes 5.1 mL of solvent with 20 mg of sorbent per analysis. A summary of analytical methods developed for SAs determination in fish is given in Table 7.

#### *1.1.4.7 Sample preparation procedures for animal feeds samples*

The last type of sample in which many analyses of SAs are carried out is animal feeds. This is because it is an easy way for the administration of antibiotics to animals. Liu et al. suggest the addition of acetonitrile in the animal feed and then, the use of the basic alumina column for the SPE clean-up of the extract [103]. This way, a linear range of 0.2-40  $\mu\text{g kg}^{-1}$ , limits of quantification between 0.5 and 20  $\mu\text{g kg}^{-1}$  and recoveries ranging from 80% to 120% can be achieved. Pietron et al. followed nearly the same procedure, without the clean-up step and the analytical figures of merit were similar to those of the previous study [104]. Although such an approach seems easy, the use of methanol or acetonitrile for SAs extraction results in a highly contaminated extract that makes the detection of SAs in low levels impossible. In this context, Patyra et al. studied different commercially available SPE cartridges and various solvent systems and found that a mixture of ethyl acetate/methanol/acetonitrile (50:25:25 v/v/v) resulted in the optimum extraction yield, whereas optimum clean-up and recovery was achieved using Strata-SCX cartridges [105]. Finally, Qiao et al. developed a novel 4-chloro-6-pyrimidinylferrocene-modified silica gel and used it as a sorbent in an SPE procedure [106]. Compared with commercial SPE sorbents, the new sorbent has excellent selectivity to retain polar and nonpolar interferences resulting in an overall simple and accurate method for the determination of trace SAs in foodstuffs. A summary of analytical methods developed for SAs determination in animal feeds is given in Table 8.

Table 6: Analytical methods developed for the determination of SAs in honey

Analytes	Method	sorbent	Extraction time (min)	Linear range (µg/kg)	LOD (µg/kg)	RSD (%)	Recovery (%)	Reference
SP, SM, STZ, SMZ, SMX, TMP, DAP, SDX, SDT	SPE and HPLC-MS/MS	Oasis HLB	5	0.-100	0.3-0.9	6-18	70-106	[107]
SM, SMM, SCP, SDX, SIZ, SDM	Sugaring-out assisted liquid-liquid extraction and HPLC-FL	-		2-200	0.6-0.9	0.3-4.4	80.9-99.6	[108]
SQX, SDX, STZ	Liquid extraction and flow injection coupled to a liquid waveguide capillary cell	-	5	6-115	1.66-1.99	-	88-112	[109]
SGN, SNL, SD, STZ, ZMR, SMZ, SDM, SMNM, SMP, SDX, SMX, SQX, SDT	Liquid extraction and HPLC-MS/MS	-	5	10-50	-	2.6-19.8	85.8-110.2	[110]
SGU, SFM, SAC, SP, STZ, SMZ, SMX, SMM, SM, SCP, SDO, SMZ, SDM	Online extraction and HPLC-FL	-	-	1-100	0.1-1.0	1-10	80-100	[111]

SM, SMZ, SDX, SIZ	Solid-phase extraction and HPLC	Graphene oxide/chitosan	5	10-10000	0.71-0.98	3.5-7.1	75.3-105.2	[33]
SD, STZ, SDD, SM, SAA, SMP, SCP, SAC, SMX, SDM	Salting Out Liquid Liquid Extraction and HPLC-UV	-	5	5-100	1.5-2	-	63.3-86.5	[37]
STZ, SP, SD	Pipette tip solid phase extraction and HPLC-UV	2-(hexyloxy) naphthalene-sulfate doped polyaniline polymer	5	50-50000	9.5-16.5	2.5-11.1	92.4-105.8	[55]
SMZ, SMP, SMD, SMX, SDM, SPP	Microwave-assisted dispersive liquid-liquid microextraction and HPLC	1-hexyl-3-methylimidazolium hexafluorophosphate	12	0.05-5.0	0.011-0.018	1.5-7.3	95.4-106.3	[60]
SMX, SMZ, SDM,	Direct injection HPLC	-	-	9-25	2.7-23.1	5-24	103-119	[112]
SA, SD, SMX, SMZ, SIX, SBA, SMA, SCP, SDM, STZ, SM, SMP, SDX	Liquid extraction and UPLC-ESI-MS/MS	-	-	0-200	0.15-0.54		81.3-86.6	[113]
SDM, SCP	SPE and HPLC-FL-MS	Oasis HLB	5	0.03-686	0.03-0.1	13.3-34.8	69.4-115	[98]
SD, SDX, SMZ, STZ	Liquid extraction and HPLC-MS	-	-	0.1-100		13.2-28.8	60.5-94.6	[97]

Table 7: Analytical methods developed for the determination of SAs in fish

Analytes	Method	sorbent	Extraction time (min)	Linear range (µg/kg)	LOD (µg/kg)	RSD (%)	Recovery (%)	Reference
SD, SMM, SDM, SMZ, SMD, SMZ	Solid-phase extraction and HPLC	Primary secondary amine	10	0.05–5.0	5.8–11.7	1.37–3.95	80.1–95.1	[114]
SD, SDMD, STZ, SA, SP, SMX, SM, SIX, SMZ	Magnetic solid phase extraction and HPLC-DAD	Fe <sub>3</sub> O <sub>4</sub> @MoS <sub>2</sub>	20	5–1000	0.40–1.5	<10	80.13–107.1	[73]
SD, STZ, SM, SDD, SMP, SMM, SCP, SDM, SMZ, SMX, SIX, SGN, SP, SMX, SQX SDX, SCIZ	UHPLC-MS	-	15	20–150	5.65 -25.8	6.7-16	-	[100]
SP, SD, STZ, SQX, SDM, SCP, SM, SMZ, SMX,	HPLC-MS/MS	-	-	85-118	-	1-6	97- 114	[99]
SA, SD, STZ, SM, SMZ, SM, SMP, SMM, SCP, SDO, SMX, SSA, SDM, SQX,	Micro-scale pipette tip-matrix solid-phase dispersion and HPLC-MS/MS	Hydrophilic–lipophilic balance material	13	1-100	4.2-16.4	1.4–10.3	70.6–95.5	[102]
SP, STZ, SMZ, SDM, SMX, SMP, SM	QuEChERS	-	-	12.5-100	1.0	-	38.4- 103.6	[101]

Table 8: Analytical methods developed for the determination of SAs in animal feeds

Analytes	Method	sorbent	Extraction time (min)	Linear range (µg/kg)	LOD (µg/kg)	RSD (%)	Recovery (%)	Reference
SD, SGD, SMZ, SM, SMX	Solid-phase extraction and HPLC-FL	Strata-SCX cartridge	15	-	34.5–79.5	-	79.3–114.0	[105]
SMZ, SDM	Solid-phase extraction and HPLC	4-chloro-6-pyrimidinyl ferrocene-modified silica gel	-	10-5000	2–5	1.69-2.5	72.4-93.6	[106]
SD, SP, SM, SMDZ, SMZ, SMP, SMX, SDM, SPZ, SD, SCR, SMM, STZ, SAA, SA, SQX	Solid phase extraction and UHPLC–MS–MS.	OASIS MCX	35	0.2-40	0.5-20	-	80-120	[103]



### 1.1.5 Objectives and Scope

Sulfonamides belong to one of the many classes of compounds of particular interest to analytical chemists. This is for two main reasons: First, they have a negative impact on the environment, and hence, the legislation (details are given in Appendix) for their detection is becoming stricter. Secondly, they exist in various matrices making it difficult for them to develop a “one and only” method for their analysis. Based on the principle that the future of analytical chemistry lies, to a great extent, in sample preparation, this research focuses mainly on the development of novel separation-extraction procedures, using (nano)materials and then on the development of analytical methods for the HPLC-based determination of sulfonamides.

Instead of developing only nanomaterials that would be used in magnetic dispersive solid-phase procedures and would result in minor advancement of the specific field, different approaches were attempted resting on the concept of (nano)materials and chemical analysis. In this context, two different functionalized melamine sponges, a magnetic ionic liquid and a magnetic nanomaterial were developed and further used for sulfonamides. This way, alternative sample preparation procedures were developed which can be used depending on the circumstances. Moreover, the development of such alternatives not only serves the purpose of sulfonamides detection but also meets the need for greener and more miniaturized analytical methods.

Details of the four developed sorbent materials (i. melamine sponges functionalized with graphene, ii. Melamine sponges decorated with copper sheets, iii. magnetic ionic liquid based on dysprosium and iv. zinc ferrites) along with all the parameters of the analytical methods and performance data are given in the following chapters.

## 1.2 References

- [1] D.M. Morens, G.K. Folkers, A.S. Fauci, The challenge of emerging and re-emerging infectious diseases, *Nature*. 430 (2004) 242–249. doi:10.1038/nature02759.
- [2] D.B. McArthur, *Emerging Infectious Diseases*, *Nurs. Clin. North Am.* 54 (2019) 297–311. doi:10.1016/j.cnur.2019.02.006.
- [3] T. Burki, The Black Death, *Lancet Infect. Dis.* 10 (2010) 304. doi:10.1016/S1473-3099(10)70090-6.
- [4] R. Hoff, T.M. Pizzolato, M.S. Diaz-Cruz, Trends in sulfonamides and their by-products analysis in environmental samples using mass spectrometry techniques, *Trends Environ. Anal. Chem.* 9 (2016) 24–36. doi:10.1016/j.teac.2016.02.002.
- [5] W. Sneader, History of Sulfonamides, *Encycl. Life Sci.* (2001). doi:10.1038/npg.els.0003625.
- [6] E.E. Connor, Sulfonamide antibiotics, *Prim. Care Update Ob. Gyns.* 5 (1998) 32–35. doi:10.1016/S1068-607X(97)00121-2.
- [7] S.G. Dmitrienko, E. V. Kochuk, V. V. Apyari, V. V. Tolmacheva, Y.A. Zolotov, Recent advances in sample preparation techniques and methods of sulfonamides detection - A review, *Anal. Chim. Acta.* 850 (2014) 6–25. doi:10.1016/j.aca.2014.08.023.
- [8] Y. Zhang, W.E. Zhou, S.H. Li, Z.Q. Ren, W.Q. Li, Y. Zhou, X.S. Feng, W.J. Wu, F. Zhang, A simple, accurate, time-saving and green method for the determination of 15 sulfonamides and metabolites in serum samples by ultra-high performance supercritical fluid chromatography, *J. Chromatogr. A.* 1432 (2016) 132–139. doi:10.1016/j.chroma.2015.12.075.
- [9] A. Tacic, V. Nikolic, L. Nikolic, I. Savic, Antimicrobial sulfonamide drugs, *Adv. Technol.* (2017). doi:10.5937/savteh1701058t.
- [10] N.E. Holmes, M. Lindsay Grayson, Sulfonamides, in: *Kucers Use Antibiot. A Clin. Rev. Antibacterial, Antifung. Antiparasit. Antivir. Drugs*, Seventh Ed., 2017. doi:10.1201/9781315152110.
- [11] W. Baran, E. Adamek, J. Ziemiańska, A. Sobczak, Effects of the presence of sulfonamides in the environment and their influence on human health, *J. Hazard. Mater.* 196 (2011) 1–15. doi:10.1016/j.jhazmat.2011.08.082.
- [12] J. Jiang, G. Wang, Hazard of Sulfonamides and Detection Technology Research Progress, in: *IOP Conf. Ser. Earth Environ. Sci.*, 2017. doi:10.1088/1755-1315/100/1/012040.
- [13] M. Kester, K.D. Karpa, K.E. Vrana, *Treatment of Infectious Diseases*, Elsevier's Integr. Rev. Pharmacol. (2012) 41–78. doi:10.1016/b978-0-323-07445-2.00004-5.

- [14] Website:, (n.d.). [www.drugs.com](http://www.drugs.com) (accessed December 20, 2019).
- [15] R.S. Vardanyan, V.J. Hruby, *Antimicrobial Drugs, Synth. Essent. Drugs.* (2006) 499–523. doi:10.1016/b978-044452166-8/50033-9.
- [16] E. Scholar, *Sulfonamides, XPharm Compr. Pharmacol. Ref.* (2007) 1–4. doi:10.1016/B978-008055232-3.61013-X.
- [17] K. Park, I.S. Kwak, Disrupting effects of antibiotic sulfathiazole on developmental process during sensitive life-cycle stage of *Chironomus riparius*, *Chemosphere.* (2018). doi:10.1016/j.chemosphere.2017.09.118.
- [18] E.F. Goulden, L. Høj, M.R. Hall, Microbial management for bacterial pathogen control in invertebrate aquaculture hatcheries, *Adv. Aquac. Hatch. Technol.* (2013) 246–285. doi:10.1533/9780857097460.1.246.
- [19] N. Rajendiran, J. Thulasidhasan, Binding of Sulfamerazine and Sulfamethazine to Bovine Serum Albumin and Nitrogen Purine Base Adenine: A Comparative Study, *Int. Lett. Chem. Phys. Astron.* (2015). doi:10.18052/www.scipress.com/ilcpa.59.170.
- [20] S.E. Mason, R.E. Baynes, J.L. Buur, J.E. Riviere, G.W. Almond, Sulfamethazine water medication pharmacokinetics and contamination in a commercial pig production unit, *J. Food Prot.* (2008). doi:10.4315/0362-028X-71.3.584.
- [21] A. Dirany, I. Sirés, N. Oturan, A. Özcan, M.A. Oturan, Electrochemical treatment of the antibiotic sulfachloropyridazine: Kinetics, reaction pathways, and toxicity evolution, *Environ. Sci. Technol.* (2012). doi:10.1021/es204621q.
- [22] J.F. Huertas-Pérez, N. Arroyo-Manzanares, L. Havlíková, L. Gámiz-Gracia, P. Solich, A.M. García-Campaña, Method optimization and validation for the determination of eight sulfonamides in chicken muscle and eggs by modified QuEChERS and liquid chromatography with fluorescence detection, *J. Pharm. Biomed. Anal.* 124 (2016) 261–266. doi:10.1016/j.jpba.2016.02.040.
- [23] M.J.G. Galán, M.S. Díaz-Cruz, D. Barceló, Sulfonamide Antibiotics in Natural and Treated Waters: Environmental and Human Health Risks, in: *Handb. Environ. Chem.*, 2012: pp. 71–92. doi:10.1007/698\_2011\_129.
- [24] Y. Agersø, T. Hald, B. Helwigh, B. Borck Høg, L. Bogø Jensen, V. Frøkjær Jensen, H. Korsgaard, L. Stehr Larsen, A.M. Seyfarth, T. Struve, A.M. Hammerum, K. Gaardbo Kuhn, L.M. Lambertsen, A. Rhod Larsen, M. Laursen, E. Møller Nielsen, S.S. Olsen, A. Petersen, L. Skjøt-Rasmussen, R. L. Skov, M. Torpdahl, DANMAP 2009 - Use of antimicrobial agents and

occurrence of antimicrobial resistance in bacteria from food animals, food, and humans in Denmark, 2009. [http://www.danmap.org/~media/Projekt sites/Danmap/DANMAP reports/Danmap\\_2009.ashx](http://www.danmap.org/~media/Projekt%20sites/Danmap/DANMAP%20reports/Danmap_2009.ashx).

- [25] A. Armentano, S. Summa, S. Lo Magro, C. Palermo, D. Nardiello, D. Centonze, M. Muscarella, Rapid method for the quantification of 13 sulphonamides in milk by conventional high-performance liquid chromatography with diode array ultraviolet detection using a column packed with core-shell particles, *J. Chromatogr. A.* 1531 (2018) 46–52. doi:10.1016/j.chroma.2017.11.015.
- [26] S.G. Dmitrienko, E. V. Kochuk, V. V. Tolmacheva, V. V. Apyari, Y.A. Zolotov, Determination of the total content of some sulfonamides in milk using solid-phase extraction coupled with off-line derivatization and spectrophotometric detection, *Food Chem.* 188 (2015) 51–56. doi:10.1016/j.foodchem.2015.04.123.
- [27] N. Raza, K.H. Kim, Quantification techniques for important environmental contaminants in milk and dairy products, *TrAC - Trends Anal. Chem.* 98 (2018) 79–94. doi:10.1016/j.trac.2017.11.002.
- [28] J.M.K.J.K. Premarathne, D.A. Satharasinghe, A.R.C. Gunasena, D.M.S. Munasinghe, P. Abeynayake, Establishment of a method to detect sulfonamide residues in chicken meat and eggs by high-performance liquid chromatography, *Food Control.* 72 (2017) 276–282. doi:10.1016/j.foodcont.2015.12.012.
- [29] A. Hiba, A. Carine, A.R. Haifa, L. Ryszard, J. Farouk, Monitoring of twenty-two sulfonamides in edible tissues: Investigation of new metabolites and their potential toxicity, *Food Chem.* 192 (2016) 212–227. doi:10.1016/j.foodchem.2015.06.093.
- [30] X. Zhao, J. Wang, J. Wang, S. Wang, Development of water-compatible molecularly imprinted solid-phase extraction coupled with high performance liquid chromatography–tandem mass spectrometry for the detection of six sulfonamides in animal-derived foods, *J. Chromatogr. A.* 1574 (2018) 9–17. doi:10.1016/j.chroma.2018.08.044.
- [31] European Parliament, Directive 2013/39/EU, Off. J. Eur. Union. (2013).
- [32] Z.H.A.O. Shuo, W.A.N.G. Hao-Tian, L.I. Ke, Z. Jing, W.A.N.G. Xia-Yan, G.U.O. Guang-Sheng, Fast Determination of Residual Sulfonamides in Milk by In-Tube Solid-Phase Microextraction Coupled with Capillary Electrophoresis-Laser Induced Fluorescence, *Chinese J. Anal. Chem.* 46 (2018) e1810–e1816. doi:10.1016/S1872-2040(17)61076-4.

- [33] Y. Li, Z. Li, W. Wang, S. Zhong, J. Chen, A.J. Wang, Miniaturization of self-assembled solid phase extraction based on graphene oxide/chitosan coupled with liquid chromatography for the determination of sulfonamide residues in egg and honey, *J. Chromatogr. A*. 1447 (2016) 17–25. doi:10.1016/j.chroma.2016.04.026.
- [34] S. Ansari, M. Karimi, Recent progress, challenges and trends in trace determination of drug analysis using molecularly imprinted solid-phase microextraction technology, *Talanta*. 164 (2017) 612–625. doi:10.1016/j.talanta.2016.11.007.
- [35] Q. Zhou, Z. Fang, Highly sensitive determination of sulfonamides in environmental water samples by sodium dodecylbenzene sulfonate enhanced micro-solid phase extraction combined with high performance liquid chromatography, *Talanta*. 141 (2015) 170–174. doi:10.1016/j.talanta.2015.04.016.
- [36] S.A. Errayess, A.A. Lahcen, L. Idrissi, C. Marcoaldi, S. Chiavarini, A. Amine, A sensitive method for the determination of Sulfonamides in seawater samples by Solid Phase Extraction and UV–Visible spectrophotometry, *Spectrochim. Acta - Part A Mol. Biomol. Spectrosc.* 181 (2017) 276–285. doi:10.1016/j.saa.2017.03.061.
- [37] L. Kadziński, R. Banasiuk, B. Banecki, Determination of ten sulfonamides in honey using tetrahydrofuran Salting Out Liquid Liquid Extraction and monolithic silica column, *Lwt*. 96 (2018) 7–12. doi:10.1016/j.lwt.2018.05.007.
- [38] Y. Li, N. Zhu, T. Chen, Y. Ma, Q. Li, A green cyclodextrin metal-organic framework as solid-phase extraction medium for enrichment of sulfonamides before their HPLC determination, *Microchem. J.* 138 (2018) 401–407. doi:10.1016/j.microc.2018.01.038.
- [39] C.D. Stalikas, Y.C. Fiamegos, Microextraction combined with derivatization, *TrAC - Trends Anal. Chem.* (2008). doi:10.1016/j.trac.2008.04.005.
- [40] Y. xin She, J. Liu, J. Wang, Y. Liu, R. Wang, W. Cao, Determination of sulfonamides in bovine milk by ultra performance liquid chromatography combined with quadrupole mass spectrometry, *Anal. Lett.* (2010). doi:10.1080/00032711003698796.
- [41] R.H.M.M. Granja, A.C. de Lima, A.G. Salerno, A.C.B.A. Wanschel, Validation of a liquid chromatography with ultraviolet detection methodology for the determination of sulfonamides in bovine milk according to 2002/657/EC, *Food Control*. (2012). doi:10.1016/j.foodcont.2012.05.018.
- [42] I.A. Unsal, M. Tasan, T. Gokcen, A.C. Goren, Determination of sulfonamides in milk by ID-LC-MS/MS, *J. Chem. Metrol.* (2018). doi:10.25135/jcm.15.18.04.081.

- [43] E.P. Tolika, V.F. Samanidou, I.N. Papadoyannis, Development and validation of an HPLC method for the determination of ten sulfonamide residues in milk according to 2002/657/EC, *J. Sep. Sci.* (2011). doi:10.1002/jssc.201100171.
- [44] T. Dai, J. Duan, X. Li, X. Xu, H. Shi, W. Kang, Determination of sulfonamide residues in food by capillary zone electrophoresis with on-line chemiluminescence detection based on an Ag(III) complex, *Int. J. Mol. Sci.* (2017). doi:10.3390/ijms18061286.
- [45] X.L. Hou, G. Chen, L. Zhu, T. Yang, J. Zhao, L. Wang, Y.L. Wu, Development and validation of an ultra high performance liquid chromatography tandem mass spectrometry method for simultaneous determination of sulfonamides, quinolones and benzimidazoles in bovine milk, *J. Chromatogr. B Anal. Technol. Biomed. Life Sci.* (2014). doi:10.1016/j.jchromb.2014.05.005.
- [46] J. An, X. Wang, M. Ming, J. Li, N. Ye, Determination of sulfonamides in milk by capillary electrophoresis with PEG@MoS<sub>2</sub> as a dispersive solid-phase extraction sorbent, *R. Soc. Open Sci.* (2018). doi:10.1098/rsos.172104.
- [47] X. Jia, P. Zhao, X. Ye, L. Zhang, T. Wang, Q. Chen, X. Hou, A novel metal-organic framework composite MIL-101(Cr)@GO as an efficient sorbent in dispersive micro-solid phase extraction coupling with UHPLC-MS/MS for the determination of sulfonamides in milk samples, *Talanta*. (2017). doi:10.1016/j.talanta.2016.08.086.
- [48] A.N.M. Nasir, N. Yahaya, N.N.M. Zain, V. Lim, S. Kamaruzaman, B. Saad, N. Nishiyama, N. Yoshida, Y. Hirota, Thiol-functionalized magnetic carbon nanotubes for magnetic micro-solid phase extraction of sulfonamide antibiotics from milks and commercial chicken meat products, *Food Chem.* (2019). doi:10.1016/j.foodchem.2018.10.044.
- [49] L. Fu, H. Zhou, E. Miao, S. Lu, S. Jing, Y. Hu, L. Wei, J. Zhan, M. Wu, Functionalization of amino terminated carbon nanotubes with isocyanates for magnetic solid phase extraction of sulfonamides from milk and their subsequent determination by liquid chromatography-high resolution mass spectrometry, *Food Chem.* (2019). doi:10.1016/j.foodchem.2019.03.097.
- [50] Y. Li, X. Wu, Z. Li, S. Zhong, W. Wang, A. Wang, J. Chen, Fabrication of CoFe<sub>2</sub>O<sub>4</sub>-graphene nanocomposite and its application in the magnetic solid phase extraction of sulfonamides from milk samples, *Talanta*. 144 (2015) 1279–1286. doi:10.1016/j.talanta.2015.08.006.
- [51] Q. Gao, D. Luo, J. Ding, Y.Q. Feng, Rapid magnetic solid-phase extraction based on magnetite/silica/poly(methacrylic acid-co-ethylene glycol dimethacrylate) composite microspheres for the determination of sulfonamide in milk samples, *J. Chromatogr. A*. 1217 (2010) 5602–5609. doi:10.1016/j.chroma.2010.06.067.

- [52] V. V. Tolmacheva, V. V. Apyari, A.A. Furletov, S.G. Dmitrienko, Y.A. Zolotov, Facile synthesis of magnetic hypercrosslinked polystyrene and its application in the magnetic solid-phase extraction of sulfonamides from water and milk samples before their HPLC determination, *Talanta*. 152 (2016) 203–210. doi:10.1016/j.talanta.2016.02.010.
- [53] X. Huang, N. Qiu, D. Yuan, Simple and sensitive monitoring of sulfonamide veterinary residues in milk by stir bar sorptive extraction based on monolithic material and high performance liquid chromatography analysis, *J. Chromatogr. A*. (2009). doi:10.1016/j.chroma.2009.05.031.
- [54] C. Yu, B. Hu, C18-coated stir bar sorptive extraction combined with high performance liquid chromatography-electrospray tandem mass spectrometry for the analysis of sulfonamides in milk and milk powder, *Talanta*. 90 (2012) 77–84. doi:10.1016/j.talanta.2011.12.078.
- [55] S. Sadeghi, S. Oliaei, Nanostructured polyaniline based pipette tip solid phase extraction coupled with high-performance liquid chromatography for the selective determination of trace levels of three sulfonamides in honey and milk samples with the aid of experimental design met, *Microchem. J.* (2019). doi:10.1016/j.microc.2019.02.020.
- [56] H. Yan, N. Sun, S. Liu, K.H. Row, Y. Song, Miniaturized graphene-based pipette tip extraction coupled with liquid chromatography for the determination of sulfonamide residues in bovine milk, *Food Chem.* 158 (2014) 239–244. doi:10.1016/j.foodchem.2014.02.089.
- [57] M. Gao, H. Yan, N. Sun, Water-compatible poly (hydroxyethyl methacrylate) polymer sorbent for miniaturized syringe assisted extraction of sulfonamides in milk, *Anal. Chim. Acta.* (2013). doi:10.1016/j.aca.2013.09.026.
- [58] E. Karageorgou, N. Manousi, V. Samanidou, A. Kabir, K.G. Furton, Fabric phase sorptive extraction for the fast isolation of sulfonamides residues from raw milk followed by high performance liquid chromatography with ultraviolet detection, *Food Chem.* 196 (2016) 428–436. doi:10.1016/j.foodchem.2015.09.060.
- [59] U. Novak, A. Pohar, I. Plazl, P. Žnidaršič-Plazl, Ionic liquid-based aqueous two-phase extraction within a microchannel system, in: *Sep. Purif. Technol.*, 2012. doi:10.1016/j.seppur.2012.01.033.
- [60] X. Xu, R. Su, X. Zhao, Z. Liu, Y. Zhang, D. Li, X. Li, H. Zhang, Z. Wang, Ionic liquid-based microwave-assisted dispersive liquid-liquid microextraction and derivatization of sulfonamides in river water, honey, milk, and animal plasma, *Anal. Chim. Acta.* (2011). doi:10.1016/j.aca.2011.09.018.

- [61] R. Gao, J. Zhang, X. He, L. Chen, Y. Zhang, Selective extraction of sulfonamides from food by use of silica-coated molecularly imprinted polymer nanospheres, *Anal. Bioanal. Chem.* 398 (2010) 451–461. doi:10.1007/s00216-010-3909-z.
- [62] I.S. Ibarra, J.M. Miranda, J.A. Rodriguez, C. Nebot, A. Cepeda, Magnetic solid phase extraction followed by high-performance liquid chromatography for the determination of sulphonamides in milk samples, *Food Chem.* 157 (2014) 511–517. doi:10.1016/j.foodchem.2014.02.069.
- [63] C. Yu, B. Hu, C18-coated stir bar sorptive extraction combined with high performance liquid chromatography-electrospray tandem mass spectrometry for the analysis of sulfonamides in milk and milk powder, *Talanta.* (2012). doi:10.1016/j.talanta.2011.12.078.
- [64] V. V. Tolmacheva, V. V. Apyari, A.A. Furletov, S.G. Dmitrienko, Y.A. Zolotov, Facile synthesis of magnetic hypercrosslinked polystyrene and its application in the magnetic solid-phase extraction of sulfonamides from water and milk samples before their HPLC determination, *Talanta.* (2016). doi:10.1016/j.talanta.2016.02.010.
- [65] Y. Li, X. Wu, Z. Li, S. Zhong, W. Wang, A. Wang, J. Chen, Fabrication of CoFe<sub>2</sub>O<sub>4</sub>-graphene nanocomposite and its application in the magnetic solid phase extraction of sulfonamides from milk samples, *Talanta.* (2015). doi:10.1016/j.talanta.2015.08.006.
- [66] M.N.S. De La Cruz, R.F. Soares, A.S.F. Marques, F.R. De Aquino-Neto, Development and validation of analytical method for sulfonamide residues in eggs by liquid chromatography tandem mass spectrometry based on the comission decision 2002/657/EC, *J. Braz. Chem. Soc.* (2011). doi:10.1590/S0103-50532011000300007.
- [67] E. P. Tolika, V. F. Samanidou, I. N. Papadoyannis, Development and Validation of an HPLC Method for the Simultaneous Determination of Ten Sulfonamide Residues in Bovine, Porcine and Chicken Tissues According to 2002/657/EC, *Curr. Pharm. Anal.* (2012). doi:10.2174/157341212798995476.
- [68] Y. Xu, J. Ding, H. Chen, Q. Zhao, J. Hou, J. Yan, H. Wang, L. Ding, N. Ren, Fast determination of sulfonamides from egg samples using magnetic multiwalled carbon nanotubes as adsorbents followed by liquid chromatography-tandem mass spectrometry, *Food Chem.* 140 (2013) 83–90. doi:10.1016/j.foodchem.2013.02.078.
- [69] S. fen Yuan, Z. hua Liu, H. Yin, Z. Dang, P. xiao Wu, N. wu Zhu, Z. Lin, Trace determination of sulfonamide antibiotics and their acetylated metabolites via SPE-LC-MS/MS in wastewater and insights from their occurrence in a municipal wastewater treatment plant, *Sci. Total Environ.* (2019). doi:10.1016/j.scitotenv.2018.10.417.



- [70] K. Chullasat, P. Nurerk, P. Kanatharana, P. Kueseng, T. Sukchuay, O. Bunkoed, Hybrid monolith sorbent of polypyrrole-coated graphene oxide incorporated into a polyvinyl alcohol cryogel for extraction and enrichment of sulfonamides from water samples, *Anal. Chim. Acta.* (2017). doi:10.1016/j.aca.2017.01.052.
- [71] P.S. Peixoto, I. V. Tóth, S. Machado, L. Barreiros, A. Machado, A.A. Bordalo, J.L.F.C. Lima, M.A. Segundo, Screening of sulfonamides in waters based on miniaturized solid phase extraction and microplate spectrophotometric detection, *Anal. Methods.* (2018). doi:10.1039/c7ay02624b.
- [72] M.J. García-Galán, M.S. Díaz-Cruz, D. Barceló, Determination of 19 sulfonamides in environmental water samples by automated on-line solid-phase extraction-liquid chromatography-tandem mass spectrometry (SPE-LC-MS/MS), *Talanta.* (2010). doi:10.1016/j.talanta.2009.12.009.
- [73] Y. Zhao, R. Wu, H. Yu, J. Li, L. Liu, S. Wang, X. Chen, T.W.D. Chan, Magnetic solid-phase extraction of sulfonamide antibiotics in water and animal-derived food samples using core-shell magnetite and molybdenum disulfide nanocomposite adsorbent, *J. Chromatogr. A.* (2019). doi:10.1016/j.chroma.2019.460543.
- [74] L. Sun, L. Chen, X. Sun, X. Du, Y. Yue, D. He, H. Xu, Q. Zeng, H. Wang, L. Ding, Analysis of sulfonamides in environmental water samples based on magnetic mixed hemimicelles solid-phase extraction coupled with HPLC-UV detection, *Chemosphere.* (2009). doi:10.1016/j.chemosphere.2009.09.049.
- [75] M.M. Zheng, M.Y. Zhang, G.Y. Peng, Y.Q. Feng, Monitoring of sulfonamide antibacterial residues in milk and egg by polymer monolith microextraction coupled to hydrophilic interaction chromatography/mass spectrometry, *Anal. Chim. Acta.* (2008). doi:10.1016/j.aca.2008.07.033.
- [76] Y. Xu, J. Ding, H. Chen, Q. Zhao, J. Hou, J. Yan, H. Wang, L. Ding, N. Ren, Fast determination of sulfonamides from egg samples using magnetic multiwalled carbon nanotubes as adsorbents followed by liquid chromatography-tandem mass spectrometry, *Food Chem.* (2013). doi:10.1016/j.foodchem.2013.02.078.
- [77] J.M.K.J.K. Premarathne, D.A. Satharasinghe, A.R.C. Gunasena, D.M.S. Munasinghe, P. Abeynayake, Establishment of a method to detect sulfonamide residues in chicken meat and eggs by high-performance liquid chromatography, *Food Control.* (2017). doi:10.1016/j.foodcont.2015.12.012.

- [78] J.F. Huertas-Pérez, N. Arroyo-Manzanares, L. Havlíková, L. Gámiz-Gracia, P. Solich, A.M. García-Campaña, Method optimization and validation for the determination of eight sulfonamides in chicken muscle and eggs by modified QuEChERS and liquid chromatography with fluorescence detection, *J. Pharm. Biomed. Anal.* (2016). doi:10.1016/j.jpba.2016.02.040.
- [79] G.Z. Fang, J.X. He, S. Wang, Multiwalled carbon nanotubes as sorbent for on-line coupling of solid-phase extraction to high-performance liquid chromatography for simultaneous determination of 10 sulfonamides in eggs and pork, *J. Chromatogr. A.* (2006). doi:10.1016/j.chroma.2006.06.024.
- [80] M.M. Zheng, G.D. Ruan, Y.Q. Feng, Hybrid organic-inorganic silica monolith with hydrophobic/strong cation-exchange functional groups as a sorbent for micro-solid phase extraction, *J. Chromatogr. A.* (2009). doi:10.1016/j.chroma.2009.08.085.
- [81] P. Shi, N. Ye, Magnetite-graphene oxide composites as a magnetic solid-phase extraction adsorbent for the determination of trace sulfonamides in water samples, *Anal. Methods.* 6 (2014) 9725–9730. doi:10.1039/c4ay02027h.
- [82] A.H. Ide, S.M. Ahmad, N.R. Neng, J.M.F. Nogueira, Enhancement for trace analysis of sulfonamide antibiotics in water matrices using bar adsorptive microextraction (BA $\mu$ E), *J. Pharm. Biomed. Anal.* 129 (2016) 593–599. doi:10.1016/j.jpba.2016.07.022.
- [83] M.N.H. Rozaini, N. farihin Semail, B. Saad, S. Kamaruzaman, W.N. Abdullah, N.A. Rahim, M. Miskam, S.H. Loh, N. Yahaya, Molecularly imprinted silica gel incorporated with agarose polymer matrix as mixed matrix membrane for separation and preconcentration of sulfonamide antibiotics in water samples, *Talanta.* (2019). doi:10.1016/j.talanta.2019.02.096.
- [84] Y. Huang, M. Lu, H. Li, M. Bai, X. Huang, Sensitive determination of perfluoroalkane sulfonamides in water and urine samples by multiple monolithic fiber solid-phase microextraction and liquid chromatography tandem mass spectrometry, *Talanta.* (2019). doi:10.1016/j.talanta.2018.09.004.
- [85] C.K. Cheong, P. Hajeb, S. Jinap, M.R. Ismail-Fitry, Sulfonamides determination in chicken meat products from Malaysia, *Int. Food Res. J.* (2010).
- [86] Mehtabuddin, A.A. Mian, T. Ahmad, S. Nadeem, Z.I. Tanveer, J. Arshad, Sulfonamide residues determination in commercial poultry meat and eggs, *J. Anim. Plant Sci.* (2012).

- [87] H. Sun, A Rapid and Effective Method for Simultaneous Determination of Residual Sulfonamides and Sarafloxacin in Pork and Chicken Muscle by High Performance Liquid Chromatography with Accelerated Solvent Extractionâ€“Solid Phase Extraction Cleanup, *J. Chromatogr. Sep. Tech.* (2012). doi:10.4172/2157-7064.1000154.
- [88] H. Zhao, M. Ding, Y. Gao, W. Deng, Determination of sulfonamides in pork, egg, and chicken using multiwalled carbon nanotubes as a solid-phase extraction sorbent followed by ultra-performance liquid chromatography/tandem mass spectrometry, *J. AOAC Int.* (2014). doi:10.5740/jaoacint.13-133.
- [89] Y.P. Song, L. Zhang, G.N. Wang, J.X. Liu, J. Liu, J.P. Wang, Dual-dummy-template molecularly imprinted polymer combining ultra performance liquid chromatography for determination of fluoroquinolones and sulfonamides in pork and chicken muscle, *Food Control.* (2017). doi:10.1016/j.foodcont.2017.07.002.
- [90] X.L. Hou, Y.L. Wu, T. Yang, X.D. Du, Multi-walled carbon nanotubes-dispersive solid-phase extraction combined with liquid chromatography-tandem mass spectrometry for the analysis of 18 sulfonamides in pork, *J. Chromatogr. B Anal. Technol. Biomed. Life Sci.* (2013). doi:10.1016/j.jchromb.2013.04.014.
- [91] L. Xia, L. Liu, X. Lv, F. Qu, G. Li, J. You, Towards the determination of sulfonamides in meat samples: A magnetic and mesoporous metal-organic framework as an efficient sorbent for magnetic solid phase extraction combined with high-performance liquid chromatography, *J. Chromatogr. A.* (2017). doi:10.1016/j.chroma.2017.04.004.
- [92] X. Liu, Y. Tong, L. Zhang, Tailorable yolk-shell Fe<sub>3</sub>O<sub>4</sub>@graphitic carbon submicroboxes as efficient extraction materials for highly sensitive determination of trace sulfonamides in food samples, *Food Chem.* (2020). doi:10.1016/j.foodchem.2019.125369.
- [93] H. Yu, H. Mu, Y.M. Hu, Determination of fluoroquinolones, sulfonamides, and tetracyclines multiresidues simultaneously in porcine tissue by MSPD and HPLC-DAD, *J. Pharm. Anal.* (2012). doi:10.1016/j.jpha.2011.09.007.
- [94] G.N. Wang, L. Zhang, Y.P. Song, J.X. Liu, J.P. Wang, Application of molecularly imprinted polymer based matrix solid phase dispersion for determination of fluoroquinolones, tetracyclines and sulfonamides in meat, *J. Chromatogr. B Anal. Technol. Biomed. Life Sci.* (2017). doi:10.1016/j.jchromb.2017.09.034.
- [95] C.H. Wen, S.L. Lin, M.R. Fuh, Determination of sulfonamides in animal tissues by modified QuEChERS and liquid chromatography tandem mass spectrometry, *Talanta.* (2017). doi:10.1016/j.talanta.2016.11.006.

- [96] Z. Yan, B. Hu, Q. Li, S. Zhang, J. Pang, C. Wu, Facile synthesis of covalent organic framework incorporated electrospun nanofiber and application to pipette tip solid phase extraction of sulfonamides in meat samples, *J. Chromatogr. A*. (2019). doi:10.1016/j.chroma.2018.11.039.
- [97] S. Dluhošová, I. Borkovcová, L. Kaniová, L. Vorlová, Sulfonamide Residues: Honey Quality in the Czech Market, *J. Food Qual.* (2018). doi:10.1155/2018/2939207.
- [98] Á. Tölgyesi, R. Berky, K. Békési, S. Fekete, J. Fekete, V.K. Sharma, Analysis of sulfonamide residues in real honey samples using liquid chromatography with fluorescence and tandem mass spectrometry detection, *J. Liq. Chromatogr. Relat. Technol.* (2013). doi:10.1080/10826076.2012.685911.
- [99] J.M. Storey, S.B. Clark, A.S. Johnson, W.C. Andersen, S.B. Turnipseed, J.J. Lohne, R.J. Burger, P.R. Ayres, J.R. Carr, M.R. Madson, Analysis of sulfonamides, trimethoprim, fluoroquinolones, quinolones, triphenylmethane dyes and methyltestosterone in fish and shrimp using liquid chromatography-mass spectrometry, *J. Chromatogr. B Anal. Technol. Biomed. Life Sci.* (2014). doi:10.1016/j.jchromb.2014.09.009.
- [100] M.E. Dasenaki, N.S. Thomaidis, Multi-residue determination of seventeen sulfonamides and five tetracyclines in fish tissue using a multi-stage LC-ESI-MS/MS approach based on advanced mass spectrometric techniques, *Anal. Chim. Acta.* (2010). doi:10.1016/j.aca.2010.04.034.
- [101] K.S.D. Nunes, M.R. Assalin, J.H. Vallim, C.M. Jonsson, S.C.N. Queiroz, F.G.R. Reyes, Multiresidue Method for Quantification of Sulfonamides and Trimethoprim in Tilapia Fillet by Liquid Chromatography Coupled to Quadrupole Time-of-Flight Mass Spectrometry Using QuEChERS for Sample Preparation, *J. Anal. Methods Chem.* (2018). doi:10.1155/2018/4506754.
- [102] Q. Shen, R. Jin, J. Xue, Y. Lu, Z. Dai, Analysis of trace levels of sulfonamides in fish tissue using micro-scale pipette tip-matrix solid-phase dispersion and fast liquid chromatography tandem mass spectrometry, *Food Chem.* (2016). doi:10.1016/j.foodchem.2015.08.050.
- [103] R. Liu, P. He, Z. Li, R. Li, Simultaneous Determination of 16 Sulfonamides in Animal Feeds by UHPLC-MS-MS, *J. Chromatogr. Sci.* (2011). doi:10.1093/chrscl/49.8.640.
- [104] W.J. Pietroń, W. Cybulski, D. Krasucka, A. Mitura, K. Kos, M. Antczak, Determination of five sulfonamides in medicated feedingstuffs by liquid chromatography with ultraviolet detection, *Bull. Vet. Inst. Pulawy.* (2013). doi:10.2478/bvip-2013-0094.
- [105] E. Patyra, M. Przeniosło-Siwczynska, K. Kwiatek, Determination of sulfonamides in feeds by high-performance liquid chromatography after fluorescamine precolumn derivatization, *Molecules.* (2019). doi:10.3390/molecules24030452.

- [106] L. Qiao, X. Zhou, Y. Zhang, A. Yu, S. Zhang, Y. Wu, Determination of trace sulfonamides in foodstuffs by HPLC using a novel mixed-mode functionalized ferrocene sorbent for solid-phase extraction cleanup, *Anal. Methods*. (2016). doi:10.1039/c6ay01291d.
- [107] A. Economou, O. Petraki, D. Tsipi, E. Botitsi, Determination of a liquid chromatography-tandem mass spectrometry method for the determination of sulfonamides, trimethoprim and dapsone in honey and validation according to Commission Decision 2002/657/EC for banned compounds, *Talanta*. (2012). doi:10.1016/j.talanta.2012.03.058.
- [108] W.H. Tsai, H.Y. Chuang, H.H. Chen, Y.W. Wu, S.H. Cheng, T.C. Huang, Application of sugaring-out extraction for the determination of sulfonamides in honey by high-performance liquid chromatography with fluorescence detection, *J. Chromatogr. A*. (2010). doi:10.1016/j.chroma.2010.10.008.
- [109] T.A. Catelani, I.V. Tóth, J.L.F.C. Lima, L. Pezza, H.R. Pezza, A simple and rapid screening method for sulfonamides in honey using a flow injection system coupled to a liquid waveguide capillary cell, *Talanta*. (2014). doi:10.1016/j.talanta.2013.12.034.
- [110] E. Dubreil-Chéneau, Y. Pirotais, E. Verdon, D. Hurtaud-Pessel, Confirmation of 13 sulfonamides in honey by liquid chromatography-tandem mass spectrometry for monitoring plans: Validation according to European Union Decision 2002/657/EC, *J. Chromatogr. A*. 1339 (2014) 128–136. doi:10.1016/j.chroma.2014.03.003.
- [111] M. Sajid, N. Na, M. Safdar, X. Lu, L. Ma, L. He, J. Ouyang, Rapid trace level determination of sulfonamide residues in honey with online extraction using short C-18 column by high-performance liquid chromatography with fluorescence detection, *J. Chromatogr. A*. (2013). doi:10.1016/j.chroma.2013.09.020.
- [112] A. von Eyken, D. Furlong, S. Arooni, F. Butterworth, J.F. Roy, J. Zweigenbaum, S. Bayen, Direct injection high performance liquid chromatography coupled to data independent acquisition mass spectrometry for the screening of antibiotics in honey, *J. Food Drug Anal.* (2019). doi:10.1016/j.jfda.2018.12.013.
- [113] İ. Kivrak, Ş. Kivrak, M. Harmandar, Development of a rapid method for the determination of antibiotic residues in honey using UPLC-ESI-MS/MS, *Food Sci. Technol.* (2016). doi:10.1590/1678-457X.0037.
- [114] W. Nie, F. Wang, R. Hao, L. Zhang, Q. Chen, F. Wei, X. Li, R. Loffredo, Z. Liu, Y. Liu, New method of aqueous two phase with solid phase extraction (ATP-SPE) for detection of sulfonamides, *Microchem. J.* 150 (2019) 104076. doi:10.1016/J.MICROC.2019.104076.



## Chapter 2: Graphene-functionalized melamine sponges for microextraction of sulfonamides from food and environmental samples

### 2.1 Introduction

It is an undeniable fact that carbon-based nanomaterials are being extensively used in analytical applications [1]. A large number of them have been investigated as sorbents in sample preparation, including fullerenes, carbon nanotubes, nanofibers, nanohorns, and graphene, as well as their chemically-modified analogs. The characteristic structures of carbon-based nanomaterials allow them to interact with molecules via non-covalent forces, such as hydrogen bonding,  $\pi$ - $\pi$  stacking, electrostatic forces, van der Waals forces, and hydrophobic interactions. Taking into account the aforementioned possibilities, carbon-based nanomaterials have found a wide range of applications in different sample preparation techniques. Although the reasons for the selection of a particular allotrope over another are still being discussed, a wide variety of carbon-based materials is available and applicable to analytical procedures.

Among the various carbon-based nanomaterials that have been developed, graphene has sparked interest due to its intriguing properties. Graphene, discovered in 2004, is a novel and particularly fascinating carbon material, which has motivated an exponential amount of research from both the experimental and theoretical scientific communities in recent years [2]. Graphene is a two-dimensional nanomaterial comprised of  $sp^2$ -hybridized carbon atoms that are arranged in a honeycomb pattern [3]. It has a very high specific surface area (single-layer graphene:  $\sim 2630 \text{ m}^2 \text{ g}^{-1}$  [4]), extraordinary electrical, optical, thermal and mechanical properties. Owing to its planar structure and the high specific surface area, it is able to interact with molecules from both sides of its planar sheets via non-covalent forces [5]. On the other hand, graphene is insoluble and poorly disperses in all solvents, owing to strong electrostatic van der Waals interactions. This hinders its potential as a sorbent in analytical chemistry. However, graphene oxide (the oxidized

form of graphene) possesses multiple oxygen-containing groups (such as hydroxyl, carboxyl, and epoxy), which make it easily dispersible in water and it forms stable colloidal solutions [3,4,6]. Owing to their different polarities, due to their different functional groups, graphene can be used in reversed-phase extraction procedures, whereas graphene oxide can be used in normal-phase extraction procedures. Graphene possesses an extensive  $\pi$  delocalized electron system which has a strong affinity for (aromatic) ring structures. Thus, graphene has a high affinity for organic compounds [6].

Among others, it is reported that graphene can serve as an excellent adsorbent for SAs due to the hydrophobic and electrostatic interactions, which can be developed between them [7,8]. In this context, a few graphene-based nanocomposites have been used to develop new sample pre-treatment methods, under the principles of pipette-tip extraction [7,9] and solid-phase extraction [10]. However, the negligible dispersibility of graphene in aqueous media is a major drawback, when it is used as an adsorbent in microextraction procedures, resulting in limitations of its use [5]. Additionally, its employment in classical solid-phase extraction procedures is also limited due to: (i) the escape of tiny graphene sheets from the cartridge and (ii) the irreversible formation of agglomerates during sample passing stage [6]. To overcome these problems, graphene nanoparticles are rendered magnetic, so as they can be utilized in magnetic solid-phase extraction procedures [11–13]. An alternative of the magnetic graphene-based nanomaterials is to “immobilize” graphene onto bulk materials and employ them as a whole in extraction procedures. Cardador et al. supported graphene onto cotton fibers and then modified graphene sheets with aminosilica nanoparticles to extract polycyclic aromatic hydrocarbons, phthalates, musks, phenolic endocrine disruptors and haloacetic acids [6]. Similarly, Montesinos et al. prepared cotton-supported graphene as an extraction material, which can be employed for the extraction of multiclass pesticides from environmental waters [14]. Samanidou et al. coated cellulose-based substrates with graphene using a sol-gel procedure [15]. The modified cellulose substrate was used in a fabric sorptive phase extraction of bisphenol A and some residual monomers (e.g.



glycerolatedimethacrylate) from cow and human milk samples. The above studies are representative examples showcasing the merits of immobilizing nanomaterials in bulk, fabric substrates.

Although numerous different fabrics can be used (e.g. cotton, polyurethane foam, silk, etc.) to immobilize nanomaterials, the repeatable use can reduce their mechanical strength [16]. Therefore, more durable and low-cost materials are needed to overcome this hindrance. One such material is melamine sponge (MeS). MeS is a three-dimensional, low density, foam-like material made of formaldehyde-melamine-sodium bisulfite copolymer. It has an open-hole structure, high porosity (>99%), excellent wettability and negligible cost [17]. So far, MeS functionalizations with graphene have been reported, with the aim to alter the hydrophilicity of the resulting sponge and render them suitable for dye or oil absorption applications [18,19]. The functionalization processes reported are time-consuming and are completed in multiple steps, while in some cases they need sophisticated equipment [20,21]. In this chapter, the functionalization of MeS with graphene, employing a single-step, microwave-assisted hydrothermal process, is discussed. The graphene-functionalized MeS (GMeS) was used as an adsorbent to extract SAs from milk, egg and environmental water.

## 2.2 Material and methods

### 2.2.1 Chemicals and reagents

- Melamine sponge is commercially available and was bought from a local market.
- Sulfadiazine, sulfamerazine, sulfamethazine, and sulfacetamide (purities >99%) were purchased from Alfa Aesar (Karlsruhe, Germany).
- Sulfapyridine, sulfamethoxy-pyridazine, sulfachloropyridazine, sulfamethoxazole, sulfadimethoxine (purities >99%) were purchased from Aldrich (Sigma–Aldrich–Hellas, Greece)
- Graphite powder (99.9%) (Sigma–Aldrich–Hellas)
- H<sub>2</sub>SO<sub>4</sub> (96% w/w) (Sigma–Aldrich–Hellas)
- H<sub>3</sub>PO<sub>4</sub> (85% w/w) (Sigma–Aldrich–Hellas)
- HCl (37% w/w) (Sigma–Aldrich–Hellas)
- Trichloroacetic acid (Sigma–Aldrich–Hellas)
- H<sub>2</sub>O<sub>2</sub> (30% w/w) (Sigma–Aldrich–Hellas)
- Solvents (at least of analytical grade) (Sigma–Aldrich–Hellas).

Stock standard solutions of each compound were prepared in acetonitrile (ACN), at concentrations of 1.0 mg mL<sup>-1</sup>. Further dilutions were made in H<sub>2</sub>O:ACN (70:30, v/v). All solutions were stored in screw-capped, amber-glass vials, at -18 °C.

### 2.2.2 Instrumentation

Chromatographic separation and analysis were carried out on a Shimadzu HPLC system coupled to a Diode Array Detector (DAD). The system consisted of an LC20AD pump, a CTO 10AS column oven and an SPD-M20A DAD. The column used for separation was a Hypersil ODS (250 × 4.6 mm, 5 μm), kept at 30 °C. Injection volume was 20 μL, using a Rheodyne injector. The mobile phase consisted of water (A) and ACN (B), containing 0.1% (v/v) formic acid. The analytes were separated following a gradient elution program: from 10% to 35% B, in 30 min. The flow rate of the mobile phase was set at 1.0 mL min<sup>-1</sup>. The

detector was set at a wavelength range of 200–360 nm. Data acquisition and processing were carried out using an LC-solution software version 1.21. Peak identification was based on the comparison of retention times and UV spectra (recorded at 270 nm) with those of the authentic compounds.

The X-ray diffraction (XRD) analysis was performed on a D8 Advance diffractometer from Bruker AXS (Madison, USA) using CuK $\alpha$  ( $\lambda=1.5406$  Å) radiation. Centrifugation was conducted with a PrO-Research centrifuge (Centurion, Sci., West Sussex, UK).

### 2.2.3 Graphene oxide (GO) synthesis

Graphene oxide was synthesized following a previously reported method [22]. Briefly, 133 mL of a mixture containing conc. H<sub>2</sub>SO<sub>4</sub>/H<sub>3</sub>PO<sub>4</sub> (9:1 v/v) was added to a blend of graphite powder (1.0 g) and KMNO<sub>4</sub> (6.0 g). The resulting solution was stirred for 24 h, at ~50 °C. After cooling down to room temperature, 130 mL of water containing 6 mL of H<sub>2</sub>O<sub>2</sub>, was added in an ice bath, under vigorous stirring. The solution was left to settle overnight and then the supernatant was decanted away. The residue was stirred for 3 h at room temperature, after the addition of 30 mL of conc. HCl. The mixture was centrifuged at 4000 rpm, for 10 min and washed several times with double distilled water (DDW), till pH~5.5. Then, the remaining solid was washed three times with 25 mL of ethanol, followed by centrifugation. Finally, ethanol was discarded and the remaining GO was dried at 60 °C overnight.

### 2.2.4 Functionalization of melamine sponges

A commercially available melamine sponge was cut into cubes of 1×1×1 cm, which were rinsed with methanol and left to dry. Then, each cube was dipped in a GO dispersion (5 mg mL<sup>-1</sup>) containing 150 μg mL<sup>-1</sup> of hydrazine so that to soak up the maximum volume and then it was placed in a glass beaker. The cubes were microwaved for 2 min at 2000 W and subsequently, they were placed in an oven, at 120 °C, for 3 h to dry and were stored at room temperature, until use.

### 2.2.5 Extraction procedure

Prior to extraction, the GMeS cube was preconditioned by immersing, successively, once in methanol and three times in distilled water. After that, the GMeS cube was placed in 10 mL of sample, properly prepared (see section 2.6) and stirred for 30 min, at 600 rpm. After extraction, the GMeS was removed and placed in a syringe cartridge, where it was rinsed extensively with water and squeezed with the plunger to wash the sample away. The analytes were desorbed by adding 2×1 mL of ACN containing ammonia (5% v/v). The eluent was evaporated to dryness, under a gentle nitrogen stream. The residue was reconstituted in 100 µL of H<sub>2</sub>O: ACN mixture (70:30 v/v), ultrasonicated for 1 min and injected into the HPLC system.

### 2.2.6 Sample preparation

A 15-mL portion of milk (blank or spiked) was first defatted by centrifugation at 4 °C, at 4000 rpm, for 10 min. The upper and sedimented phases were discarded and the remaining liquid was collected. Next, proteins were precipitated and pH was adjusted to 3.0 by adding 1 mL of trichloroacetic acid aqueous solution (15% w/v) for every 10 mL of defatted milk and the solution was vortexed for 1 min, followed by centrifugation, at 4000 rpm, for 5 min. The supernatant was retracted and sodium chloride (6% w/v) was added. After repeating the centrifugation process, the supernatant was collected (approximately 10 mL) and SAs were extracted using the proposed GMeS procedure.

Whole eggs were homogenized by magnetic stirring (i.e. 900 rpm for 5 min). Then, 1.0 g was transferred to a glass beaker, followed by the addition of 8.7 mL of DDW, 0.3 mL trichloroacetic acid aqueous solution (15% w/v) (used for pH adjustment) and sodium chloride (6% w/v). Finally, the mixture was stirred for 1 min, before SAs extraction.

Lake water was not subjected to any pre-treatment (except pH adjustment to 3.0 and sodium chloride (6% w/v) addition) and SAs were extracted directly from 10 mL of the test sample, using the GMeS.

## 2.3 Results and discussion

### 2.3.1 Characterization of the GMeS

Melamine sponge can serve as a propitious material for functionalization with nanomaterials due to its open-hole structure, high porosity, and amino-groups, which are plentiful. The amino-groups of melamine can interact with the epoxy, hydroxyl and carboxyl groups of GO, under certain conditions, rendering the graphene coating stable [19]. The morphology of MeS and GMeS was observed by SEM and relevant images are shown in Figures 3-5. It can be seen (Figure 3A) that the unmodified sponge possesses a 3D interconnected porous framework, with the diameter of the skeleton ranging between 5  $\mu\text{m}$  and 7  $\mu\text{m}$  and the pore size lying between 100  $\mu\text{m}$  and 200  $\mu\text{m}$ , thus facilitating the embodiment of GO. Moreover, it can be seen (Figure 4(B–E)) that the skeleton of the non-functionalized MeS is very smooth. After hydrothermal treatment–functionalization, the GMeS maintains its 3D structure but the diameter of the melamine skeleton is reduced to 3–5  $\mu\text{m}$  (Figure 5(A, B)). Graphene sheets are embodied in the skeleton of the MeS by virtue of the dispersibility of GO in water and the ease of soaking it up by MeS. Graphene sheets are interconnected as well as connected with the melamine skeleton (Figure 3C) due to the favorable chemical interfacial interaction between the GO (epoxy-groups) and the melamine skeleton (amino-groups). The surface of the resulting graphene sheets is full of wrinkles (Figure 5(D–H)), which is a typical characteristic of its structure.

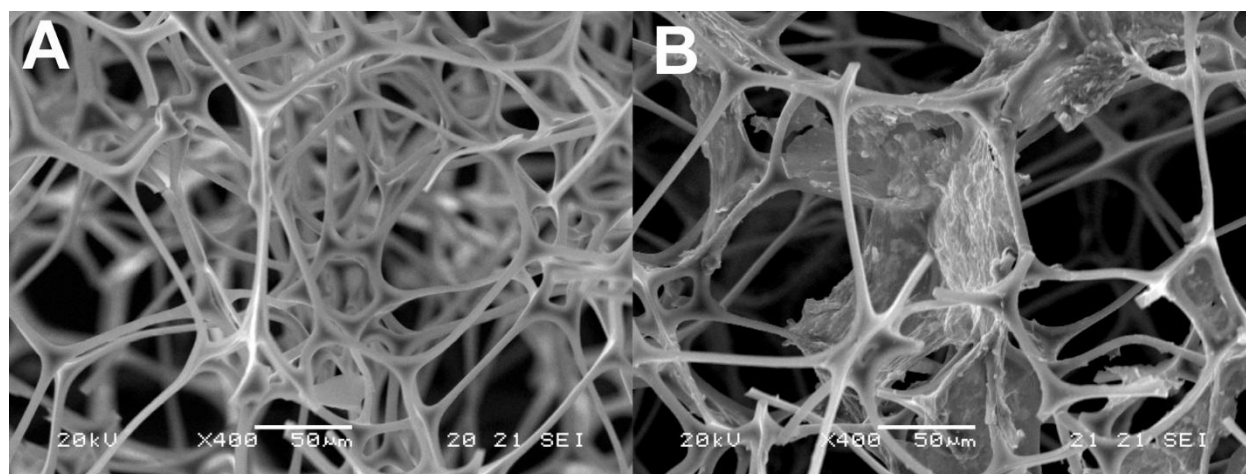


Figure 3: SEM images of MeS before (A) and after (B) functionalization with graphene (GMeS).

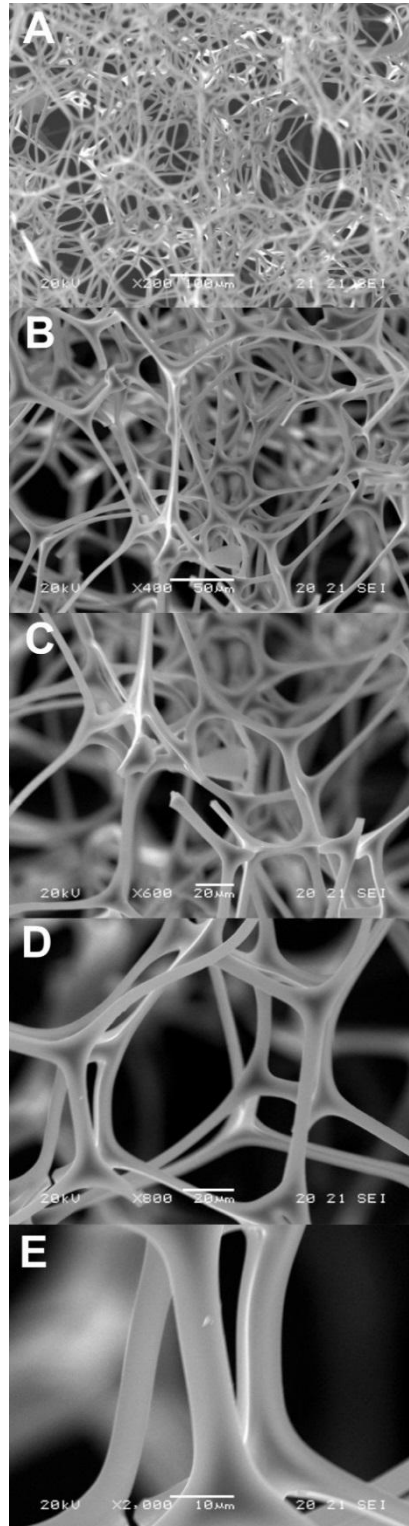


Figure 4: SEM images of MeS in various magnifications (scale bars: 100  $\mu\text{m}$  (A), 50  $\mu\text{m}$  (B), 20  $\mu\text{m}$  (C), 20  $\mu\text{m}$  (D) and 10  $\mu\text{m}$  (E)).

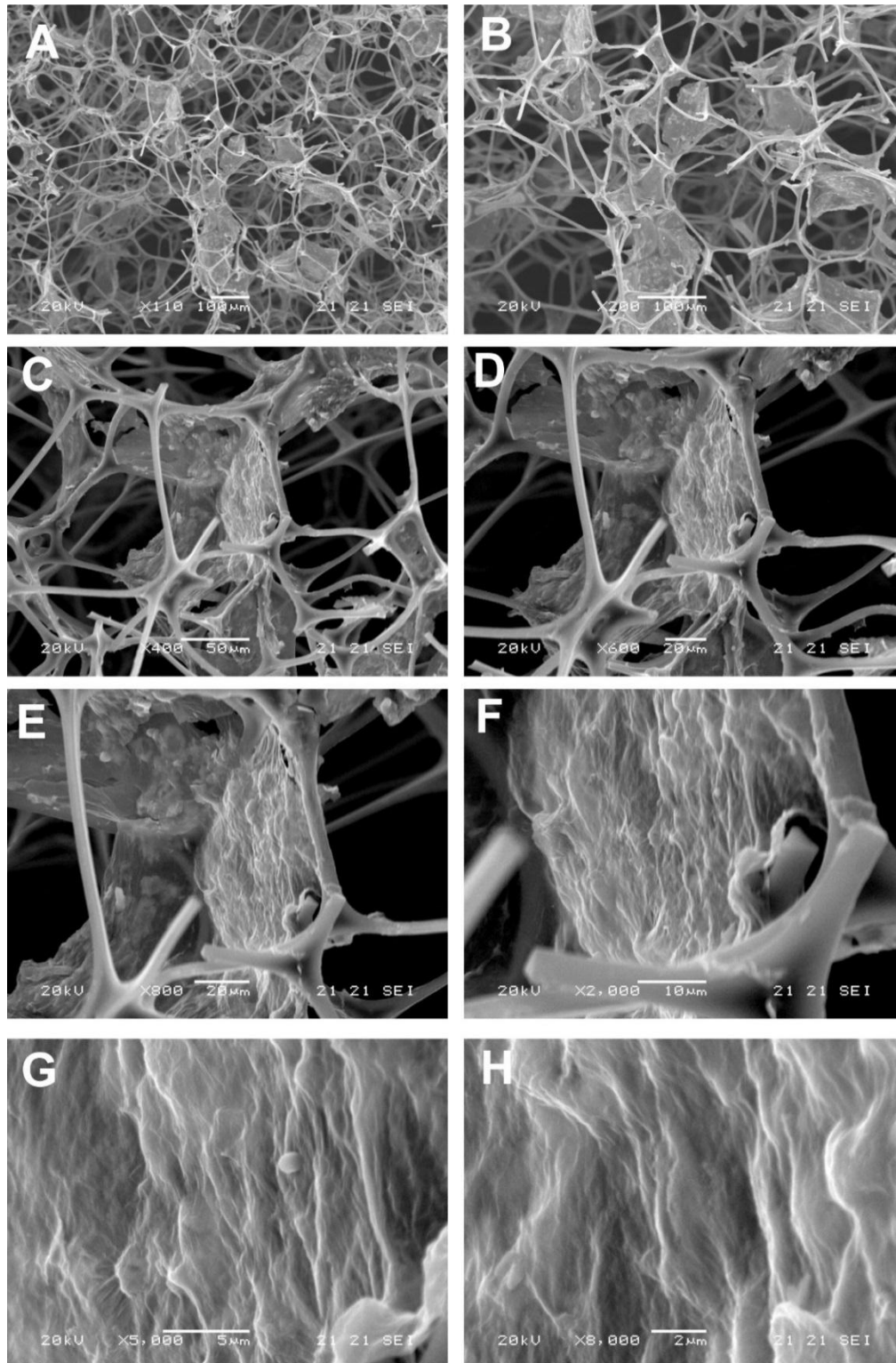


Figure 5: SEM images of GMeS in various magnifications (scale bars: 100  $\mu\text{m}$  (A), 100  $\mu\text{m}$  (B), 50  $\mu\text{m}$  (C), 20  $\mu\text{m}$  (D), 20  $\mu\text{m}$  (E) 10  $\mu\text{m}$  (F) 5  $\mu\text{m}$  (G) and 5  $\mu\text{m}$  (H)).

The XRD spectra of the pristine graphite, the synthesized GO and the GMeS can be seen in Figures 6-8, respectively. A sharp diffraction peak at  $26.6^\circ$  in the XRD spectrum of graphite is attributed to interlayer (002) spacing ( $d = 0.33$  nm). After oxidation, the peak shifted to  $10.1^\circ$ , bespeaking an increase in the interlayer spacing ( $d = 0.88$  nm) due to the addition of oxygen-containing groups. Finally, the XRD spectrum of the GMeS shows that the (002) diffraction peak was red-shifted to  $21.9^\circ$  ( $d = 0.41$  nm) and broadened, suggesting a reduction in the quantity of oxygen-containing groups (the interlayer spacing is lower than in GO but higher than in graphite) and successful reduction of GO to graphene.

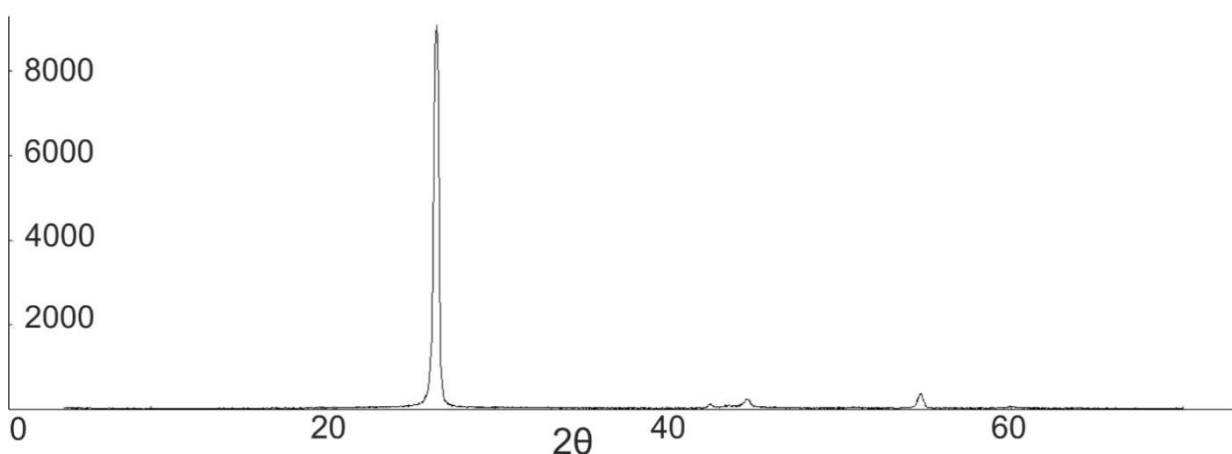


Figure 6: XRD spectrum of graphite.

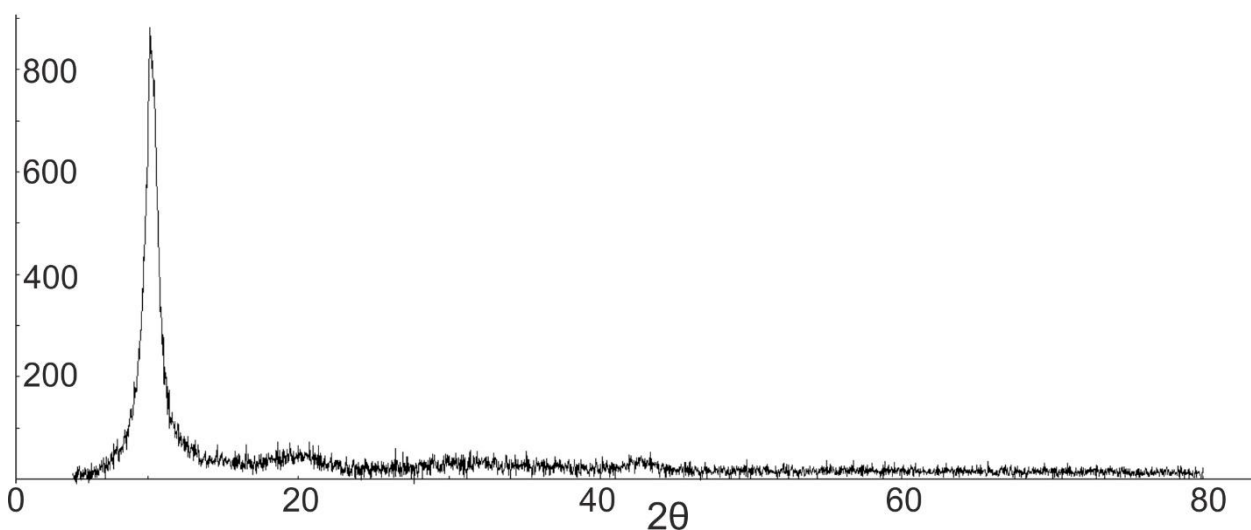


Figure 7: XRD spectrum of graphene oxide.



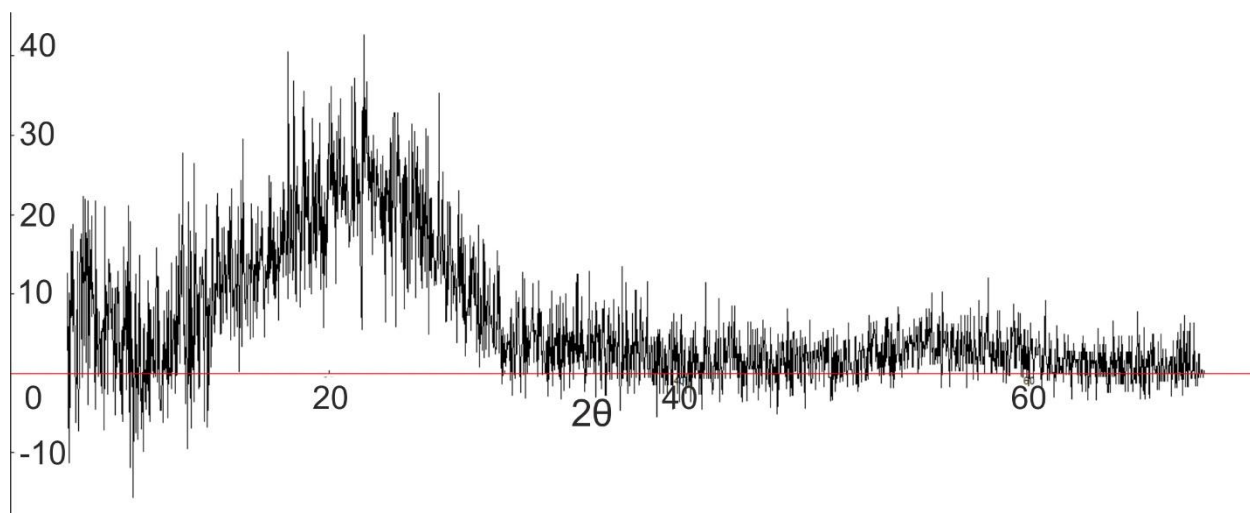
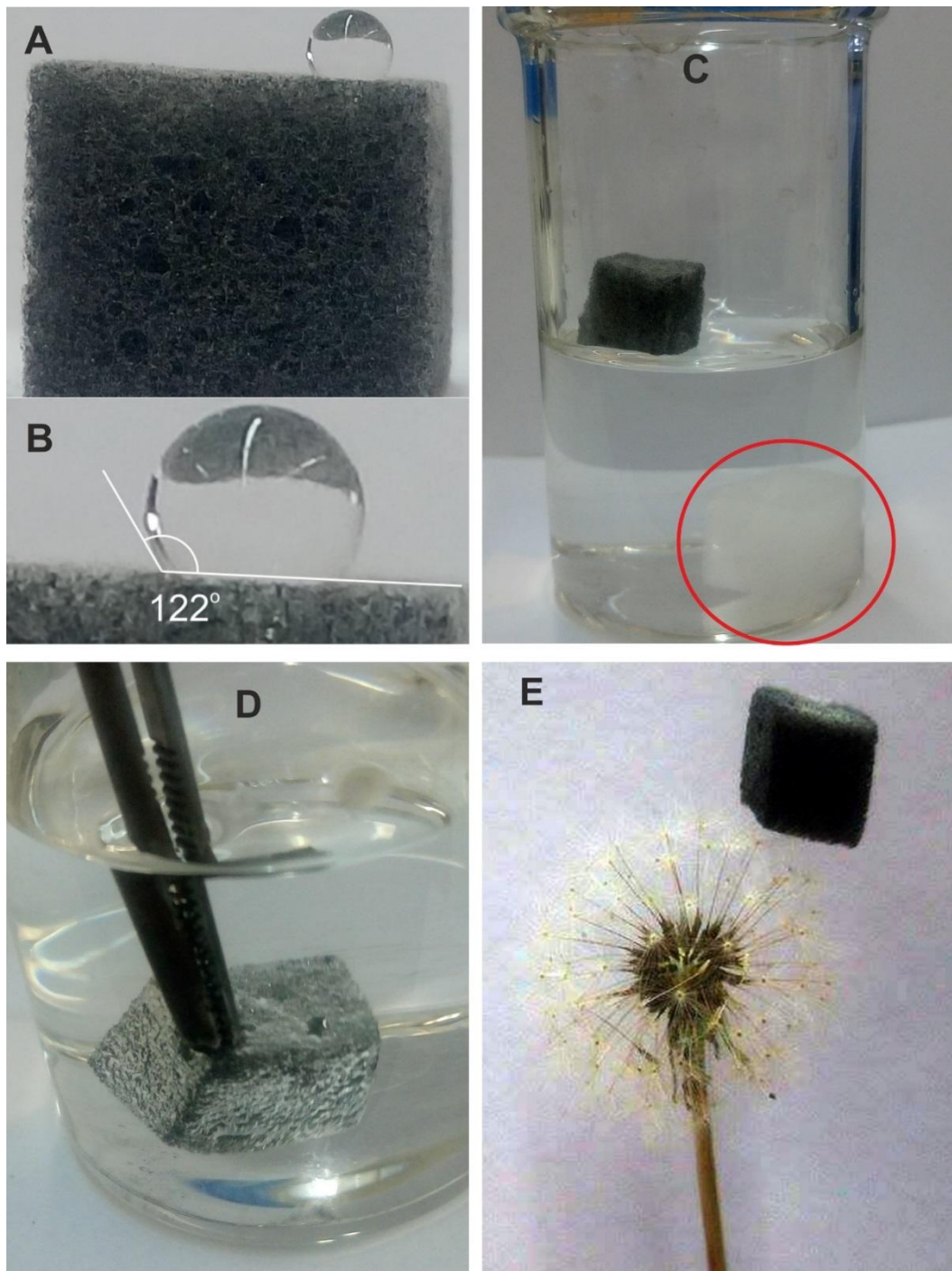


Figure 8: XRD spectrum of GMeS.

Due to the functionalization with graphene, the white color of MeS turned black and the material was rendered hydrophobic. The GMeS showed great water repellency, (Figure 9(A, B)), and it is obvious that a water droplet on the surface of the GMeS has an almost spherical shape with a contact angle of around  $122^\circ$ . The highly hydrophobic nature of the GMeS did not allow it to sink to the bottom of a beaker filled with water (upper left sponge, in Figure 9(C)), in contrast to the non-functionalized MeS (lower right corner, in Figure 9(C)). When external force was applied to submerge the GMeS in the water, the surface of the GMeS was similar to a silver mirror when viewed from a glancing angle (Figure 9(D)) [17]. Finally, the GMeS was extremely light (Figure 9(E)).

### 2.3.2 Synthesis optimization

Parameters of the synthesis were optimized in order to achieve maximum adsorption of SAs. The evaluation of the adsorption capability of the resulting GMeS in each case was conducted in a DDW test sample, spiked with  $200 \mu\text{g L}^{-1}$  of each sulfonamide. The criterion used for the evaluation was the extraction yield of the total SAs content. The parameters optimized were: the concentration of the GO in the aqueous dispersion, the quantity of hydrazine, the microwave intensity and time and the number of coatings.



*Figure 9: Images of (A) water droplet on the surface of a GMeS, (B) contact angle of a water droplet, (C) MeS and GMeS in a glass beaker with water, (D) GMeS immersed in water and (E) GMeS on top of a dandelion flower.*

### 2.3.2.1 GO concentration and hydrazine quantity

The concentration of GO in the dispersion was the first parameter to be optimized since the adsorption of SAs is directly affected by the quantity of the extracting phase. Six aqueous dispersions containing 1, 2, 3, 4, 5 and 10 mg mL<sup>-1</sup> of GO were prepared and used to functionalize the pristine MeS. The results showed that 5 mg mL<sup>-1</sup> of GO is sufficient to achieve the optimum adsorption (Figure 10). A higher concentration of GO (10 mg mL<sup>-1</sup>) did not improve the extraction yield. To ensure that the functionalization is indispensable for the extraction of analytes, a non-functionalized MeS was tested for its capability to adsorb the selected SAs. The results showed that without functionalization, the MeS could adsorb up to 5% of the total concentration of SAs.

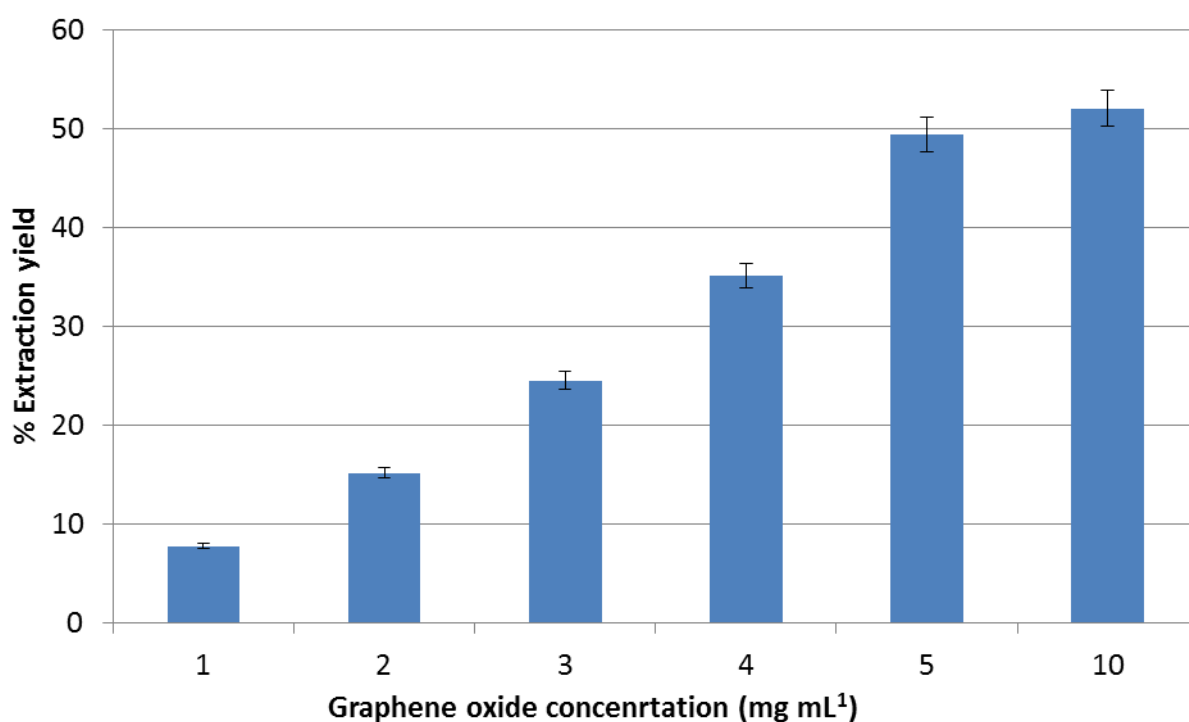


Figure 10: % Extraction yield of GMeS cubes, prepared using various concentrations of GO.

In the proposed synthesis, hydrazine was used to convert GO into its reduced form, since it has been shown that the oxygen content of GO interferes with the adsorption of SAs because water clusters are formed around the oxygen-containing groups, thus reducing the number of available adsorption sites [8]. On the basis of the above discussion, the adsorption on GMeS, synthesized in the presence of different quantities of hydrazine, showed that even at a low concentration of hydrazine ( $50 \mu\text{g mL}^{-1}$ ) the adsorption can be enhanced by almost 30% (Figure 11). An increase in hydrazine up to  $150 \mu\text{g mL}^{-1}$  showed a further increase in the adsorption efficiency, whereas even higher concentrations proved to be hardly suitable. Although Liu et al. have suggested that the adsorption of SAs on reduced GO is based on hydrophobic and electrostatic interactions between graphene and SAs, in our case,  $\pi$ - $\pi$  and hydrophobic interactions were found to be the dominant adsorption mechanisms (more details are discussed later on) [8]. The two aforementioned mechanisms justify the noticeable enhancement in adsorption efficiency which is achieved by GMeS, functionalized in the presence of hydrazine.

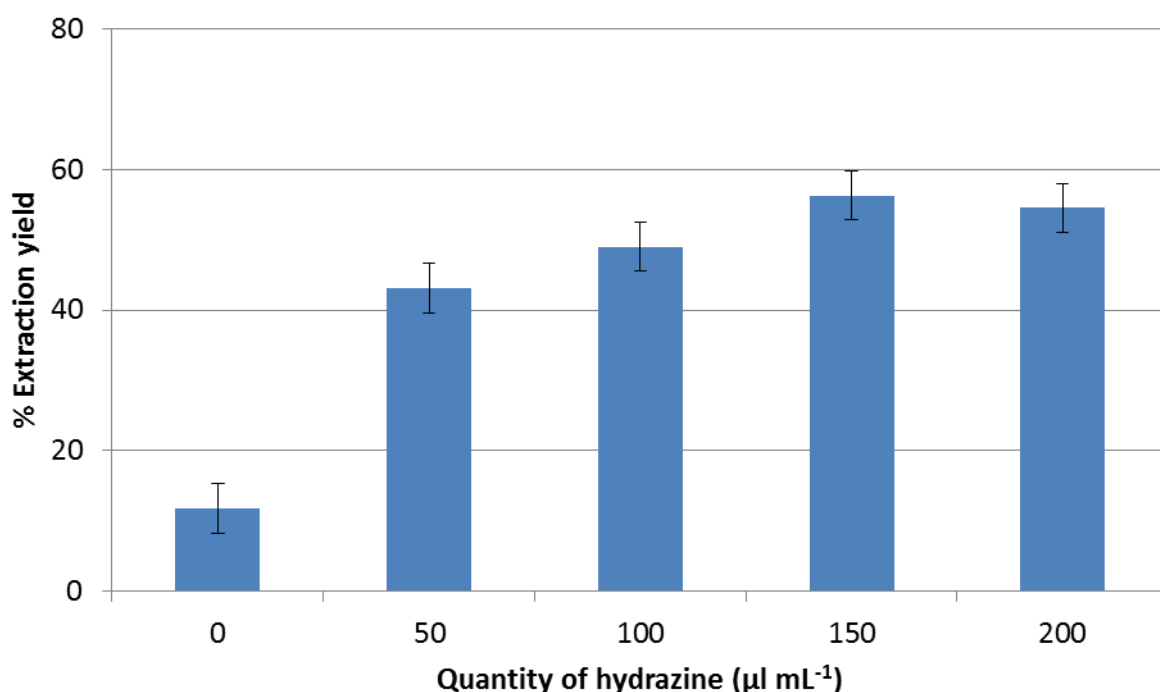


Figure 11: % Extraction yield of GMeS cubes, prepared using various amounts of hydrazine.

### 2.3.2.2 Microwave intensity and time

The intensity of the microwaves was studied in the range of 400–2000 W. It was found that the higher the intensity of the microwave, the better the adsorption capability of the resulting GMeS (Figure 12). This can be justified by the fact that microwaves assist the reduction of GO, resulting in better adsorption of SAs. Furthermore, the microwave time was examined, as the last important parameter affecting the functionalized sponge. The results showed that 2-min irradiation is adequate to achieve maximum adsorption efficiency of SAs (it is enhanced by almost 20% as compared to 1-min irradiation) (Figure 13). During the above experiments, visual inspection of the GMeS showed that short irradiation time and/or low microwave intensity resulted in functionalized MeS whose color was not black. In this case, the dark color of the adsorber faded effortlessly when GMeS was placed in water because graphene is loosely retained on the sponge.

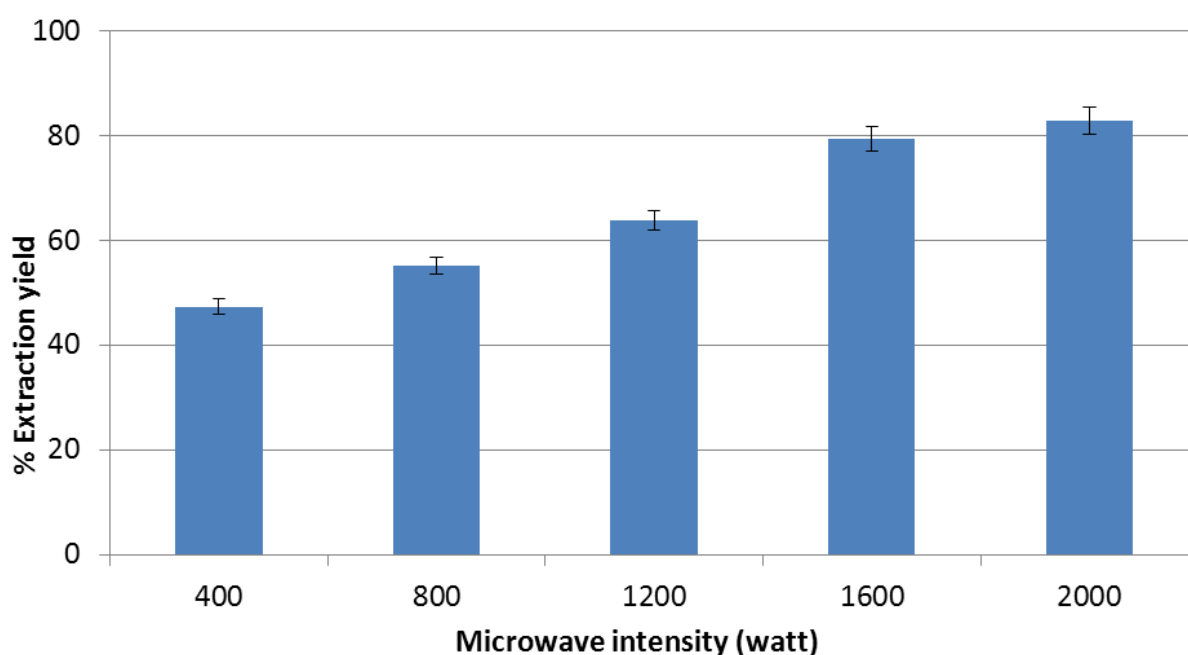


Figure 12: % Extraction yield of GMeS cubes, prepared using various intensities of microwave.

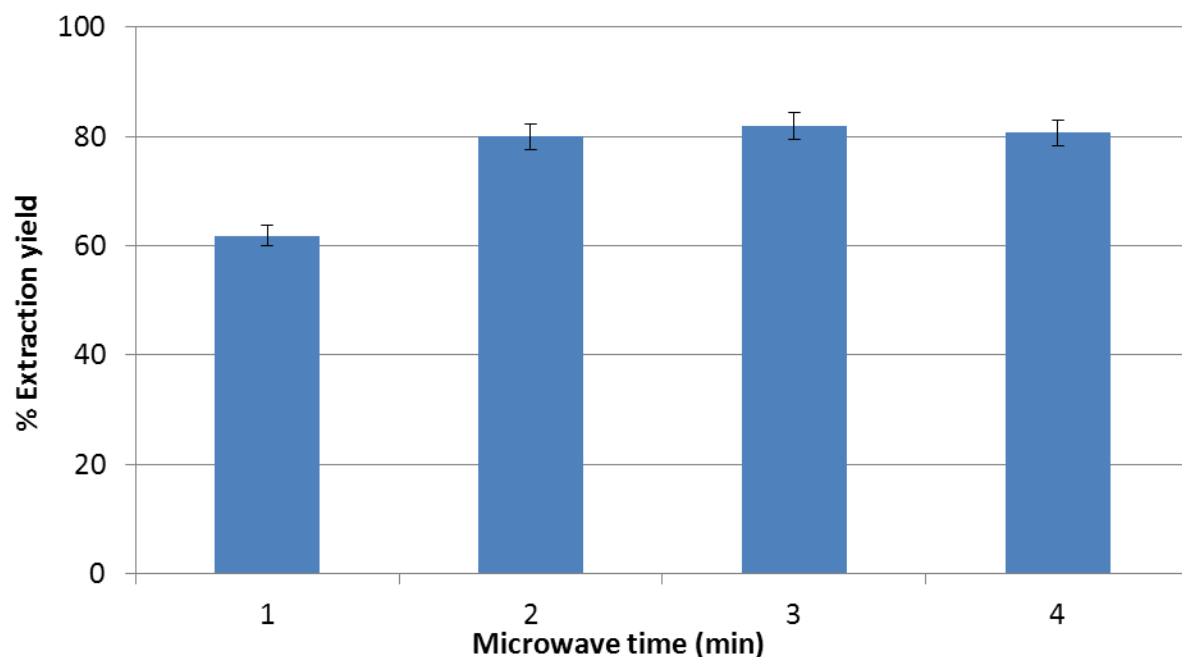


Figure 13: % Extraction yield of GMeS cubes, prepared by microwaving for various times.

#### 2.3.2.3 Times of functionalization

The final step of the synthesis was to examine whether more repetitions of the immersion-irradiation procedure could possibly benefit the adsorption. Four GMeS were prepared, each one functionalized once more than the previous one, resulting in GMeS functionalized up to four times. The adsorption results showed no significant difference among the four different GMeS (less than 5% increase of adsorption between the GMeS functionalized once and four times). Therefore, there is no need to repeat the functionalization process.

According to the results presented so far, it can be inferred that the proposed synthetic procedure is fast (it takes only 2 min), while the resulting GMeS can efficiently extract the SAs in a reproducible way (the reproducibility of the extraction from different batches of functionalized GMeS was satisfactory). The simplicity of the method, in terms of equipment and precursors, renders the synthetic procedure advantageous, compared to previously reported methods [18–21,23]. Furthermore, the cost-effective and energy-efficient character and the maximum incorporation of the precursor materials are major benefits that bring the method one step closer to adhering to the principles of green chemistry.

### 2.3.3 Optimization of the proposed procedure

All optimization experiments were carried out in aqueous standard solutions of the SAs. The optimum conditions established were subsequently checked for their appropriateness to the rest of the matrixes. Relevant experiments evidenced that these conditions were also applicable to milk and egg matrixes. In addition, matrix-matched testing samples of milk and egg samples were analyzed to achieve optimum and reproducible extraction results.

#### 2.3.3.1 Effect of the pH-mechanism of interaction

Sulfonamides contain two different ionizable functional groups, one aromatic amine (able to gain a proton) and a sulfonamide group with an acidic nitrogen atom (able to release a proton) [24]. Variations in the pH of a solution result in ionization of the two functional groups, thus altering the dominant form of the SAs. As a result, the different ionization forms are expected to interact, to a different degree, with the sorbent. This hypothesis is validated by the results presented in Figure 14, where it is obvious that the optimum pH for SAs adsorption is 3.0, whereas lower or higher pH values result in a decrease in the adsorption for all SAs. At pH values close to 3.0, the neutral and positively-charged forms of SAs co-exist according to their dissociation constant and speciation diagrams [25,26] while the remaining oxygen groups on the surface of graphene are also in their neutral form, according to the point of zero charge of graphene [8]. Taking into account the above and the reduced adsorption of SAs when they exist in their anionic or cationic form, strong electrostatic interactions between SAs and GMeS are not anticipated and hence, this is not the dominant mechanism of adsorption, in this case. However, weak electrostatic interactions (van der Waals forces) due to the presence of electronegative atoms in the SAs could not be ruled out, suggesting that they can serve as an auxiliary adsorption mechanism.

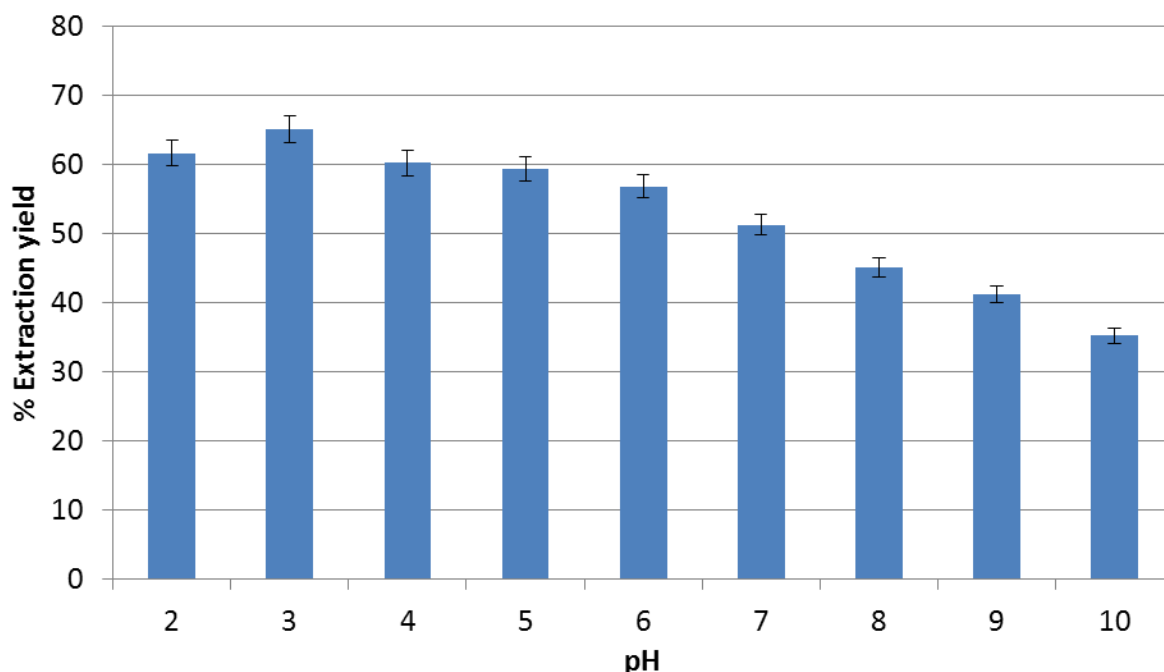


Figure 14: Effect of the pH on the adsorption efficiency of the SAs on GMeS.

According to Peng et al., the  $\pi$ - $\pi$  interactions between molecules containing aromatic rings and graphene are increased as the number of aromatic rings increases [27]. All of the SAs studied have two aromatic rings in their structure, except for sulfacetamide – which has only one – yet its sorption behavior was comparable to those of the rest of SAs. Therefore,  $\pi$ - $\pi$  interactions between the SAs and the graphene of GMeS are present and expected to be sufficiently strong [27]. This notion is strengthened also by the findings in Section 3.2.1., since the reduction of GO towards graphene increased the aromatic ring area, available for  $\pi$ - $\pi$  interactions, significantly, increasing the adsorption potential of the GMeS. Another possible mechanism of interaction between SAs and GMeS is the hydrophobic interaction. Since SAs are ionizable, as mentioned above, their hydrophobicity (expressed by  $\log K_{ow}$ ) is affected by the pH value of the solution. The neutral form of the SAs has the highest  $\log K_{ow}$  compared to the two ionizable forms and hence higher hydrophobicity. Although at pH 3.0 the neutral and the cationic form of SAs co-exist, the major fraction is the neutral species. Hence, hydrophobic interactions are



likely to be established and contribute to the overall adsorption process. This is further justified by the adsorption behavior of individual sulfonamides, under the same pH conditions (data not shown). From the data, it seems that the higher the  $\log K_{ow}$  value of a SA, the higher its adsorption percentage. For instance, for sulfamethoxypyridazine and sulfadimethoxine (whose main difference is a methoxy group and the difference between their  $\log K_{ow}$  values is higher than 1), it was found that the latter was adsorbed more effectively by nearly 10%. Likewise, in the case of sulfapyridine and sulfamerazine, the former was adsorbed by almost 8% more than the latter. On the contrary, sulfadiazine, sulfamerazine and sulfamethazine (differing in the number of methyl groups and in the slightly higher  $\log K_{ow}$  values of the two last) it was found that all three compounds were equally adsorbed (less than 2% difference in their adsorption), strengthening the above claim. All the above are also in agreement with the aforementioned results, according to which GO-functionalized MeS (less hydrophobic) showed lower adsorption efficiency compared to the GMeS (more hydrophobic). Overall, it can be concluded that the two governing mechanisms of adsorption are  $\pi$ - $\pi$  and hydrophobic interactions, whereas a minor contribution from electrostatic interactions cannot be ruled out.

#### ***2.3.3.2 Effect of the ionic strength***

The effect of ionic strength on the adsorption of SAs was examined using NaCl and Na<sub>2</sub>SO<sub>4</sub> at concentrations ranging between 0 and 10% (w/v) (Figures 15 and 16). The addition of NaCl up to 6% (w/v) caused a salting-out effect, resulting in an increase of the extraction efficiency. However, higher concentrations proved to be deteriorating, since they slightly decreased the extraction efficiency by 10%. In this case, as the salt content increases, cation- $\pi$  interactions between sodium cations and the aromatic rings of the SAs or the aromatic rings of the graphene from GMeS may contribute to the decrease in the overall efficiency. When Na<sub>2</sub>SO<sub>4</sub> was used to increase the ionic strength, the extraction was significantly reduced, compared to the absence of salt. It is likely that cation- $\pi$  interactions are expected to be twice as higher as in the case of NaCl. Moreover, an increase in the viscosity of the solution is probable (due to an increase in the electrostatic

attraction between water layers) decelerating the percolation of the solution into the holes of the GMeS and resulting in lower mass transfer [28]. Consequently, the addition of 6% (w/v) NaCl was selected to enhance the overall extraction efficiency.

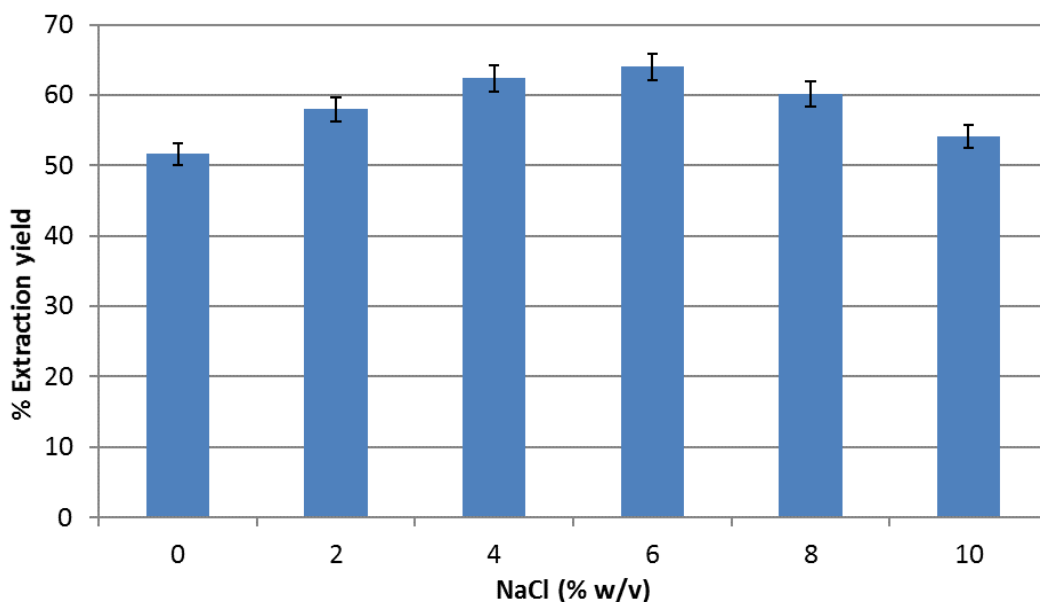


Figure 15: Adsorption efficiency of the proposed method in solutions containing different concentrations of NaCl.

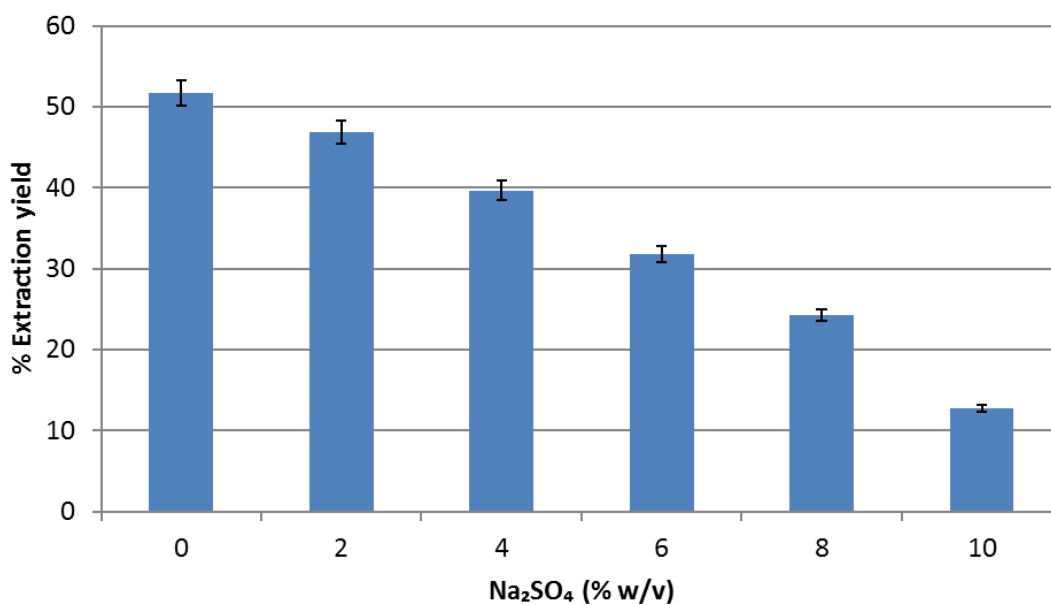


Figure 16: Adsorption efficiency of the proposed method in solutions containing different concentrations of Na<sub>2</sub>SO<sub>4</sub>.

### *2.3.3.3 Other extraction parameters*

The effect of temperature on the extraction efficiency was examined. The extraction was conducted at three different temperatures (i.e. 25, 35 and 45 °C) and the results showed a minor increase (<4%) of the extraction efficiency, at 45 °C. This could be possibly due to the lower viscosity of the aqueous solution at this temperature. However, since the increase is trivial no temperature control was selected simplifying the procedure.

Next, the volume of the solution, the concentration of analytes, the amount of GMeS and stirring time and rate were optimized. Although the optimum stirring rate is associated with all of the above parameters, the experiments conducted showed that low stirring rates (< 500 rpm) were inadequate to achieve high extraction yields. High stirring rates (>700 rpm) hindered the extraction process, due to the formation of a deep vortex in the glass beaker, which sucked down the GMeS. In this way, not all the surface of the GMeS was in contact with the solution, thus uniform percolation through the holes of the GMeS was not feasible. Additionally, due to the vortex formation, air bubbles were trapped on the surface of the GMeS, blocking the percolation of the solution and levitating the GMeS to the surface of the solution. A stirring rate of 600 rpm was found proper.

As regards sample volume, 10, 20 and 30 mL were tested for their suitability. Initially, three different test volumes were spiked with the same amount of analytes (20 µL from a stock standard solution containing 100 µg mL<sup>-1</sup> of each SA) and the results showed a gradual decrease in the extraction efficiency, as the volume increases (a decrease from ~11% to 22% by increasing the volume from 20 mL to 30 mL). Afterward, at a constant concentration of analytes, the adsorption was tested by altering simultaneously the sample volume (10–30 mL), the number of GMeS cubes (1/2, 1 and 2) and the stirring time (10, 20 and 30 min), resulting in a total of 27 experiments. The results are portrayed in Figure 17. It is noteworthy that instead of using a single GMeS cube of 2 × 2 × 2 cm it was more preferable to use two 1 × 1 × 1 cm cubes so that the solution can percolate

more efficiently through the network of holes in smaller cubes. From the results, it is obvious that the optimum extraction yield is achieved using one GMeS for 10 mL of sample, after 30 min of stirring. Although it would be expected that the extraction yield achieved by two GMeS would be higher, this was not the case with sample volumes of 10 and 20 mL. Due to the small volumes used, the two GMeS could not move freely in the glass beaker and the percolation into the holes was possibly not efficient, resulting in an overall less efficient adsorption. When 30 mL were used, the two GMeS showed higher adsorption compared to the half and the entire GMeS cube, but still, it was not as satisfactory (14% less), as in the case of 10 mL, with one GMeS for 30 min.

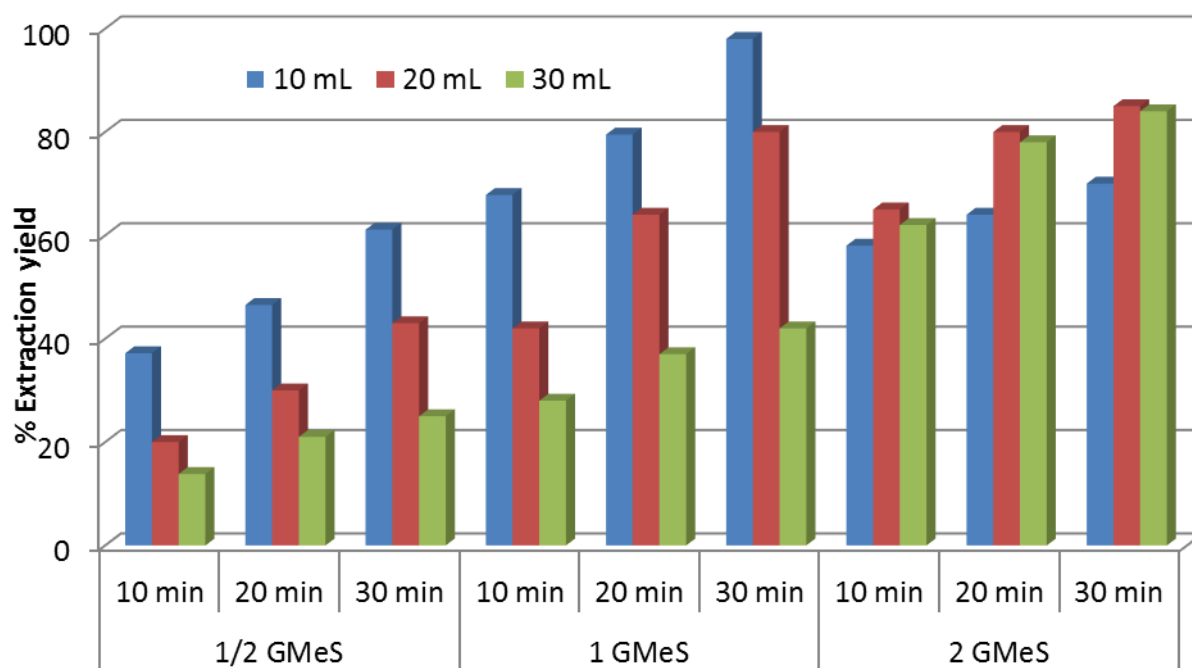


Figure 17: Effect of sample volume, amount of adsorbent and extraction time on the efficiency of the method.

#### 2.3.3.4 Elution conditions

The desorption of SAs was optimized by testing ACN, methanol, and isopropanol. Among the three solvents tested, ACN exhibited the highest elution yield, followed by methanol and isopropanol. However, the elution was still inadequate to recover quantitatively all

analytes from GMeS (recoveries <40%). In order to increase the desorption yield, formic acid or ammonia was added at various percentages (1–5% v/v) to increase the acidity or alkalinity. The addition of formic acid was not more efficient than pure ACN; on the contrary, the addition of 5% ammonia in ACN increased desorption yield significantly. This is reasonable and in accordance with the results from the pH optimization of adsorption since it was found that the alkaline environment does not favor the adsorption, resulting in an increase in the desorption yield. Higher concentrations of ammonia did not further improve the desorption yield, so, ACN containing 5% (v/v) ammonia was selected as the optimum elution solvent. Finally, as regards the volume of the eluent, it was found that two successive elutions with 1 mL of the solvent were adequate to completely desorb the SAs.

#### 2.3.4 Method validation

Three different matrices were used to assess the applicability of the developed method: two animal-derived foods (i.e. milk and eggs) and an environmental water sample. Before discussing the analytical merits of the method, it is worth mentioning that the chromatograms of the blank samples (Figures 18-20) are free from interfering peaks, signifying that the extraction procedure acts also as a clean-up step and highlighting the benefit of the proposed extraction procedure. The linearity of the method was evaluated by preparing matrix-matched calibration curves of spiked matrices, for all SAs, in the range of 1–200  $\mu\text{g kg}^{-1}$  for milk, 1–200  $\mu\text{g L}^{-1}$  for lake water and 10–200  $\mu\text{g kg}^{-1}$  for eggs (except sulfacetamide for which the calibration curve was prepared in the range 1–200  $\mu\text{g kg}^{-1}$ ). The equations of the calibrations curves along with the coefficients of determination and the other analytical characteristics of the method can be seen in detail, in Tables 9-11 for milk, eggs and lake water respectively, while a summary of the analytical merits is presented in Table 12.

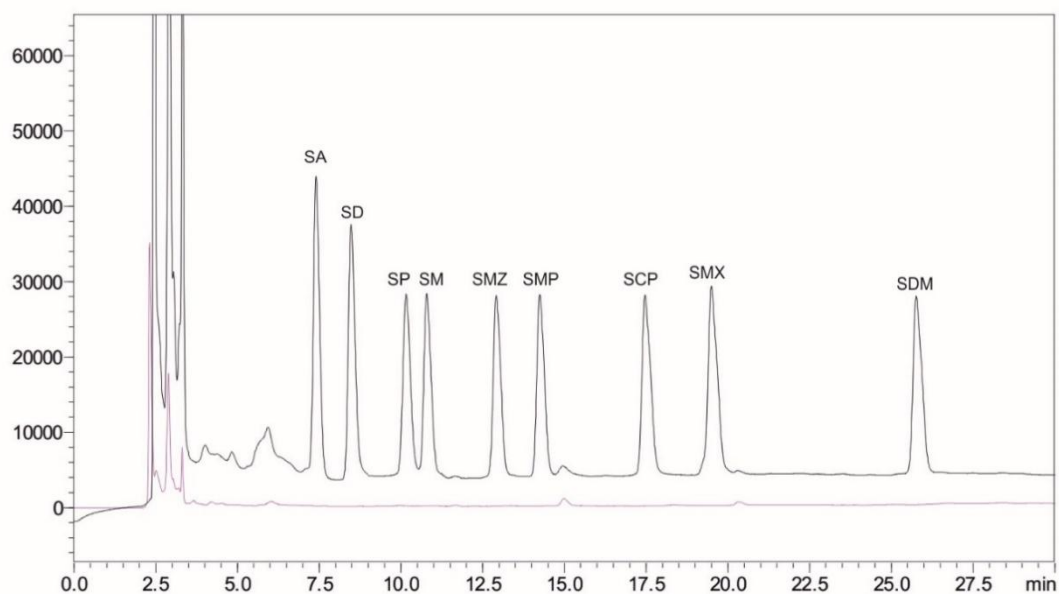


Figure 18: Chromatograms of a blank milk sample (lower chromatogram) and a spiked milk sample with  $50 \mu\text{g kg}^{-1}$  of SAs, at 270 nm. Peak assignment: sulfacetamide (SA), sulfadiazine (SD), sulfapyridine (SP), sulfamerazine (SM), sulfamethazine (SMZ), sulfamethoxyipyridazine (SMP), sulfachloropyridazine (SCP), sulfamethoxazole (SMX), sulfadimethoxine (SDM).

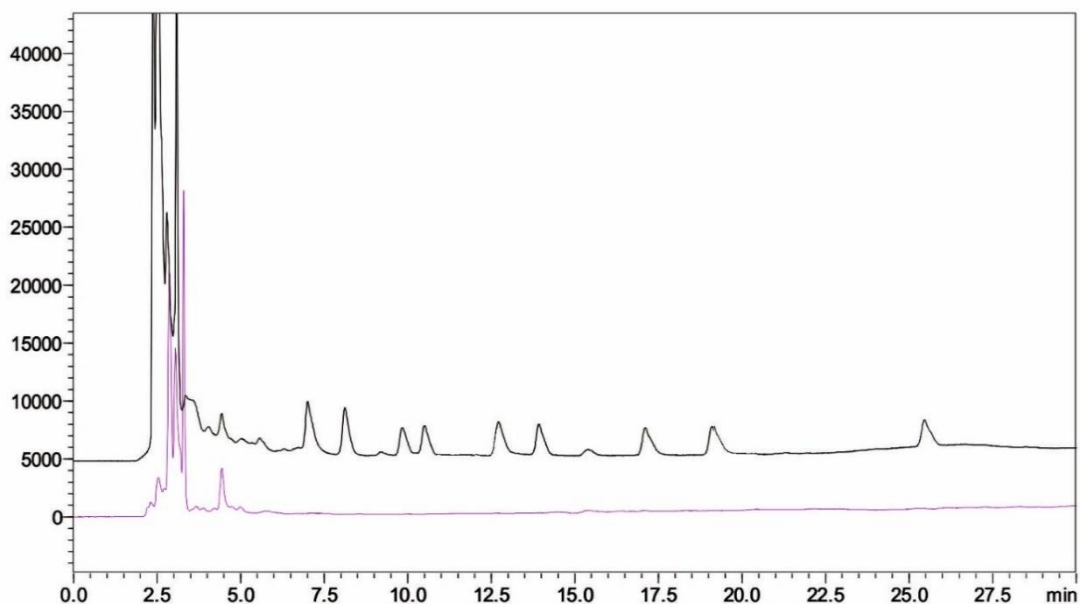


Figure 19: Chromatograms (270 nm) of a blank egg sample (lower chromatogram) and an egg sample spiked with  $50 \mu\text{g kg}^{-1}$  of SAs (upper chromatogram).

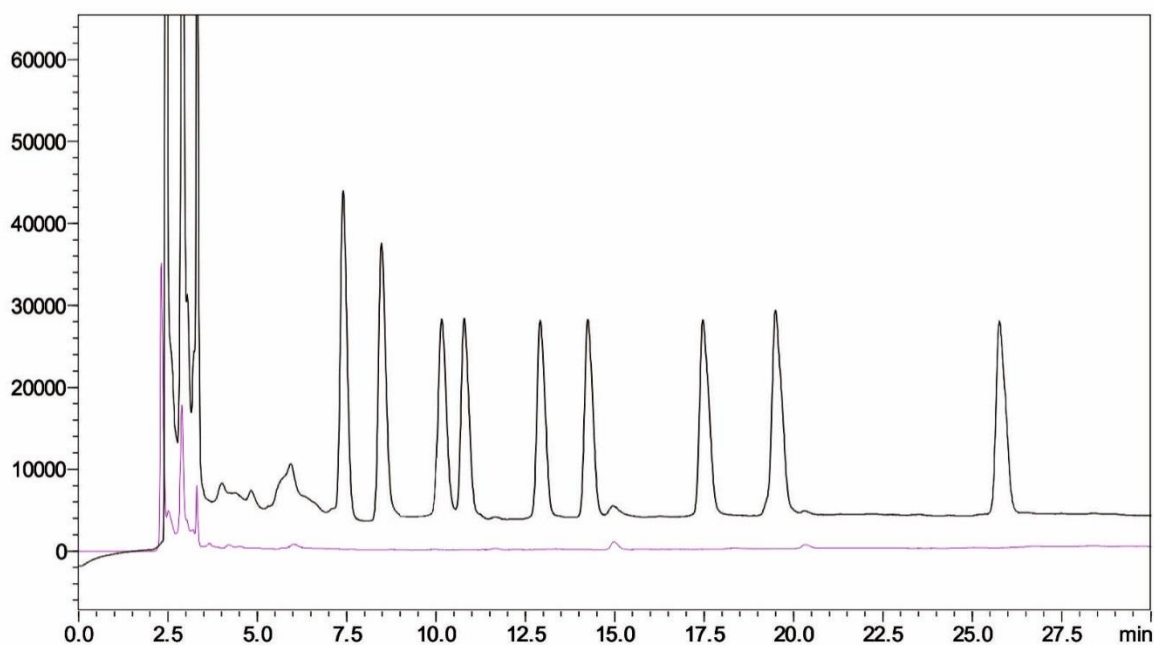


Figure 20: Chromatograms (270 nm) of a blank lake water sample (lower chromatogram) and a lake water sample spiked with  $50 \mu\text{g L}^{-1}$  of SAs (upper chromatogram).

Linearities were calculated in the studied concentration ranges, for all SAs, with the coefficients of determination ( $R^2$ ) being higher than 0.9968, 0.9938 and 0.9984 in the case of milk, eggs and lake water respectively, implying good linearity. The limits of quantification (calculated as the signal-to-noise ratio  $\geq 10$ ) for the SAs ranged between  $0.31 \mu\text{g kg}^{-1}$  and  $1.3 \mu\text{g kg}^{-1}$  for the food matrices and  $0.10 \mu\text{g L}^{-1}$  and  $0.29 \mu\text{g L}^{-1}$  in lake water. The precision of the method was calculated as the relative standard deviation (RSD) within-day and between three different days by analyzing three samples, spiked with a low concentration of the analytes ( $10 \mu\text{g kg}^{-1}$ ). Within-day RSD and inter-day RSD ranged between 3.1-7.9% and 3.5-10.1% for all three matrices.

Table 9: Analytical characteristics of the proposed method for SAs determination in milk; LOQ: limit of quantification, RSD: relative standard deviation, enrichment factor (ratio of the peak area after the extraction and a standard), matrix effect (calculated by the areas of spiked extraction solution and spiked matrix samples)

SAs	linear equation	coefficient of determination ( $R^2$ )	LOQ ( $\mu\text{g kg}^{-1}$ )	RSD (%)		Recovery (%)		EF	ME (%)
				within-day (n=3)	between-day (n=3×3)	10 $\mu\text{g kg}^{-1}$	100 $\mu\text{g kg}^{-1}$		
SA	$y=11166x+24831$	0.9982	0.44	7.3	8.2	91	102	99	6
SD	$y=11023x+2036$	0.9992	0.90	4.9	6.7	105	97	94	10
SP	$y=8160x+5695$	0.9971	0.50	3.2	6.6	101	97	96	16
SM	$y=8192x+2222$	0.9987	0.50	5.5	7.6	90	97	95	-1
SMZ	$y=8287x+4413$	0.9983	0.53	4.9	7.6	90	96	96	-2
SMP	$y=8483x+4780$	0.9968	0.91	6.2	8.0	92	95	97	-7
SCP	$y=9591x+3640$	0.9987	0.34	5.9	8.0	91	100	95	3
SMX	$y=9572x+4871$	0.9975	0.31	3.1	5.6	104	100	100	14
SDM	$y=9088x+6928$	0.9971	0.81	7.9	10.1	97	101	97	0



Table 10: Analytical characteristics of the proposed method for SAs determination in eggs; LOQ: limit of quantification, RSD: relative standard deviation, enrichment factor (ratio of the peak area after the extraction and a standard), matrix effect (calculated by the areas of spiked extraction solution and spiked matrix samples)

SAs	linear equation	coefficient of determination ( $R^2$ )	LOQ ( $\mu\text{g kg}^{-1}$ )	RSD (%)		Recovery (%)		EF	ME (%)
				within-day (n=3)	between-day (n=3×3)	10 $\mu\text{g kg}^{-1}$	100 $\mu\text{g kg}^{-1}$		
SA	$y=1141x+11122$	0.9956	0.96	6.8	8.0	106	108	8	7
SD	$y=944+6570.6$	0.9971	0.97	4.7	6.2	93	96	9	-9
SP	$y=723x+2732$	0.9966	1.11	3.7	6.8	95	94	8	-12
SM	$y=727x+3966$	0.9977	1.01	5.0	7.7	106	94	9	-10
SMZ	$y=870x+4891$	0.9938	1.09	5.1	6.9	98	108	10	1
SMP	$y=769x+3608$	0.9966	1.12	5.4	7.7	90	91	9	-15
SCP	$y=778.x+5102$	0.9939	1.06	6.4	8.1	90	91	9	-15
SMX	$y=869x+6795$	0.9940	1.08	3.6	5.2	91	96	10	-8
SDM	$y=746x+3209$	0.9965	1.32	6.9	9.4	93	92	10	-16

Table 11: Analytical characteristics of the proposed method for SAs determination in lake water; LOQ: limit of quantification, RSD: relative standard deviation, enrichment factor (ratio of the peak area after the extraction and a standard), matrix effect (calculated by the areas of spiked extraction solution and spiked matrix samples)

SAs	linear equation	coefficient of determination ( $R^2$ )	LOQ ( $\mu\text{g L}^{-1}$ )	RSD (%)		Recovery (%)		ME EF (%)	
				within-day (n=3)	between-day (n=3×3)	10 $\mu\text{g L}^{-1}$	100 $\mu\text{g L}^{-1}$		
SA	$y=14012x+7791$	0.9996	0.29	3.2	3.8	103	105	98	7
SD	$y=13422x+6422$	0.9990	0.27	2.7	3.5	99	100	96	7
SP	$y=10219x+3835$	0.9995	0.12	3.9	5.3	97	98	96	3
SM	$y=10206x+5511$	0.9995	0.12	3.3	4.7	97	99	99	3
SMZ	$y=10669x+12912$	0.9986	0.11	4.0	5.5	96	99	99	6
SMP	$y=11092x+12126$	0.9987	0.11	3.4	4.8	95	97	96	7
SCP	$y=11503x+3089$	0.9984	0.11	3.4	4.3	96	99	97	4
SMX	$y=12022x+12379$	0.9989	0.10	2.9	3.9	98	96	96	5
SDM	$y=11286x+14295$	0.9985	0.11	4.2	5.5	93	96	97	5

Table 12: Summary of the analytical characteristics of the developed method for each matrix; LOQ: limit of quantification, RSD: relative standard deviation, enrichment factor (ratio of the peak area after the extraction and a standard), matrix effect (calculated by the areas of spiked extraction solution and spiked matrix samples)

Matrix	Coefficient of determination (R <sup>2</sup> )	LOQ μg kg <sup>-1</sup>	RSD (%)		Recovery (%)		Enrichment factor	Matrix effect (%)
			within-day (n=3)	between-day (n=2 × 3)	10 μg kg <sup>-1</sup>	100 μg kg <sup>-1</sup>		
milk	> 0.9968	0.31-0.91	3.1-7.9	5.6-10.1	90-105	95-102	94-100	-7 – 16
egg	> 0.9938	0.96-1.32	5.0-6.9	5.2-9.4	90-106	90-108	8-10	-16 – 7
lake water	> 0.9984	0.10-0.29	2.7-4.2	3.5-5.5	93-103	96-105	96-99	3 – 7

Recoveries of the analytes were determined at two concentrations: the maximum residue limit of SAs (100 μg kg<sup>-1</sup>) and ten times lower (10 μg kg<sup>-1</sup>). They were found to be in the range of 90-106% and 90%-108% for the low and the high concentration, respectively, in all matrices. Enrichment factors (EF) were determined by calculating the ratio of the chromatographic peak area of each sulfonamide after the extraction procedure to the area of a standard solution, directly injected [29]. They were found to range between 94 and 100 for milk and lake water samples, while ten times lower enrichment factors were achieved in the case of eggs (between 8 and 10). Finally, the matrix effect was evaluated for each SA using Eq. (1), by comparing the peak areas of spiked extraction solutions (x<sub>1</sub>) with the peak areas of spiked matrices (x<sub>2</sub>), according to a previous report [29].

$$\text{Matrix effect (\%)} = \frac{x_2 - x_1}{x_1} \times 100 \quad (1)$$

As regards milk samples, it can be seen that the values range between -7% to 16%, indicating that the signal of sulfamerazine, sulfamethazine, and sulfamethoxypridazine is

suppressed. The opposite holds true for the rest of SAs. In the case of the egg, the results show that except for sulfacetamide and sulfamethazine, all analytes exhibit suppressed signals. Finally, as regards the lake water matrix effect, it was found to be relatively low causing no significant interference in the analytical procedure. Since all matrix effect values were lower than 20%, the matrix effect can be considered insignificant. As a consequence, standard calibration curves can also be used for quantification purposes, although the matrix-matched calibration is more preferable. All the aforementioned analytical merits of the proposed method advocate for a procedure that adheres to SANCO/12571/2013 guideline for both food matrices.

### 2.3.5 Comparison with other analytical methods

The method proposed herein was compared with previously reported for the detection of SAs in similar matrices, in terms of time required for adsorbent synthesis and the major analytical characteristics (i.e. linear range, LOD, RSD, recovery). As it can be seen from Table 13, most of the adsorbents employed in previous reports are complex, that is to say, more steps and consequently more time is required for their synthesis (up to 72 h has been reported) compared to the GMeS, which takes only 2 min to prepare. The analytical figures of merit of the method are comparable with those attained by other approaches involving different sample pretreatment procedures. The LODs achieved are better than those of previous methods (optical detectors) or rival them (mass spectrometric (MS) or MS/MS detectors). Moreover, the recoveries achieved are higher, the RSD is low and the proposed method is suitable for routine analysis or even more for fast screening of the SAs since it covers their maximum residue limits set. Finally, the GMeS can be reused with an observed loss of extraction capability less than 7%, but the negligible cost and effort needed to synthesize it make its reuse unnecessary.

## 2.4 Conclusions

In this study, the functionalization of MeS with graphene is described. This new type of sorbent material takes advantage of the extractive properties of graphene and is utilized to develop a simple procedure for the detection of SAs in milk, eggs and lake water. The speedy procedure for functionalization with graphene (requires only 2 min), the negation of the need for procedures of sorbent isolation (e.g. centrifugation or magnetic removal) and the absence of matrix effects render it suitable for routine analysis. The proposed extraction protocol combined with HPLC-UV determination could be applied for the sensitive analysis of trace SAs in food and environmental samples. It is conceivable that GMeS can be operative not only in the case of SAs but also for other analytes that can interact with graphene. However, this is the first time that the GMeS is utilized successfully in an extraction procedure.

Table 13: Comparison of the developed procedure with other analytical methods.

Analytes	Method	Adsorbent	Synthesis time*	Extraction time	Matrix	Linear range ( $\mu\text{g/L}$ or $\mu\text{g/Kg}$ )	LOD ( $\mu\text{g/L}$ or $\mu\text{g/Kg}$ ) (S/N = 3)	RSD (%)	Recovery (%)	Reference
SMX, SD, SMZ, SDM, SM, SM	Dispersive solid phase extraction and HPLC-UV	SMX imprinted acrylamide functionalized silica nanoparticles	~72 h	45 min (+ 10 min centrifugation)	milk	50-20000	2.81-14.6	3.5-7.5	69.8-87.4	[30]
					eggs			2.3-6.3	73.2-89.1	
SM, SML, SDX, SMX, SIX	Self-assembled solid phase extraction and HPLC-UV	Graphene oxide/chitosan	~14 h	~10 min	eggs	10-10000	0.71-0.98	5.2-13.5	75.3-105.2	[31]
					honey			4.7-12.6	81.2-101	
SD, SM, SMX, SMM, SMD, SDM, SQX	Magnetic dispersive solid phase extraction and LC-MS/MS	Magnetic multiwalled carbon nanotubes	~16 h	15 min	eggs	10-1000	1.4-2.8	73.8-96.2	74-96	[32]
SD, STZ, SMZ, SMP, SCP, SMX, SIX, SDM, SQX	Magnetic dispersive solid phase extraction and HPLC-DAD	Magnetite-embedded with silica functionalized with phenyl chains	~17 h	~20 min	milk	30-800	7-14	<10	81.8-114.9	[33]
SM, SML, SDX, SMX, SIX	Dispersive solid phase extraction and HPLC-UV	CoFe <sub>2</sub> O <sub>4</sub> -graphene	~7 h	22 min (+ 5 min precondition)	milk	20-50000	1.16-1.59	2.4-4.3	62.0-104.3	[12]

SD, SM, SMZ, SML, SMX, SDM	Stir bar sorptive extraction and HPLC-MS/MS	C <sub>18</sub> coated stir bar	~10 min	10 min (+10 min elution)	milk	0.1-2000	0.9-10.5	7.3-16.7	87-120	[34]
					milk powder				80-115	
SCP, STZ, SP, SMD, SM, SMZ, SMP, SDM, SML, SA SMM	Dispersive solid phase extraction and HPLC-MS	Magnetite/silica/poly (methacrylic acid-co-ethylene glycol dimethacrylate)	~40 h	15 sec	milk	0.05-20	0.0005-0.0495	<13	87.6-115.6	[35]
SD, SDMD, STZ	Magnetic dispersive solid phase extraction and HPLC-DAD	Fe <sub>3</sub> O <sub>4</sub> -graphene oxide	~1 h	20 min	water	200-20000	50-100	5.38-9.03	67.4-119.9	[36]
SA, SD, SP, SM, SMZ, SMP, SCP, SMX, SDM	Extraction and HPLC-DAD	Graphene-functionalized melamine sponges	2 min	30 min	milk	1-200	0.10-0.30	3.1-7.9	95-102	This method
					eggs	10-200	0.32-0.44	5.0-6.9	90-108	
					lake water	1-200	0.03-0.09	2.7-4.2	96-105	

\*Graphene oxide synthesis and drying steps were not taken into account for approximate synthesis time estimation.

The results of the above study have been published in the *Journal of Chromatography A*

Journal of Chromatography A, 1522 (2017) 1–8



Contents lists available at ScienceDirect

Journal of Chromatography A

journal homepage: [www.elsevier.com/locate/chroma](http://www.elsevier.com/locate/chroma)



Full length article

## Graphene-functionalized melamine sponges for microextraction of sulfonamides from food and environmental samples



Theodoros Chatzimitakos<sup>a</sup>, Victoria Samanidou<sup>b</sup>, Constantine D. Stalikas<sup>a,\*</sup>

<sup>a</sup> Laboratory of Analytical Chemistry, Department of Chemistry, University of Ioannina, 45110 Ioannina, Greece

<sup>b</sup> Laboratory of Analytical Chemistry, Department of Chemistry, Aristotle University of Thessaloniki, 54124 Thessaloniki, Greece

### ARTICLE INFO

#### Article history:

Received 24 July 2017

Received in revised form 1 September 2017

Accepted 19 September 2017

Available online 20 September 2017

#### Keywords:

Graphene

Melamine sponge

Sulfonamides

HPLC

Milk-egg

Microextraction

### ABSTRACT

The study describes the functionalization of melamine sponges with graphene and its use as an adsorbent for the microextraction of sulfonamides from food and environmental samples. The graphene-functionalized melamine sponge (GMeS) was prepared by an easy, one-step procedure, which complies with the principles of green chemistry and is proved advantageous over previously described methods. The applicability of the GMeS in extraction procedures was studied and an analytical method for the determination of sulfonamides in milk, eggs and lake water was developed and validated according to SANCO/12571/2013 guideline. The developed method was highly accurate and reproducible, while the limits of quantification were found to be relatively low ( $0.31\text{--}0.91\ \mu\text{g kg}^{-1}$ ,  $0.96\text{--}1.32\ \mu\text{g kg}^{-1}$  and  $0.10\text{--}0.29\ \mu\text{g L}^{-1}$  in the case of milk, eggs and lake water respectively). Furthermore, matrix effects were absent in all cases, since the microextraction procedure serves also as a clean-up step. The low cost of synthesis, the environmentally friendly conditions, the efficiency and high extraction recoveries are some additional advantages of the proposed procedure. To the best of our knowledge, this is the first time that a GMeS is prepared in a straightforward way and used for analytical purposes.

© 2017 Elsevier B.V. All rights reserved.



## 2.5 References

- [1] B.T. Zhang, X. Zheng, H.F. Li, J.M. Lin, Application of carbon-based nanomaterials in sample preparation: A review, *Anal. Chim. Acta.* 784 (2013) 1–17. doi:10.1016/j.aca.2013.03.054.
- [2] D. Chen, H. Feng, J. Li, Graphene Oxide: Preparation, Functionalization, and Electrochemical Applications, *Chem. Rev.* 112 (2012) 6027–6053. doi:10.1021/cr300115g.
- [3] R. Sitko, B. Zawisza, E. Malicka, Graphene as a new sorbent in analytical chemistry, *TrAC - Trends Anal. Chem.* 51 (2013) 33–43. doi:10.1016/j.trac.2013.05.011.
- [4] S. Ge, F. Lan, F. Yu, J. Yu, Applications of graphene and related nanomaterials in analytical chemistry, *New J. Chem.* 39 (2015) 2380–2395. doi:10.1039/c4nj01783h.
- [5] T. Chatzimitakos, C. Stalikas, Carbon-Based Nanomaterials Functionalized with Ionic Liquids for Microextraction in Sample Preparation, *Separations.* 4 (2017) 14. doi:10.3390/separations4020014.
- [6] M.J. Cardador, E. Papparizou, M. Gallego, C. Stalikas, Cotton-supported graphene functionalized with aminosilica nanoparticles as a versatile high-performance extraction sorbent for trace organic analysis, *J. Chromatogr. A.* 1336 (2014) 43–51. doi:10.1016/j.chroma.2014.02.013.
- [7] N. Sun, Y. Han, H. Yan, Y. Song, A self-assembly pipette tip graphene solid-phase extraction coupled with liquid chromatography for the determination of three sulfonamides in environmental water, *Anal. Chim. Acta.* 810 (2014) 25–31. doi:10.1016/j.aca.2013.12.013.
- [8] F.F. Liu, J. Zhao, S. Wang, B. Xing, Adsorption of sulfonamides on reduced graphene oxides as affected by pH and dissolved organic matter, *Environ. Pollut.* 210 (2016) 85–93. doi:10.1016/j.envpol.2015.11.053.
- [9] H. Yan, N. Sun, S. Liu, K.H. Row, Y. Song, Miniaturized graphene-based pipette tip extraction coupled with liquid chromatography for the determination of sulfonamide residues in bovine milk, *Food Chem.* 158 (2014) 239–244. doi:10.1016/j.foodchem.2014.02.089.
- [10] L. Chen, T. Zhou, Y. Zhang, Y. Lu, Rapid determination of trace sulfonamides in fish by graphene-based SPE coupled with UPLC/MS/MS, *Anal. Methods.* 5 (2013) 4363–4370. doi:10.1039/c3ay40523k.
- [11] Y.B. Luo, Z.G. Shi, Q. Gao, Y.Q. Feng, Magnetic retrieval of graphene: Extraction of sulfonamide antibiotics from environmental water samples, *J. Chromatogr. A.* 1218 (2011) 1353–1358. doi:10.1016/j.chroma.2011.01.022.

- [12] Y. Li, X. Wu, Z. Li, S. Zhong, W. Wang, A. Wang, J. Chen, Fabrication of CoFe<sub>2</sub>O<sub>4</sub>-graphene nanocomposite and its application in the magnetic solid phase extraction of sulfonamides from milk samples, *Talanta*. 144 (2015) 1279–1286. doi:10.1016/j.talanta.2015.08.006.
- [13] Z. Li, Y. Li, M. Qi, S. Zhong, W. Wang, A.J. Wang, J. Chen, Graphene-Fe<sub>3</sub>O<sub>4</sub> as a magnetic solid-phase extraction sorbent coupled to capillary electrophoresis for the determination of sulfonamides in milk, *J. Sep. Sci.* 39 (2016) 3818–3826. doi:10.1002/jssc.201600308.
- [14] I. Montesinos, A. Sfakianaki, M. Gallego, C.D. Stalikas, Graphene-coated cotton fibers as a sorbent for the extraction of multiclass pesticide residues from water and their determination by gas chromatography with mass spectrometry, *J. Sep. Sci.* 38 (2015) 836–843. doi:10.1002/jssc.201400957.
- [15] V. Samanidou, O. Filippou, E. Marinou, A. Kabir, K.G. Furton, Sol-gel-graphene-based fabric-phase sorptive extraction for cow and human breast milk sample cleanup for screening bisphenol A and residual dental restorative material before analysis by HPLC with diode array detection, *J. Sep. Sci.* 40 (2017) 2612–2619. doi:10.1002/jssc.201700256.
- [16] J. Lv, B. Wang, Q. Ma, W. Wang, L. Zeng, M. Li, A. Li, X. Zhao, J. Li, Q. Xiang, H. Li, Y. Li, C. Zhao, D. Xiang, Preparation of superhydrophobic melamine sponges decorated with polysiloxane nanotubes by plasma enhanced chemical vapor deposition (PECVD) method for oil/water separation, *Mater. Res. Express*. 5 (2018). doi:10.1088/2053-1591/aad0e1.
- [17] Y. Yang, Y. Deng, Z. Tong, C. Wang, Multifunctional foams derived from poly(melamine formaldehyde) as recyclable oil absorbents, *J. Mater. Chem. A*. 2 (2014) 9994–9999. doi:10.1039/c4ta00939h.
- [18] J. Zhao, Q. Guo, X. Wang, H. Xie, Y. Chen, Recycle and reusable melamine sponge coated by graphene for highly efficient oil-absorption, *Colloids Surfaces A Physicochem. Eng. Asp.* 488 (2016) 93–99. doi:10.1016/j.colsurfa.2015.09.048.
- [19] T. Liu, G. Zhao, W. Zhang, H. Chi, C. Hou, Y. Sun, The preparation of superhydrophobic graphene/melamine composite sponge applied in treatment of oil pollution, *J. Porous Mater.* 22 (2015) 1573–1580. doi:10.1007/s10934-015-0040-8.
- [20] K. Hou, Y. Jin, J. Chen, X. Wen, S. Xu, J. Cheng, P. Pi, Fabrication of superhydrophobic melamine sponges by thiol-ene click chemistry for oil removal, *Mater. Lett.* (2017). doi:10.1016/j.matlet.2017.05.062.
- [21] S. Song, H. Yang, C. Su, Z. Jiang, Z. Lu, Ultrasonic-microwave assisted synthesis of stable reduced graphene oxide modified melamine foam with superhydrophobicity and high oil adsorption capacities, *Chem. Eng. J.* (2016). doi:10.1016/j.cej.2016.07.086.

- [22] M. Serrano, T. Chatzimitakos, M. Gallego, C.D. Stalikas, 1-Butyl-3-aminopropyl imidazolium-functionalized graphene oxide as a nanoadsorbent for the simultaneous extraction of steroids and  $\beta$ -blockers via dispersive solid-phase microextraction, *J. Chromatogr. A.* 1436 (2016) 9–18. doi:10.1016/j.chroma.2016.01.052.
- [23] Q. Du, Y. Zhou, X. Pan, J. Zhang, Q. Zhuo, S. Chen, G. Chen, T. Liu, F. Xu, C. Yan, A graphene-melamine-sponge for efficient and recyclable dye adsorption, *RSC Adv.* (2016). doi:10.1039/c6ra08412e.
- [24] N. Şanlı, S. Şanlı, G. Özkan, A. Denizli, Determination of pKa values of some sulfonamides by LC and LC-PDA methods in acetonitrile-water binary mixtures, *J. Braz. Chem. Soc.* (2010).
- [25] X. Yu, L. Zhang, M. Liang, W. Sun, pH-dependent sulfonamides adsorption by carbon nanotubes with different surface oxygen contents, *Chem. Eng. J.* (2015). doi:10.1016/j.cej.2015.05.044.
- [26] R.M.P. Leal, L.R.F. Alleoni, V.L. Tornisiello, J.B. Regitano, Sorption of fluoroquinolones and sulfonamides in 13 Brazilian soils, *Chemosphere.* (2013). doi:10.1016/j.chemosphere.2013.03.018.
- [27] B. Peng, L. Chen, C. Que, K. Yang, F. Deng, X. Deng, G. Shi, G. Xu, M. Wu, Adsorption of Antibiotics on Graphene and Biochar in Aqueous Solutions Induced by  $\pi$ - $\pi$  Interactions, *Sci. Rep.* (2016). doi:10.1038/srep31920.
- [28] T. Chatzimitakos, C. Binellas, K. Maidatsi, C. Stalikas, Magnetic ionic liquid in stirring-assisted drop-breakup microextraction: Proof-of-concept extraction of phenolic endocrine disrupters and acidic pharmaceuticals, *Anal. Chim. Acta.* 910 (2016) 53–59. doi:10.1016/j.aca.2016.01.015.
- [29] N.S. Pano-Farias, S.G. Ceballos-Magaña, R. Muñiz-Valencia, J.M. Jurado, Á. Alcázar, I.A. Aguayo-Villarreal, Direct immersion single drop micro-extraction method for multi-class pesticides analysis in mango using GC–MS, *Food Chem.* (2017). doi:10.1016/j.foodchem.2017.05.030.
- [30] R. Gao, J. Zhang, X. He, L. Chen, Y. Zhang, Selective extraction of sulfonamides from food by use of silica-coated molecularly imprinted polymer nanospheres, *Anal. Bioanal. Chem.* (2010). doi:10.1007/s00216-010-3909-z.
- [31] Y. Li, Z. Li, W. Wang, S. Zhong, J. Chen, A.J. Wang, Miniaturization of self-assembled solid phase extraction based on graphene oxide/chitosan coupled with liquid chromatography for the determination of sulfonamide residues in egg and honey, *J. Chromatogr. A.* (2016). doi:10.1016/j.chroma.2016.04.026.

- [32] Y. Xu, J. Ding, H. Chen, Q. Zhao, J. Hou, J. Yan, H. Wang, L. Ding, N. Ren, Fast determination of sulfonamides from egg samples using magnetic multiwalled carbon nanotubes as adsorbents followed by liquid chromatography-tandem mass spectrometry, *Food Chem.* (2013). doi:10.1016/j.foodchem.2013.02.078.
- [33] I.S. Ibarra, J.M. Miranda, J.A. Rodriguez, C. Nebot, A. Cepeda, Magnetic solid phase extraction followed by high-performance liquid chromatography for the determination of sulphonamides in milk samples, *Food Chem.* (2014). doi:10.1016/j.foodchem.2014.02.069.
- [34] C. Yu, B. Hu, C18-coated stir bar sorptive extraction combined with high performance liquid chromatography-electrospray tandem mass spectrometry for the analysis of sulfonamides in milk and milk powder, *Talanta.* (2012). doi:10.1016/j.talanta.2011.12.078.
- [35] Q. Gao, D. Luo, J. Ding, Y.Q. Feng, Rapid magnetic solid-phase extraction based on magnetite/silica/poly(methacrylic acid-co-ethylene glycol dimethacrylate) composite microspheres for the determination of sulfonamide in milk samples, *J. Chromatogr. A.* (2010). doi:10.1016/j.chroma.2010.06.067.
- [36] P. Shi, N. Ye, Magnetite-graphene oxide composites as a magnetic solid-phase extraction adsorbent for the determination of trace sulfonamides in water samples, *Anal. Methods.* (2014). doi:10.1039/c4ay02027h.

## Chapter 3: Melamine sponge decorated with copper sheets as a material with outstanding properties for microextraction of sulfonamides prior to their determination by high-performance liquid chromatography

### 3.1 Introduction

As discussed in Chapter 2, the use of sponge or sponge-like materials is an up-and-coming concept in liquid sample preparation techniques [1–3]. Although their employment in passive air sampling is well known, sponge-like materials are scarcely employed for the extraction of analytes from aqueous matrices, due to their low extraction potential [1,4]. One of the most widely exploited materials for such purposes is polyurethane foam. In the last five years, there has been an increasing number of articles that attempt to modify the surface of polyurethane foam in an effort to enhance its extraction capability [5–7]. However, such modifications are difficult to conduct for preparing big batches of modified foams; along with the relatively high cost, their applicability is limited. Another type of sponge-like material is graphene foams. Different graphene and graphene-composite foams have been prepared and used in extraction procedures, taking advantage of the extraction capability of graphene [3,8–10]. The preparation of graphene-based foams is based mainly on the self-assembly of the reduced graphene oxide, under specific conditions and the disadvantages of graphene foams lie exactly at this point. Since it is difficult to control the conditions, the preparation of foams with specific characteristics (e.g. porosity, mechanical stability, etc.) is rendered laborious [11,12]. At the present time, there is a trend for the fabrication of carbon-coated commercial polymeric sponges due to their low cost and availability [13,14]. Melamine sponge (MeS) is a rising star among these materials. It is a low-density sponge with very high porosity (>99%) and an open-hole structure, with negligible cost to obtain [15,16]. MeS consists of a formaldehyde-melamine-sodium bisulfite copolymer that endows it with excellent wettability/hydrophilicity. Because of

the presence of functional groups, MeS is amenable to functionalization in order to tune its hydrophilicity or render it hydrophobic [17]. Such modifications have enabled the application of MeS-based hydrophobic materials to oil-adsorption removal [15,17]. However, their potential to be used in microextraction is yet to be explored. Recently, we proposed a modification of MeS with graphene in a one-step, fast procedure and utilized, for the first time, the produced graphene-MeS in a microextraction procedure [13]. To the best of our knowledge, there are not yet other reports that utilize MeS for such a purpose.

The affinity of melamine with copper is well known and has been employed to detect the one in the presence of the other, interchangeably or even to prepare complexes [18–20]. Due to the presence of melamine in the building blocks of MeS, a high affinity for copper is anticipated. In a previous study, Yang et al. coated polyester-cotton fabrics with copper and the modified fabrics were rendered suitable for oil-water separation taking advantage of the hydrophobic properties of copper [21]. It is likely that in a similar manner, a copper-loaded MeS (CuMeS) might exhibit hydrophobic properties that make it suitable for microextraction purposes.

In this Chapter, the development of a copperized sponge-based material via a fast reduction approach is described. The prepared CuMeS is expected to be hydrophobic, owing to the presence of metallic copper and, what is more, it is anticipated to be propitious to interact with SAs due to their high affinity with copper. To the best of our knowledge, this is the first attempt to develop a selective and sensitive sample microextraction procedure for the detection of SAs, capitalizing on the affinity of copper for sulfonamides.

## 3.2 Material and methods

### 3.2.1 Chemicals and reagents

- Melamine sponge is commercially available and was bought from a local market.
- Sulfadiazine, sulfathiazole, and sulfamethazine (purities >99%) were purchased from Alfa Aesar (Karlsruhe, Germany).
- Sulfapyridine, sulfamethoxy pyridazine, sulfachloropyridazine, sulfamethoxazole, sulfadimethoxine, sulfisoxazole and sulfaquinoxaline (purities >99%) were purchased from Aldrich Sigma–Aldrich (Steinheim, Germany)
- Copper (II) acetate (98%), Sigma–Aldrich (Steinheim)
- Hydrazinium hydroxide (~100%), Sigma–Aldrich (Steinheim)
- Trichloroacetic acid, Sigma–Aldrich (Steinheim)
- Copper powder, Fluka (Seelze)
- Solvents (at least of analytical grade) Sigma–Aldrich (Steinheim).

Stock standard solutions of each compound were prepared in acetonitrile (ACN), at concentrations of 1.0 mg mL<sup>-1</sup>. Further dilutions were made in H<sub>2</sub>O:ACN (70:30, v/v). All solutions were stored in screw-capped, amber-glass vials, at -18 °C.

### 3.2.2 Instrumentation

X-ray diffraction (XRD) analysis was performed on a D8 Advance diffractometer from Bruker AXS (Madison, USA) using CuK $\alpha$  ( $\lambda = 1.5406 \text{ \AA}$ ) radiation. Chromatographic separation and analysis were carried out on a Shimadzu (Kyoto, Japan) HPLC system coupled to a SPD-M20A Diode Array Detector (DAD). The column used for separation was a Hypersil ODS (250  $\times$  4.6 mm, 5  $\mu$ m particle size) from Thermo Fisher Scientific, kept at 30 °C in a CTO 10AS column oven. Samples were injected using a Rheodyne injector and injection volume was 20  $\mu$ L. The mobile phase consisted of water (A) and acetonitrile (B), containing 0.1% (v/v) formic acid. The SAs were separated following a gradient elution program from 10% to 35% B in 30 min. The mobile phase was delivered using a LC20AD

pump, at a flow rate of  $1.0 \text{ mL min}^{-1}$ . The detector was set at a wavelength range of 200–360 nm. Data acquisition and processing were carried out using an LC-solution software version 1.21. Peak identification was based on the comparison of retention times and UV spectra (recorded at 270 nm) with those of the authentic compounds. The SEM images were acquired using a JSM 5600 system from Jeol (Nieuw-Vennep, Netherlands), operating at 20 kV.

### 3.2.3 Decoration of melamine sponge with copper sheet

A MeS was firstly cut into cubes of  $1 \times 1 \times 1 \text{ cm}$ , rinsed with ethanol and left to dry. In a glass beaker, 10 mL of aqueous copper acetate solution ( $0.025 \text{ mol L}^{-1}$ ) was heated to ca  $70 \text{ }^\circ\text{C}$  and a MeS cube was soaked in it. Hydrazine was added dropwise, under stirring, up to a final concentration of  $0.65 \text{ mol L}^{-1}$ . The whole procedure was conducted under continuous nitrogen bubbling. After 30 min, the CuMeS cube was taken out and transferred to degassed distilled water and stirred vigorously during a washing step, to remove loosely bound copper. The water was replaced several times with fresh one until no floating particulate matter could be seen and the resulting CuMeS was used directly for microextraction.

### 3.2.4 Extraction procedure

In a typical procedure, 35 mL of sample (prepared according to the procedure of Section 2.5) were transferred to a glass beaker and a CuMeS cube was immersed in it. After stirring for 30 min, the CuMeS cube was removed and placed in a syringe cartridge to facilitate the washing with distilled water and the elution step. The excess water was removed by mechanical squeezing with a plunger and 2 mL of acetonitrile containing 3% (v/v) ammonia, percolated into the modified sponge to elute the adsorbed SAs. The eluent was evaporated to dryness, under a gentle nitrogen stream, reconstituted in 100  $\mu\text{L}$  of a mixture of  $\text{H}_2\text{O}$ :acetonitrile (70:30 v/v) using ultrasonication for 1 min and finally injected into the HPLC system.



### 3.2.5 Sample preparation

Milk samples were defatted by centrifugation at 4 °C, at 4000 rpm, for 10 min. The middle phase was retracted and 1 mL of 15% w/v trichloroacetic acid solution per 10 mL of defatted milk sample was added. After vortexing for 1 min and centrifuging under the above conditions, the supernatant was retracted and subjected to further analysis. No pH adjustment was needed since the added trichloroacetic acid lowered the pH of milk to ~3.

Lake water was filtered through a Whatman paper filter to remove particulate matter and the pH was adjusted to 3.0 using HCl 1.0 mol L<sup>-1</sup>.

### 3.3 Results and discussion

#### 3.3.1 Characterization

The XRD pattern of CuMeS is depicted in Figure 21. As it can be seen, there are four characteristic peaks, at  $43.4^\circ$  (1,1,1), at  $50.4^\circ$  (2,0,0), at  $74.1^\circ$  (2,2,0) and at  $89.9^\circ$  (3,1,1), all of which are characteristic of a face-centered cubic metallic copper phase [22,23]. Moreover, peaks that can be attributed to copper oxides (e.g.  $36.6^\circ$ ) are absent, bespeaking the lack of oxides or other impurities.

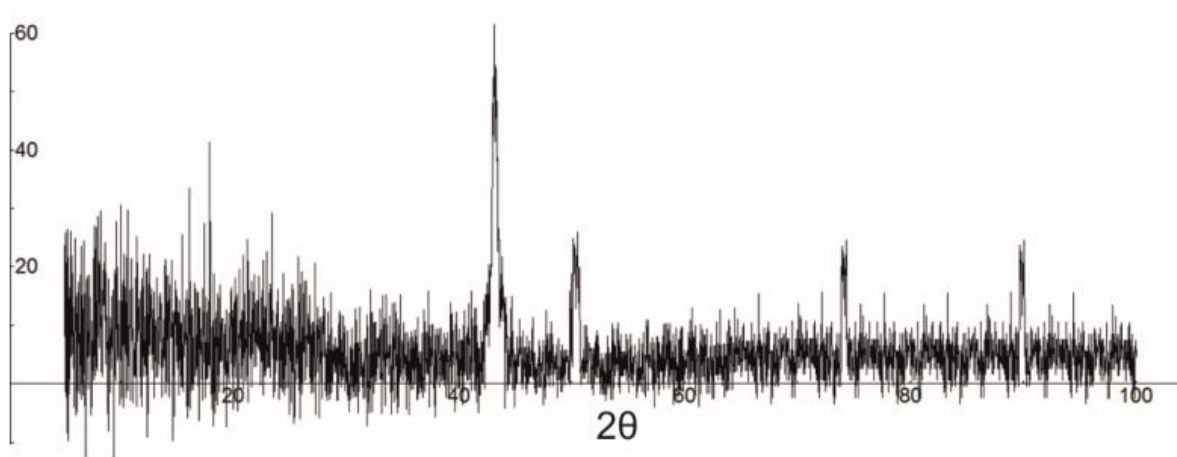


Figure 21: XRD pattern of CuMeS.

The SEM images (Figure 22(A–H)) of the bare and copper-modified MeS cubes were acquired, so as to observe their morphology. Bare MeS has an interconnected 3D network with pores, whose diameter range between 100 and 200  $\mu\text{m}$ . Following the modification procedure detailed herein, it can be seen that the 3D network becomes filled with copper sheets. Copper is retained within MeS due to their favorable chemical interaction and finally, a copperized sponge-based material is obtained. This decoration proceeds smoothly through the formation of a clearly visible copper mirror on the walls of the reaction vessel (Figure 23(A)) and through the change of the color of MeS from

white to metallic-copper-red (Figure 23(B)). Once in water, CuMeS cubes float on the surface signifying a reasonably greater hydrophobicity than that of bare MeS (Figure 23(C and D)).

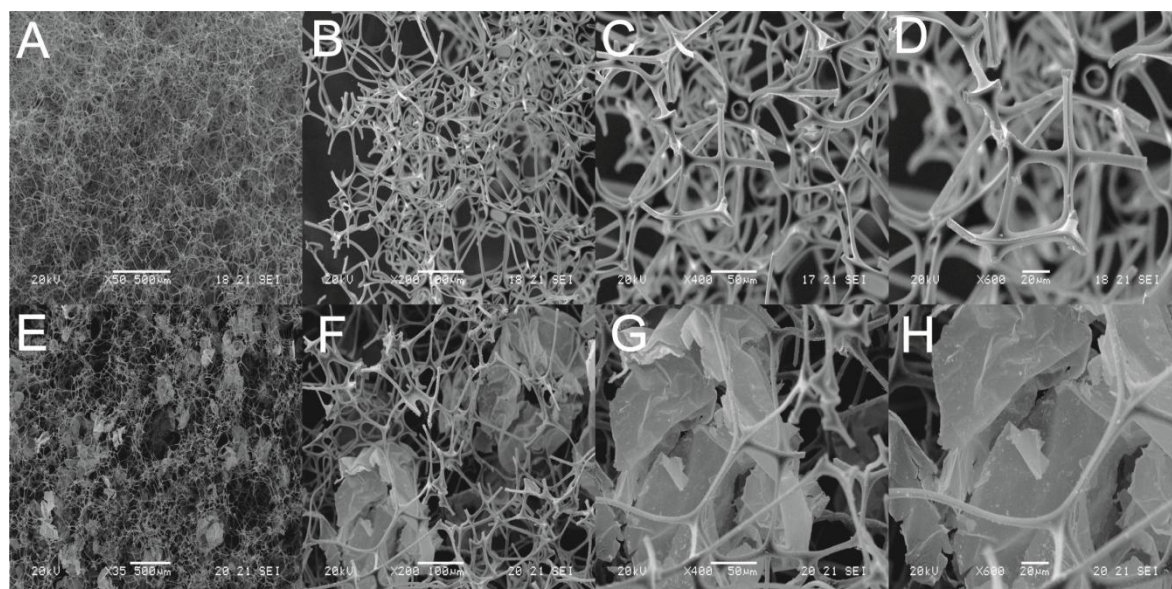


Figure 22: SEM images of MeS (A–D) and CuMeS (E–H) in various magnifications (scale bars: 500  $\mu\text{m}$  (A, E), 100  $\mu\text{m}$  (B, F), 50  $\mu\text{m}$  (C, G) and 20  $\mu\text{m}$  (D, H)).

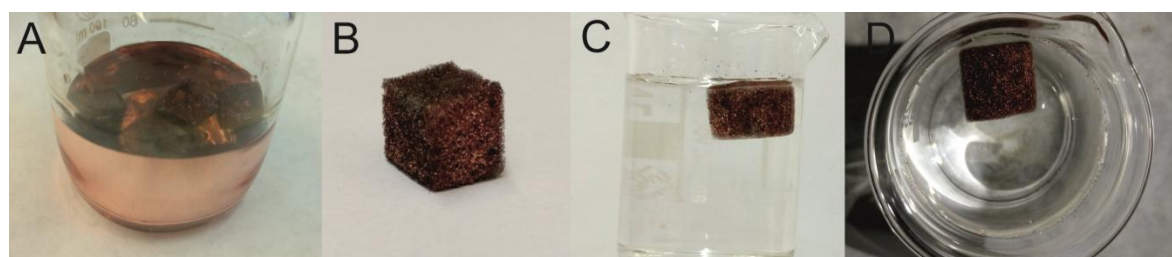


Figure 23: Copper mirror formed on the surface of the reaction glass beaker during decoration of MeS (A). The produced CuMeS (B) and its behavior in water (C, D).

### 3.3.2. Synthesis optimization

In order to achieve maximum loading of MeS with copper, the conditions of synthesis were properly handled and examined. The use of different copper salts was the first parameter tested, followed by the concentrations of salt and hydrazine, temperature and time of treatment and finally, by the number of modification times. The criterion used to select the optimum synthesis conditions was the total adsorption capability of the resulting CuMeS, for a mixture of ten SAs ( $150 \mu\text{g mL}^{-1}$  each), although the adsorption of each SA also was taken into account (a complete list of the examined SAs along with their physicochemical characteristics can be seen in Table 1). Single MeS cubes ( $1 \times 1 \times 1 \text{ cm}$ ,  $\sim 10 \text{ mg}$  each) were used throughout the experiments for the optimization of the synthesis unless otherwise stated.

#### 3.3.2.1 Copper salt

The first parameter examined was the copper salt for the formation of CuMeS. To this end, copper sulfate, copper acetate, and copper chloride were tested. In each case, a proper amount of salt was added to the water so that the final concentration of copper ions was kept constant, while the final hydrazine concentration was fixed at  $0.8 \text{ mol L}^{-1}$ . In all three cases, the formation of metallic copper onto the MeS was visible; however, during the washing step, the loss/bleeding of copper from CuMeS fabricated from copper sulfate and copper chloride was pronounced and it was much higher than that from CuMeS synthesized from copper acetate. Moreover, the extraction capabilities of the first two CuMeS were decreased by almost 55% compared to CuMeS produced from copper acetate. This is in line with the lower content of copper in these CuMeS. In addition, previous studies have proven that different salts are able to produce different sizes of copper, which can justify the variations in extraction yield [22,23]. Thus, copper acetate was used to functionalize MeS with metallic copper sheets due to the improved extraction potential of the resulting CuMeS for SAs.

### *3.3.2.2 Copper acetate concentrations and reduction conditions*

For the purpose of achieving maximum loading of MeS with copper sheets, the concentration of copper acetate was varied. At the same time, hydrazine quantity was increased proportionally to ensure an invariable excess of the reducing agent. Thus, given the sufficient reduction of copper ions by hydrazine, any differences observed in the extraction efficiency should be due to the loading of the prepared CuMeS with copper. The concentration of copper acetate (and hence of  $\text{Cu}^{2+}$ ) was examined in the range of  $0.005\text{--}0.05\text{ mol L}^{-1}$ . Figure 24 depicts the total adsorption efficiency for the mixture of SAs. The adsorption was similar for all SAs, except for sulfamethoxypyridazine and sulfachloropyridazine, for which an increase in the adsorption efficiency was more pronounced compared to that for the rest of SAs. It is evident that as the concentration of copper acetate increases the adsorption efficiency increases up to a concentration of  $0.025\text{ mol L}^{-1}$ . At lower tested concentrations, after completion of the reaction, no deposition of a copper film/mirror on the walls of the reaction vessel was observed, hinting that the amount of copper ions was insufficient to fully decorate the MeS. The concentration of  $0.025\text{ mol L}^{-1}$  of copper acetate was sufficient to load the MeS cube while the excess copper developed a thin copper film/mirror on the reaction vessel. A two-fold increase in copper acetate concentration resulted in CuMeS with the same adsorption efficiency. Therefore, for maximum loading of copper on MeS, the above concentration was selected as the optimum and used for conducting further experiments. Following a gravimetric analysis of CuMeS (obtained using the optimum conditions, as explained subsequently) it was found that each MeS cube (weighing  $10.0 \pm 0.1\text{ mg}$ ) is regarded as fully loaded when  $12.0 \pm 0.3\text{ mg}$  of copper are attached. Higher concentrations of copper acetate did not result in a higher content of copper on MeS, which agreed with the findings of the adsorption efficiency of the different CuMeS.

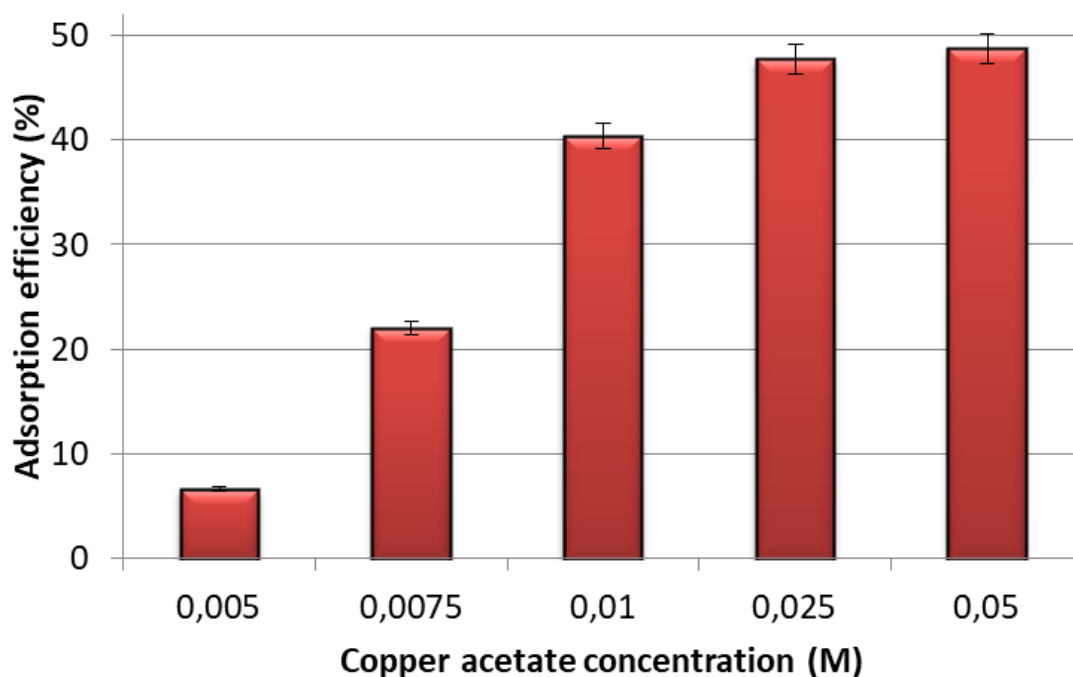
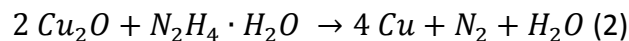
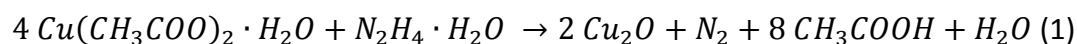


Figure 24: Effect of copper acetate concentration on the adsorption efficiency of the resulting CuMeS for a mixture of 10 SAs ( $150 \mu\text{g mL}^{-1}$  each) (number of replicate analysis=3).

Prior to examining the effect of hydrazine concentrations, a milder reducing agent was examined in order to replace hydrazine. Although complete formation of metallic copper was observed on and inside the 3D network of MeS using ascorbic acid, the adsorption capability of the prepared CuMeS was nearly 50% lower than that prepared using hydrazine. This could be due to the size of the synthesized copper sheets, which depends on the reducing agent used (hydrazine results in typically smaller copper sheets compared to ascorbic acid) [24]. As regards the optimum concentration of hydrazine, using a constant concentration of copper acetate (i.e.  $0.025 \text{ mol L}^{-1}$ ), different CuMeS were prepared at hydrazine concentrations in the range of  $0.05\text{--}1.0 \text{ mol L}^{-1}$ . The results showed that hydrazine concentrations lower than  $0.65 \text{ mol L}^{-1}$  resulted in CuMeS, which had virtually no adsorption capability for SAs (adsorption  $<5\%$  in all cases) (Figure 25). Visual inspection of the CuMeS prepared under the above-mentioned concentrations of hydrazine, showed that CuMeS were black-colored, with negligible signs of copper

metallic color (which is clearly visible in the cases of hydrazine concentration above 0.65 mol L<sup>-1</sup>). Furthermore, in the washing step, a lot of the loaded copper was removed, resulting in sponges with lower copper content. This could justify the insignificant adsorption capability of the CuMeS. On the contrary, when the reaction was carried out in solutions containing hydrazine concentration above 0.65 mol L<sup>-1</sup>, metallic copper was visible in the entire CuMeS cube (see Figure 23B). These findings evidenced that there is a threshold of hydrazine concentration (close to 0.6 mol L<sup>-1</sup>), above which metallic copper is formed, whereas at lower concentrations copper oxides (mainly Cu<sub>2</sub>O) are the dominant species. According to previous studies, at low concentrations of hydrazine Cu<sub>2</sub>O is formed [22]. Taking into consideration the color changes during synthesis, the two aforementioned facts hint towards a mechanism of metallic copper formation that takes place through the formation of oxides, as depicted by Eqs. (1) and (2) [23].



No differences in the extraction yield of SAs were noticed among CuMeS cubes produced from hydrazine at concentrations of 0.65, 0.8 and 1.0 mol L<sup>-1</sup>. Excess hydrazine can reduce copper acetate to pure metallic copper and the formed copper sheets homogeneously coat the MeS by the in-situ reduction growth method. Thus, a concentration of 0.65 mol L<sup>-1</sup> was selected as the optimum so as to minimize hydrazine use.

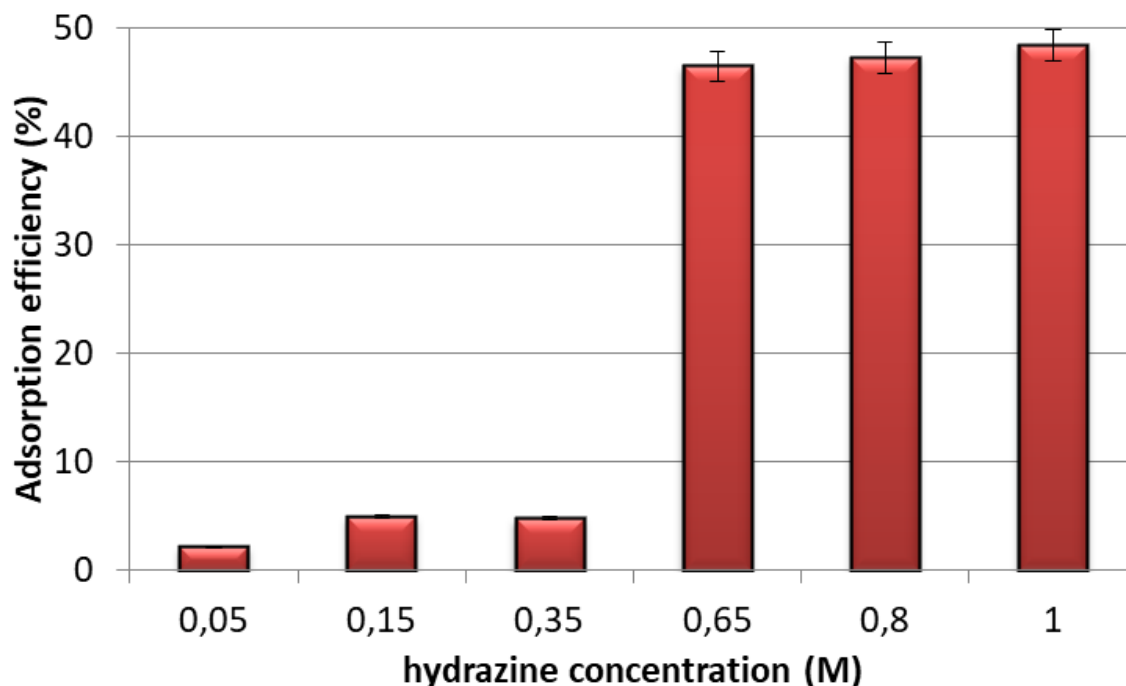


Figure 25: Effect of hydrazine concentration on the adsorption efficiency of the resulting CuMeS for a mixture of 10 SAs ( $150 \mu\text{g mL}^{-1}$  each) (number of replicate analysis=3).

### 3.3.2.3 Synthesis pH, time and temperature

The modification of CuMeS cubes with copper was conducted in both acidic (no adjustment was needed since acetate ions result in pH = 4) and alkaline environment (pH = 10) and the resulting CuMeS were compared. In the former case, cubes were left intact after the washing step while in the latter they became almost completely uncovered of copper (the white color of the MeS was revealed in this case). As expected, the CuMeS produced in alkaline conditions did not show any adsorption capability due to the low copper load. Deng et al. have reported that the pH affects the progress of copper ions reduction [25]. They proposed that in alkaline solutions containing ammonia, copper (II)-ammonia complexes are formed, resulting in decreased reduction rate and in more stable growth of copper sheets. On the contrary, the bubbles which are rapidly released in acidic media, produce more copper nuclei that aggregate in larger agglomerates. Presumably, in a more acidic environment, the melamine moieties in MeS ( $\text{pK}_a \sim 5.0$ ) are



protonated, forming melaminium cations and/or dications [18]. Therefore, interactions between copper (electron donor) and melaminium (di)cations (electron acceptor) are favored. This, however, is not the case in alkaline conditions.

The next parameter tested was the copper-loading temperature. It has been reported that elevated temperatures, at around 70 °C, hasten the reduction of copper ions to metallic copper [24]. Although in our experiments the formation of copper can be achieved at room temperature (under stirring, overnight), it was found that heating at 70 °C dramatically reduces the time needed to complete the reaction (~30 min). Reactions conducted under heating or no heating in different time periods for the preparation of CuMeS (until the copper film/mirror was seen on the walls of the reaction vessel) had the same adsorption efficiency. Thus, the temperature does not affect the adsorption capability but only the speed of decoration of MeS with copper. A 30-min reaction period, at 70 °C is adequate to prepare CuMeS. At shorter time periods (e.g. 5, 10 and 15 min) the reaction was not completed and the CuMeS cubes were not efficient for SAs adsorption. Moreover, high variations in the adsorption behavior were noticed between different batches of CuMeS. Generally, the reaction was completed when the solution turned from light blue to deep blue, yellow, brown and henna, before discoloration occurred. As already mentioned, a thin mirror-like, copper film is deposited on the vessel walls during the process, which takes approximately 25 min to form. However, 30 min was the time selected to conduct experiments in order to ensure completion of the functionalization.

#### ***3.3.2.4 Times of modification and synthesis scale-up***

A CuMeS cube which was produced following the aforementioned optimized procedure was subjected to a second modification cycle (under the same conditions), in an effort to further increase the amount of copper in MeS. The results did not show any increase in the copper content (and no change in the adsorption efficiency), demonstrating that maximum loading of MeS with copper was attained in a single decoration step. Finally,

the potential to produce simultaneously more than one CuMeS, in a single pot was examined. A scale-up synthesis was carried out with ten MeS cubes in a single synthesis and it was found that within-batch and between-batch adsorption reproducibility was highly satisfactory (the relative standard deviation was 3.6% and 4.4% for within-batch and between-batch CuMeS, respectively. Number of replicate analyses = 5). Thus, the proposed synthesis can be scaled up for the easier production of more than one CuMeS cube, at a time.

### **3.3.3 Optimization of the proposed procedure**

#### **3.3.3.1 Effect of pH-mechanism of interaction**

The first parameter that is expected to play a significant role in the extraction of SAs from CuMeS is the pH of the solution due to the ionizable nature of the SAs. From Figure 26 it is apparent that acidic pH values favor the adsorption of SAs; as the pH increases the adsorption is hindered. The optimum pH value was found to be 3.0. At this pH, SAs co-exist in their neutral and positively charged form. At pH values where the neutral form dominates, the adsorption is significantly lower, hinting at weaker hydrophobic interactions between the neutral form of SAs and CuMeS. Therefore, it is considered reasonable that SAs interact with the CuMeS through, primarily, the protonated aromatic amine. On the contrary, the nitrogen of the sulfonamide group is not expected to contribute to the overall interaction mechanism, since it does not affect positively the adsorption efficiency in the protonated or deprotonated state. At pH lower than 3.0, extensive leaching of copper from the CuMeS occurred (the CuMeS regained the white color of MeS) and adsorption of SAs was not feasible.

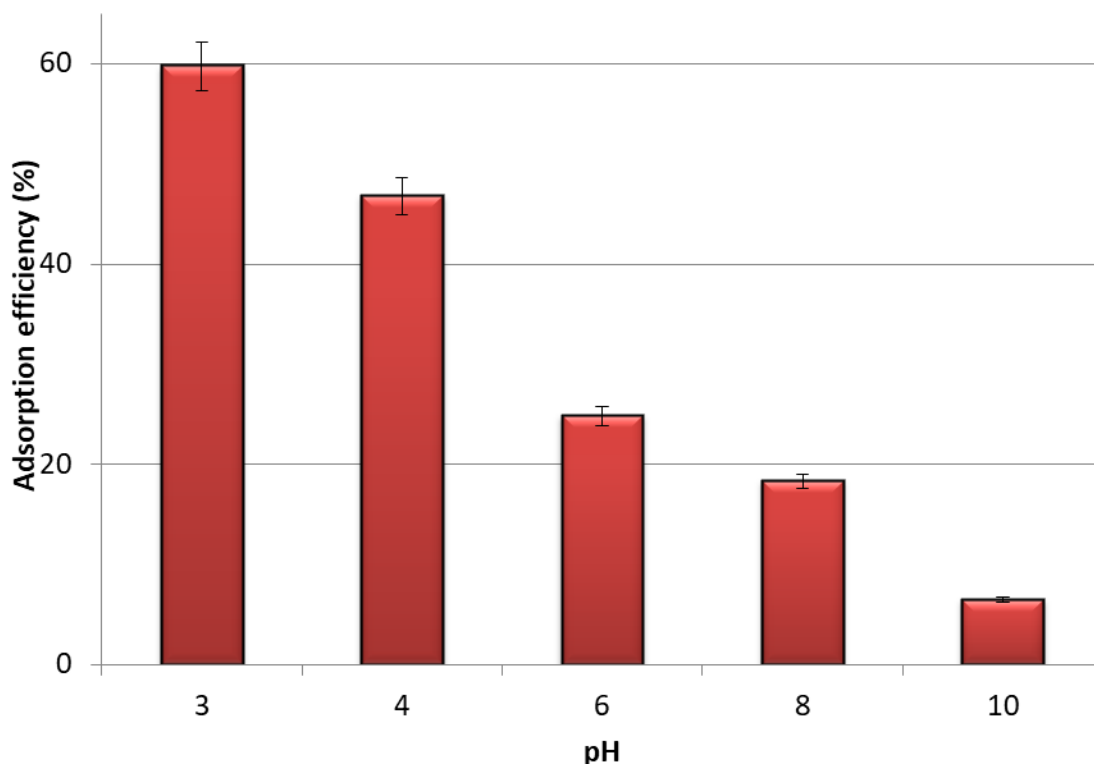


Figure 26: Effect of the pH on the adsorption efficiency of CuMeS for a mixture of 10 SAs ( $150 \mu\text{g mL}^{-1}$  each) (number of replicate analysis=3).

According to Kremer et al., there are four possible interactions between sulfonamides and copper ions [26]. Typically, sulfonamides can act: (I) as monodentate ligands through the aromatic amine nitrogen or the nitrogen atom of the heterocycle, (II) as bidentate ligands through the sulfonamide nitrogen atom and nitrogen atom of the heterocycle, (III) as bridges between two copper ions through the aromatic amine nitrogen and nitrogen atom of the heterocycle, or (IV) as bidentate ligands through the sulfonamide nitrogen atom and nitrogen atom of the heterocycle and simultaneously, as bridges with another copper ion through the aromatic amine nitrogen. In our case, the second type of interaction (i.e. II) is not applicable since it cannot explain the observed difference of the protonated states of aromatic amine nitrogen that alter the adsorption efficiency. The substituted aromatic rings in all examined SAs are basic, indicating that a lone pair of electrons, not belonging to the aromatic system, exists. In acidic environment, the basic

aromatic rings tend to form (aromatic) cations and the nitrogen atoms of the aromatic heterocycles are also expected to interact with copper. To strengthen this notion, specific data about the adsorption of individual SAs on CuMeS were exploited. Sulfacetamide does not contain a (substituted) aromatic ring to function as a ligand and as a result, the adsorption can be achieved only through the aromatic amine. Our data showed relatively low adsorption (~20%) at pH = 3, definitely lower than the yields achieved for the rest of the SAs examined. This is attributed to the lack of a substituted aromatic ring, verifying that aromatic nitrogens contribute to the adsorption mechanism significantly. Thus, the first type of above-mentioned interactions (i.e. I) is not applicable in this instance, since both nitrogen atoms contribute simultaneously to the overall adsorption. To figure out the exact mechanism that governs the interaction of SAs with CuMeS, the adsorption behavior towards 2,2-bipyridine and 4,4-bipyridine was examined. The 2,2-bipyridine acts as a bidentate ligand for one copper ion, while 4,4-bipyridine acts as a bridge between two metal ions. Relevant experiments revealed that high affinity with CuMeS exists in the case of 4,4-bipyridine, contrary to 2,2-bipyridine which is not adsorbed at all. This finding suggests that the fourth type of interaction (i.e. IV) is unlikely to be the case, alluding to the third interaction mechanism (i.e. III), where SAs act as bridges between two metallic centers. Bare MeS was also examined for assessing its extraction capability. The results showed trivial adsorption of SAs (~3%), suggesting weak or no interactions.

Other interactions which can potentially take place between CuMeS and SAs during the extraction of SAs are hydrophobic. A closer look at the adsorption behavior of the individual SAs revealed a gradual increase in the adsorption percentages as the logKow of analytes increase (e.g. sulfadiazine whose logKow is -0.12 is adsorbed by 25% less efficiently than sulfadimethoxine, whose logKow is 1.5). Thus, hydrophobic interactions between CuMeS and different SAs are also applicable, in our case.

### *3.3.3.2 Effect of the ionic strength*

Generally, increasing the ionic strength of a solution results in an improvement in the extraction efficiency, when salting-out effect plays a crucial role in the procedure. In order to examine this effect, NaCl or Na<sub>2</sub>SO<sub>4</sub> was added to aqueous samples, at a concentration up to 15% (w/v) (in increments of 3%) and the adsorption capability of the CuMeS was evaluated. As can be seen in Figure 27, the addition of Na<sub>2</sub>SO<sub>4</sub> up to 15% (w/v) neither favored nor hindered significantly the extraction of SAs from CuMeS (only a minor decrease of ~3% was noticed when the maximum tested concentration of Na<sub>2</sub>SO<sub>4</sub> was used). On the other hand, a pronounced decrease in the extraction capability was noticed when NaCl was used. The increase in the viscosity of the solution could conceivably decelerate the percolation of the solution through the 3D network of the CuMeS. However, this does not happen with Na<sub>2</sub>SO<sub>4</sub>. Moreover, the presence of sodium cations does not have an impact on the extraction efficiency, since a similar trend was not noticed with Na<sub>2</sub>SO<sub>4</sub>. Thus, the observed decrease is solely attributed to the presence of chloride ions. When 3% NaCl was used, the sample solution containing a CuMeS cube turned from colorless to cloudy due to the formation of the water-insoluble copper (I) chloride. At higher concentrations of NaCl, the solution was transparent hinting at a reaction between copper (I) chloride with excess chloride ions, which formed soluble copper (II) chloride. The above findings are in accordance with earlier reports, which described the corrosion/dissolution of copper in chloride solutions [27,28]. Lower concentrations of chloride ions, up to 150 mM were not found to affect adversely the extraction efficiency (~2%). Thus, the proposed method can safely be used for milk (the free chloride concentration is around 30 mM [29] and surface water samples (commonly, they contain less than 150 mM chloride ions [30]).

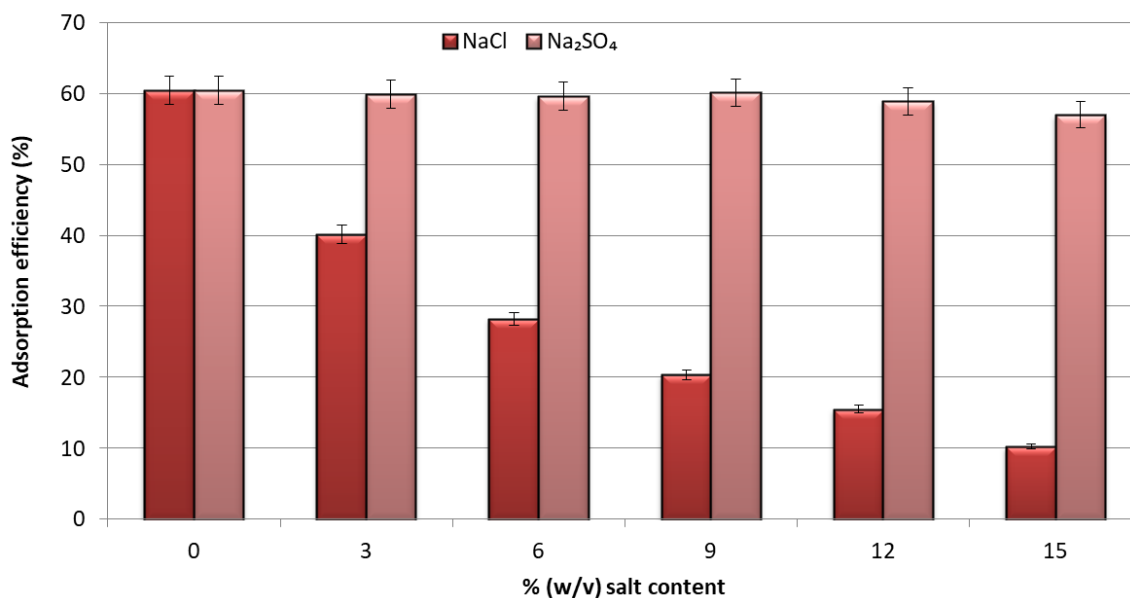


Figure 27: Effect of the ionic strength of the sample on the adsorption efficiency of the method for a mixture of 10 SAs ( $150 \mu\text{g mL}^{-1}$  each) (number of replicate analysis=3).

### 3.3.3.3 Other extraction parameters

The microextraction of SAs was conducted at three different temperatures (i.e. 25, 35 and 45 °C). The results showed a trifling increase in the extraction efficiency (~4%) when temperature increased from 25 to 45 °C. This is probably ascribed to the lower viscosity of the sample at higher temperatures. Thus, further experiments were conducted without temperature control, simplifying the overall procedure.

The sample volume, the amount of CuMeS, the concentration of analytes and stirring rate and time were finally studied to select the optimum working conditions. Firstly, four sample volumes were examined (i.e. 20, 35, 50 and 75 mL), spiked with the same amount of SAs (20  $\mu\text{L}$  from a  $100 \mu\text{g mL}^{-1}$  stock standard solution). The results showed an insignificant decrease in the extraction efficiency (<7%) up to a volume of 50 mL, while a sharp decrease (~20%) was noticed when 75 mL of sample was used. Before proceeding, preliminary experiments were conducted at three different stirring rates (i.e. 300, 600 and 900 rpm) and the results showed no difference in the adsorption efficiency. For

further experiments, a moderate stirring speed of 600 rpm was employed. Next, the adsorption was examined by altering simultaneously the sample volume (20–50 mL) at the same concentration of analytes, stirring time (10–30 min) and number of CuMeS cubes ( $\frac{1}{2}$ , 1 and 2), resulting in a total of 27 experiments. The use of  $\frac{1}{2}$  CuMeS cube resulted in lower extraction yields (Figure 28), compared to one or two CuMeS cubes. Maximum extraction efficiency was achieved using an entire CuMeS cube, either in 20 or 35 mL of sample, after 30 min of stirring. In order to achieve higher enrichment factors, 35 mL of sample was used for further experiments. The use of two CuMeS cubes resulted in the same maximum extraction efficiency as with one. Cube with dimensions twice as big as that of  $1 \times 1 \times 1$  cm was not examined since the percolation of the solution through the cube is expected to be less efficient [13]. Thus, the use of a second cube was not deemed necessary and was avoided for reasons of simplicity.

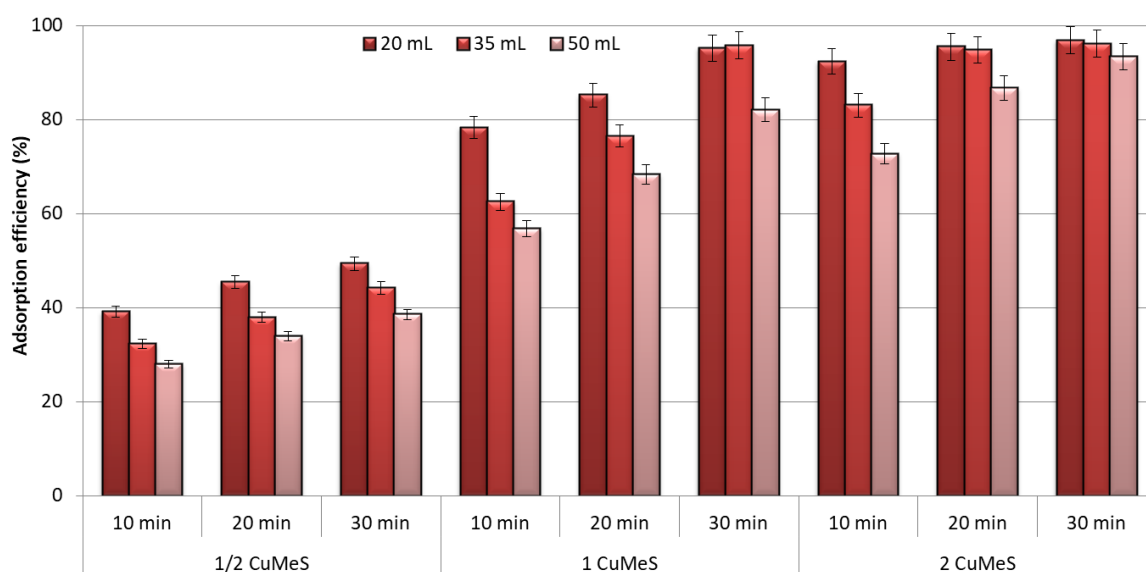


Figure 28: Effect of sample volume, amount of adsorbent and extraction time on the efficiency of the method (number of replicate analysis = 3).

Stirring rate was tested once again, under the aforementioned optimum parametric conditions. The results verified that stirring rate does not affect the overall extraction procedure. Under optimum conditions, 12 and 60 mg of copper powder (the same amount of Cu as with copper-decorated MeS and five times more) were used to compare CuMeS performance with plain copper. The two tested portions of copper powder adsorbed nearly 30 and 45% of SAs, respectively, in contrast to CuMeS which adsorbed almost 100% of the total SAs content. The observed difference could be attributed to the high hydrophobicity of copper powder. On account of this, the powder had the tendency to remain on the surface of the sample, despite the vigorous stirring applied. Therefore, CuMeS was proved vastly superior over copper powder.

#### **3.3.3.4 Elution conditions**

Acetonitrile and methanol were examined for their ability to elute the adsorbed SAs. Relevant experiments revealed that methanol is unsuitable for the elution since it leads to corrosion of copper and thus, to leaching from the CuMeS, without, however, eluting SAs (elution yield was lower than 20% for all SAs) [31]. Elution with acetonitrile was found to be inadequate (between 35 and 48%) and hence, the addition of formic acid (acidic conditions) and ammonia (alkaline conditions) were examined. Only the addition of ammonia increased significantly the elution yield. The addition of formic acid caused an increase of ~5% only for sulfadiazine, sulfapyridine, sulfathiazole and sulfamethazine while ammonia increased the elution yield up to 75% for all SAs. Ammonia displaces SAs from the adsorbent to form copper ammine complexes, thus, favoring the elution of SAs. Next, the content of ammonia was examined in the range of 1–5% (v/v) and it was found that the addition of 3% (v/v) ammonia was sufficient to achieve total elution of the SAs. Finally, relevant experiments revealed that a single elution with 2 mL of the solvent was enough for the recovery of SAs.



### **3.3.4 Method validation according to the commission decision 657/2002/EC**

The adsorption potential of the as-synthesized CuMeS for SAs, was examined using lake-water and milk. Method validation was carried out according to the Commission Decision 657/2002/EC, using spiked lake water and milk samples. The linearity, selectivity, accuracy, precision, sensitivity, decision limit, and detection capability were assessed, using the abovementioned guidelines [32–34].

#### **3.3.4.1 Linearity and sensitivity**

For each of the two examined matrices, 8-points matrix-matched calibration curves were prepared and they were used to validate the assays. The calibration lines were linear in the range of 0.05–150  $\mu\text{g L}^{-1}$  and 0.5–150  $\mu\text{g L}^{-1}$  for lake water and milk, respectively and the coefficients of determination ( $R^2$ ) were above 0.9973 and 0.9964, respectively, bespeaking good linearity. The limits of detection were calculated and found to be in the range of 0.008–0.0019  $\mu\text{g L}^{-1}$  for lake water and 0.077–0.350  $\mu\text{g L}^{-1}$  for milk samples. All the above data can be seen in detail in Tables 14 and 15.

#### **3.3.4.2 Selectivity**

Selectivity was evaluated by analyzing blank samples of lake water and milk. The samples were checked for interferences at the retention times, where SAs are eluted. Representative chromatograms of the blank samples are depicted in Figures 29 and 30. It is evident that the eluents are free from interfering peaks, suggesting that the proposed CuMeS-based procedure acts both as extraction and clean-up for the quantitative determination of SAs.

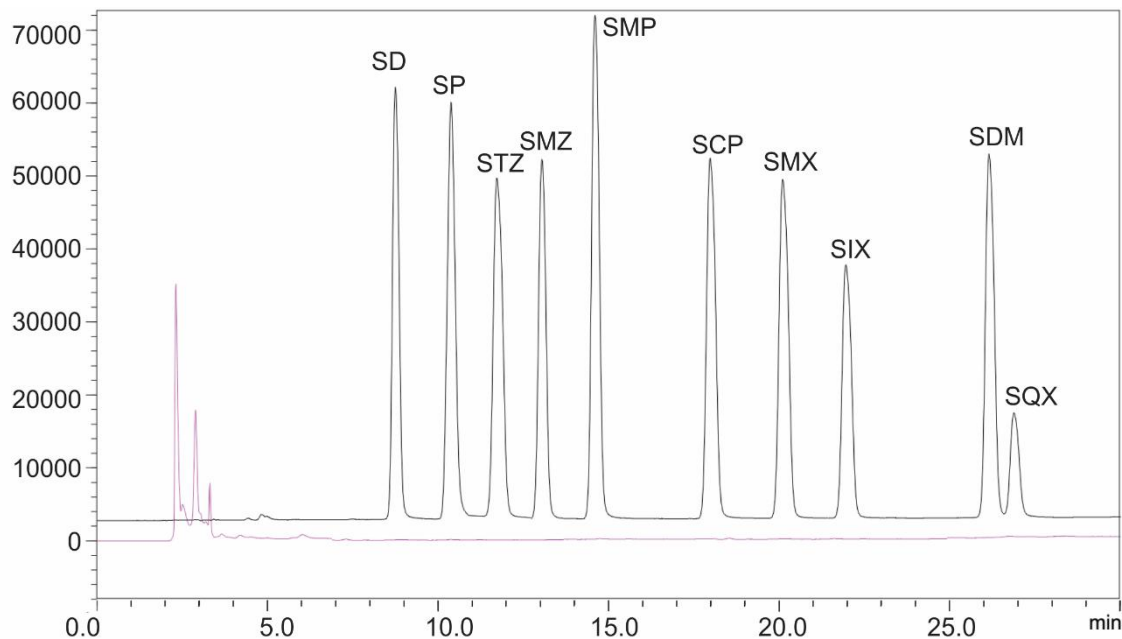


Figure 29: Chromatograms (at 270 nm) of a blank lake water sample (lower chromatogram) and a lake water sample spiked with  $50 \mu\text{g L}^{-1}$  of SAs (upper chromatogram).

#### 3.3.4.3 Accuracy and precision

Within-day and between-day precision of the method were calculated as the relative standard deviation (RSD) of five samples analyzed on the same day and three samples on five consecutive days, spiked with 50, 100 and  $150 \mu\text{g L}^{-1}$  of each SA (i.e. 0.5, 1.0 and 1.5 times the maximum residue limits (MRL) for SAs according to the European Union). For lake water samples, within-day RSD and between-day RSDs ranged between 4.1–5.9% and 4.9–7.3%, respectively. Likewise, within-day RSD and between-day RSDs for milk samples were in the range of 6.0–8.7% and 6.4–9.9%, respectively. Next, recoveries of SAs were calculated at three concentrations and were found to be between 89 and 104% for lake water and 88–97% for milk. Finally, enrichment factors (EFs) were calculated according to our previous study [13]. For lake water, EFs were between 234 and 463 and for milk they ranged between 25 and 41. The aforementioned results for all analytes are listed in Tables 16,17.

Table 14: Analytical characteristics of the proposed method for SAs determination in lake water

SAs	linear equation	coefficient of determination ( $R^2$ )	LOQ ( $\mu\text{g L}^{-1}$ )	Recovery (%)			EF	CCa (MRL $\text{L}^{-1}$ )	CCb (MRL $\text{L}^{-1}$ )
				0.1 $\mu\text{g L}^{-1}$	0.5 $\mu\text{g L}^{-1}$	5.0 $\mu\text{g L}^{-1}$			
SD	$y=34240x-20216$	0.9973	0.034	92	95	96	264	109.5	119.2
SP	$y=40434x-30183$	0.9974	0.037	93	94	96	320	108.0	116.4
STZ	$y=34429x-24236$	0.9976	0.034	94	95	102	270	107.7	115.6
SMZ	$y=31969x-23486$	0.9974	0.039	90	93	96	330	107.5	115.4
SMP	$y=45830x-29923$	0.9976	0.025	89	94	99	463	108.5	116.9
SCP	$y=38541x-23644$	0.9978	0.029	94	94	98	388	106.7	113.8
SMX	$y=37561x-22875$	0.9981	0.032	91	95	96	352	108.0	116.6
SIX	$y=27542x-14688$	0.9985	0.048	92	94	96	252	109.0	118.7
SDM	$y=37916x-22687$	0.9979	0.028	91	96	104	338	107.7	115.9
SQX	$y=13364x-29671$	0.9920	0.057	90	98	99	234	106.7	113.9

Table 15: Analytical characteristics of the proposed method for SAs determination in milk samples

SAs	linear equation	coefficient of determination ( $R^2$ )	LOQ ( $\mu\text{g L}^{-1}$ )	Recovery (%)			EF	CCa (MRL $\text{kg}^{-1}$ )	CCb (MRL $\text{kg}^{-1}$ )
				1 $\mu\text{g L}^{-1}$	10 $\mu\text{g L}^{-1}$	25 $\mu\text{g L}^{-1}$			
SD	$y=3531x-2400$	0.9984	0.36	89	91	94	25	111.3	122.8
SP	$y=4047x-1461$	0.9974	0.26	92	93	95	34	111.6	123.0
STZ	$y=3406x-2547$	0.9981	0.33	91	91	97	37	112.5	124.4
SMZ	$y=3204x-2802$	0.9972	0.32	90	94	96	32	112.5	124.8
SMP	$y=4606x-1907$	0.9980	0.23	90	92	95	41	111.2	122.6
SCP	$y=3890x-3098$	0.9985	0.36	91	91	94	36	111.8	123.6
SMX	$y=3560x-834$	0.9981	0.30	89	91	94	33	111.8	123.8
SIX	$y=2683x-1248$	0.9979	0.41	88	91	90	25	113.3	126.7
SDM	$y=3815x-5923$	0.9972	0.29	90	89	93	36	111.6	123.5
SQX	$y=1325x-3256$	0.9964	1.05	89	93	95	41	113.6	127.4

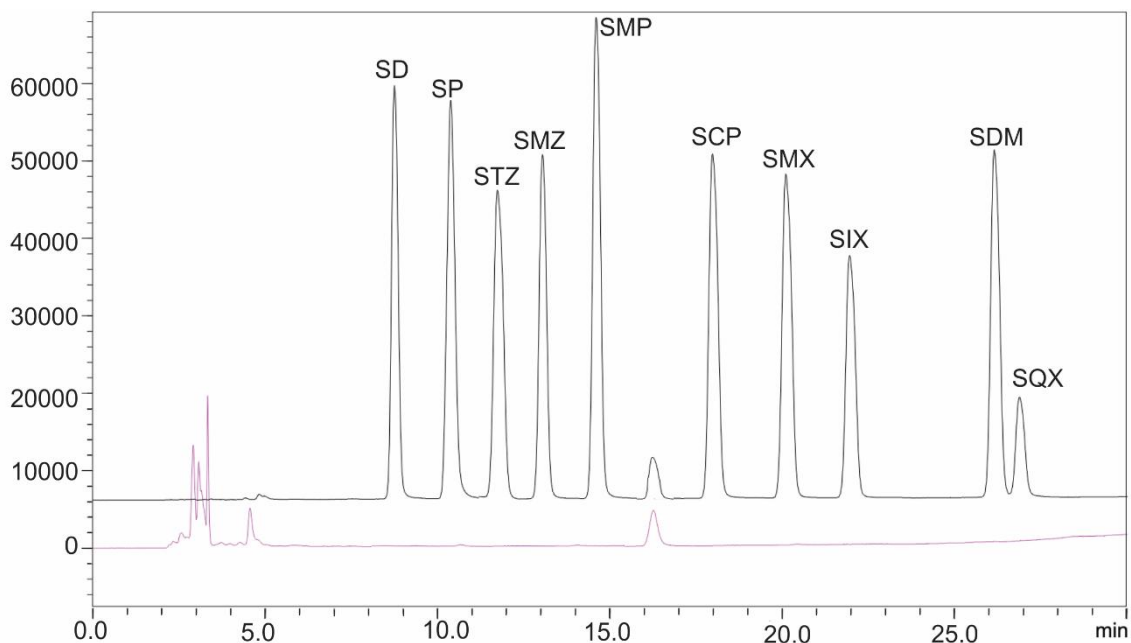


Figure 30: Chromatograms (at 270 nm) of a blank milk sample (lower chromatogram) and a milk sample spiked with  $50 \mu\text{g L}^{-1}$  of SAs (upper chromatogram).

#### 3.3.4.4 Decision limit and detection capability

According to the Commission Decision 657/2002/EC two novel criteria must be calculated: the  $CC\alpha$  (i.e. limit of decision) and  $CC\beta$  (i.e. capability of detection), which are defined as “the limit at and above which it can be concluded, with an error probability of  $\alpha$ , that a sample is noncompliant” and “the smallest content of the substance that may be detected, identified, and/or quantified in a sample with an error probability of  $\beta$ ”, respectively. To calculate  $CC\alpha$ , 20 lake water and milk samples were spiked with the maximum residue limit of the SAs (i.e.  $100 \mu\text{g L}^{-1}$ ). More specifically,  $CC\alpha$  was the mean measured concentration of the samples plus 1.64 times the corresponding standard deviation. Similarly,  $CC\beta$  was calculated using 20 samples spiked with the respective  $CC\alpha$  values plus 1.64 times the corresponding standard deviation. The data are given in Tables 16 and 17. Overall, it can be deduced that the proposed method is suitable for the sensitive and selective extraction of SAs from environmental water and milk samples. Due to the wide linear range, which covers concentrations of SAs above and well below the maximum residue limit and the highly satisfactory recoveries, the method can be applied for routine analysis and is comparable or even better than those published so far (see Table 18).

Table 16: Relative standard deviations of lake water samples spiked with three different concentrations of SAs (i.e 0.5, 1.0 and 1.5 times the maximum residue limits (MRL))

SAs	50 µg L <sup>-1</sup> (i.e 0.5 MRL)		100 µg L <sup>-1</sup> (i.e MRL)		150 µg L <sup>-1</sup> (i.e 1.5 MRL)	
	within-day (n=5)	between-day (n=3×5)	within-day (n=5)	between-day (n=3×5)	within-day (n=5)	between-day (n=3×5)
SD	4.8	6.2	5.8	6.2	5.1	5.6
SP	5.1	6.8	4.9	5.0	4.3	6.6
STZ	5.9	6.0	4.7	5.8	5.1	5.7
SMZ	5.2	5.6	4.6	4.9	5.0	5.1
SMP	4.5	5.7	5.2	5.8	4.8	5.4
SCP	5.7	7.3	4.1	6.2	4.1	5.3
SMX	5.3	6.4	4.9	6.9	4.1	6.5
SIX	5.7	6.2	5.5	6.4	4.3	5.9
SDM	5.4	6.0	4.7	6.5	4.4	6.1
SQX	5.7	7.1	4.1	7.0	5.6	6.5

Table 17: Relative standard deviations of milk samples spiked with three different concentrations of SAs (i.e. 0.5, 1.0 and 1.5 times the maximum residue limits (MRL))

SAs	50 µg kg <sup>-1</sup> (i.e. 0.5 MRL)		100 µg kg <sup>-1</sup> (i.e. MRL)		150 µg kg <sup>-1</sup> (i.e. 1.5 MRL)	
	within-day (n=5)	between-day (n=3×5)	within-day (n=5)	between-day (n=3×5)	within-day (n=5)	between-day (n=3×5)
SD	7.4	8.9	6.9	9.1	6.5	7.2
SP	6.9	8.8	7.1	8.3	6.0	7.4
STZ	7.1	7.7	7.6	7.9	6.7	7.6
SMZ	8.2	9.1	7.6	9.3	6.1	7.3
SMP	7.9	9.4	6.8	9.9	7.0	8.4
SCP	7.7	9.0	7.2	9.7	7.0	7.7
SMX	7.2	8.0	7.2	8.7	6.5	6.7
SIX	7.7	9.3	8.1	9.2	6.2	7.2
SDM	8.7	9.6	7.1	7.8	6.1	6.4
SQX	7.9	8.4	8.3	9.4	6.9	6.9

### 3.4 Conclusions

Melamine sponge is a promising alternative to common polyurethane or graphene sponges or other sponge-like materials, due to its many inherent advantages. Decorating the MeS with metallic copper using the proposed procedure has proved to be an easy and efficient way to alter the properties of the MeS. The CuMeS was used to develop a sample preparation procedure for the extraction of SAs from environmental water and milk samples. To the best of our knowledge, this is the first time that a sample preparation procedure takes advantage of the high affinity of copper with for SAs. Owing to this, high sensitivity and fairly good selectivity are ensured by the developed method. The low detection limits, wide linear range, highly satisfactory recoveries and repeatability of the method, highlight the merits of CuMeS for SAs microextraction. The proposed method was validated according to Commission Decision 657/2002/EC. Finally, the modification endows CuMeS with hydrophobicity due to the presence of copper, a benefit that can be further exploited for other applications.



Table 18: Comparison with other analytical methods

Analytes	Method	Adsorbent	Synthesis time*	Matrix	Linear range (µg/L or µg/Kg)	LOD (µg/L or µg/Kg) (S/N = 3)	RSD (%)	Recovery (%)	Reference	
SD, SM, SMZ, SML, SMX, SDM	Stir bar sorptive extraction and HPLC-MS/MS	C <sub>18</sub> coated stir bar	~10 min	milk	0.1-2000	0.9-10.5	7.3-16.7	87-120	[35]	
				milk powder				80-115		
STZ, SMX, SDM and trimethoprim	Bar adsorptive microextraction and HPLC-DAD	Polystyrene-divinylbenzene polymer coated stir bars	-	Tap, estuarine and wastewater	0.16-8.00	0.08-0.16	<15.2	63.8-84.2	[36]	
SD, STZ, SMZ, SMP, SCP, SMX, SIX, SDM, SQX	Magnetic dispersive solid phase extraction and HPLC-DAD	Magnetite-embedded with silica functionalized with phenyl chains	~17 h	milk	30-800	7-14	<10	81.8-114.9	[37]	
SMX, SD, SMZ, SDM, SM	Dispersive solid phase extraction and HPLC-UV	SMX imprinted acrylamide functionalized silica nanoparticles	~72 h	milk	50-20000	2.81-14.6	3.5-7.5	69.8-87.4	[38]	
				eggs				2.3-6.3		73.2-89.1
				honey				4.7-12.6		81.2-101
SMP, SMZ, SMX, SCP	Magnetic solid-phase extraction and HPLC-Amperometric detector	Magnetic hypercrosslinked polystyrene	~2 h	water	2.0-200	0.21-0.33	3-10	84-105	[39]	
				milk	10-400	2.0-2.5				

SM, SML, SDX, SMX, SIX	Dispersive solid phase extraction and HPLC-UV	CoFe <sub>2</sub> O <sub>4</sub> -graphene	~7 h	milk	20-50000	1.16-1.59	2.4-4.3	62.0-104.3	[40]
SP, SM, SDX, SCP, SMM	Magnetic dispersive solid phase extraction and HPLC-UV	Fe <sub>3</sub> O <sub>4</sub> @SiO <sub>2</sub> @G	-	Lake, sewage and waste water	0.5-100	0.09-0.16	<10.7	74.2-104.1	[41]
SA, SD, SP, SM, SMZ, SMP, SCP, SMX, SDM	Extraction and HPLC-DAD	Graphene-functionalized melamine sponges	2 min	milk	1-200	0.10-0.30	3.1-7.9	95-102	[13]
				eggs	10-200	0.32-0.44	5.0-6.9	90-108	
				lake water	1-200	0.03-0.09	2.7-4.2	96-105	
SD, SP, STZ, SMZ, SMP, SCP, SMX, SIX, SDM, SQX	Extraction and HPLC-DAD	Melamine sponge decorated with copper sheets	30 min	lake water	0.05-150	0.009-0.019	4.1-7.0	89-102	This work
				milk	0.5-150	0.075-0.35	6.8-9.9	88-97	

\*Graphene oxide synthesis and drying steps were not taken into account for the estimation of approximate synthesis time.

The results of the above study have been published in the *Journal of Chromatography A*



Contents lists available at ScienceDirect

Journal of Chromatography A

journal homepage: [www.elsevier.com/locate/chroma](http://www.elsevier.com/locate/chroma)



## Melamine sponge decorated with copper sheets as a material with outstanding properties for microextraction of sulfonamides prior to their determination by high-performance liquid chromatography



Theodoros G. Chatzimitakos, Constantine D. Stalikas\*

Laboratory of Analytical Chemistry, Department of Chemistry, University of Ioannina, 45110 Ioannina, Greece

### ARTICLE INFO

#### Article history:

Received 3 February 2018  
Received in revised form 29 March 2018  
Accepted 6 April 2018  
Available online 7 April 2018

#### Keywords:

Melamine sponge  
Metallic copper sheets  
Microextraction of sulfonamides  
Milk  
HPLC

### ABSTRACT

In this study, the modification/loading of melamine sponge with metallic copper sheets (CuMeS) is discussed. The CuMeS is prepared in a fast, single-step procedure, where concurrent production of copper oxides is avoided. The as-prepared CuMeS is utilized to develop a sensitive and selective sample preparation procedure to extract sulfonamides (SAs) from milk and water samples. The surface of the resulting CuMeS, after drying is rendered hydrophobic enabling hydrophobic interactions. To the best of our knowledge, this is the first time that the benefits of the high affinity of copper for SAs are reaped for analytical purposes. Due to the high selectivity, the proposed CuMeS-based procedure acts both as extraction and clean-up for the quantitative determination of SAs. The analytical method developed herein, which is based on the extractive potential of CuMeS, has the merits of wide linearity (including concentrations above and below the maximum residue limit of SAs), low limits of quantification ( $0.025\text{--}0.057\ \mu\text{g L}^{-1}$  for lake water and  $0.23\text{--}1.05\ \mu\text{g L}^{-1}$  for milk samples), high enrichment factors and highly satisfactory recoveries and repeatability. The analytical method is validated according to the Commission Decision 657/2002/EC. Owing to the low cost of CuMeS and the straightforward procedure followed the proposed method can be applied to routine analysis of SAs.

© 2018 Elsevier B.V. All rights reserved.

### 3.5 References

- [1] J. Han, Z. Cao, W. Qiu, W. Gao, J. Hu, B. Xing, Probing the specificity of polyurethane foam as a 'solid-phase extractant': Extractability-governing molecular attributes of lipophilic phenolic compounds, *Talanta*. 172 (2017) 186–198. doi:10.1016/j.talanta.2017.05.020.
- [2] X. Yang, Y.H. Han, L.H. Wang, Synthesis of Sponge-Like Material for the Extraction of Fluoroquinolones in Milk, *Adv. Mater. Res.* 1035 (2014) 231–234. doi:10.4028/www.scientific.net/amr.1035.231.
- [3] X. Gao, H. Yue, S. Huang, X. Lin, X.P.A. Gao, B. Wang, L. Yao, W. Wang, E. Guo, Synthesis of graphene/ZnO nanowire arrays/graphene foam and its application for determination of folic acid, *J. Electroanal. Chem.* 808 (2018) 189–194. doi:10.1016/j.jelechem.2017.12.017.
- [4] F.M. Jaward, N.J. Farrar, T. Harner, A.J. Sweetman, K.C. Jones, Passive Air Sampling of PCBs, PBDEs, and Organochlorine Pesticides Across Europe, *Environ. Sci. Technol.* 38 (2004) 34–41. doi:10.1021/es034705n.
- [5] J.O. Vinhal, C.F. Lima, R.J. Cassella, Polyurethane foam loaded with sodium dodecylsulfate for the extraction of “quat” pesticides from aqueous medium: Optimization of loading conditions, *Ecotoxicol. Environ. Saf.* 131 (2016) 72–78. doi:10.1016/j.ecoenv.2016.05.012.
- [6] E.A. Moawed, A.B. Abulkibash, M.F. El-Shahat, Synthesis of tannic acid azo polyurethane sorbent and its application for extraction and determination of atrazine and prometryn pesticides in foods and water samples, *Environ. Nanotechnology, Monit. Manag.* 3 (2015) 61–66. doi:10.1016/j.enmm.2015.02.001.
- [7] E.A. Moawed, A.M. Radwan, Application of acid modified polyurethane foam surface for detection and removing of organochlorine pesticides from wastewater, *J. Chromatogr. B Anal. Technol. Biomed. Life Sci.* 1044–1045 (2017) 95–102. doi:10.1016/j.jchromb.2016.12.041.
- [8] S. Jayanthi, A. Mukherjee, K. Chatterjee, A.K. Sood, A. Misra, Tailored nitrogen dioxide sensing response of three-dimensional graphene foam, *Sensors Actuators, B Chem.* 222 (2016) 21–27. doi:10.1016/j.snb.2015.08.041.
- [9] A.T.E. Vilian, S. An, S.R. Choe, C.H. Kwak, Y.S. Huh, J. Lee, Y.K. Han, Fabrication of 3D honeycomb-like porous polyurethane-functionalized reduced graphene oxide for detection of dopamine, *Biosens. Bioelectron.* 86 (2016) 122–128. doi:10.1016/j.bios.2016.06.022.
- [10] X. Wang, X. Guo, J. Chen, C. Ge, H. Zhang, Y. Liu, L. Zhao, Y. Zhang, Z. Wang, L. Sun, Au nanoparticles decorated graphene/nickel foam nanocomposite for sensitive detection of hydrogen peroxide, *J. Mater. Sci. Technol.* 33 (2017) 246–250. doi:10.1016/j.jmst.2016.11.029.

- [11] J. Bai, A. Zhou, Z. Huang, J. Wu, H. Bai, L. Li, Ultra-light and elastic graphene foams with a hierarchical structure and a high oil absorption capacity, *J. Mater. Chem. A* 3 (2015) 22687–22694. doi:10.1039/c5ta06204g.
- [12] Z. Dai, L. Liu, X. Qi, J. Kuang, Y. Wei, H. Zhu, Z. Zhang, Three-dimensional Sponges with Super Mechanical Stability: Harnessing True Elasticity of Individual Carbon Nanotubes in Macroscopic Architectures, *Sci. Rep.* 6 (2016). doi:10.1038/srep18930.
- [13] T. Chatzimitakos, V. Samanidou, C.D. Stalikas, Graphene-functionalized melamine sponges for microextraction of sulfonamides from food and environmental samples, *J. Chromatogr. A* 1522 (2017) 1–8. doi:10.1016/j.chroma.2017.09.043.
- [14] H. Sun, A. Li, Z. Zhu, W. Liang, X. Zhao, P. La, W. Deng, Superhydrophobic activated carbon-coated sponges for separation and absorption, *ChemSusChem* 6 (2013) 1057–1062. doi:10.1002/cssc.201200979.
- [15] Y. Yang, Y. Deng, Z. Tong, C. Wang, Multifunctional foams derived from poly(melamine formaldehyde) as recyclable oil absorbents, *J. Mater. Chem. A* 2 (2014) 9994–9999. doi:10.1039/c4ta00939h.
- [16] K. Hou, Y. Jin, J. Chen, X. Wen, S. Xu, J. Cheng, P. Pi, Fabrication of superhydrophobic melamine sponges by thiol-ene click chemistry for oil removal, *Mater. Lett.* 202 (2017) 99–102. doi:10.1016/j.matlet.2017.05.062.
- [17] J. Zhao, Q. Guo, X. Wang, H. Xie, Y. Chen, Recycle and reusable melamine sponge coated by graphene for highly efficient oil-absorption, *Colloids Surfaces A Physicochem. Eng. Asp.* 488 (2016) 93–99. doi:10.1016/j.colsurfa.2015.09.048.
- [18] A.B. Wiles, D. Bozzuto, C.L. Cahill, R.D. Pike, Copper (I) and (II) complexes of melamine, *Polyhedron* 25 (2006) 776–782. doi:10.1016/j.poly.2005.08.022.
- [19] O.S. Taskin, N. Ersoy, A. Aksu, B. Kiskan, N. Balkis, Y. Yagci, Melamine-based microporous polymer for highly efficient removal of copper(II) from aqueous solution, *Polym. Int.* 65 (2016) 439–445. doi:10.1002/pi.5074.
- [20] N. Bhawawet, S. Fuangswasdi, A. Imyim, Determination of Melamine Based on the Formation of an Insoluble Copper-Melamine Complex and Flame Atomic Absorption Spectrometry, *Anal. Lett.* 47 (2014) 1931–1937. doi:10.1080/00032719.2014.888728.
- [21] W. Yang, J. Li, P. Zhou, L. Zhu, H. Tang, Superhydrophobic copper coating: Switchable wettability, on-demand oil-water separation, and antifouling, *Chem. Eng. J.* 327 (2017) 849–854. doi:10.1016/j.cej.2017.06.159.

- [22] Y. Kobayashi, T. Shirochi, Y. Yasuda, T. Morita, Metal-metal bonding process using metallic copper nanoparticles prepared in aqueous solution, *Int. J. Adhes. Adhes.* 33 (2012) 50–55. doi:10.1016/j.ijadhadh.2011.11.002.
- [23] D. Deng, Y. Jin, Y. Chen, T. Qi, F. Xiao, Preparation of copper nanoparticles with low sintering temperature, 2012. doi:10.1109/EMAP.2012.6507927.
- [24] V. Andal, G. Buvaneswari, Effect of reducing agents in the conversion of Cu<sub>2</sub>O nanocolloid to Cu nanocolloid, *Eng. Sci. Technol. an Int. J.* 20 (2017) 340–344. doi:10.1016/j.jestch.2016.09.003.
- [25] D. Deng, Y. Jin, Y. Cheng, T. Qi, F. Xiao, Copper nanoparticles: Aqueous phase synthesis and conductive films fabrication at low sintering temperature, *ACS Appl. Mater. Interfaces.* 5 (2013) 3839–3846. doi:10.1021/am400480k.
- [26] E. Kremer, G. Facchin, E. Estévez, P. Alborés, E.J. Baran, J. Ellena, M.H. Torre, Copper complexes with heterocyclic sulfonamides: Synthesis, spectroscopic characterization, microbiological and SOD-like activities: Crystal structure of [Cu(sulfisoxazole)<sub>2</sub>(H<sub>2</sub>O)<sub>4</sub>] · 2H<sub>2</sub>O, *J. Inorg. Biochem.* 100 (2006) 1167–1175. doi:10.1016/j.jinorgbio.2006.01.042.
- [27] A. El Warraky, H.A. El Shayeb, E.M. Sherif, Pitting corrosion of copper in chloride solutions, *Anti-Corrosion Methods Mater.* 51 (2004) 52–61. doi:10.1108/00035590410512735.
- [28] K. Rhattas, M. Benmessaoud, M. Doubi, N. Hajjaji, A. Srhiri, Corrosion Inhibition of Copper in 3% NaCl Solution by Derivative of Aminotriazole, *Mater. Sci. Appl.* 02 (2011) 220–225. doi:10.4236/msa.2011.24028.
- [29] F. Gaucheron, The minerals of milk, *Reprod. Nutr. Dev.* 45 (2005) 473–483. doi:10.1051/rnd:2005030.
- [30] N. Graham, Guidelines for Drinking-Water Quality, 2nd edition, Addendum to Volume 1 – Recommendations, World Health Organisation, Geneva, 1998, 36 pages, 1999. doi:10.1016/s1462-0758(00)00006-6.
- [31] J. Banaś, B. Stypuła, K. Banaś, J. Światowska-Mrowiecka, M. Starowicz, U. Lelek-Borkowska, Corrosion and passivity of metals in methanol solutions of electrolytes, in: *J. Solid State Electrochem.*, 2009: pp. 1669–1679. doi:10.1007/s10008-008-0649-5.
- [32] E. Dubreil-Chéneau, Y. Pirotais, E. Verdon, D. Hurtaud-Pessel, Confirmation of 13 sulfonamides in honey by liquid chromatography-tandem mass spectrometry for monitoring plans: Validation according to European Union Decision 2002/657/EC, *J. Chromatogr. A.* 1339 (2014) 128–136. doi:10.1016/j.chroma.2014.03.003.

- [33] E. Karageorgou, N. Manousi, V. Samanidou, A. Kabir, K.G. Furton, Fabric phase sorptive extraction for the fast isolation of sulfonamides residues from raw milk followed by high performance liquid chromatography with ultraviolet detection, *Food Chem.* 196 (2016) 428–436. doi:10.1016/j.foodchem.2015.09.060.
- [34] J. Peris-Vicente, J. Esteve-Romero, S. Carda-Broch, Validation of Analytical Methods Based on Chromatographic Techniques: An Overview, in: *Anal. Sep. Sci.*, 2015: pp. 1757–1808. doi:10.1002/9783527678129.assep064.
- [35] C. Yu, B. Hu, C18-coated stir bar sorptive extraction combined with high performance liquid chromatography-electrospray tandem mass spectrometry for the analysis of sulfonamides in milk and milk powder, *Talanta.* 90 (2012) 77–84. doi:10.1016/j.talanta.2011.12.078.
- [36] A.H. Ide, S.M. Ahmad, N.R. Neng, J.M.F. Nogueira, Enhancement for trace analysis of sulfonamide antibiotics in water matrices using bar adsorptive microextraction (BA $\mu$ E), *J. Pharm. Biomed. Anal.* 129 (2016) 593–599. doi:10.1016/j.jpba.2016.07.022.
- [37] I.S. Ibarra, J.M. Miranda, J.A. Rodriguez, C. Nebot, A. Cepeda, Magnetic solid phase extraction followed by high-performance liquid chromatography for the determination of sulphonamides in milk samples, *Food Chem.* 157 (2014) 511–517. doi:10.1016/j.foodchem.2014.02.069.
- [38] R. Gao, J. Zhang, X. He, L. Chen, Y. Zhang, Selective extraction of sulfonamides from food by use of silica-coated molecularly imprinted polymer nanospheres, *Anal. Bioanal. Chem.* 398 (2010) 451–461. doi:10.1007/s00216-010-3909-z.
- [39] V. V. Tolmacheva, V. V. Apyari, A.A. Furletov, S.G. Dmitrienko, Y.A. Zolotov, Facile synthesis of magnetic hypercrosslinked polystyrene and its application in the magnetic solid-phase extraction of sulfonamides from water and milk samples before their HPLC determination, *Talanta.* 152 (2016) 203–210. doi:10.1016/j.talanta.2016.02.010.
- [40] Y. Li, X. Wu, Z. Li, S. Zhong, W. Wang, A. Wang, J. Chen, Fabrication of CoFe<sub>2</sub>O<sub>4</sub>-graphene nanocomposite and its application in the magnetic solid phase extraction of sulfonamides from milk samples, *Talanta.* 144 (2015) 1279–1286. doi:10.1016/j.talanta.2015.08.006.
- [41] Y.B. Luo, Z.G. Shi, Q. Gao, Y.Q. Feng, Magnetic retrieval of graphene: Extraction of sulfonamide antibiotics from environmental water samples, *J. Chromatogr. A.* 1218 (2011) 1353–1358. doi:10.1016/j.chroma.2011.01.022.





## Chapter 4: Enhanced magnetic ionic liquid-based dispersive liquid-liquid microextraction of triazines and sulfonamides through a one-pot, pH-modulated approach

### 4.1 Introduction

An ongoing trend in microextraction in chemical analysis is the use of ionic liquids (ILs). Commonly, ILs are molten salts at temperatures below 100 °C. They are composed of organic or inorganic ions, the wide variety of which can result in approximately 10<sup>18</sup> ionic liquids when diverse cations and anions are combined [1,2]. So far, ILs have been employed for the separation of various compounds using dispersive liquid-liquid microextraction, single drop microextraction, hollow fiber membrane liquid-phase microextraction and solid-phase microextraction, among others [3–9].

A more advanced, interesting concept of IL-based microextraction is the magnetic separation of the ILs from the analyzed matrix. To achieve separation and circumvent the laborious harvesting of ILs, magnetic ILs (MILs) have been developed by incorporating paramagnetic components in the IL chemical structure. Such MILs retain the advantageous properties of ILs and concurrently they strongly respond to external magnetic fields [10,11]. Owing to this improvement, the employment of MILs in microextraction has been rendered easier and new microextraction modes have become available, such as dispersive liquid-liquid microextraction with magnetic retrieval and stir-bar dispersive liquid microextraction [12,13]. The tetrachloroferrate anion was among the first paramagnetic components used for rendering the ILs magnetic [14]. However, the applicability of tetrachloroferrate-based MILs in microextraction is limited, due to hydrolysis of the anion which gives rise to low harvest efficiency of MILs [15]. As an alternative, MILs with transition or rare-earth metals have been developed and are less prone to hydrolysis while possessing increased magnetic moments [16,17]. Despite the improvements in the paramagnetic components of the MILs which are aimed at improving their magnetic properties, MILs have some drawbacks when they are

considered for analytical methodologies. For example, the hydrophilic nature of MILs limits their potential for aqueous-based applications. Increasing the alkyl-chain length of the components or introducing alternative ions (e.g., trihexyl(tetradecyl)phosphonium and Aliquat 336) addresses this issue and improves their extractive potential towards different groups of analytes, resulting in more use in hydrophobic MILs [11,15]. Moreover, the high viscosity of MILs intended for dispersive liquid-liquid microextraction is another drawback, due to their poor dispersibility and tendency to tightly adhere to the surface of the vessel walls [13,18].

Typical dispersive liquid-liquid microextraction procedures that employ MILs as extractants are based on vigorous stirring of the MIL drop resulting in many smaller dispersed droplets. However, the phenomenon of MIL drop breakage is uncontrolled and the density and size of the formed droplets is random, or widely distributed. This has an impact on the reproducibility/repeatability and efficiency of the microextraction method employed. Another factor that can affect the analytical figures of merit of a relevant analytical method is the viscosity of the MIL employed. The direct addition of an exact amount of a viscous MIL is a tricky task, resulting in variations of the MIL amount added between samples due to the uncontrolled size of the drop that is formed on a pipette tip.

Water pollution is a matter of high concern due to the increasing number of organic pollutants with adverse health effects detected in aquatic environments. The overuse and improper discharge of agricultural pesticides and veterinary drugs can lead to contamination of surface waters with relevant compounds [19]. Triazines (TZs) constitute a major class of herbicides that have been used for more than 50 years in weed control. Due to their high water solubility and persistence in water and organisms, they are invariably an environmental safety concern [20]. Moreover, owing to their endocrine-disrupting, teratogenic and carcinogenic effects, they pose a threat to human and animal health [21,22]. Sulfonamides (SAs) are a class of broad-spectrum antibacterial compounds that are widely administered in livestock animals and are among the most commonly

used classes of antibiotics in Europe [23,24]. They are harmful or highly toxic compounds (according to different risk assessment criteria), which can potentially cause cancer to humans, while their presence in the environment can also promote the development of antibiotic resistance [24–26]. The hazardous nature of the above classes of compounds has led regulatory agencies to establish maximum residue limits at 0.1 µg/L for each herbicide and 100 µg L<sup>-1</sup> for SAs [23,27].

In this chapter, we report an enhanced variant of MIL-based dispersive liquid-liquid microextraction which combines a water insoluble solid support and the [P<sub>66614</sub><sup>+</sup>][Dy(III)(hfacac)<sub>4</sub><sup>-</sup>] MIL (trihexyl(tetradecyl)phosphonium tetrakis (hexafluoroacetylaceto)dysprosate(III)) in a one-pot, pH-modulated procedure for the microextraction of TZs and SAs. The solid supporting material was mixed with the MIL to overcome difficulties regarding the weighing of the MIL and to assist in the control of uniform dispersion of the MIL, thus rendering the whole extraction procedure more reproducible. The employed pH-modulation during the microextraction procedure makes feasible the one-pot extraction of SAs and TZs from a single sample.

## 4.2 Material and methods

### 4.2.1 Chemicals and reagents

- Manganese(II) chloride tetrahydrate, Alfa Aesar (Ward Hill, MA, USA).
- Nickel(II) chloride (98%), Acros Organics (Morris Plains, NJ, USA)
- Ammonium hydroxide (28–30% solution in water), Acros Organics (Morris Plains, NJ)
- 1,1,1,5,5,5-hexafluoroacetylacetone (99%), Acros Organics (Morris Plains, NJ)
- Anhydrous diethyl ether (99.0%), Avantor Performance Materials Inc. (Center Valley, PA, USA)
- Trihexyl(tetradecyl) phosphonium chloride (97.7%), Strem Chemicals (Newburyport, MA, USA)
- Cobalt(II) chloride hexahydrate (98.0%), Sigma-Aldrich (St. Louis, MO, USA)
- Dysprosium(III) chloride hexahydrate (99.9%), Sigma-Aldrich (St. Louis, MO)
- Gadolinium(III) chloride hexahydrate (99.9%), Sigma-Aldrich (St. Louis, MO)
- Quartz silica (50–70 mesh particle size), Sigma–Aldrich (Steinheim, Germany)
- Silica (35–70 mesh), Sigma–Aldrich (Steinheim)
- Sodium chloride, Sigma–Aldrich (Steinheim)
- Sodium sulfate, Sigma–Aldrich (Steinheim)
- Trisodium citrate, Sigma–Aldrich (Steinheim)
- Sodium hydroxide, Sigma–Aldrich (Steinheim)
- Hydrochloric acid, Sigma–Aldrich (Steinheim)
- Sulfadiazine, and sulfamethazine (purities >99%) were purchased from Alfa Aesar (Karlsruhe, Germany).
- Sulfapyridine, sulfamerazine, sulfamethoxypyridazine, sulfachloropyridazine, sulfamethoxazole, sulfadimethoxine and sulfisoxazole (purities >99%) were purchased from Aldrich Sigma–Aldrich (Steinheim)
- Solvents (at least of analytical grade) Sigma–Aldrich (Steinheim).

Stock standard solutions of each compound were prepared in acetonitrile (ACN) at concentrations of  $1.0 \text{ mg mL}^{-1}$ . All solutions were stored in screw-capped, amber-glass vials at  $-18 \text{ }^{\circ}\text{C}$ .

#### 4.2.2 Instrumentation

Chromatographic separation and analysis were carried out on a Shimadzu HPLC system coupled to a Diode Array Detector (DAD). The system consisted of a LC20CE pump, a CTO 10AS column oven, a SPD-M20 A DAD and a Hypersil ODS column ( $250 \times 4.6 \text{ mm}$ ,  $5 \text{ }\mu\text{m}$ ) kept at  $30 \text{ }^{\circ}\text{C}$ . The sample was injected using a Rheodyne injector and the injection volume was  $20 \text{ }\mu\text{L}$ . The mobile phase consisted of water (A) and ACN (B), containing  $0.1\%$  (v/v) formic acid. The analytes were separated following a gradient elution program from  $10\%$  to  $55\%$  B (the MIL is completely soluble in this range), in  $50 \text{ min}$ . The flow rate of the mobile phase was set at  $1.0 \text{ mL min}^{-1}$ . The detector was set at a wavelength range of  $220\text{--}360 \text{ nm}$ . Data acquisition and processing were carried out using an LC-solution software version 1.21. Peak identification was based on the comparison of retention times and UV spectra (recorded at  $270 \text{ nm}$ ) with those of the authentic compounds.

#### 4.2.3 MIL synthesis

To prepare MILs containing the transition metals (i.e. Co, Mn and Ni), first  $10 \text{ mmol}$  of ammonium hydroxide were dissolved in  $30 \text{ mL}$  ethanol. After sealing the reaction vessel with a rubber septum, hexafluoroacetylacetone ( $10 \text{ mmol}$ ) was added dropwise at a rate of approximately  $1 \text{ mL min}^{-1}$  to the ethanolic solution. After the white vapor settles,  $3.3 \text{ mmol}$  of either cobalt(II) chloride hexahydrate, or manganese(II) chloride tetrahydrate or nickel(II) chloride, respectively were added. After stirring for  $5 \text{ h}$  at room temperature, the solvent was removed under vacuum and the resulting product was redissolved in  $20 \text{ mL}$  of diethyl ether. Then, deionized water was added several times in the above solution for cleaning, until the aqueous phase yielded no precipitate during a  $\text{AgNO}_3$  test. Diethyl

ether was removed under vacuum and the ammonium-metal hfacac salt was dried, overnight at 50 °C, under vacuum. Then, 1 mmol of the ammonium-metal hfacac salt was added to 1 mmol of the purified phosphonium chloride salt and dissolved in 30 mL of methanol. After overnight stirring at room temperature, the solvent was removed and the resulting product was redissolved in 20 mL of diethyl ether. Then, deionized water was added several times in the above solution for cleaning, until the aqueous phase yielded no precipitate during a AgNO<sub>3</sub> test. Diethyl ether was removed under vacuum and the MIL was dried, overnight at 50 °C, under vacuum. The rare earth based MILs were prepared according to the above procedure using 10 mmol of ammonium hydroxide, 10 mmol of hexafluoroacetylacetone, 2.5 mmol dysprosium(III) chloride hexahydrate or gadolinium(III) chloride hexahydrate, and finally, 1.2 mmol of the anion salt was mixed to 1 mmol of purified phosphonium chloride salt. When not in use, the MIL solvents were stored in a desiccator.

#### 4.2.4 Sample preparation

Water samples from Pamvotis Lake (Ioannina, Greece) and effluents of the municipal treatment plant of Ioannina were collected and filtered (to remove particulate matter). Finally, the pH was adjusted to 9.0 through the addition of NaOH solution.

#### 4.2.5 Extraction procedure

An aliquot of 75 mL of a sample was transferred to a glass beaker and 15 g of trisodium citrate was added. After complete dissolution, 500 mg of a [P<sub>66614</sub><sup>+</sup>][Dy(III)(hfacac)<sub>4</sub><sup>-</sup>]-quartz silica mixture (1:20 w/w) was added under stirring, at ~700 rpm, resulting in the formation of tiny droplets. After 10 min, the pH was adjusted to 3.0 using hydrochloric acid and the mixture was stirred for an additional 5 min. Then, the MIL droplets were harvested using a neodymium cylinder magnet and the MIL was diluted to 300 µL with acetonitrile. Finally, the solution was filtered through a 0.20 µm syringe filter (Corning®) and injected into the HPLC system for further separation and analysis.

## 4.3 Results and discussion

### 4.3.1 Selection of the solid supporting material

In dispersive liquid-liquid microextraction, the formation of as small as possible droplets is highly favorable to achieve maximum performance of the extraction procedure [28]. To overcome hindrances regarding the manipulation and dispersibility of the MIL (as mentioned in the introduction), solid supporting materials were examined, which were mixed together with the MIL prior to microextraction. By mixing the MIL with the solid support, the weighing of the whole mixture was easier than weighing the neat viscous MIL. Thus, it is ensured that always the same exact amount of MIL is used for the microextraction procedure. Ideally, the MIL should be physically deposited on the solid support since strong interactions are not favorable. Moreover, the solid support should separate fast from the MIL so that all droplets progressively formed would be available for extraction in a reasonable length of time. Finally, it should not be able to adsorb the desired analytes at the expense of MILs, thus lowering the achieved recoveries.

In our case, the solid supports which were mixed with the MIL included soluble inorganic salts and insoluble silica and quartz silica microparticles. For inorganic salts, it is conceivable that they possess a dual role: first to assist in the dispersion and secondly to enhance the extraction in case salting out plays a key positive role. Similarly, silica microparticles were examined since they could also assist in the dispersion, while they could also adsorb potential interfering compounds due to their surface chemistry. At first, sodium chloride and sodium sulfate were tested. Although the produced MIL-salt mixture seemed homogenous, aggregates were formed when it was added to the water requiring more time to dissolve and, as a consequence, a low amount of dispersed MIL in the form of droplets was observed. Subsequently, silica microparticles were tested. The mixture was “sticky”, not homogenized completely with the silica and most of the MIL remained on the walls of the mixing glassware. When added to water, the MIL could not easily be released and part of it was retained on the silica microparticles. Moreover, part of SAs and TZs were adsorbed by silica microparticles. To avoid laborious deactivating

procedures, quartz silica was further employed. When transferred to an aqueous sample under stirring, quartz silica particles carrying the MIL as extraction phase were dispersed homogeneously in the bulk phase and the MIL was released easily (in less than 1 min) with the aid of stirring, resulting in the formation of tiny droplets. In this manner, the droplets were dispersed in the bulk of the sample, while quartz silica settled at the bottom. Additionally, in the optimum conditions for the extraction (as will be explained later on), it was found that quartz silica cannot extract either SAs or TZs. Quartz silica was finally selected as the most suitable solid supporting material. Visual inspection during microextraction experiments revealed that droplets were more homogenous, reproducible and smaller compared to those without the use of solid support. Therefore, the available interface is higher when quartz silica is used while the dispersion phenomenon is less random and more controlled. Moreover, the size of the droplets was dependent on the ratio of quartz silica to MIL. Taking advantage of this, we examined different ratios in order to identify the optimal one that yielded the highest efficiency and most reproducible results. The ratios examined were: 1:5, 1:10, 1:20, 1:30 and 1:40 (MIL:quartz silica w/w), using two different sample volumes (i.e., 25 and 75 mL). Ratios of 1:5 and 1:10 resulted in decreased extraction yields due to the large-size droplets formed in the solution. In the case of ratios of 1:30 and 1:40, the droplets formed were so tiny that the extraction yields were decreased due to the high number of droplets that adhered to the beaker wall, resulting in lower overall extraction yields. The ratio 1:20 yielded the highest yield (almost 15% higher than other ratios). Therefore, this ratio was used for further experiments. To test the superiority of the procedure using the solid support over traditional MIL dispersive microextraction [12], both procedures were applied under the same conditions (i.e., sample volume: 20 and 75 mL, amount of MIL: 25 mg, stirring rate: 700 rpm and stirring time: 15 min, using the pH-modulated approach, *vide infra*) and were compared. The results were conclusive for the superiority of the quartz silica-MIL over the bare-MIL dispersive microextraction procedure, since the former was found to be nearly 20% more efficient with regard to the extraction of TZs



and almost 13% for SAs. Moreover, the reproducibility of microextraction, when the solid support was used was higher compared to the other method (the average relative standard deviation of five experiments for all analytes was 4.9 and 8.6 for the proposed and MIL dispersive microextraction procedure, respectively).

Before studying other parameters that affect the microextraction procedure, we made a comparison with other MILs for their extraction potential. For this study, another rare earth based MIL (i.e.  $[P_{66614}^+][Gd(III)(hfacac)_4^-]$ ) and some transition metal-based MILs ( $[P_{66614}^+][Co(II)(hfacac)_3^-]$ ,  $[P_{66614}^+][Mn(II)(hfacac)_3^-]$  and  $[P_{66614}^+][Ni(II)(hfacac)_4^-]$ ) were used. All five tested MILs had the same extraction behavior for both classes of compounds. Since the transition-based MILs possess three hexafluoroacetylacetonate ligands coordinated to the metal instead of four and present the same adsorption efficiency, it can be deduced that the anion does not play any role in the extraction of the analytes. Therefore, the selection of  $[P_{66614}^+][Dy(III)(hfacac)_4^-]$  was based solely on its effective magnetic moment, which is higher than the rest of the tested MILs [15]. Due to this, it could be harvested more easily and efficiently than the other studied MILs.

#### 4.3.2 Optimization of extraction

Parameters affecting the extraction were optimized to achieve maximum efficiency. In all cases, distilled water spiked with  $100 \mu\text{g L}^{-1}$  of each analyte was used to assess the performance of the extraction procedure as a function of several tested parameters. The criterion used for the evaluation of the different parameters was the average extraction yield of the total SAs and TZs content. The parameters studied were the pH, ionic strength, stirring time and rate, sample volume, and the amount of extracting phase.

#### 4.3.2.1 pH-modulation for extraction

Due to the ionizable nature of SAs and TZs, pH is expected to play a significant role in their extraction. By properly modulating the pH in a one-pot experiment both classes of analytes can be extracted efficiently in a single MIL dosage. To further explore the applicability of this concept, we initially examined the extraction efficiency in the pH range 2–10 for both classes of compounds. As expected, in more alkaline conditions, the transfer of TZs is favored (optimum pH = 9.0); on the contrary, SAs are extracted more efficiently under acidic conditions (optimum pH = 3.0) (Figure 31). In both cases, it can also be seen that the extraction yield decreases significantly as the pH either decreases (in the case of TZs) or increases (in the case of SAs), resulting in less than 5% extraction yield. Generally, the adsorption of SAs is favored under acidic conditions, where the neutral or deprotonated species dominate [26]. However, it is known that TZs hydrolyze in a strongly acidic environment [21,22] and, therefore, they are commonly extracted under neutral or alkaline conditions.

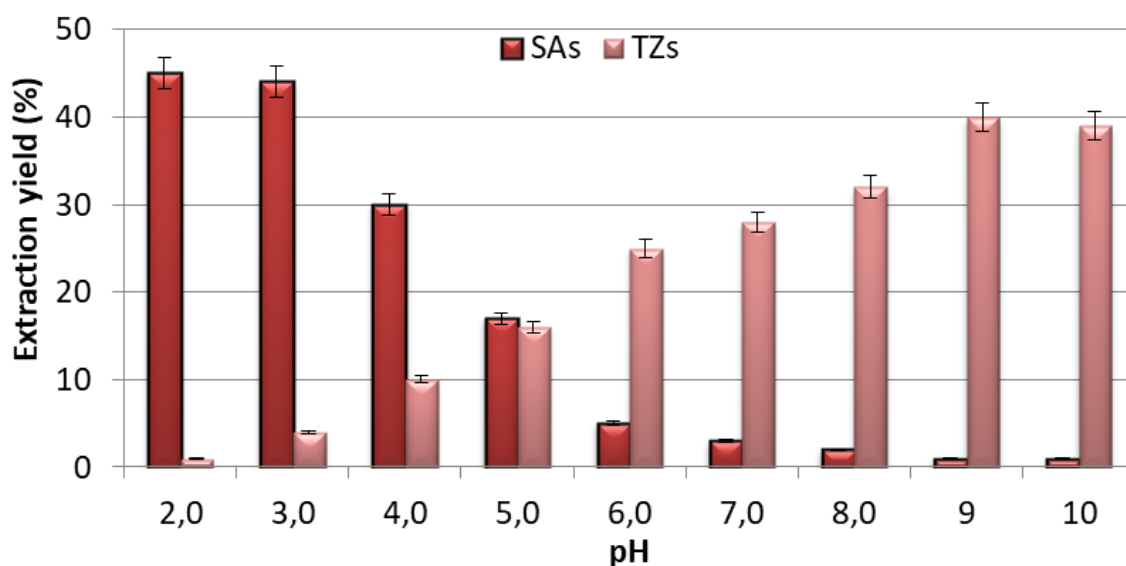


Figure 31: Effect of sample pH on the extraction of a mixture of SAs and TZs, containing  $100 \mu\text{g L}^{-1}$  of each (number of replicate analysis = 3).

The next step was to test the concurrent extraction of SAs and TZs in two ways: (I) by initially adjusting the pH to 3.0 and then increasing the pH of the solution to 9.0 and (II) by performing the opposite procedure of (I). The results demonstrate that the first (I) approach results in poor extraction of TZs while for SAs the extraction yield was satisfactory. This can be explained by the following. Firstly, the TZs studied herein have a  $pK_a$  between 1.0 and 4.3 and at pH 3.0 they co-exist in their neutral and protonated form. Thus, it can be deduced that their protonated form is extracted less efficiently than their neutral form, which dominates in the alkaline environment. Secondly and more importantly, TZs hydrolyze in strongly acidic environment, as mentioned above; this accounts for their decreased extraction yield at low pH. Due to this, TZs cease to exist in the working pH, in their native form and this accounts for the negligible extraction yield recorded. On the contrary, when the second way (II) was employed, TZs were extracted efficiently in the alkaline pH, while the subsequent decrease in the pH resulted in a satisfactory extraction of SAs. Moreover, the decrease in the pH was not accompanied by desorption of TZs from the MIL. This hints towards a mechanism that is not dependent upon the ionization of TZs and MIL. We have already concluded (Section 3.1) that the anion of the MIL does not play any role in the extraction. It is most likely that the procedure proceeds through interactions with the cation. Considering the hydrophobic nature of the cation (due to alkyl chains), hydrophobic interactions arise, mainly, between the cation of the MIL and TZs. Therefore, the extraction of both classes of compounds from a single sample, with a single MIL dosage is possible, without loss of efficiency for either class.

#### **4.3.2.2 Ionic strength**

One of the most exploited parameters during the optimization of a microextraction procedure is the ionic strength due to the so-called salting-out effect. On the other hand, as the ionic strength of a solution increases along with the favorable salting-out effect, secondary phenomena occur such as the increase in the viscosity of the solution, which often hinders the extraction process. In our case, three different salts, namely sodium

chloride, sodium sulfate, and trisodium citrate were employed to increase the ionic strength of the solution up to 30% w/v. For the sake of simplicity, the results depicted in Figure 32 represent the average extraction yield of both SAs and TZs. As can be seen, the higher amount of each of the three salts produced an increase in the extraction efficiency. This increase is more pronounced with trisodium citrate followed by sodium sulfate and sodium chloride. This is due to the different ionic strength that the salts exhibit. Apparently, the increase in extraction efficiency is attributed to the salting out effect, which lowers the solubility of organic compounds in aqueous media, thus, favoring their extraction [29,30].

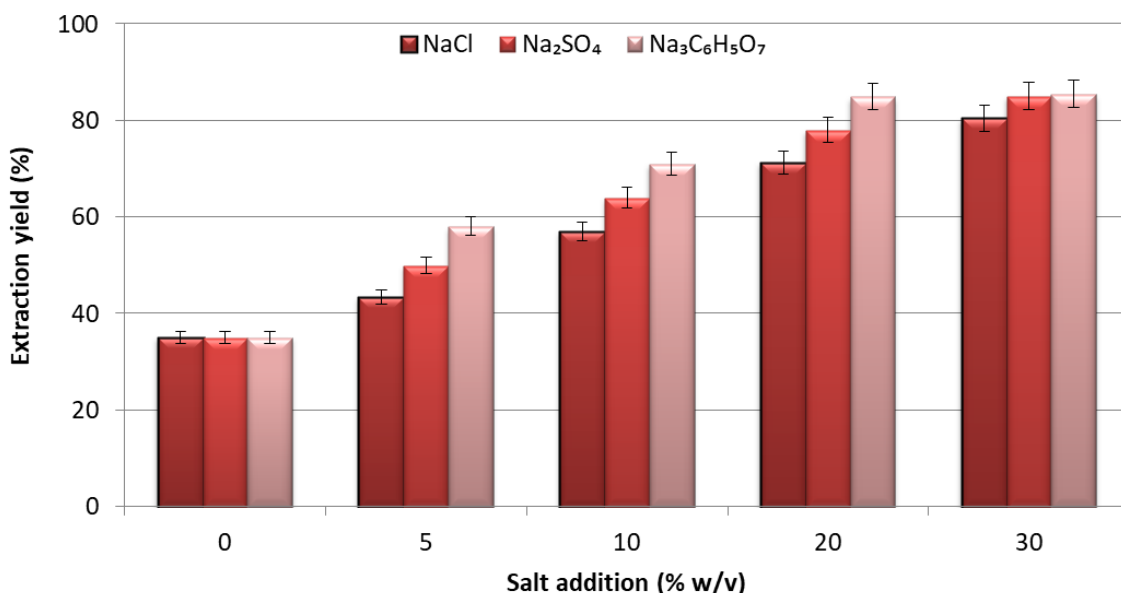


Figure 32: Addition of different salts to increase the ionic strength of the solution and the respective extraction efficiency for a mixture of SAs and TZs, containing  $100 \mu\text{g L}^{-1}$  of each (number of replicate analysis = 3).

Another secondary effect concomitant of the presence of high salt content is the reduction of the diffusion rate of the analytes, especially for less polar ones. Due to the polar to intermediate polar nature of the target analytes, this effect does not significantly affect the extraction efficiency [31]. Aside from the salting-out effect on the extraction

yield, the same experiments showed that as the ionic strength increases, the magnetic retrieval of the MIL was rendered easier and the tendency of the MIL droplets to adhere to the beaker wall was significantly lower. Although this does not affect the extraction yield, it favors the magnetic retrieval and thus, the reproducibility/repeatability of the procedure. Based on the results above, the addition of 20% w/v trisodium citrate was chosen in conducting further experiments, as a compromise of maximum efficiency and less consumption of salt.

#### ***4.3.2.3 Other extraction parameters***

Extraction experiments were conducted at three different temperatures (i.e., 25, 35 and 45 °C) to assess the effect of temperature on the extraction efficiency. The results showed that as temperature increases, there is a trivial increase (<5%) in the extraction efficiency of only TZs. Hence, no temperature control was used for further experiments. Stirring rate was set to a predetermined value without being optimized in relation to the other parameters. It was observed that stirring rates < 500 rpm resulted in poor extraction yields, due to the partial attachment of droplets on the magnetic stirring bar and rates >900 rpm caused the formation of unfavorable bubbles in the solution that assisted in the MIL droplets adhering to the beaker walls. Thus, a moderate-high stirring rate (i.e., 700 rpm) was found to be optimum and was employed for all experiments.

The next parameters optimized were the volume of the sample and the amount of the extracting phase. With regard to sample volume, the volumes 25, 50, 75 and 100 mL were initially tested by spiking with the same amount of analytes. Results showed a minor decrease in the extraction efficiency (<7%) up to 75 mL of sample, while a more pronounced decrease (~25%) was noticed for 100 mL. Subsequently, sample volumes of 25, 50 and 75 mL at the same concentration of analytes and sorbent amounts of 150, 300 and 500 mg were examined and assessed. From Figure 33, it can be seen that 500 mg of the MIL-quartz silica mixture was needed in all three tested sample volumes to achieve total extraction of the analytes. Therefore, this amount along with 75 mL of sample was selected to achieve high enrichment factors.

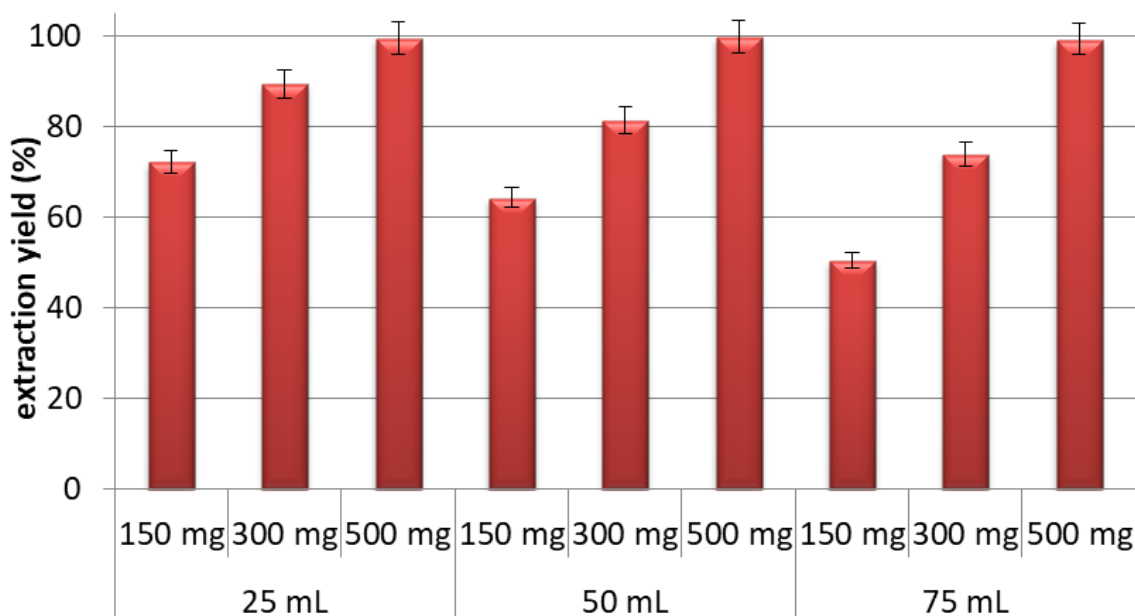


Figure 33: Effect of sample volume and amount of extracting phase on the efficiency of the method (number of replicate analysis = 3).

An extraction time up to 30 min in increments of 5 min was studied separately for both SAs and TZs. The results showed that complete extraction of TZs and SAs can be achieved within 10 min and 5 min, respectively. Prolonged extraction times resulted in yields that were neither improved nor lessened for any of the tested compounds. Thus, the overall procedure can be completed in 15 min, which is a rather short period of time for analysis of two classes of compounds.

#### 4.3.3. Analytical figures of merit

After optimizing all parameters that affect the extraction, an analytical method was developed for the determination of SAs and TZs. The solutes selected herein are representative and the method can be used for other compounds of the same category (e.g. sulfathiazole, simazine, etc.). As a proof-of-concept, the method was used to determine the concentration of the compounds in lake water and effluent from a municipal wastewater treatment plant. A chromatogram of spiked and non-spiked

effluent can be seen in Figure 34. The analytical characteristics of the developed procedure are listed in Tables 19 and 20. In all cases, SAs were quantified at the absorption maxima of 270 nm and TZs at 260 nm. The calibration curves were prepared using water spiked with the analytes in the range of 0.2–75  $\mu\text{g L}^{-1}$  and 0.1–75  $\mu\text{g L}^{-1}$  for TZs and SAs, respectively. For both classes of compounds, the coefficients of determination ( $R^2$ ) were higher than 0.9970, suggesting good linearity. The limits of quantification (achieved by decreasing the analyte concentration up to a signal-to-noise ratio = 10) ranged between 0.034 and 0.088  $\mu\text{g L}^{-1}$  for SAs and 0.041 and 0.091  $\mu\text{g L}^{-1}$  for TZs. The LOQs were lower than the maximum residue levels established for these analytes. The enrichment factors (EF) (calculated according to our previous study [13]) were found to be between 51 and 71 for SAs and between 20 and 41 for TZs. The extraction percentage (E%) (calculated according to our previous study [13]) was higher than 98% and 95% for SAs and TZs, respectively. The precision of the method was calculated as the relative standard deviation of five different samples, analyzed on the same day and three different samples on five consecutive days. The values were in the range of 5.2–7.3% (within-day) and 6.0–8.1% (between-day). Since no residues of the analytes were detected, relative recoveries of the examined compounds were calculated from the two water samples that were both spiked at two concentration levels (i.e., 0.2 and 1.0  $\mu\text{g L}^{-1}$  of each analyte). For municipal treatment plant water, recoveries were in the range of 89–96 % and 91–101% for 0.2 and 1.0  $\mu\text{g L}^{-1}$ , respectively. Likewise, recoveries from lake water were between 94 and 99% for the low concentration and 95 and 99% for the high concentration.

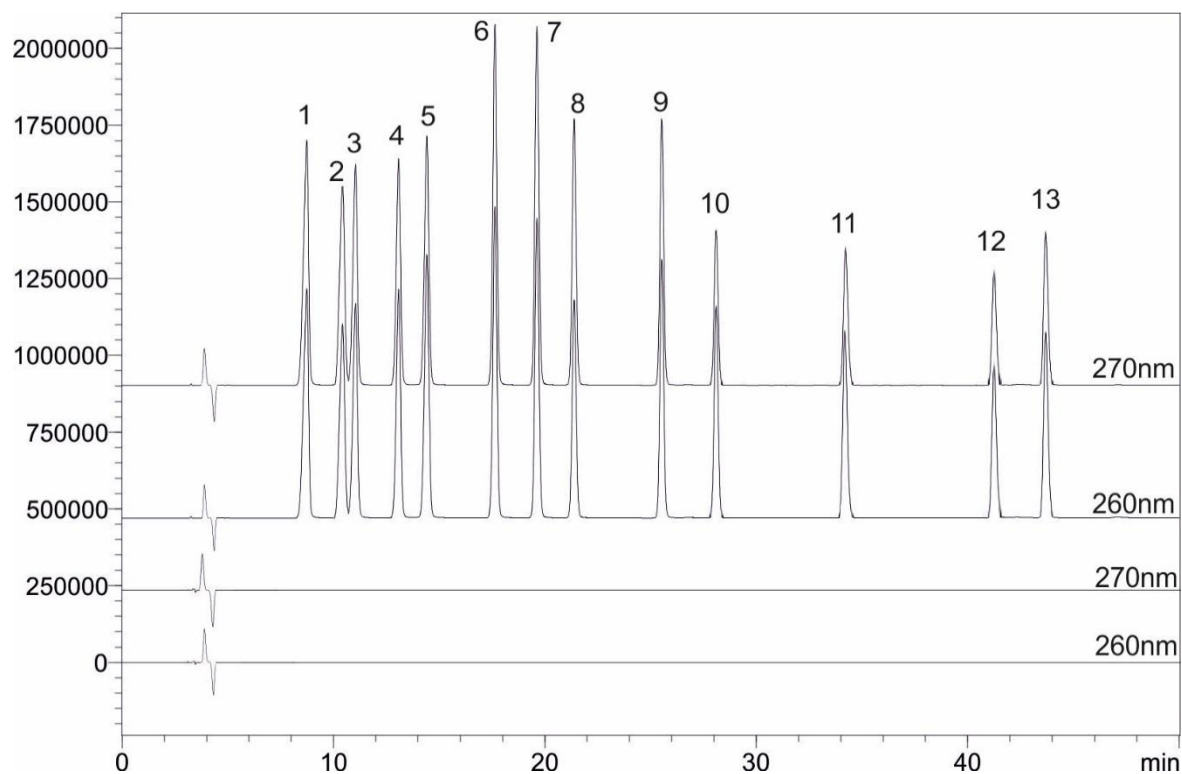


Figure 34: Chromatograms of the extract (obtained with the proposed procedure) of an effluent from municipal treatment plant, spiked with  $50 \mu\text{g L}^{-1}$  SAs and TZs (two upper) and non-spiked (two lower), at two different wavelengths. Peak assignment: 1. sulfadiazine, 2. sulfapyridine, 3. sulfamerazine, 4. sulfamethazine, 5. sulfamethoxy pyridazine, 6. sulfachloropyridazine, 7. sulfamethoxazole, 8. sulfisoxazole, 9. sulfadimethoxine, 10. terbuthryn, 11. atrazine, 12. propazine, 13. Terbutylazine.



Table 19: Analytical figures of merit of the developed MIL-based microextraction procedure

Compound	Slope $\pm$ error	Intercept $\pm$ error	Standard error of the regression	Coefficient of determination ( $R^2$ )	LOQ ( $\mu\text{g L}^{-1}$ )
SD	28983 $\pm$ 755	11735 $\pm$ 3458	7979	0.9973	0.054
SP	12406 $\pm$ 237	11394 $\pm$ 1843	2488	0.9975	0.088
SM	22967 $\pm$ 587	11510 $\pm$ 2688	6548	0.9984	0.054
SMZ	22279 $\pm$ 460	14255 $\pm$ 2167	4838	0.9970	0.063
SMP	25021 $\pm$ 563	15331 $\pm$ 2578	5933	0.9985	0.057
SCP	33142 $\pm$ 560	30116 $\pm$ 2576	5931	0.9980	0.036
SMX	34189 $\pm$ 730	22849 $\pm$ 3346	7659	0.9988	0.034
SIX	23989 $\pm$ 578	22985 $\pm$ 6465	6599	0.9970	0.042
SDM	23148 $\pm$ 485	39335 $\pm$ 2222	5838	0.9969	0.045
Terbuthryn	8368 $\pm$ 154	23333 $\pm$ 5473	7792	0.9983	0.041
Atrazine	6845 $\pm$ 136	21602 $\pm$ 4829	9521	0.9980	0.051
Propazine	6480 $\pm$ 195	17088 $\pm$ 6957	3717	0.9975	0.091
Terbutylazine	6841 $\pm$ 187	22427 $\pm$ 6671	3153	0.9973	0.044

Table 20: Enrichment factors (EF), Extraction percentages (E%), Relative standard deviations (RSD) and Relative recoveries of the developed MIL-based microextraction procedure

Compound	EF	E%	RSD (%)		Relative Recovery (%) <sup>A</sup>		Relative Recovery (%) <sup>B</sup>	
			within-	between-	0.2 µg	1.0 µg	0.2 µg	1.0 µg
			day (n=5)	day (n=3×5)	L <sup>-1</sup>	L <sup>-1</sup>	L <sup>-1</sup>	L <sup>-1</sup>
SD	71	99	5.2	7.2	95	97	99	99
SP	68	99	7.3	7.9	93	95	94	95
SM	69	99	5.4	6.0	95	101	94	95
SMZ	71	99	6.6	8.1	92	98	96	98
SMP	71	99	6.0	6.4	90	94	97	99
SCP	68	99	7.0	8.1	95	100	96	97
SMX	68	99	5.3	7.0	96	99	94	96
SIX	65	99	6.0	7.6	94	97	95	99
SDM	51	98	5.0	6.5	92	94	94	97
terbuthryn	41	97	5.1	6.4	92	97	94	97
atrazine	37	97	5.5	7.3	92	95	94	95
propazine	20	95	6.9	7.7	89	91	96	98
terbutylazine	40	98	5.5	6.9	89	94	94	98

<sup>A</sup> effluent from municipal wastewater treatment plant,

<sup>B</sup> lake water

As it can be seen from Table 21, the proposed procedure is advantageous in terms of (relative) recoveries and repeatability (expressed as relative standard deviation), highlighting the superiority for the determination of both classes of compounds. Most importantly, the proposed procedure can be used, simultaneously, for the extraction of both classes, compared to the other methods which are specific for only one class of them.

Table 21: Comparison of the developed procedure with other analytical methods

Analytes	Method	Extractant	Matrix	Linear range ( $\mu\text{g/L}$ or $\mu\text{g/kg}$ )	LOD ( $\mu\text{g/L}$ ) (S/N = 3)	RSD (%)	(Relative)Rec overy (%)	Reference
STZ, SMX, SDM and trimethoprim	Bar adsorptive microextraction and HPLC-DAD	Polystyrene- divinylbenzene polymer coated stir bars	Tap, estuarine and wastewater	0.16-8.00	0.08-0.16	<15.2	63.8-84.2	[32]
SMP, SMZ, SMX and SCP	Magnetic solid- phase extraction and HPLC- Amperometric detector	Magnetic hypercrosslinked polystyrene	water	2.0-200	0.21-0.33	3-10	84-105	[33]
SP, SM, SDX, SCP and SMM	Magnetic dispersive solid phase extraction and HPLC-UV	$\text{Fe}_3\text{O}_4@\text{SiO}_2@\text{G}$	Lake, sewage and waste water	0.5-100	0.09-0.16	<10.7	74.2-104.1	[34]
SA, SD, SP, SM, SMZ, SMP, SCP, SMX and SDM	Extraction and HPLC-DAD	Graphene-functionalized melamine sponges	lake water	1-200	0.03-0.09	2.7-4.2	96-105	[35]
Cyanazine, atrazine and simazine	Ionic liquid dispersive liquid- phase microextraction and HPLC-UV	1-Octyl-3- methylimidazolium hexafluorophosphate ([C8MIM][PF6])	river, underground, drainage and wastewater	0.5-80 for cyanazine and 1.0-100 for simazine and atrazine	0.05-0.06	4.8-8.9	85.1-100	[36]

Ametryn, atrazine, cyanazine, prometryn, propazine, simazine, simetryn, terbuthylazine and terbutryn	Solid-phase extraction and HPLC-DAD	Oasis HLB	tap water	0.02-0.1	0.010-0.023	3.8-11.7	86-110	[37]
Atrazine, ametryn, simetryn, propazine	Solid-phase extraction and HPLC-DAD	Double water compatible molecularly imprinted polymers	tap and river water	50-1000	3.2-8.6	1.33-4.73	69.2-95.4	[38]
SD, SP, SM, SMZ, SMP, SCP, SMX, SIX, SDM, terbuthryn, atrazine, propazine, terbuthylazine	Magnetic ionic liquid-based dispersive liquid- liquid microextraction using a one-pot, pH modulated approach and HPLC-DAD	[P66614 <sup>+</sup> ][Dy(III)(hfacac) <sub>4</sub> ]	lake water and effluent from a municipal wastewater treatment plant	0.1-100 for SAs and 0.2-75 for TZs	0.011-0.029 for SAs and 0.013-0.030 for TZs	5.2-7.3	90-101 for SAs and 89-98 for TZs	This work

#### 4.4 Conclusions

In this chapter, an advanced dispersive liquid-liquid microextraction method using MILs was developed. One major improvement was the use of quartz-silica as solid supporting material for the MIL microextraction mode. The use of the solid support renders handling of the MIL easier as well as significantly increases the reproducibility and efficiency of the method. Using a pH-modulated approach, the extraction of SAs and TZs could be performed in a one-pot procedure from the same sample in a short period of time allowing each class to be extracted separately at different sample pH. The enhanced method has suitable precision, good recovery and sensitivity and the achieved LOQs make feasible the determination of the compounds at levels below the maximum residue limits, as defined by regulatory agencies.

The results of the above study have been published in the *Journal of Chromatography A*

Journal of Chromatography A, 1571 (2018) 47–54



Contents lists available at ScienceDirect

Journal of Chromatography A

journal homepage: [www.elsevier.com/locate/chroma](http://www.elsevier.com/locate/chroma)



## Enhanced magnetic ionic liquid-based dispersive liquid-liquid microextraction of triazines and sulfonamides through a one-pot, pH-modulated approach



Theodoros G. Chatzimitakos<sup>a</sup>, Stephen A. Pierson<sup>b</sup>, Jared L. Anderson<sup>b</sup>,  
Constantine D. Stalikas<sup>a,\*</sup>

<sup>a</sup>Laboratory of Analytical Chemistry, Department of Chemistry, University of Ioannina, 45110 Ioannina, Greece

<sup>b</sup>Department of Chemistry, Iowa State University, Ames, IA, 50010 United States

### ARTICLE INFO

#### Article history:

Received 17 March 2018

Received in revised form 4 July 2018

Accepted 4 August 2018

Available online 7 August 2018

#### Keywords:

Enhanced magnetic ionic liquid-based  
microextraction  
Sulfonamides  
Triazines  
pH-modulated procedure  
HPLC-DAD

### ABSTRACT

In this study, an enhanced variant of magnetic ionic liquid (MIL)-based dispersive liquid-liquid microextraction is put forward. The procedure combines a water insoluble solid support and the  $[P_{66614}^+][Dy(III)(hfacac)_4^-]$  MIL, in a one-pot, pH-modulated procedure for microextraction of triazines (TZs) and sulfonamides (SAs). The solid supporting material was mixed with the MIL to overcome difficulties concerning the weighing of MIL and to control the uniform dispersion of the MIL, rendering the whole extraction procedure more reproducible. The pH-modulation during extraction step makes possible the one-pot extraction of SAs and TZs, from a single sample, in 15 min. Overall, the new analytical method developed enjoys the benefits of sensitivity (limits of quantification: 0.034–0.091  $\mu\text{g L}^{-1}$ ) and precision (relative standard deviation: 5.2–8.1%), while good recoveries (i.e., 89–101%) were achieved from lake water and effluent from a municipal wastewater treatment plant. Owing to all of the above, the new procedure can be used to determine the concentrations of SAs and TZs at levels below the maximum residue limits.

© 2018 Elsevier B.V. All rights reserved.

## 4.5 References

- [1] B.K. Kim, E.J. Lee, Y. Kang, J.J. Lee, Application of ionic liquids for metal dissolution and extraction, *J. Ind. Eng. Chem.* (2018). doi:10.1016/j.jiec.2017.12.038.
- [2] A.J. Carmichael, K.R. Seddon, Polarity study of some 1-alkyl-3-methylimidazolium ambient-temperature ionic liquids with the solvatochromic dye, Nile Red, *J. Phys. Org. Chem.* (2000). doi:10.1002/1099-1395(200010)13:10<591::AID-POC305>3.0.CO;2-2.
- [3] Ł. Marcinkowski, F. Pena-Pereira, A. Kloskowski, J. Namieśnik, Opportunities and shortcomings of ionic liquids in single-drop microextraction, *TrAC - Trends Anal. Chem.* (2015). doi:10.1016/j.trac.2015.03.024.
- [4] S.R. Wang, S. Wang, Ionic liquid-based hollow fiber-supported liquid-phase microextraction enhanced electrically for the determination of neutral red, *J. Food Drug Anal.* (2014). doi:10.1016/j.jfda.2014.03.006.
- [5] M.J. Trujillo-Rodríguez, P. Rocío-Bautista, V. Pino, A.M. Afonso, Ionic liquids in dispersive liquid-liquid microextraction, *TrAC - Trends Anal. Chem.* (2013). doi:10.1016/j.trac.2013.06.008.
- [6] T.D. Ho, A.J. Canestraro, J.L. Anderson, Ionic liquids in solid-phase microextraction: A review, *Anal. Chim. Acta.* (2011). doi:10.1016/j.aca.2011.03.034.
- [7] T. Chatzimitakos, C. Stalikas, Carbon-Based Nanomaterials Functionalized with Ionic Liquids for Microextraction in Sample Preparation, *Separations*. 4 (2017) 14. doi:10.3390/separations4020014.
- [8] T.D. Ho, C. Zhang, L.W. Hantao, J.L. Anderson, Ionic liquids in analytical chemistry: Fundamentals, advances, and perspectives, *Anal. Chem.* (2014). doi:10.1021/ac4035554.
- [9] K.D. Clark, M.N. Emaus, M. Varona, A.N. Bowers, J.L. Anderson, Ionic liquids: solvents and sorbents in sample preparation, *J. Sep. Sci.* (2018). doi:10.1002/jssc.201700864.
- [10] E. Santos, J. Albo, A. Irabien, Magnetic ionic liquids: Synthesis, properties and applications, *RSC Adv.* (2014). doi:10.1039/c4ra05156d.
- [11] K.D. Clark, O. Nacham, J.A. Purslow, S.A. Pierson, J.L. Anderson, Magnetic ionic liquids in analytical chemistry: A review, *Anal. Chim. Acta.* (2016). doi:10.1016/j.aca.2016.06.011.
- [12] A. Chisvert, J.L. Benedé, J.L. Anderson, S.A. Pierson, A. Salvador, Introducing a new and rapid microextraction approach based on magnetic ionic liquids: Stir bar dispersive liquid microextraction, *Anal. Chim. Acta.* (2017). doi:10.1016/j.aca.2017.06.024.

- [13] T. Chatzimitakos, C. Binellas, K. Maidatsi, C. Stalikas, Magnetic ionic liquid in stirring-assisted drop-breakup microextraction: Proof-of-concept extraction of phenolic endocrine disrupters and acidic pharmaceuticals, *Anal. Chim. Acta.* 910 (2016) 53–59. doi:10.1016/j.aca.2016.01.015.
- [14] T. Yao, S. Yao, Magnetic ionic liquid aqueous two-phase system coupled with high performance liquid chromatography: A rapid approach for determination of chloramphenicol in water environment, *J. Chromatogr. A.* (2017). doi:10.1016/j.chroma.2016.12.039.
- [15] S.A. Pierson, O. Nacham, K.D. Clark, H. Nan, Y. Mudryk, J.L. Anderson, Synthesis and characterization of low viscosity hexafluoroacetylacetonate-based hydrophobic magnetic ionic liquids, *New J. Chem.* (2017). doi:10.1039/c7nj00206h.
- [16] R.E. Del Sesto, T.M. McCleskey, A.K. Burrell, G.A. Baker, J.D. Thompson, B.L. Scott, J.S. Wilkes, P. Williams, Structure and magnetic behavior of transition metal based ionic liquids, *Chem. Commun.* (2002). doi:10.1039/b711189d.
- [17] P. Nockemann, B. Thijs, N. Postelmans, K. Van Hecke, L. Van Meervelt, K. Binnemans, Anionic rare-earth thiocyanate complexes as building blocks for low-melting metal-containing ionic liquids, *J. Am. Chem. Soc.* (2006). doi:10.1021/ja0640391.
- [18] V. Vičkačkaitė, A. Padarauskas, Ionic liquids in microextraction techniques, *Cent. Eur. J. Chem.* (2012). doi:10.2478/s11532-012-0023-4.
- [19] P. Du, M. Jin, C. Zhang, G. Chen, X. Cui, Y. Zhang, Y. Zhang, P. Zou, Z. Jiang, X. Cao, Y. She, F. Jin, J. Wang, Highly sensitive detection of triazophos pesticide using a novel bio-bar-code amplification competitive immunoassay in a micro well plate-based platform, *Sensors Actuators, B Chem.* (2018). doi:10.1016/j.snb.2017.10.075.
- [20] M. Mei, X. Huang, X. Yang, Q. Luo, Effective extraction of triazines from environmental water samples using magnetism-enhanced monolith-based in-tube solid phase microextraction, *Anal. Chim. Acta.* (2016). doi:10.1016/j.aca.2016.08.001.
- [21] X. Liu, C. Liu, P. Wang, G. Yao, D. Liu, Z. Zhou, Effervescence assisted dispersive liquid-liquid microextraction based on cohesive floating organic drop for the determination of herbicides and fungicides in water and grape juice, *Food Chem.* (2018). doi:10.1016/j.foodchem.2017.08.100.
- [22] Y. Wang, Y. Sun, B. Xu, X. Li, R. Jin, H. Zhang, D. Song, Magnetic ionic liquid-based dispersive liquid-liquid microextraction for the determination of triazine herbicides in vegetable oils by liquid chromatography, *J. Chromatogr. A.* (2014). doi:10.1016/j.chroma.2014.11.009.



- [23] S.G. Dmitrienko, E. V. Kochuk, V. V. Apyari, V. V. Tolmacheva, Y.A. Zolotov, Recent advances in sample preparation techniques and methods of sulfonamides detection - A review, *Anal. Chim. Acta.* (2014). doi:10.1016/j.aca.2014.08.023.
- [24] J.F. Huertas-Pérez, N. Arroyo-Manzanares, L. Havlíková, L. Gámiz-Gracia, P. Solich, A.M. García-Campaña, Method optimization and validation for the determination of eight sulfonamides in chicken muscle and eggs by modified QuEChERS and liquid chromatography with fluorescence detection, *J. Pharm. Biomed. Anal.* (2016). doi:10.1016/j.jpba.2016.02.040.
- [25] W. Baran, E. Adamek, J. Ziemiańska, A. Sobczak, Effects of the presence of sulfonamides in the environment and their influence on human health, *J. Hazard. Mater.* (2011). doi:10.1016/j.jhazmat.2011.08.082.
- [26] A. Armentano, S. Summa, S. Lo Magro, C. Palermo, D. Nardiello, D. Centonze, M. Muscarella, Rapid method for the quantification of 13 sulphonamides in milk by conventional high-performance liquid chromatography with diode array ultraviolet detection using a column packed with core-shell particles, *J. Chromatogr. A.* (2018). doi:10.1016/j.chroma.2017.11.015.
- [27] EU, Directive 2013/39/EU of the European Parliament and of the Council of 12 August 2013 amending Directives 2000/60/EC and 2008/105/EC as regards priority substances in the field of water policy, *Off. J. Eur. Union.* (2013).
- [28] H. Yu, J. Merib, J.L. Anderson, Faster dispersive liquid-liquid microextraction methods using magnetic ionic liquids as solvents, *J. Chromatogr. A.* (2016). doi:10.1016/j.chroma.2016.08.007.
- [29] T. Chatzimitakos, V. Exarchou, S.A. Ordoudi, Y. Fiamegos, C. Stalikas, Ion-pair assisted extraction followed by <sup>1</sup>H NMR determination of biogenic amines in food and biological matrices, *Food Chem.* 202 (2016) 445–450. doi:10.1016/j.foodchem.2016.02.013.
- [30] M. Serrano, T. Chatzimitakos, M. Gallego, C.D. Stalikas, 1-Butyl-3-aminopropyl imidazolium-functionalized graphene oxide as a nanoadsorbent for the simultaneous extraction of steroids and  $\beta$ -blockers via dispersive solid-phase microextraction, *J. Chromatogr. A.* 1436 (2016) 9–18. doi:10.1016/j.chroma.2016.01.052.
- [31] L. Xu, C. Basheer, H.K. Lee, Developments in single-drop microextraction, *J. Chromatogr. A.* (2007). doi:10.1016/j.chroma.2006.10.073.

- [32] A.H. Ide, S.M. Ahmad, N.R. Neng, J.M.F. Nogueira, Enhancement for trace analysis of sulfonamide antibiotics in water matrices using bar adsorptive microextraction (BA $\mu$ E), *J. Pharm. Biomed. Anal.* 129 (2016) 593–599. doi:10.1016/j.jpba.2016.07.022.
- [33] V. V. Tolmacheva, V. V. Apyari, A.A. Furletov, S.G. Dmitrienko, Y.A. Zolotov, Facile synthesis of magnetic hypercrosslinked polystyrene and its application in the magnetic solid-phase extraction of sulfonamides from water and milk samples before their HPLC determination, *Talanta*. 152 (2016) 203–210. doi:10.1016/j.talanta.2016.02.010.
- [34] Y.B. Luo, Z.G. Shi, Q. Gao, Y.Q. Feng, Magnetic retrieval of graphene: Extraction of sulfonamide antibiotics from environmental water samples, *J. Chromatogr. A*. 1218 (2011) 1353–1358. doi:10.1016/j.chroma.2011.01.022.
- [35] T. Chatzimitakos, V. Samanidou, C.D. Stalikas, Graphene-functionalized melamine sponges for microextraction of sulfonamides from food and environmental samples, *J. Chromatogr. A*. 1522 (2017) 1–8. doi:10.1016/j.chroma.2017.09.043.
- [36] Q.X. Zhou, Y.Y. Gao, Combination of ionic liquid dispersive liquid-phase microextraction and high performance liquid chromatography for the determination of triazine herbicides in water samples, *Chinese Chem. Lett.* (2014). doi:10.1016/j.ccllet.2014.01.026.
- [37] E. Beceiro-González, M.J. González-Castro, R. Pouso-Blanco, S. Muniategui-Lorenzo, P. López-Mahía, D. Prada-Rodríguez, A simple method for simultaneous determination of nine triazines in drinking water, *Green Chem. Lett. Rev.* (2014). doi:10.1080/17518253.2014.944940.
- [38] S. Xu, H. Lu, L. Chen, Double water compatible molecularly imprinted polymers applied as solid-phase extraction sorbent for selective preconcentration and determination of triazines in complicated water samples, *J. Chromatogr. A*. (2014). doi:10.1016/j.chroma.2014.05.026.

## Chapter 5: Zinc ferrite as a magnetic sorbent for the dispersive micro solid-phase extraction of sulfonamides and their determination by HPLC

### 5.1 Introduction

As shown in Chapter 3, metals show an affinity for SAs and for complexes, as well. Aside from copper, cadmium [1,2] mercury [3,4] and zinc [5–7] have also a high affinity for SAs. Zinc, it goes without saying that it could be a candidate for such purposes as it has the least impact on the environment. So far, zinc has been tailored into several nanomaterials but it has scarcely been used as a sorbent, except for lead ions [8] and methyl blue [9]. To avoid time-consuming steps, magnetic materials have been employed in dispersive solid-phase extraction procedures for various analytes [10,11]. Therefore, zinc ferrites could be good candidates to meet the requirements for a sorbent for novel applications. In this chapter, the synthesis of zinc ferrite, which is a material with enhanced magnetic properties is discussed, along with the examination of its potential as a sorbent for SAs extraction. Owing to the presence of zinc, SAs can readily be extracted from matrixes employing the magnetic zinc ferrite with the least environmental consequences. Lastly, an analytical method for the determination of SAs in lake water and egg samples was developed which has the merits of simplicity and selectivity, low matrix effect and good recoveries. Moreover, the method can claim adherence to the principles of green chemistry as few synthetic steps are involved and reduction of the use or generation of hazardous substances is achieved.

## 5.2 Materials and methods

### 5.2.1 Chemicals and reagents

- Sulfacetamide, sulfadiazine, sulfapyridine, sulfamerazine, sulfathiazole, sulfamethazine, sulfamethoxypyridazine, sulfachlorpyridazine, sulfamethoxazole, sulfisoxazole, sulfadimethoxine, and sulfaquinoxaline (purities >99%) were purchased from Aldrich Sigma–Aldrich (Steinheim, Germany)
- Zinc nitrate, Alfa Aesar (Karlsruhe, Germany)
- iron (III) chloride, Alfa Aesar (Karlsruhe)
- sodium hydroxide, Alfa Aesar (Karlsruhe)
- Solvents (at least of analytical grade) Sigma–Aldrich (Steinheim).

Stock solutions of SAs ( $1.0 \text{ mg mL}^{-1}$ ) were prepared in acetonitrile and stored at screw-capped, amber-glass vials, at  $-18 \text{ }^\circ\text{C}$ . Doubly-distilled water was used throughout the study.

### 5.2.2 Instrumentation

A D8 Advance diffractometer from Bruker AXS (Madison, USA) using CuK $\alpha$  ( $\lambda=1.5406 \text{ \AA}$ ) radiation was used for X-ray diffraction (XRD) analysis. The specific surface areas were calculated based on nitrogen adsorption-desorption porosimetry according to the BET method. The determination of the isotherms was carried out on an Autosorb-1 porosimeter from Quantachrom Instruments (Boynton Beach, USA). The magnetic properties of the respective nanomaterials were examined on a vibrating magnetometer (LakeShore 7300, Westerville, OH, USA), at room temperature. A Shimadzu (Kyoto, Japan) HPLC system consisting of a DGU-20A3R online degassing unit, two LC20AD pumps, a SIL-20AC HT autosampler, a CTO 20AC column oven and an SPD-M20A Diode Array Detector, was used for separation and analysis of the samples. The sample injection volume was  $20 \text{ }\mu\text{L}$ . A Hypersil Gold ( $250 \times 4.6 \text{ mm}$ ,  $5 \text{ }\mu\text{m}$  particle size) column from Thermo Fisher Scientific was used for the separation of SAs. The temperature of the column was held constant at  $30 \text{ }^\circ\text{C}$ . The analytes were separated by applying a gradient elution program using water (A) and

acetonitrile (B) containing 0.1% (v/v) formic acid. In 30 min, the concentration of B was increased from 10% to 35% and then kept at 35% for 5 more minutes. The flow rate of the mobile phase was 1.0 mL min<sup>-1</sup>. The detector was set at a wavelength range of 200–360 nm. Peak identification was achieved by comparing the retention times and UV spectra (recorded at 270 nm) of peaks in samples with those of pure compounds.

### 5.2.3 Zinc ferrites synthesis

The synthesis of zinc ferrites was based on a co-precipitation process, reported in a previous study [12]. In brief, 10 mL of zinc nitrate solution (0.462 mol L<sup>-1</sup>) and 10 mL of iron (III) chloride (1.368 mol L<sup>-1</sup>) were placed in a glass beaker and heated at 80 °C, for 30 min. Then, sodium hydroxide solution (5 mol L<sup>-1</sup>) was added dropwise under vigorous stirring, until pH = 11. After heating at 80 °C for an additional 2 h, under stirring, the mixture was centrifuged at 5000 rpm, for 5 min. The precipitate was washed three times with water and twice with ethanol and then placed in an oven at 60 °C, overnight. The resulting solid material was ground to a fine powder.

### 5.2.4 Ultrasound-assisted dispersive micro solid-phase procedure

In a glass beaker, 20 mL of sample and 3 g of sodium sulfate were added. The solution was stirred at 900 rpm until the salt was completely dissolved and then, 20 mg of zinc ferrites were added, followed by ultrasonication for 15 s. After 30 min of stirring at 900 rpm, the sorbent was harvested using a neodymium magnet and washed twice with distilled water. For the desorption of the analytes, 2 mL of acetonitrile, containing 2% v/v formic acid was added after discarding the water and the mixture was ultrasonicated for 30 s. Then, the organic solvent was transferred to an Eppendorf tube and evaporated to dryness, under a gentle nitrogen stream. Finally, 100 µL of water : acetonitrile mixture (90:10 v/v) was added and after ultrasonication for 1 min, a portion of the sample was injected into the HPLC system.

### 5.2.5 Sample preparation

Egg samples (purchased from a local market at Ioannina, Greece) were prepared by homogenizing whole eggs (without the addition of any solvent) by magnetic stirring at 900 rpm, for 5 min. In a glass beaker, 2 mL of the homogenized eggs and 18 mL of water were transferred and mixed thoroughly by magnetic stirring. Finally, the pH was adjusted to 6.0, using a hydrochloric acid solution ( $0.5 \text{ mol L}^{-1}$ ).

Lake water was collected from Lake Pamvotis (Ioannina, Greece). All samples were filtered through a  $0.45 \mu\text{m}$  filter membrane to remove particulate matter and the pH was adjusted to 6.0 using a hydrochloric acid solution of  $0.5 \text{ mol L}^{-1}$ .

## 5.3 Results and discussion

### 5.3.1 Synthesis optimization

In order to achieve optimum extraction efficiency, parameters associated with the synthesis of zinc ferrites were optimized. The use of different zinc salts, the zinc-to-iron ratio, salts concentration, reaction time, reaction temperature and the need for calcination of zinc ferrite were studied in detail. The optimum synthesis conditions were selected by evaluating the synthesized zinc ferrite for its extraction efficiency (%) in an aqueous solution containing a mixture of twelve SAs ( $100 \mu\text{g mL}^{-1}$  each).

#### 5.3.1.1 Effect of zinc salt

For the synthesis of zinc ferrite, different amounts of zinc salts of sulfate, acetate, nitrate, and chloride were used so that the concentration of zinc ions was constant. In all cases, the synthesized zinc ferrites were adequately magnetic to be harvested. As can be seen from Figure 35, the different counter ions do not affect the produced zinc ferrites, since their extraction efficiency does not differ from each other ( $t < 0.05$ ). Further experiments were carried out using zinc nitrate as a zinc ion source, which is in accordance with the original synthesis method [12].

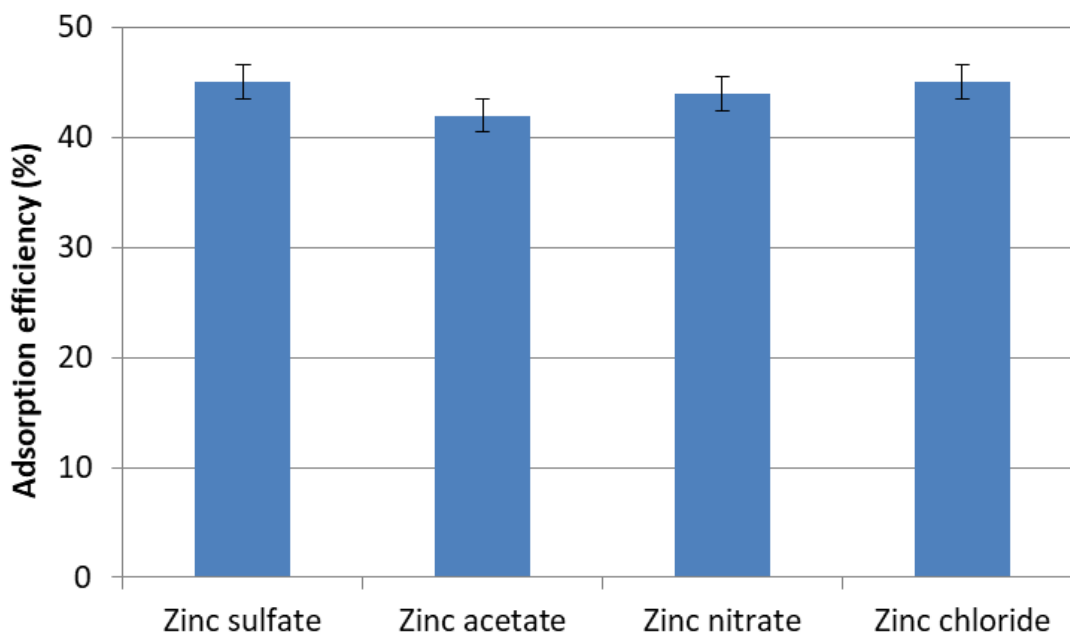


Figure 35: Effect of using different zinc salts during the synthesis of zinc ferrites on their adsorption efficiency for SAs (number of replicate analysis = 3).

#### 5.3.1.2 Zinc-to-iron molar ratio in the co-precipitation process

As the magnetic properties of zinc ferrites are speculated to derive from ferrite and the extraction is achieved, mainly, through zinc, the zinc-to-iron molar ratio in the reaction medium for the synthesis of zinc ferrites is expected to have a serious impact on the extraction efficiency. In order to develop the optimum material for the adsorption of SAs, zinc ferrites with initial zinc-to-iron molar ratios of 1:5, 1:3, 1:2, 1:1, 2:1, 3:1 and 5:1 were synthesized. The synthesized materials with molar ratios of 2:1, 3:1 and 5:1 were not magnetic while that with a molar ratio of 1:1 was barely magnetic. Hence, they were not tested further. With regard to the other three materials, their adsorption efficiencies can be seen in Figure 36. The material with a zinc-to-iron molar ratio of 1:5 had the lowest total adsorption efficiency (16%) among the three tested materials most likely because the zinc content is the lowest. Although it would be expected that the material with the molar ratio of 1:2 would be more efficient than that with 1:3, this was not the case. Specifically, after the extraction procedure, a considerable amount of particles were not



able to be harvested, thus, resulting in an overall low extraction efficiency of SAs. As a consequence, the material with a zinc-to-iron molar ratio of 1:3 proved to be the most efficient since it combines both good magnetic properties and efficient adsorption.

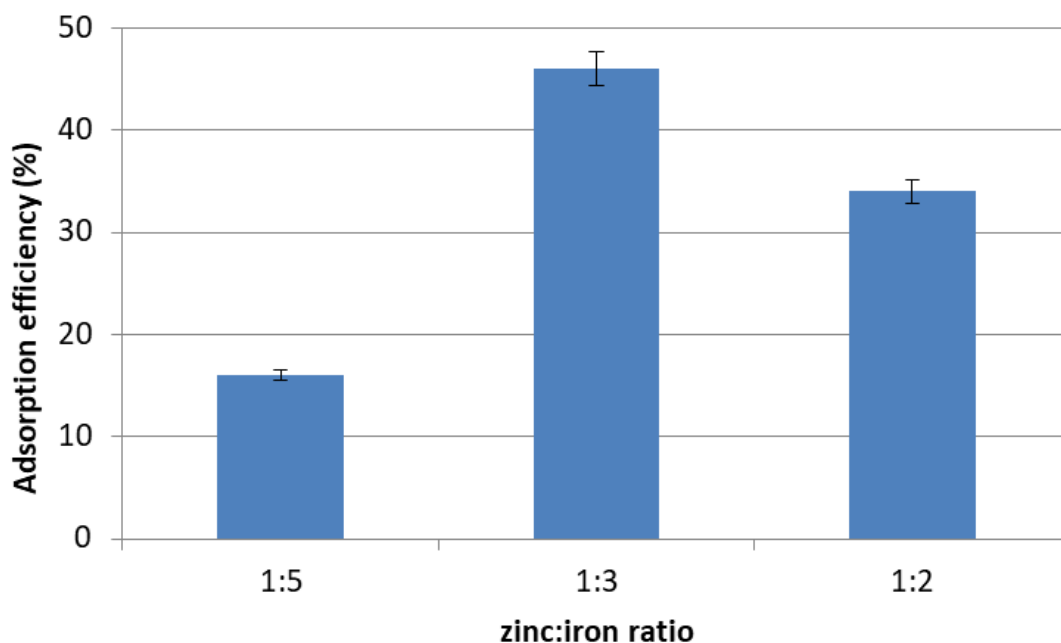


Figure 36: Effect of different zinc: iron molar ratios during the synthesis of zinc ferrites on their adsorption efficiency for SAs (number of replicate analysis = 3).

#### 5.3.1.3 Reaction temperature, time and calcination

Zinc ferrites were prepared at different temperatures (i.e. 25 °C, 50 °C and 80 °C). The results demonstrated that the temperature of 80 °C produces the optimum material. The materials prepared at the two other temperatures exhibited ~25% lower adsorption efficiency. Similarly, zinc ferrites heated for different time periods (i.e. 30 min, 60 min, 120 min and 360 min) were synthesized and the efficiency of the extraction acquired a maximum with the material prepared at 120 min. Finally, we examined the effect of annealing the sorbent at 500 °C for 8 h, as conducted in a previous report [12]. The annealed zinc ferrites retained their magnetic properties and no difference was observed in the adsorption efficiency of SAs, between the annealed and non-annealed zinc ferrites. Finally, the within-

batch and between-batch reproducibility of the synthesis were evaluated in terms of the relative standard deviation of five replicate analyses. The results were highly satisfactory, as within-batch and between-batch reproducibilities were 4.1% and 4.8%, respectively.

### 5.3.2 Characterization

After the optimization procedure, the optimum zinc ferrite material (as described in section 2.3) was characterized. Figure 37 depicts the XRD pattern of the synthesized sorbent. From the diffraction peaks, it can be inferred that the particles have a cubic spinel structure with space group  $Fd\bar{3}m$ . This is in accordance with previous reports [12–14]. Since no other peaks were detected, it can be concluded that the synthesized material is of high purity. Using Scherrer's equation the mean particle size was calculated to be  $11\pm 3$  nm.

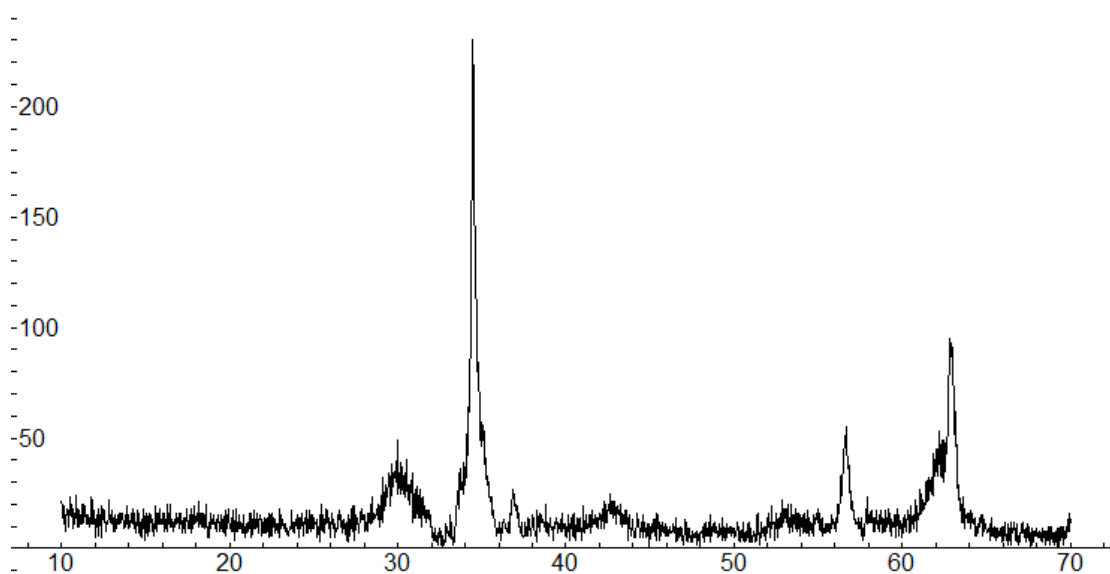


Figure 37: XRD pattern of the synthesized zinc ferrites.

The magnetization property was investigated at room temperature by measuring the magnetization curves (Figure 38). The saturation magnetization is  $29.8 \text{ emu g}^{-1}$ , indicating that the magnetic composite has high magnetism which ensures complete magnetic separation, under an external magnetic field.

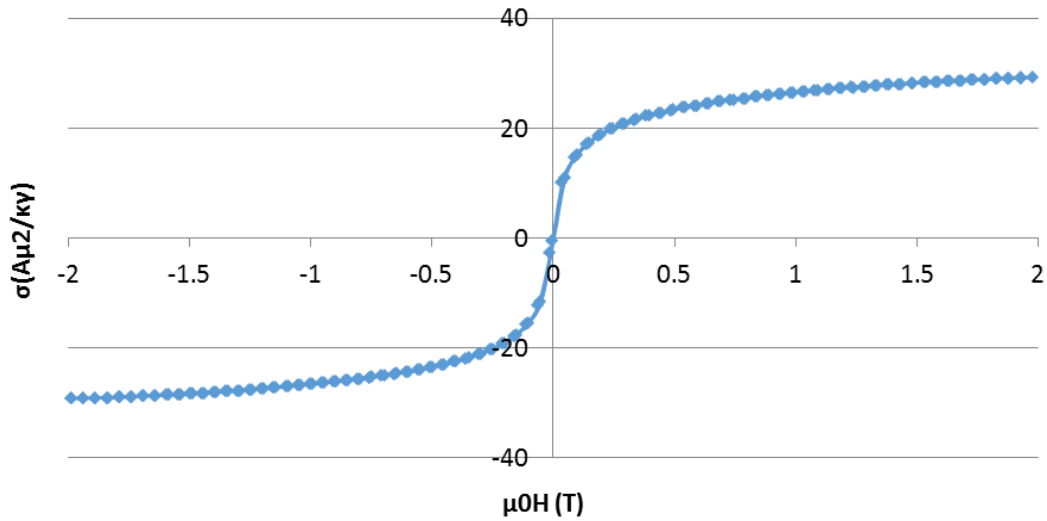


Figure 38: Magnetization curves of the synthesized zinc ferrite.

The surface properties of the synthesized adsorbent were characterized by nitrogen adsorption-desorption measurements. The nitrogen sorption isotherms of the zinc ferrite are shown in Figure 39. A moderate specific surface area was obtained which was calculated as  $124 \text{ m}^2 \text{ g}^{-1}$ .

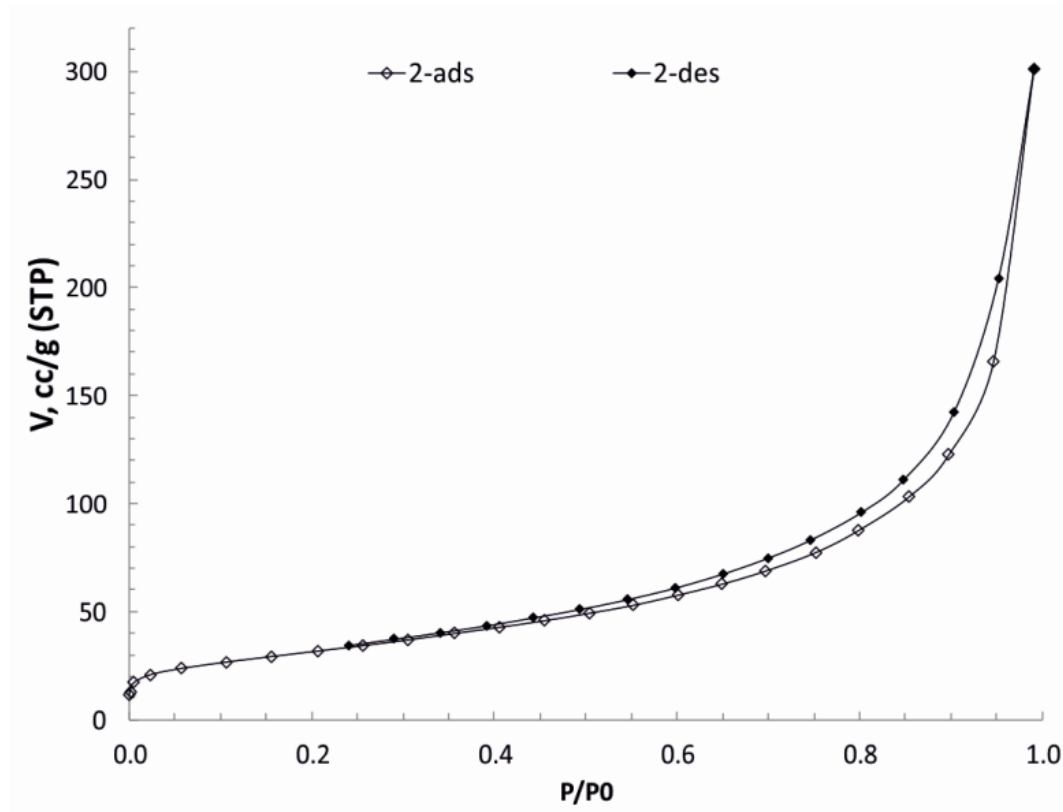


Figure 39: Nitrogen adsorption-desorption isotherms for the synthesized zinc ferrite.

### 5.3.3 Optimization of the extraction procedure

#### 5.3.3.1 Effect of the pH – Mechanism of interaction

The first parameter examined to optimize the ultrasound-assisted dispersive micro solid-phase procedure was sample pH, considering the ionizable character of SAs. As can be seen from Figure 40, optimum extraction was achieved at sample pH 6.0. The adsorption efficiency for all examined SAs follows the same trend at different pH values, except for sulfacetamide and sulfisoxazole, which were adsorbed ~12% at pH 4.0. Since the adsorption for most SAs was independent of sample pH, this bespeaks a mechanism that is also pH-independent in the studied range. Yuan et al. studied sulfadiazine complexes with zinc and found that the metal can be coordinated to the nitrogen atom of the pyrimidine ring, the nitrogen of the sulfonamide group and the oxygen atom of the sulfonyl group [7]. At pH 5–8 the neutral and negatively-charged forms of SAs coexist. As the adsorption of SAs was not affected in this range, the interactions with the ionizable sulfonamide nitrogen atom are not expected to occur and as such, the analytes interact with zinc, via the nitrogen of pyrimidine or the oxygen atom. However, this is not the case for sulfacetamide and sulfisoxazole, because they do not possess a pyrimidine ring. Sulfacetamide does not contain an aromatic ring either; so it should interact with zinc, primarily, through the oxygen atom and secondly via the sulfonamide nitrogen, which is negatively charged at pH 6.0, where its adsorption is the highest. Similar interactions occur, also, for sulfisoxazole which contains an isoxazole ring, instead of a pyrimidine ring. Although an isoxazole ring is also contained in sulfamethoxazole, its adsorption was not affected by the sample pH, as happened with sulfisoxazole. From the chemical structures of these two compounds, it can be seen that in sulfamethoxazole the nitrogen atom of the isoxazole ring is in position 2 in the ring (starting the numbering from the carbon that bonds with the sulfonamide nitrogen), as occurs with the nitrogen atoms of the pyrimidine rings. However, in sulfisoxazole the nitrogen atom is in position 3, hindering its interaction with zinc. Therefore, all three mechanisms are applicable in our case, with the most favorable to be the interaction via the pyrimidine nitrogen.

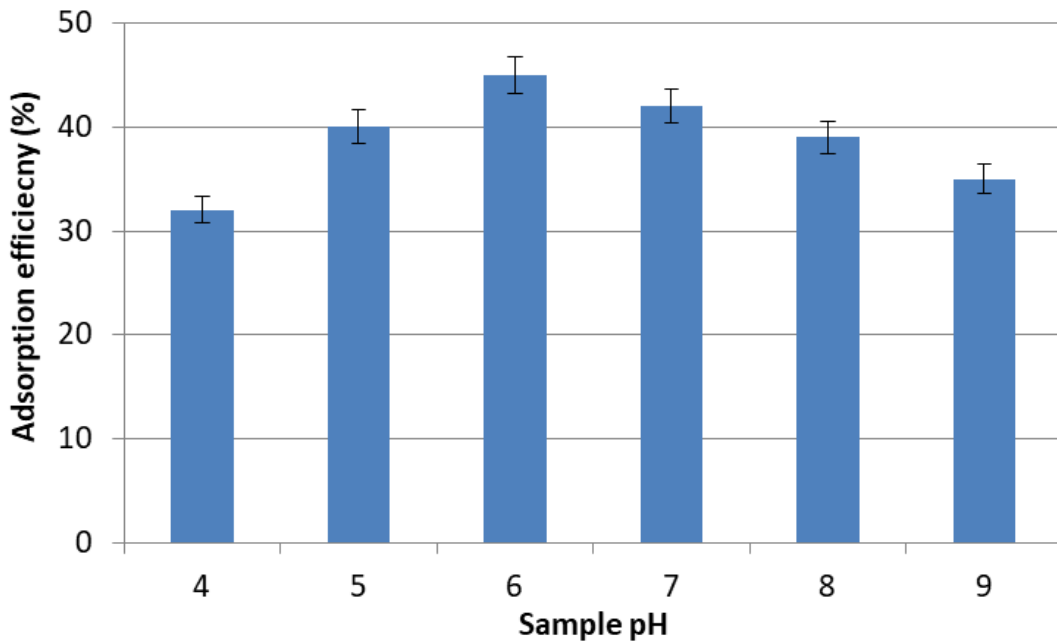


Figure 40: Effect of the pH on the adsorption efficiency of SAs on zinc ferrites (number of replicate analysis = 3).

### 5.3.3.2 Ionic strength

The effect of ionic strength on the adsorption efficiency of SAs from zinc ferrites was examined, using sodium chloride or sodium sulfate at concentrations up to 30% w/v in increments of 5%. As can be seen in Figure 41, the addition of both salts drastically improved the adsorption efficiency of SAs. This is due to the decrease of SAs solubility, owing to the salting-out effect, which promotes their adsorption on zinc ferrite [15,16]. Maximum adsorption efficiency was attained by the addition of either 25% w/v sodium chloride or 15% w/v sodium sulfate. This can be attributed to the different ionic strength that the two salts exhibit. For further experiments, 15% w/v sodium sulfate was added, so as to achieve the highest adsorption efficiencies.

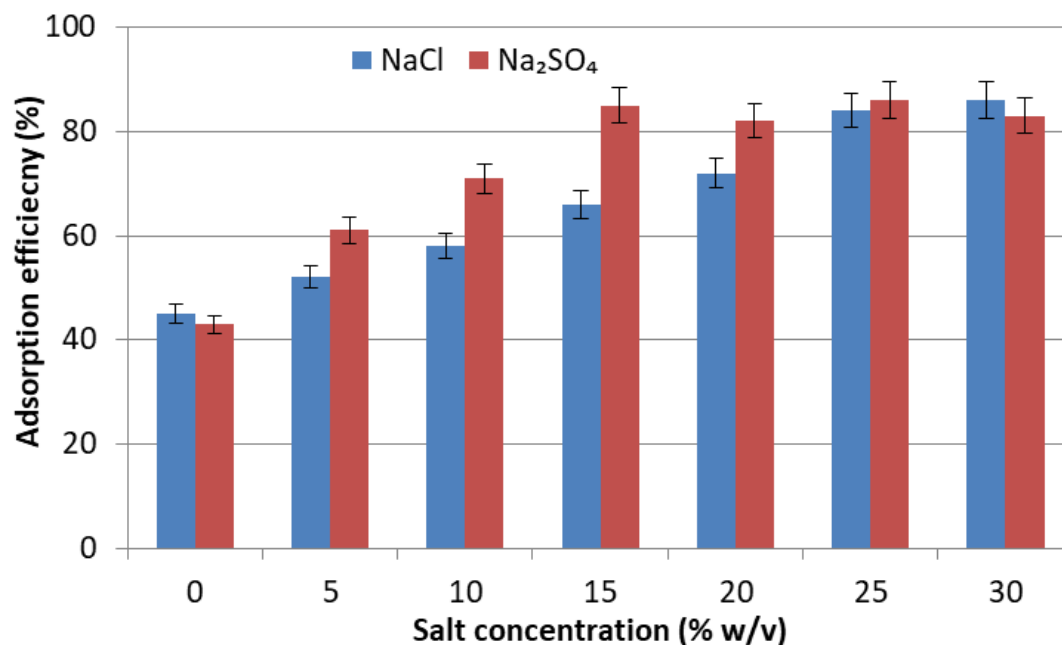


Figure 41: Effect of increasing ionic strength on the adsorption efficiency of SAs from zinc ferrites (number of replicate analysis = 3).

### 5.3.3.3 Other extraction parameters

Three different temperatures (i.e. 25, 35 and 45 °C) were tested. As temperature increases, a negligible decrease of the adsorption efficiency was recorded (~6% decrease at 45 °C, compared to 25 °C). Therefore, no temperature control was employed for further experiments. Next, we studied the impact of the stirring rate at the adsorption efficiency. Three stirring rates (300, 600 and 900 rpm) were examined for this purpose. The stirring rate of 300 rpm was found unsuitable since particles are attached to the magnetic bar during the ultrasound-assisted dispersive micro solid-phase procedure. Although no difference in the adsorption efficiencies was visible at the other two stirring rates, that of 900 rpm was selected to achieve fast mass transfer rates.

Finally, the sample volume, the amount of sorbent and the extraction time were studied, in order to define the optimum parameters. Four different sample volumes (10, 20, 30 and 50 mL), spiked with the same amount of SAs (100 µg mL<sup>-1</sup> each) were initially tested. A minor decrease in the adsorption efficiency (<8%) was recorded up to 30 mL sample

volume, while a more sharp decrease (~22%) in the adsorption efficiency was recorded for 50 mL sample volume. Based on the above, we carried out experiments by altering simultaneously the three aforementioned parameters (sample volume: 10, 20 and 30 mL; extraction time: 10, 20 and 30 min; sorbent amount: 10, 20 and 30 mg). The results can be seen in Figure 42, where the maximum overall adsorption of SAs was achieved at 20 and 30 mg of zinc ferrite. To minimize the sorbent consumption, 20 mg of sorbent was selected as the optimum. As far as sample volume and extraction time are concerned, when 20 mg of sorbent was used, optimum results were obtained when SAs were extracted from 10 mL of sample for 20 min or 20 mL of sample for 30 min. A combination of a high sample volume and a long extraction time (i.e. 20 mL and 30 min) was selected in order to obtain the highest enrichment factors.

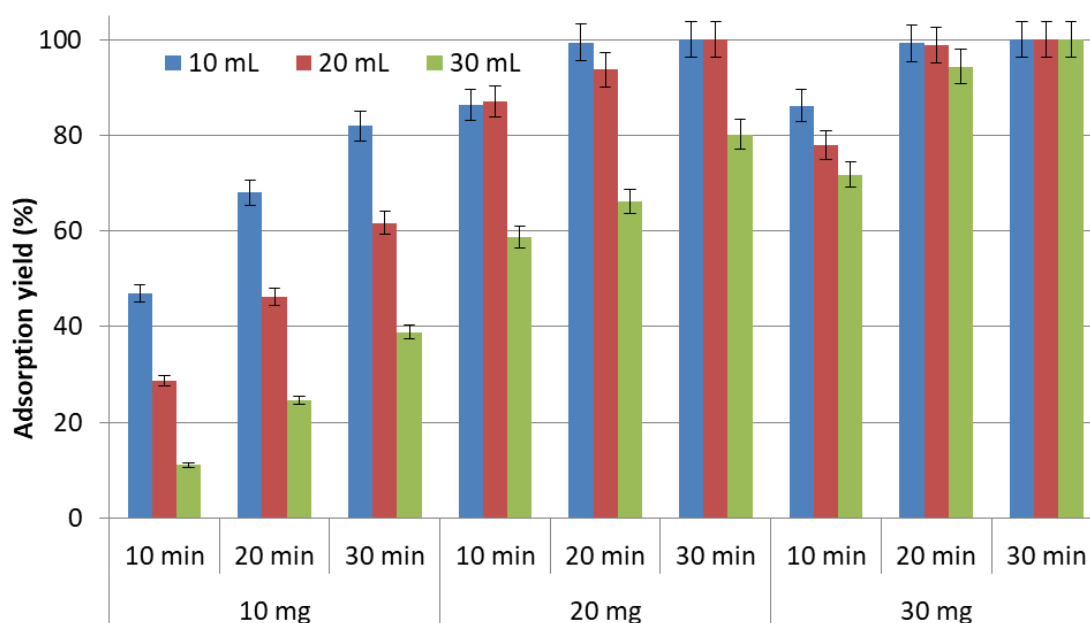


Figure 42: Effect of different sample volume, sorbent mass and extraction time on the adsorption efficiency of SAs from zinc ferrites (number of replicate analysis = 3).

#### 5.3.4 Optimization of the elution conditions

For the elution of SAs, initially, 1 mL of acetonitrile and methanol were used. When acetonitrile was used the elution yield was ~45%, whereas for methanol the elution was ~10% lower. Therefore, acetonitrile was selected as the optimum solvent. Formic acid and ammonia were added to acetonitrile at various percentages (1–5% v/v, in increments of 1%) to heighten the elution by the addition of acid or base. When ammonia was added, no improvement was recorded. When 2% of formic acid was used, a 20% increase of the elution yield was recorded, while higher concentrations of formic acid did not further improve the elution, after the ultrasound-assisted dispersive micro solid-phase extraction procedure. Finally, a second elution step was employed, using 1 mL of acidified acetonitrile and it was found that the extraction yield of SAs reached 100%. To simplify the elution, a single elution step with 2 mL of acidified acetonitrile was finally adopted, which was as efficient as that with two elution steps of 1 mL of solvent each.

#### 5.3.5 Method validation

Under the optimum conditions, the analytical figures of merit of the analytical method were evaluated. A representative chromatogram of the extract obtained from a spiked egg sample and a non-spiked sample can be seen in Figure 43. Calibration plots were prepared by analyzing water samples spiked with SAs from 250  $\mu\text{g L}^{-1}$  up to the limit of quantification (LOQ). The limits of quantification (calculated by decreasing the analyte concentration until the signal-to-noise ratio was 10), were between 0.06  $\mu\text{g L}^{-1}$  and 0.11  $\mu\text{g L}^{-1}$  (a complete list of the analytical figures of merit is provided in Tables 22 and 23). The equations of the calibration curves, the coefficients of determination ( $R^2$ ) and the other analytical figures of merit are listed in Tables 22 and 2. The  $R^2$  values ranged between 0.9983 and 0.9998, implying good linearity. Next, the % matrix effect for egg and lake water samples were evaluated according to our previous report [17]. The matrix effect was between -7% and 8% for lake water samples and between -8% and 3% for egg samples. Because all values were <20%, no significant interferences, due to matrix effect



occur in the analytical method. Therefore, there is no need to prepare matrix-matched calibration curves for either matrix. The enrichment factors (calculated according to our previous reports [18]) were in the range of 112–138 and 111–141 for lake water and egg samples, respectively. Next, the precision of the method was evaluated for both matrices. Five different samples were analyzed on the same day and three different samples were analyzed each day, for three consecutive days and the relative standard deviations (RSDs) of the results were calculated. For egg samples, the RSD values were between 4.0 and 7.2 for within-day analyses and between 5.7 and 8.1 for between-day analyses. In regard to lake water samples, the RSD values were between 3.4 and 6.8 for within-day analyses and between 4.2 and 8.4 for between-day analyses. Finally, the relative recoveries of SAs from both matrixes were calculated, by spiking them with  $0.3 \mu\text{g L}^{-1}$  ( $\sim 3$  times the LOQ) and  $1.0 \mu\text{g L}^{-1}$  ( $\sim 10$  times the LOQ), since no SAs residues were detected by the analysis of blank samples. The recoveries for egg samples were in the range of 88–98% and 92–99% for the lower and upper tested concentrations, respectively. For lake water samples, the recoveries were in the ranges of 91–99% and 95–101% for the lower and upper tested concentrations, respectively. The above figures of merit support an analytical method that can lend itself to the sensitive detection of SAs.

Table 22: Analytical figures of merit of the developed ultrasound-assisted dispersive micro solid-phase procedure for SAs detection in egg and lake water samples

SAs	linear equation	coefficient of determination ( $R^2$ )	LOQ ( $\mu\text{g kg}^{-1}$ )	Enrichment factor		Matrix effect (%)	
				Lake water	Eggs	Lake water	Eggs
SA	$y=132x+4030$	0.9993	0.062	131	132	2	-5
SD	$y=70x+1846$	0.9989	0.060	128	135	6	-2
SP	$y=71x+7290$	0.9985	0.103	130	135	-3	-4
SM	$y=82x+3201$	0.9986	0.085	112	111	-6	-8
STZ	$y=105x+8030$	0.9993	0.117	138	115	7	-4
SMZ	$y=78x+8584$	0.9991	0.093	135	116	1	-6
SMP	$y=99x+6545$	0.9983	0.095	116	119	-4	3
SCP	$y=100x+7733$	0.9988	0.065	129	141	8	-4
SMX	$y=144x+4927$	0.9985	0.085	116	121	7	2
SIX	$y=108x+9358$	0.9994	0.098	131	124	1	-1
SDM	$y=101x+8774$	0.9983	0.108	138	128	-3	-4
SQX	$y=61x+5360$	0.9998	0.075	129	123	-7	-3

Table 23: Relative standard deviations and relative recoveries of SAs from egg and lake water samples with the developed ultrasound-assisted dispersive micro solid-phase procedure

SAs	Eggs				Lake water			
	RSD (%)		Relative recovery (%)		RSD (%)		Relative recovery (%)	
	within-day	between-day	0.3 $\mu\text{g L}^{-1}$	1 $\mu\text{g L}^{-1}$	within-day	between-day	0.3 $\mu\text{g L}^{-1}$	1 $\mu\text{g L}^{-1}$
	(n=5)	(n=3×3)			(n=5)	(n=3×3)		
SA	4.9	6.6	92	93	3.6	4.2	94	97
SD	6.3	7.2	93	94	3.4	6.1	93	97
SP	4.0	5.7	96	99	5.4	6.5	91	96
SM	5.4	7.8	98	99	4.6	7.9	92	98
STZ	6.8	8.1	93	97	5.0	6.1	99	101
SMZ	7.2	7.8	96	98	5.6	6.9	91	96
SMP	5.8	7.9	91	92	4.3	6.5	96	97
SCP	5.5	7.7	91	95	5.1	6.1	94	101
SMX	5.4	6.2	88	93	6.8	8.4	93	95
SIX	7.0	7.7	95	99	6.1	6.9	96	98
SDM	4.1	6.9	92	96	4.0	7.1	95	99
SQX	5.4	7.9	92	94	4.5	7.2	97	98

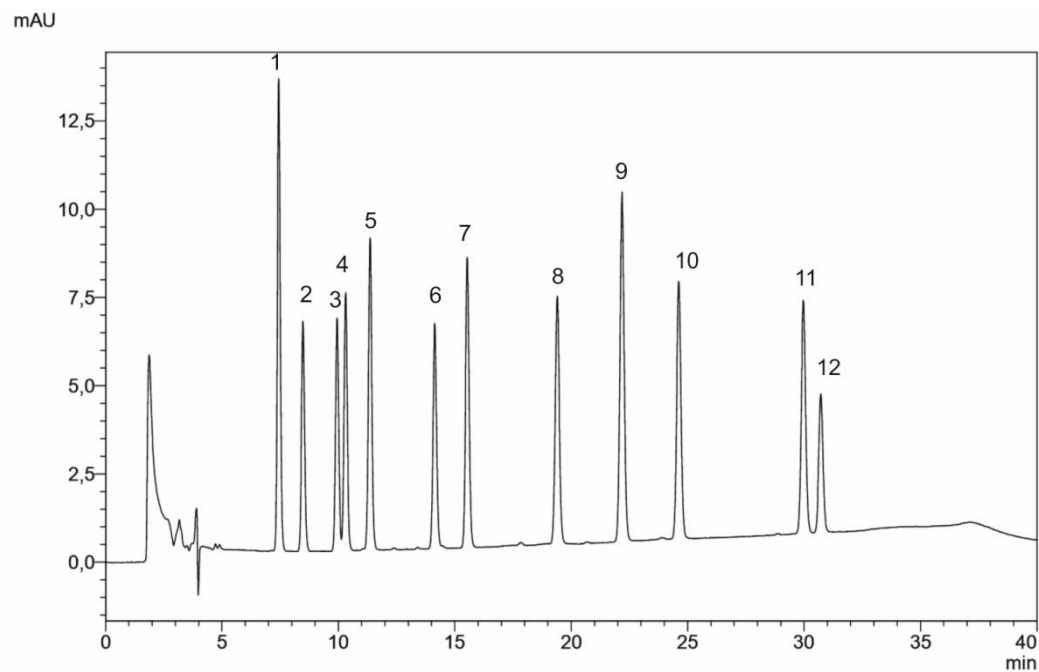


Figure 43: Chromatogram of the extract obtained with the developed procedure from egg sample spiked with  $3.75 \mu\text{g mL}^{-1}$  of each sulfonamide; 1: sulfacetamide; 2: sulfadiazine; 3: sulfapyridine; 4: sulfamerazine; 5: sulfathiazole; 6: sulfamethazine; 7: sulfamethoxypyridazine; 8: sulfachlorpyridazine; 9: sulfamethoxazole; 10: sulfisoxazole; 11: sulfadimethoxine; 12: sulfaquinoxaline

## 5.4 Conclusions

In this study, we used, for the first time, zinc ferrites as a sorbent for SAs extraction from lake water and egg samples. The material was utilized under the principles of the magnetic ultrasound-assisted dispersive micro solid-phase extraction so that it can easily be harvested after the extraction step. Due to the high affinity of zinc ferrite for SAs, an efficient and selective analytical method was developed. The wide linear range, low limits of quantification, low matrix effects and the good recoveries are among the benefits of the developed procedure. Overall, it was highlighted that zinc ferrites can be used in analytical chemistry, while the utilization of their affinity towards SAs can be the basis for the development of future applications, taking advantage of similar affinities of metals for other organic compounds. The developed procedure is green, sustainable and can be used as an alternative to or a substitute for existing methods for the determination of SAs.

The results of the above study have been published in *Microchemical Journal*

Microchemical Journal 155 (2020) 104670



ELSEVIER

Contents lists available at ScienceDirect

Microchemical Journal

journal homepage: [www.elsevier.com/locate/microc](http://www.elsevier.com/locate/microc)



## Zinc ferrite as a magnetic sorbent for the dispersive micro solid-phase extraction of sulfonamides and their determination by HPLC



Theodoros Chatzimitakos, Constantine Stalikas\*

Laboratory of Analytical Chemistry, Department of Chemistry, University of Ioannina, 45110 Ioannina, Greece

### ARTICLE INFO

#### Keywords:

Zinc ferrite  
Dispersive micro solid-phase extraction  
Sulfonamide extraction  
Lake water  
Eggs  
HPLC

### ABSTRACT

In this study, the use of zinc ferrites in a magnetic, ultrasound-assisted dispersive micro solid-phase extraction procedure for the determination of sulfonamides is developed. Zinc ferrites can efficiently and selectively extract sulfonamides from environmental and food matrixes. Their synthesis is straightforward, and the resulting material exhibits favorable magnetic properties for its harvesting, after extraction. As a proof of concept, an analytical method was developed for the determination of sulfonamides in lake water and egg samples using high-performance liquid chromatography with diode array detection. The new procedure exhibits low limits of quantification ( $0.06$  up to  $0.11 \mu\text{g L}^{-1}$ ), low matrix effect (from  $-8\%$  to  $8\%$ ), acceptable recoveries ( $88$ – $101\%$ ) and satisfactory enrichment factors ( $111$ – $141$ ). Moreover, the method has a wide linear range (up to  $250 \mu\text{g L}^{-1}$ ) making it possible to determine sulfonamides at concentrations above and below the maximum residue limit. Due to the aforementioned merits, the few synthetic steps required and the efficiency of sample preparation, the developed method can be used for the routine analysis of sulfonamides. Moreover, this study highlights the affinity of zinc for sulfonamides, a property that has never reaped before in analytical chemistry.

## 5.5 References

- [1] M.S. Parihar, F. Khan, Stability constants and thermodynamic parameters of cadmium complexes with sulfonamides and cephalosporin, *Eclat. Quim.* 33 (2008). doi:10.1590/S0100-46702008000100004.
- [2] J.L. Evelhoch, D.F. Bocian, J.L. Sudmeier, Evidence for Direct Metal-Nitrogen Binding in Aromatic Sulfonamide Complexes of Cadmium(II)-Substituted Carbonic Anhydrases by Cadmium-113 Nuclear Magnetic Resonance, *Biochemistry.* 20 (1981) 4951–4954. doi:10.1021/bi00520a022.
- [3] B.F. Senkal, E. Yavuz, Sulfonamide based polymeric sorbents for selective mercury extraction, *React. Funct. Polym.* 67 (2007) 1465–1470. doi:10.1016/j.reactfunctpolym.2007.07.017.
- [4] S. Bellú, E. Hure, M. Trapé, M. Rizzotto, E. Sutich, M. Sigrist, V. Moreno, The interaction between mercury(II) and sulfathiazole, *Quim. Nova.* 26 (2003) 188–192. doi:10.1590/S0100-40422003000200008.
- [5] J.R.A. Diaz, M. Fernández Baldo, G. Echeverría, H. Baldoni, D. Vullo, D.B. Soria, C.T. Supuran, G.E. Camí, A substituted sulfonamide and its Co (II), Cu (II), and Zn (II) complexes as potential antifungal agents, *J. Enzyme Inhib. Med. Chem.* 31 (2016) 51–62. doi:10.1080/14756366.2016.1187143.
- [6] A.M. Cappalonga, R.S. Alexander, D.W. Christianson, Structural comparison of sulfodiimine and sulfonamide inhibitors in their complexes with zinc enzymes, *J. Biol. Chem.* 267 (1992) 19192–19197. doi:10.2210/pdb1cps/pdb.
- [7] R.X. Yuan, R.G. Xiong, Z.F. Chen, P. Zhang, H.X. Ju, Z. Dai, Z.J. Guo, H.K. Fun, X.Z. You, Crystal structure of zinc(II) 2-sulfanilamidopyrimidine: A widely used topical burn drug, *J. Chem. Soc. Dalton Trans.* (2001) 774–776. doi:10.1039/b100901j.
- [8] S. Azizi, M.M. Shahri, R. Mohamad, Green synthesis of zinc oxide nanoparticles for enhanced adsorption of lead ions from aqueous solutions: Equilibrium, kinetic and thermodynamic studies, *Molecules.* 22 (2017). doi:10.3390/molecules22060831.
- [9] F. Zhang, J. Lan, Y. Yang, T. Wei, R. Tan, W. Song, Adsorption behavior and mechanism of methyl blue on zinc oxide nanoparticles, *J. Nanoparticle Res.* 15 (2013). doi:10.1007/s11051-013-2034-2.
- [10] A. Ríos, M. Zougagh, M. Bouri, Magnetic (nano)materials as an useful tool for sample preparation in analytical methods. A review, *Anal. Methods.* 5 (2013) 4558–4573. doi:10.1039/c3ay40306h.

- [11] L. Xie, R. Jiang, F. Zhu, H. Liu, G. Ouyang, Application of functionalized magnetic nanoparticles in sample preparation, *Anal. Bioanal. Chem.* 406 (2014) 377–399. doi:10.1007/s00216-013-7302-6.
- [12] K. El Maalam, L. Fkhar, Z. Mahhouti, O. Mounkachi, M. Aitali, M. Hamedoun, A. Benyoussef, The effects of synthesis conditions on the magnetic properties of zinc ferrite spinel nanoparticles, in: *J. Phys. Conf. Ser.*, 2016. doi:10.1088/1742-6596/758/1/012008.
- [13] P.M. Prithviraj Swamy, S. Basavaraja, A. Lagashetty, N. V. Srinivas Rao, R. Nijagunappa, A. Venkataraman, Synthesis and characterization of zinc ferrite nanoparticles obtained by self-propagating low-temperature combustion method, *Bull. Mater. Sci.* (2011). doi:10.1007/s12034-011-0323-x.
- [14] N.M. Deraz, A. Alarifi, Microstructure and magnetic studies of zinc ferrite nano-particles, *Int. J. Electrochem. Sci.* (2012).
- [15] T. Chatzimitakos, V. Exarchou, S.A. Ordoudi, Y. Fiamegos, C. Stalikas, Ion-pair assisted extraction followed by <sup>1</sup>H NMR determination of biogenic amines in food and biological matrices, *Food Chem.* 202 (2016) 445–450. doi:10.1016/j.foodchem.2016.02.013.
- [16] M. Serrano, T. Chatzimitakos, M. Gallego, C.D. Stalikas, 1-Butyl-3-aminopropyl imidazolium-functionalized graphene oxide as a nanoadsorbent for the simultaneous extraction of steroids and  $\beta$ -blockers via dispersive solid-phase microextraction, *J. Chromatogr. A.* 1436 (2016) 9–18. doi:10.1016/j.chroma.2016.01.052.
- [17] T. Chatzimitakos, V. Samanidou, C.D. Stalikas, Graphene-functionalized melamine sponges for microextraction of sulfonamides from food and environmental samples, *J. Chromatogr. A.* 1522 (2017) 1–8. doi:10.1016/j.chroma.2017.09.043.
- [18] T. Chatzimitakos, C. Binellas, K. Maidatsi, C. Stalikas, Magnetic ionic liquid in stirring-assisted drop-breakup microextraction: Proof-of-concept extraction of phenolic endocrine disrupters and acidic pharmaceuticals, *Anal. Chim. Acta.* 910 (2016) 53–59. doi:10.1016/j.aca.2016.01.015.



## Appendix: Commission Decision 657/2002/EC

To ensure consumer safety, many countries have established legislation regarding the maximum residue limits of SAs in food products. According to the “**Marketing Authorization for Maximum Residue Limits for Veterinary Drugs in Foods**” issued from the Government of Canada in 2013, “A maximum residue limit (MRL) is an amount of drug residue that — if present in the tissue of a food animal or a food product derived from a food-producing animal that has been treated with a veterinary drug — will not pose an unacceptable risk to the safety of the food. This residue, at this level, is considered to pose no adverse health effects if ingested daily by humans over a lifetime.”

On 26 June 1990 the European Council legislated **Council Regulation (EEC) No 2377/90**, laying down a Community procedure for the establishment of maximum residue limits of veterinary medicinal products in foodstuffs of animal origin. According to this regulation, the MRL for SAS was set at  $100 \mu\text{g kg}^{-1}$  for fat, kidney, liver, muscle and milk from either cattle or sheep. The MRL stands both for each sulfonamide individually and for the total content of SAs in the food products. Likewise, the Government of Canada, set an MRL of 0.1 ppm for each sulfonamide and in total. Also, the World Health Organization and the Food and Agriculture Organization of the United States issued the “Maximum residue limits (MRLs) and risk management recommendations (RMRs) for residues of veterinary drugs in foods, CX/MRL 2-2018” in which the MRL for sulfadimidine was set to  $100 \mu\text{g kg}^{-1}$  for fat, kidney, liver and muscle, while for milk it was set to  $25 \mu\text{g L}^{-1}$ .

Later on **Commission Decision 657/2002/EC** was announced, concerning the performance of analytical methods, and the interpretation of the results. According to this decision, the following definitions were given:

- Accuracy means the closeness of agreement between a test result and the accepted reference value. It is determined by determining trueness and precision.
- Alpha ( $\alpha$ ) error means the probability that the tested sample is compliant, even though a non-compliant measurement has been obtained (false non-compliant decision).

- Analyte means the substance that has to be detected, identified and/or quantified and derivatives emerging during its analysis
- Beta ( $\beta$ ) error means the probability that the tested sample is truly non-compliant, even though a compliant measurement has been obtained (false compliant decision).
- Bias means the difference between the expectation of the test result and an accepted reference value.
- Decision limit ( $CC\alpha$ ) means the limit at and above which it can be concluded with an error probability of  $\alpha$  that a sample is non-compliant.
- Detection capability ( $CC\beta$ ) means the smallest content of the substance that may be detected, identified and/or quantified in a sample with an error probability of  $\beta$ . In the case of substances for which no permitted limit has been established, the detection capability is the lowest concentration at which a method is able to detect truly contaminated samples with a statistical certainty of  $1 - \beta$ . In the case of substances with an established permitted limit, this means that the detection capability is the concentration at which the method is able to detect permitted limit concentrations with a statistical certainty of  $1 - \beta$ .
- Minimum required performance limit (MRPL) means minimum content of an analyte in a sample, which at least has to be detected and confirmed. It is intended to harmonise the analytical performance of methods for substances for which no permitted limit has been established.
- Performance characteristic means functional quality that can be attributed to an analytical method. This may be for instance specificity, accuracy, trueness, precision, repeatability, reproducibility, recovery, detection capability and ruggedness
- Precision means the closeness of agreement between independent test results obtained under stipulated (predetermined) conditions. The measure of precision usually is expressed in terms of imprecision and computed as standard deviation of the test result. Less precision is determined by a larger standard deviation.
- Repeatability means precision under repeatability conditions

- Repeatability conditions means conditions where independent test results are obtained with the same method on identical test items in the same laboratory by the same operator using the same equipment
- Reproducibility means precision under reproducibility conditions
- Reproducibility conditions means conditions where test results are obtained with the same method on identical test items in different laboratories with different operators using different equipment
- During the analysis of samples the recovery shall be determined in each batch of samples, if a fixed recovery correction factor is used. If the recovery is within limits, the fixed correction factor may then be used. Otherwise the recovery factor obtained for that specific batch shall be used, unless the specific recovery factor of the analyte in the sample is to be applied in which case the standard addition procedure or an internal standard shall be used for the quantitative determination of an analyte in a sample.
- A method shall be able to distinguish between the analyte and the other substances under the experimental conditions. An estimate to which extent this is possible has to be provided. Strategies to overcome any foreseeable interference with substances when the described measuring technique is used, e.g. homologues, analogues, metabolic products of the residue of interest have to be employed. It is of prime importance that interference, which might arise from matrix components, is investigated.

In order for an analytical method to comply with the criteria applicable for the relevant performance characteristics, method validation must take place. For quantitative screening methods the detection limit  $CC\beta$ , precision, selectivity/specificity and applicability/ruggedness must be verified. For a quantitative confirmatory method, the above along with decision limit  $CC\alpha$  and recovery must be calculated. For HPLC-UV based methods, the absorption maxima in the spectrum of the analyte shall be at the same wavelengths as those of the calibration standard within a margin determined by the resolution of the detection system. For diode array detection, this is typically within  $\pm 2$  nm. The spectrum of the analyte above 220 nm shall, for those parts of the two spectra

with a relative absorbance  $\geq 10\%$ , not be visibly different from the spectrum of the calibration standard. This criterion is met when firstly the same maxima are present and secondly when the difference between the two spectra is at no point observed greater than 10% of the absorbance of the calibration standard. In the case computer-aided library searching and matching are used, the comparison of the spectral data in the test samples to that of the calibration solution has to exceed a critical match factor. This factor shall be determined during the validation process for every analyte on the basis of spectra for which the criteria described above are fulfilled. Variability in the spectra caused by the sample matrix and the detector performance shall be checked.

## Conclusions

In this thesis, four analytical methods have been developed to address the need for sensitive detection of sulfonamides and also to meet the need for greener and more miniaturized analytical methods. The analytical methods are based on the development of alternative sample preparation procedures capitalizing on the extractive properties of four, novel, (nano)materials. The first method was based on the use of graphene functionalized melamine sponges which can be prepared in only 2 min. The analytical figures of merit of the method are comparable with those attained by other approaches involving different sample pretreatment procedures. The limits of detection achieved are superior than those of previous methods (optical detectors) or rival them (mass spectrometric (MS) or MS/MS detectors), while based on the rest analytical figures of merit, the developed method is suitable for routine analysis or even more for fast screening of the sulfonamides. Next, melamine sponges were decorated with metallic copper in an easy and efficient way, resulting in a sorbent material that can be used in a sample preparation procedure with low detection limits, wide linear range, highly satisfactory recoveries, and repeatability. However, the main benefit of this method is its fairly good selectivity, which derives from the high affinity of copper for sulfonamides, a property that has not been, so far, exploited for analytical purposes. The two above studies can pave the way for the development of more melamine sponge-based sorbent materials, since melamine sponges are a promising alternative to common polyurethane or graphene sponges or other sponge-like materials, due to its many inherent advantages.

The third analytical method is an advanced dispersive liquid-liquid microextraction method using magnetic ionic liquids. This method differs from others previously described since two major improvements were achieved. The first major improvement is the use of quartz-silica as solid supporting material for the magnetic ionic liquid-based microextraction. The use of solid support renders the handling of the magnetic ionic liquid easier and significantly increases the reproducibility and efficiency of the method. The second major improvement is the use of a pH-modulated approach. Using this approach not only sulfonamides but also triazines can be extracted in a one-pot procedure from the same sample, in a short period of time allowing each class the

analytes to be extracted separately at different sample pH. The enhanced method exhibits favorable analytical figures of merit, making feasible the determination of the compounds at levels below the maximum residue limits, as defined by regulatory agencies. The development of this method addresses the flaws of existing procedures to enhance them. Moreover, it paves the way for the development of similar procedures where more than one class of compounds are extracted from the same matrix with minor modifications, by using fewer chemicals and meeting the need for greener analytical methods.

Finally, in the fourth developed method, zinc ferrites were used for the first time as a sorbent for sulfonamides extraction. The material was utilized under the principles of the magnetic ultrasound-assisted dispersive micro solid-phase extraction so that it can easily be harvested after the extraction step. Due to the high affinity of zinc ferrite for sulfonamides, an efficient and selective analytical method was developed. The wide linear range, low limits of quantification, low matrix effects and the good recoveries are among the benefits of the developed procedure. This method along with the second one (utilizing melamine sponges decorated with copper sheets) highlight that zinc ferrites and melamine sponges decorated with copper sheets can be useful alternatives in analytical chemistry, and reaping their affinity towards SAs can be the basis for the development of future applications, taking advantage of similar affinities of metals for other organic compounds.

From all the above it can be concluded that using the proposed (nano)materials, novel sample preparation procedures can be followed for the extraction of sulfonamides from food matrices. The developed methods can be used as alternatives for routine sulfonamide detection, while their cost and analysis time are reduced compared to previously described methods. Moreover, no expensive equipment (e.g. MS/MS) is needed to achieve satisfactory results. The fact that the separation and detection of sulfonamides were based on an HPLC-DAD system makes the proposed methods even more affordable for any analytical laboratory.

## List of Book Chapters, Journal Papers and Conference Presentations

- Book Chapters
4. ***“Synthesis of carbon nanodots and their therapeutic applications”*** A. Kasouni, T. Chatzimitakos, C. Stalikas in: Biosynthesized Nanomaterials, In Press, Elsevier
  3. ***“Antimicrobial properties of carbon quantum dots”*** T. Chatzimitakos, C. Stalikas in: Nanotoxicity: Prevention, and Antibacterial applications of Nanomaterials, Rajendran S., et.al (eds), In Press, Elsevier
  2. ***“Carbon nanodots from natural (re)sources: A new perspective on analytical chemistry”*** T. Chatzimitakos, C. Stalikas in: “Handbook of Nanomaterials in Analytical Chemistry: Modern Trends in Analysis, Hussain C. (eds), 2020, pages 3-28, Elsevier
  1. ***“Metabolic fingerprinting of bacteria exposed to nanomaterials, using online databases, NMR and high-resolution mass spectrometry”*** T. Chatzimitakos, C. Stalikas in Methods in Molecular Biology: Nanotoxicity Methods and Protocols, 2019, 1894, pages 271-280, Springer
- Publications
- 22) ***“Cannabinol in the spotlight: Toxicometabolomic study and behavioral analysis of zebrafish embryos exposed to the unknown cannabinoid”***  
Ieremias Chousidis, Theodoros Chatzimitakos, Dimitrios Leonardos, Michaela Filiou, Constantine Stalikas, Ioannis Leonardos  
Chemosphere, In press
  - 21) ***“Zinc ferrite as a magnetic sorbent for the dispersive micro solid-phase extraction of sulfonamides and their determination by HPLC”***  
T. Chatzimitakos, C. Stalikas  
Microchemical Journal, Volume 155, June 2020, Article Number: 104670
  - 20) ***“Exploring the antibacterial potential and unraveling the mechanism of action of non-doped and heteroatom-doped carbon nanodots”***  
T. Chatzimitakos, A. Kasouni, A. Troganis, C. Stalikas  
Journal of Nanoparticle Research, Volume 22, January 2020, Article Number: 36

**19) "Magnetic graphene oxide as a convenient nanosorbent to streamline matrix solid-phase dispersion towards the extraction of pesticides from vegetables and their determination by GC-MS"**

T. Chatzimitakos, K. Karali, C. Stalikas

Microchemical Journal, Volume 151, December 2019, Article Number: 104247

**18) "Bioimaging applications of carbon nanodots: A review"**

A. Kasouni, T. Chatzimitakos, C. Stalikas

C Journal of Carbon Research, Volume 5, April 2019, Article Number: 19

**17) "Matrix solid-phase dispersion based on magnetic ionic liquids: An alternative sample preparation approach for the extraction of pesticides from vegetables"**

T. Chatzimitakos, J. Anderson, C. Stalikas

Journal of Chromatography A, Volume 1581-1582, December 2018, Pages 168-172

**16) "Enhanced magnetic ionic liquid-based dispersive liquid-liquid microextraction of triazines and sulfonamides through a one-pot, pH-modulated approach"**

T. Chatzimitakos, S. Pierson, J. Anderson, C. Stalikas

Journal of Chromatography A, Volume 1571, October 2018, Pages 47-54

**15) "Melamine sponge functionalized with urea-formaldehyde co-oligomers as a sorbent for the solid-phase extraction of hydrophobic analytes"**

M. García-Valverde, T. Chatzimitakos, R. Lucena, S. Cárdenas, C. Stalikas

Molecules, Issue 10, October 2018,

**14) "Human fingernails as an intriguing precursor for the synthesis of nitrogen and sulfur-doped carbon dots with strong fluorescent properties: Analytical and bioimaging applications"**

T. Chatzimitakos, A. Kasouni, L. Sygellou, I. Leonardos, A. Troganis, C. Stalikas

Sensors and Actuators B: Chemical, Volume 267, August 2018, Pages 494-501

**13) "Melamine sponge decorated with copper sheets as a novel material for microextraction of sulphonamides prior to their HPLC determination"**

T. Chatzimitakos, C. Stalikas

Journal of Chromatography A, Volume 1554, June 2018, Pages 28-36



**12) "Carbonization of human fingernails: Towards the sustainable production of multifunctional nitrogen- and sulfur-co doped carbon quantum dots as highly luminescent probe with extra cell proliferative/migration properties"**

T. Chatzimitakos, A. Kasouni, A. Troganis, C. Stalikas

ACS Applied Materials & Interfaces, Volume 10, May 2018, Pages 16024-16032

**11) "Selective FRET-based sensing of 4-nitrophenol and cell imaging capitalizing on the fluorescent properties of carbon nanodots from apple seeds"**

A. Chatzimakou, T. Chatzimitakos, A. Kasouni, L. Sygellou, A. Avgeropoulos, C. Stalikas, Sensors and Actuators B: Chemical, Volume 258, April 2018, Pages 1152-1160

**10) "Two of a kind but different: Luminescent carbon quantum dots from Citrus peels for iron and tartrazine sensing and cell imaging"**

T. Chatzimitakos, A. Kasouni, L. Sygellou, A. Avgeropoulos, A. Troganis, C. Stalikas, Talanta, Volume 175, December 2017, Pages 305-312

**9) "Graphene-functionalized melamine sponges for microextraction of sulfonamides from food and environmental samples"**

T. Chatzimitakos, V. Samanidou, C. Stalikas, Journal of Chromatography A, Volume 1522, November 2017, Pages 1-8

**8) "Carbon-based nanomaterials functionalized with ionic liquids for microextraction in sample preparation"**

T. Chatzimitakos, C. Stalikas, Separations, Volume 4, Issue 2, April 2017, Article Number: 14

**Received Separations Best Paper Award 2019 from all papers published between 1 January 2017 and 31 December 2018**

**7) "Qualitative alterations of bacterial metabolome after exposure to metal nanoparticles with bactericidal properties: A comprehensive workflow based on <sup>1</sup>H NMR, UHPLC-HRMS, and metabolic databases"**

T. Chatzimitakos, C. Stalikas, Journal of Proteome Research, Volume 15, Issue 9, September 2016, Pages 3322-3330

**6) "Antibacterial, anti-biofouling and antioxidant prospects of metal based nanomaterials"**

T. Chatzimitakos, A. Kallimanis, A. Avgeropoulos, C. Stalikas

CLEAN – Soil, Air, Water, Volume 44, Issue 7, July 2016, Pages 794-802,

**5) "Ion-pair assisted extraction followed by <sup>1</sup>H NMR determination of biogenic amines in food and biological matrices"**

T. Chatzimitakos, V. Exarchou, S. Ordoudi, Y. Fiamegos, C. Stalikas  
Food Chemistry, Volume 202, July 2016, Pages 445-450

**4) "1-Butyl-3-aminopropyl imidazolium-functionalized graphene oxide as a nanoadsorbent for the simultaneous extraction of steroids and β-blockers via dispersive solid-phase microextraction"**

M. Serrano, T. Chatzimitakos, M. Gallego, C. Stalikas  
Journal of Chromatography A, Volume 1436, Issue 4, March 2016, Pages 9-18

**3) "Magnetic ionic liquid in stirring-assisted drop-breakup microextraction: Proof-of-concept extraction of phenolic endocrine disrupters and acidic pharmaceuticals"**

T. Chatzimitakos, C. Binellas, K. Maidatsi, C. Stalikas  
Analytica Chimica Acta, Volume 910, Issue 3, March 2016, Pages 53-59

**2) "Octyl-modified magnetic graphene as a sorbent for the extraction and simultaneous determination of fragrance allergens, musks, and phthalates in aqueous samples by gas chromatography with mass spectrometry"**

K. Maidatsi, T. Chatzimitakos, V. Sakkas, C. Stalikas  
Journal of Separation Science, Volume 38, Issue 21, November 2015, Pages 3758-3765,

**1) "In situ trapping of As, Sb and Se hydrides on nanometer-sized ceria-coated iron oxide – silica and slurry suspension introduction to ICP-OES"**

A. Dados, E. Kartsiouli, T. Chatzimitakos, C. Papastephanou, C. Stalikas  
Talanta, Volume 130, Issue 1 December 2014, Pages 142-147

Oral presentations **6) "Enhanced variants of microextraction procedures based on magnetic ionic liquids"**, at "11<sup>th</sup> International Conference on Instrumental methods of analysis: Modern Trends and applications", 22-25 September 2019, Ioannina, Greece

**5) "Detection of hexavalent chromate, cell bioimaging and promotion of cell cycle: three applications of carbon quantum dots with high quantum yield, from human fingernails"**, at "5<sup>th</sup> Conference of Department of Chemistry of University of Ioannina", 29-30 September 2017, Ioannina, Greece

4) **“Antibacterial properties of three metal nanoparticles - method development for the metabolomic study of bacteria exposed to the nanomaterials”**, at *“22<sup>nd</sup> PanHellenic Chemistry Conference”*, 2-4 December 2016, Thessaloniki, Greece

3) **“Chemical composition of *Carassius gibelio roes* – Comparison with commercially available products”**, at *“16<sup>th</sup> PanHellenic Conference of Ichthyology”*, 6-9 October 2016, Kavala, Greece

2) **“Synthesis of luminescent carbon quantum dots from orange peels for the detection of iron in biological fluids and cell bioimaging”**, at *“14<sup>th</sup> PanHellenic Conference of Clinical Chemistry”*, 29 September - 1 October 2016, Ioannina, Greece

1) **“Dispersive liquid-liquid microextraction method using magnetic ionic liquids for the determination of phenolic endocrine disrupters and acidic pharmaceuticals in aqueous matrices”**, at *“8<sup>th</sup> European Conference on Pesticides and Related Organic Micropollutants in the Environment & 14<sup>th</sup> Symposium on Chemistry and Fate of Modern Pesticides”*, 18-21 September 2014, Ioannina, Greece

Poster presentations 13) **“Effect of Cannabinol on Zebrafish larvae (*Danio Rerio* Hamilton 1822): Metabolomic study using 1H-NMR”**, at *“13<sup>th</sup> Cyprus-Greece Chemistry conference”*, 31 October-3 November 2019, Nicosia, Greece

12) **“Metabolomic profiling of zebrafish with nmr and LC-MS/MS after exposure to non-doped, n-doped and n,s-doped carbon nanodots”**, at *“11<sup>th</sup> International Conference on Instrumental methods of analysis: Modern Trends and applications”*, 22-25 September 2019, Ioannina, Greece

11) **“Synthesis of magnetic bimetallic Fe-Cu nanoparticles for the dispersive microextraction of emerging pollutants”**, at *“11<sup>th</sup> International Conference on Instrumental methods of analysis: Modern Trends and applications”*, 22-25 September 2019, Ioannina, Greece

10) **“Magnetic graphene oxide solid-phase extraction of selected pharmaceuticals from environmental waters”**, at *“11<sup>th</sup> International Conference on Instrumental methods of analysis: Modern Trends and applications”*, 22-25 September 2019, Ioannina, Greece

- 9) **“Melamine sponge functionalized with graphene for the microextraction and detection of sulfonamides in food and environmental water samples”** at *“5<sup>th</sup> Conference of Department of Chemistry of University of Ioannina”*, 29-30 September 2017, Ioannina, Greece
- 8) **“Investigation of the antibacterial properties of non-doped, nitrogen-, nitrogen/sulfur-doped quantum dots from citric acid: study of the bacterial metabolomic fingerprints”** at *“22<sup>nd</sup> PanHellenic Chemistry Conference”*, 2-4 December 2016, Thessaloniki, Greece
- 7) **“Synthesis of luminescent carbon quantum dots from human nails for the detection of colorant E110 and cell imaging”** at *“22<sup>nd</sup> PanHellenic Chemistry Conference”*, 2-4 December 2016, Thessaloniki, Greece
- 6) **“Synthesis of luminescent carbon quantum dots from selected citrus fruits: Application in cell bioimaging and analysis of iron and tartrazine (E102)”** at *“22<sup>nd</sup> PanHellenic Chemistry Conference”*, 2-4 December 2016, Thessaloniki, Greece
- 5) **“Luminescent carbon quantum dots from human nails: a novel nanomaterial for cell bioimaging”**, at *“14<sup>th</sup> PanHellenic Conference of Clinical Chemistry”*, 29 September - 1 October 2016, Ioannina, Greece
- 4) **“Metabolomic study and impact of iron, copper and iron-copper nanoparticles on gram positive and negative bacteria”**, at *“8<sup>th</sup> European Conference on Pesticides and Related Organic Micropollutants in the Environment & 14<sup>th</sup> Symposium on Chemistry and Fate of Modern Pesticides”*, 18-21 September 2014, Ioannina, Greece
- 3) **“Octylamine-modified magnetic graphene as a sorbent for the extraction and simultaneous determination of fragrance-allergens, musks and phthalates in aqueous matrices”**, at *“8<sup>th</sup> European Conference on Pesticides and Related Organic Micropollutants in the Environment & 14<sup>th</sup> Symposium on Chemistry and Fate of Modern Pesticides”*, 18-21 September 2014, Ioannina, Greece
- 2) **“Graphene-based magnetic nanosorbents for the enrichment of environmental organic pollutants prior to their determination by gas chromatography-mass spectrometry”**, at *“17<sup>th</sup> International Symposium on Environmental Pollution and its Impact on Life in the Mediterranean Region 2013”*, 28 September-1 October 2013, Istanbul, Turkey

1) ***“Selective ion-pair assisted extraction and H-NMR determination of biogenic amines in various matrices”***, at ***“8<sup>th</sup> International Conference on Instrumental Methods of Analysis: Modern Trends and Applications (IMA)”***, 15-19 September 2013, Thessaloniki, Greece

Honours and awards Received ***Separations Best Paper Award 2019*** from all papers published between 1 January 2017 and 31 December 2018 for the review article ***“Carbon-based nanomaterials functionalized with ionic liquids for microextraction in sample preparation”***

**Scholarship** from General Secretariat of Research and Technology and the Hellenic Institute of Research and Innovation for the PhD studies